# Impact on Seismic Capacity of Unreinforced Masonry Houses- By varying the Geometrical Parameters of Terraced House

Master of Science Thesis

Ashwin Ganesh Kumar
21 December 2016


Delft University of Technology

DIANA FEA BV

Thesis for the degree of Master of Science in Civil Engineering

Faculty of Civil Engineering and Geosciences
Structural Engineering, Structural Mechanics

Delft University of Technology, the Netherlands

Author: Ashwin Ganesh Kumar
Student number: 4401425
E-mail: a.ganeshkumar@student.tudelft.nl

**Thesis committee:**
Dr. Ir. M.A.N. Hendriks (TU Delft, Structural Mechanics) - Chairman
Prof. Dr. Ir. J.G. Rots (TU Delft, Structural Mechanics)
Dr. Ir. K.C. Terwel (TU Delft, Building Engineering)
Dr. Ir. G.M.A. Schreppers (Diana FEA BV)

# Summary

In the last few years, increasing seismic activity is observed in the province of Groningen, The Netherlands; due to extraction of natural gas. This has an impact on the buildings located in that region, as they are composed of unreinforced masonry. As these buildings are not designed to withstand earthquakes, their assessment has now become a necessity.

The master thesis project is focusing on the seismic assessment of Dutch Terraced houses. It is based on a specific case study corresponding to the terraced houses with the presence of timber diaphragms.

From the available literature, it is evident that varying the geometrical parameters of a structure does alter the capacity on a global scale. This led to the main research objective of this project, which is to determine the impact on the seismic capacity of unreinforced masonry houses, by varying the geometrical parameters of the terraced houses. And the main objective is supported by two questions:

- What effect does inclusion of lintel beams have on the capacity of the structure?
- How does the capacity of the structure vary if the geometrical characteristics like openings in walls, inclusion/exclusion of staircase openings are altered?

A finite element model was generated for the case study. The model was created by using the language python, so as to parametrize based on user-defined values. The methodology developed focuses on the global capacity of the structure. The need to develop the variations with respect to the geometry resulted in the development of case study with fixed parameters. The modelling strategy involves the use of 2D curved shell elements, monotonic pushover analysis with uniform load application by equivalent acceleration method (EQUIAC) where all the elements in the model are subjected to an acceleration load in a specified direction, and engineering masonry model was adopted with fixed material parameters. The load increment on met followed was force controlled, with force convergences norm with arc-length criteria and an iterative Regular Newton Raphson solution method.

Two analysis were performed on the case study; eigenvalue and monotonic pushover analysis. In the pushover analysis for the case study different stages were observed from the shear drift curves. They are:

1 Pre-Crack Stage
2 First Crack Stage
3 Crack Propagation Stage
4 Collapse Stage

The crack patterns observed in the case study corresponds to different failure modes stated in the literature.

This was followed by varying the geometrical parameters of the structure. The parametrized script resulted in creating various models with minimum pre-processing time. The variations were based on the definition of irregularity index stated in the literature. The variations are:

1 Variations excluding Irregularity
2 Vertical Irregularity – varying the width of openings
3 Horizontal Irregularity – varying the height of openings
4 Number of Openings

All these variations were subjected to monotonic pushover analysis and comparison was done with respect to the case study. A sensitivity analysis was performed to see the effect on the capacity of the structure due to the irregularity index. This was then accompanied by the interpretation on the irregularities by plotting the capacity of the structure with the irregularity index of that variation.

Different failure mechanisms were observed by varying the irregularity and irregularity index. The inclusion of lintel beams improves the capacity of structure, as the masonry elements located above the openings are supported by the beams. The inclusion of staircase openings resulted in a stiffer behaviour of the structure, because the openings are supported by timber beams which are directly connected to the wall without any springs. So the nodes of the beam and the masonry wall share all degrees of freedom. Increasing the irregularity index, results in a lower capacity of the structure; due to the increased area of openings in the wall. The irregularity index, gives a clear picture on the effect of the capacity of the structure.

It is recommended that further research focuses on the detailed modelling of cavity walls, and also the inclusion of soil-structure interaction. A more sophisticated approach would be to define the irregularity index for all walls, and also local index and the percentage of masonry area for a better classification. More variation studies on the index, would lead to the developing of empirical models for the seismic assessment of the structure.

# Preface

In this document the results of the master's project, carried out for the company DIANA FEA BV, are reported. This thesis is part of the master's program Structural Mechanics at Delft University of Technology. Structural Mechanics is one of the specialization of the master track Structural Engineering.

In December 2015 the question was raised by me with the guidance from DIANA FEA BV- What is the seismic capacity of unreinforced masonry houses, by varying the geometrical parameters of the terraced house. This also involved in creating a template using the language Python, which can be run on DIANA Interactive Environment.

I would like to thank my supervisors for their support during my research. I am very pleased with the guidance Dr. Max Hendriks gave me during the project and the perspective to keep in mind the bigger picture. I want to thank Professor Jan Rots for his help with in-depth questions about the modelling aspects of terraced houses in the finite element software. I want to thank Dr. Ir. K.C. Terwel for his support with the practical problems from the building engineer point of view. I want to thank Dr. Gerd-Jan Schreppers for his constant support and motivation, in guiding me through this entire period of my research. I am also very grateful for the opportunity that he gave me to work at DIANA FEA BV and cooperate with very talented people. During my stay I have gained impeccable experience and a good understanding of computer programming and Finite Element Analyses.

Finally I want to thank family and friends for their mental support during the project.

Ashwin Ganesh Kumar
Delft, December 21, 2016

# Contents

# 1 Introduction

Until recent years, The Netherlands was a country with no earthquakes. But recently the exploitation of natural gas, which started in the early 1960s has resulted in the induced earthquakes. The gas fields are located in the Northern part of the Netherlands- Groningen. As the gas extraction was carried out despite initial low magnitude earthquakes, in the subsequent years the number increased which is now one of the key issues in the province of Groningen.
The area is quite populated with unreinforced masonry houses. The residential buildings are classified into terraced houses, semi-detached, detached, labourers cottages, and large masonry villas. In this research, terraced houses of sub-typology T1 (Structural Upgrade Study, Arup 2013) is taken into account.

**Fig. 1.1.:** DUTCH TERRACED HOUSES

## 1.1 Research Objectives

The main objective of this thesis is non-linear seismic assessment of unreinforced masonry houses subjected to earthquake loading by varying the geometrical characteristics. The area taken into consideration is Groningen, with epicentre at Loppersum. It was chosen to develop prototype fit-for-purpose software application using the programming language python to steer the DIANA Finite Element Software programme. The analysis procedure investigated here is Pushover.

To support the above mentioned objective, the following questions are considered key to be answered in this research:

- What effect does inclusion of lintel beams have on the capacity of the structure?
- How does the capacity of the structure vary if the geometrical characteristics like openings in walls, inclusion/exclusion of staircase openings are altered?

## 1.2 Methodology

To fulfil the outcome of the research objective a method had to be drafted. A brief overview is given about the method, and the assumptions made in this research are explained in detail in the subsequent chapters.

DIANA FEA BV has already developed a prototype-fit-for purpose application called as Quake, which was highly automated in the pre-processing stage. However the application had its own limitations. It was limited to the geometrical shape of a rectangular box, there was no option to include a terraced roof which is abundant in number in the province of Groningen. It was just restricted to exterior walls, the inclusion of interior walls as a structural member was lacking in the Quake application. As a result, this led to the parametrized python script. The script is flexible, that it can be used to generate different geometries. The main advantage of the script is the reduced pre-processing time. The elements which were not taken into account for modelling includes the foundation, soil-structure interaction etc. These are left out to simplify the modelling process.

When the case study has been modelled various analysis were carried out and conclusions were drawn accordingly. The variation of geometrical characteristics like varying the size of openings, inclusion/exclusion of openings and inclusion/exclusion of lintel beams etc. were carried out.

## 1.3 Case Study

The case study that was taken into consideration was a row of four terraced houses. These buildings were built during 1950s and each unit consists of two floors and an attic. In this research only one house is modelled, even though the script can already be extended to a line of terraced houses. The structure has masonry walls, timber floors, timber roofs and joists lying on a concrete foundation. The masonry façades of every unit, and side walls at the left and right of the four houses are of cavity walls with a thickness of 250mm. The solid and interior walls of every unit has a thickness of 120mm. In this research only the inner leaf has been modelled and outer leaf is taken into consideration as a translational mass. The plan, front-view of the row house and section-view of a single house are shown in the figures 1.2 and 1.3. More detailed information about the building dimensions and detailing are given in the Appendix B.1.

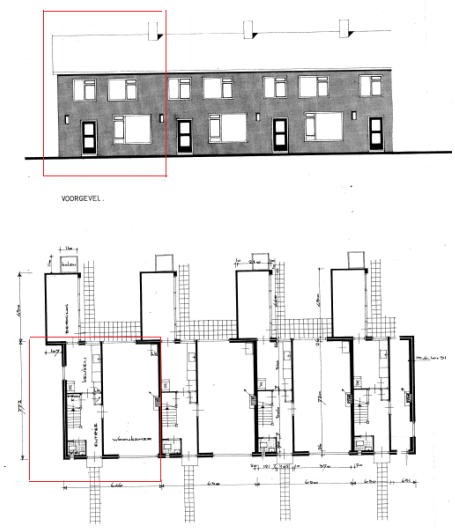

Fig. 1.2.: TERRACED-HOUSE PLAN AND FRONT VIEW

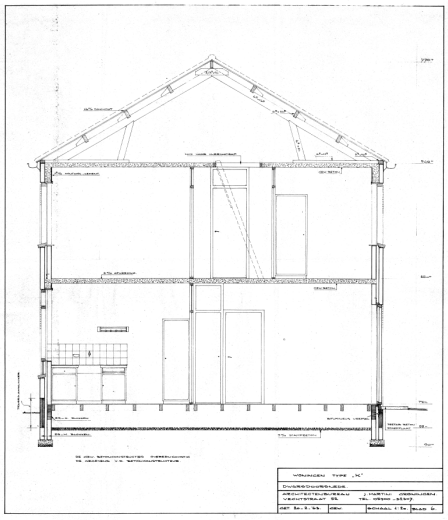

Fig. 1.3.: SECTION VIEW

## 1.4 Synopsis

This thesis report is organised in the following way. The first step that was taken in this research was to get the background knowledge on the behaviour of unreinforced masonry and also to get an insight on the different types of failure mechanisms associated with masonry. As the main objective is to assess the variation of geometrical characteristics in a terraced house, a brief overview about the geometrical irregularity has been given. The background theory on different ways to assess the seismic capacity of the structures has been explained with focus on pushover analysis.

In the next chapter, a detailed explanation is given how the case study has been modelled and what are the assumptions made behind this case study has been described. Adding to this, the key element in schematisation of the built structure into a finite element model and the properties associated with it are described in detail.

As the case study has been modelled, the next chapter deals with the interpretation of analysis results. The main analysis procedures are Eigenvalue and Pushover analysis. And this chapter is followed by the variation studies where different variations have been carried out like inclusion/exclusion of lintel beams, inclusion/exclusion of openings, varying the size of openings etc. A sensitivity analysis has been carried out and proper interpretations were made.

The last part of this report is the chapter where conclusions have been drawn from the above analysis and the research questions which supports the main objective of the thesis has been answered, and which was followed by recommendations for future research.

# Literature Study

# 2

The scope of this literature study is to give a comprehending view on the seismic response of masonry houses; and how it depends on the geometrical characteristics and structural connections in the masonry houses. So to begin with, it is very essential to understand the behaviour of material and have an overview about failure modes. Following this, a brief description is given on how structural irregularities(geometric variation) significantly affect the performance of masonry houses. As a next step specific characteristics with regards to structural connections in masonry houses are elaborated. A brief introduction is given on how the masonry houses have been modelled using 2-D curved shell elements. The methods to analyse the seismic behaviour of structure are elaborated and emphasis is given to Pushover analysis, which further extends to sensitivity analysis based on key parameters.

## 2.1 Masonry

Most of the masonry structures that are present today is made of brick units with mortar joints, which act as connection between the bricks. This makes masonry as a composite material. The properties of masonry usually vary depending on the type of bricks and mortar used. According to *Mosalam, Glascoe, & Bernier, 2009* the additional factors which affect the behaviour of masonry are the dimensions of units, mortar width and orientation of the units. The construction method that would be given primary importance in this report is Unreinforced Masonry (URM) which is traditionally used for masonry structures.

### 2.1.1 Material Properties of Masonry

As already mentioned, masonry mechanical properties are mainly dependent on units and mortars used. The weakest point in the composite is the interface between unit and mortar. Therefore, the non-linear behaviour of the interface is of high importance to determine the behaviour of the composite. Two different failure modes have been observed with respect to the interface, Mode I and Mode II failure, which can be related to tensile and shear failures respectively.
*Mode I Failure*
From the deformation controlled tests, an exponential tensioning softening curve is obtained. The fracture energy in this type of failure ranges from $0.005$ to $0.025 J/mm^2$.

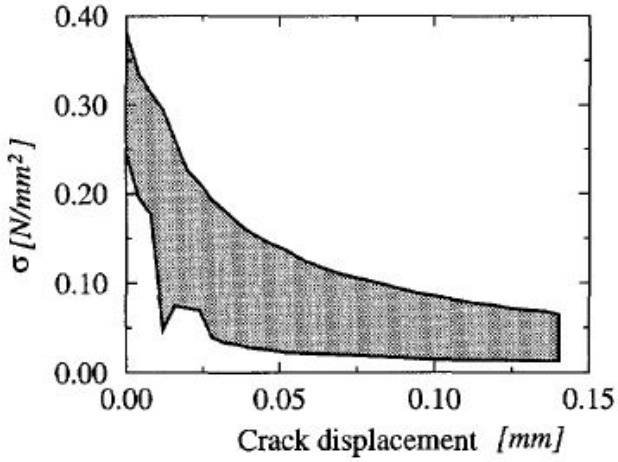


**Fig. 2.1.:** TYPICAL EXPERIMENTAL STRESS-CRACK DISPLACEMENT RESULTS FOR SOLID CLAY BRICK MASONRY: ENVELOPE OF THREE TESTS (LOURENCO (1996))

*Mode II Failure*

The results from these tests revealed that shear behaviour is characterized by a gradual decrease in strength until it reaches a gradual non-zero constant stress level, as shown in Figure 2.2 . The other noticeable relationship is that there is a linear relationship between confining stress and Mode II fracture energy, which is nothing but a Coulomb type of friction.

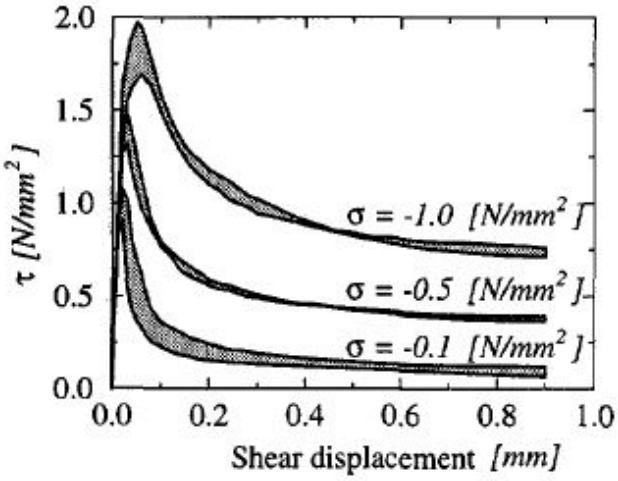


**Fig. 2.2.:** STRESS-DISPLACEMENT DIAGRAM FOR DIFFERENT NORMAL STRESS LEVELS: ENVELOPE OF THREE TESTS (LOURENCO (1996))

Another important factor which adds to material properties of masonry are the loading angle with respect to the material aspects as shown in Figure 2.3.

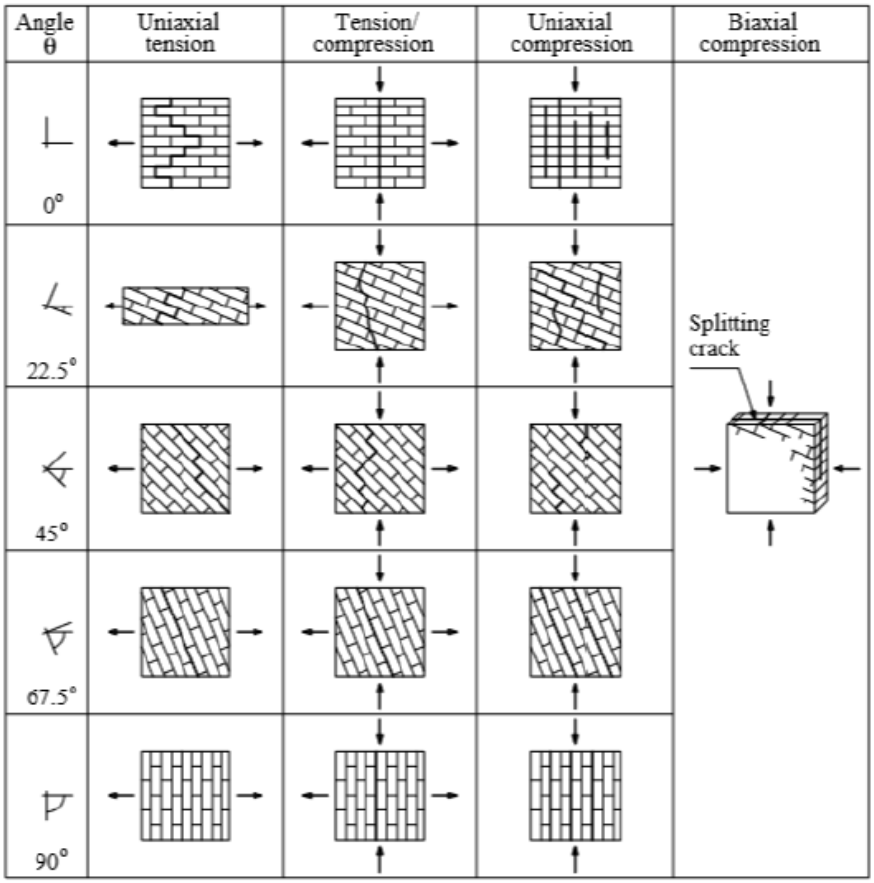


**Fig. 2.3.:** MODES OF FAILURE OF SOLID CLAY UNITS MASONRY UNDER BIAXIAL LOADING, DHANASEKAR et al. (1985)

### 2.1.2 Numerical Modelling Of Masonry Structures

A composite material-masonry shows anisotropic behaviour. This arises due to specific arrangement of units and joints. The modelling of masonry elements using finite elements can be achieved in different ways ranging from a detailed micro level approach to a macro level approach, where the wall is considered as continuum. In this research, a macro-model approach will be adopted; where the properties of all components are smeared out and can be applied with curved shell elements.

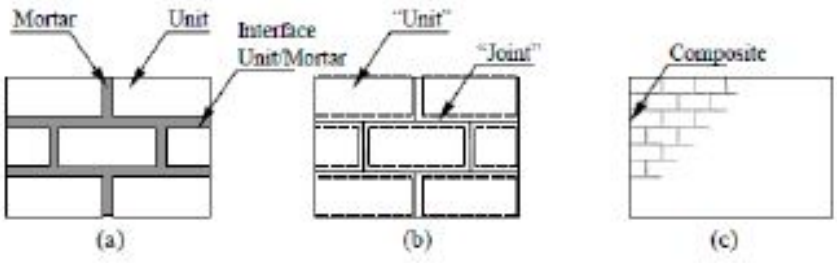


**Fig. 2.4.:** MODELLING STRATEGIES- MASONRY STRUCTURES:(A) DETAILED MICRO-MODELLING; (B) SIMPLIFIED MICRO-MODELLING; (C) MACRO-MODELLING. (LOURENCO, 2013)

## 2.2 Failure Mechanisms

Post-earthquake investigations and experimental research have shown that the typical failure mechanisms of a URM building are grouped into the following categories (Deppe 1988, Boussabah 1992, Bruneau 1994a, 1994b, 1995, Tomazevic 1999, Peralta et al. 2000):

- Lack of Anchorage
- Anchor Failure
- In-Plane Failure (URM Walls)
- Out-of Plane Failure (URM Walls)
- Combined In-Plane and Out-of Plane Failure
- Diaphragm related Failure

### 2.2.1 In-Plane Failure

Excessive bending or shear can cause in-plane failures. Especially for walls, shear in-plane failures are common. In masonry façades, the shear failures also occur in spandrels and piers. Flexural failure is also a possible failure mechanism, resulting in cracking at both ends of a URM elements. These are defined as global response mechanisms.

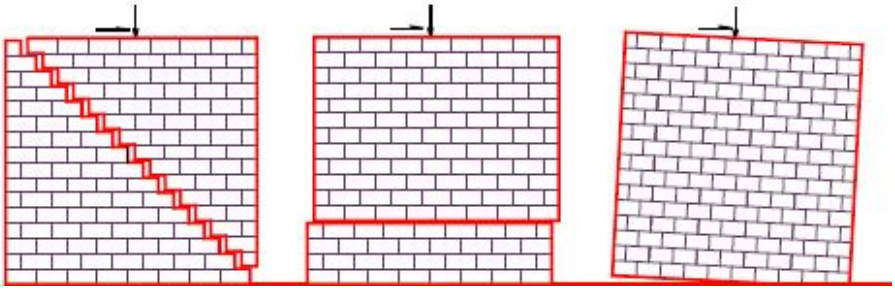

Fig. 2.5.: IN-PLANE FAILURE MECHANISMS- SHEAR FAILURE, SLIDING FAILURE, FLEXURAL FAILURE (ELGAWADY, BADOUX, AND LESTUZZI, 2006)

### 2.2.2 Out-of Plane Failure

When the wall bends in the lateral direction i.e. the weakest direction due to small thickness; out-of plane failure occurs. This type of failure occurs usually due to poor connection between walls or floors. Possible Out-of Plane failure mechanisms are shown in Figure 2.6.

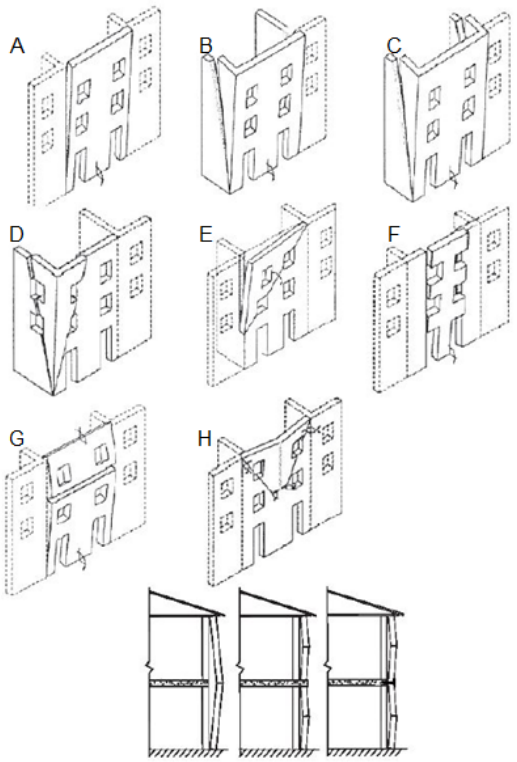


Fig. 2.6.: OUT-OF-PLANE PLANE FAILURE MECHANISMS (A) VERTICAL OVERTURNING (B) OVERTURNING WITH 1 SIDE WING (C) OVERTURNING WITH 2 SIDE WINGS (D) CORNER FAILURE (E) PARTIAL OVERTURNING (F) VERTICAL STRIP OVERTURNING (G) VERTICAL ARCH (H) HORIZONTAL ARCH(RESTREPO-VELEZ AND MAGENES, 2004; AYALA AND SPERANZA, 2003)

### 2.2.3 Diaphragm related Failure

Properly anchored URM walls behaves out-of plane, as they are dynamically excited by floor diaphragms at the ends. The flexibility of diaphragm has considerable impact on the seismic response of URM Walls. The failure of wood diaphragm itself has rarely been observed in previous earthquakes as there are several other mechanisms which dominates the failure of Unreinforced Masonry Walls (URM).

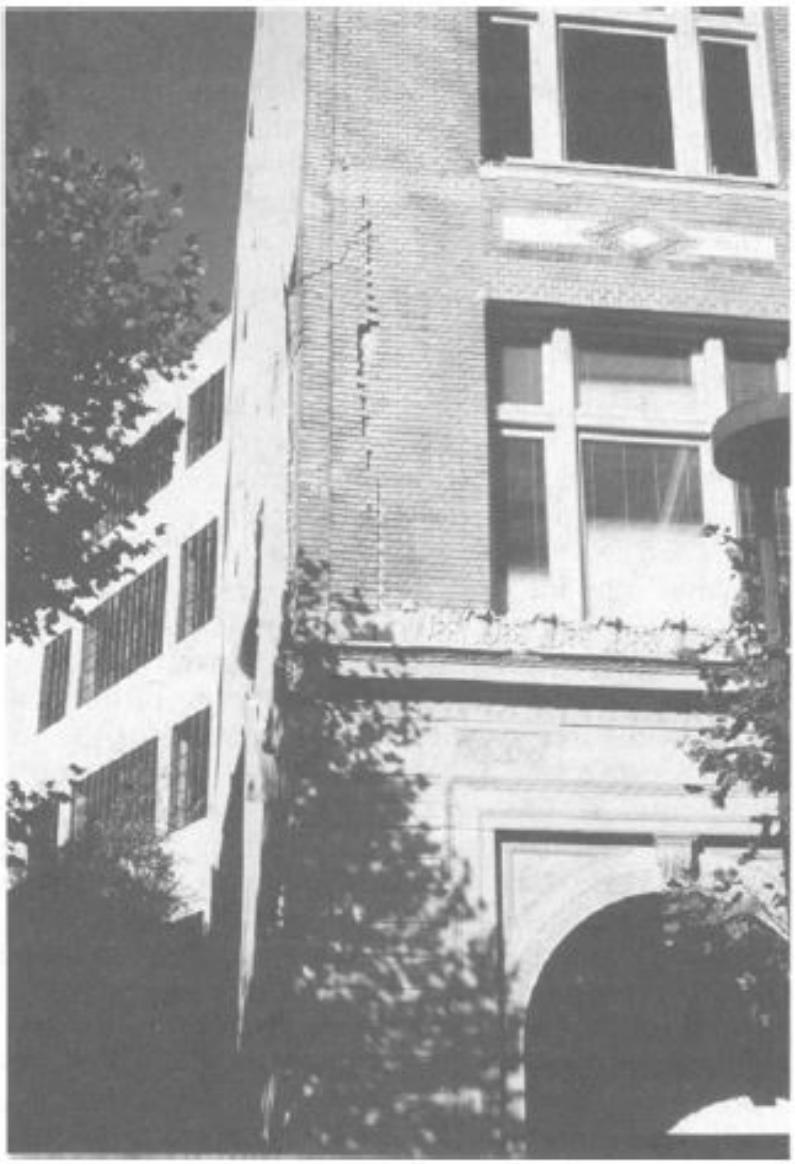

**Fig. 2.7.:** DIAPHRAGM-INDUCED CORNER DAMAGE TO URM PIER (OAKLAND, LOMA PRIETA EARTHQUAKE)

## 2.3 Structural Irregularities

One of the significant factors which affects the seismic performance of URM structures is the structural irregularity on the walls (Parisi, F. and Augenti, N. (2013)). Irregularity can be of different types, which includes misalignment of openings in the vertical and/or horizontal directions, or varying the number of openings per story.

(a)

(b)

(c)

(d)

**Fig. 2.8.:** WALLS MISALIGNED IN (a) VERTICAL MISALIGNMENT (b) HORIZONTAL MISALIGNMENT (c) COMBINED MISALIGNMENT (d) DIFFERENT NUMBER OF OPENINGS

Irregular layout of openings causes non-uniform distribution of loads in the walls but also concentration of seismic strength and drift demands in some parts of the wall. This can lead to unfavourable conditions causing seismic vulnerability of the wall, which was shown by past experimental tests (Yi T, Moon FL, Leon RT, Kahn LF. (2006)). In other words, structural irregularities have a significant effect on the seismic response of the masonry buildings, because on one hand damage is initiated by irregularities, but on the other hand it is the key feature of seismic response.

## 2.4 Timber Diaphragms

The floors which are made of timber in URM buildings typically includes sheathing, joists, and blocks. Observations from the past earthquakes and experimental research on similar typologies has revealed that wood diaphragms behaves in a distinct way that have significant effects on the overall response of the building. Timber floors are usually one-way or two-way oriented, but from the typologies found in Groningen, one-way timber diaphragms are more common.

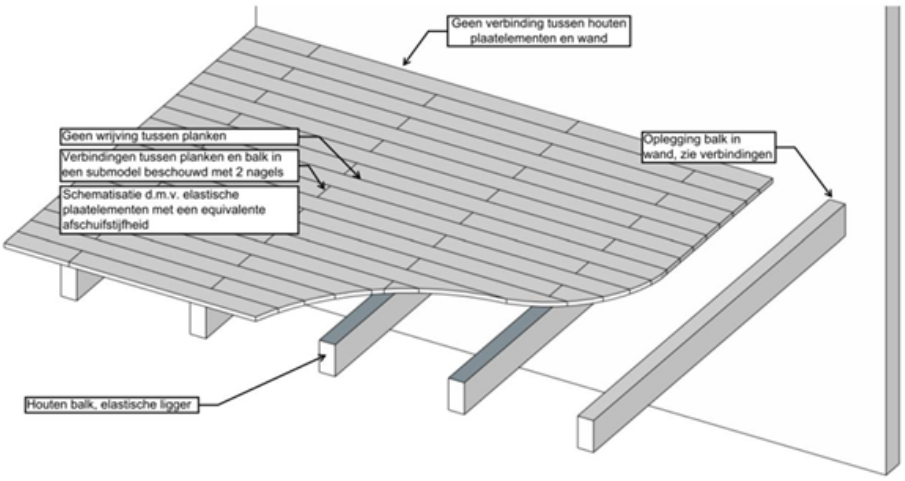


**Fig. 2.9.:** LAYOUT OF ONE-WAY TIMBER FLOORS (BRIGNOLA, PODESTA, AND PAMPANIN, 2008)

The main features which contribute to the flexibility of timber diaphragms are: (a) In-plane Stiffness; and (b) connections. The flexibility of a single sheath $\delta$ can be evaluated with three contributions namely:

- Flexural deformation of single sheath ( $\delta'$ );
- Shear deformation of single sheath ( $\delta''$ );
- Rotation caused by the nail slips ( $\delta'''$ ).

The three contributions mentioned above are expressed by the equation given below (Brignola, Podesta, & Pampanin, 2008):

$$\delta = \delta' + \delta'' + \delta''' = (\frac{F'}{k_{ser}}.\frac{2}{s_n} + \frac{\chi}{GA}.F + \frac{l^2}{12EI}.F).l$$

where:
$\frac{F'}{k_ser}$ - Nail slip from shear force F;
$k_{ser}$ - Nail deformability;
$\chi$ - Shear Factor;
G - Shear Modulus of planks;
E - Flexural Modulus parallel to the grain of the planks;
A - Area of plank section;
I - Moment of Inertia of plank section;
$s_n$ - Nails spacing;

The flexibility of the diaphragm makes it support the out-of-plane wall as a spring support. The failure of wood diaphragm as such is very rare (from previous earthquake observations) as several other failure mechanisms are more dominant which includes inadequate connections between the diaphragm and masonry walls. From previous experimental research it is found that the interaction between timber diaphragms, masonry walls, and the connections between them play an important role on the seismic response of URM houses.

## 2.5 Seismic Analysis

Earthquakes in Groningen are caused due to human activities and they differ from the usual earthquakes which is a sudden slip of tectonic plates. These are induced earthquakes and the seismic assessment of structures subjected to these can be captured by different methods. The analysis are usually classified as Static and Dynamic. However in this report, only certain type of analysis are going to be performed. Nevertheless, a brief description is given about different types of analysis. They are:

- Eigenvalue Analysis
- Response Spectrum Analysis
- Pushover Analysis
- Non-Linear Time History Analysis

### 2.5.1 Eigenvalue Analysis

The most usual step when performing dynamic analysis in a structure is to implement eigenvalue analysis to determine the natural frequencies and mode shapes of the structure. The mode shapes give an indication of how the structure will behave dynamically. And the structure tends to vibrate in its natural frequencies. The aforementioned properties are functions of structural properties and boundary conditions.
The procedure to find the natural frequencies and modes by excluding the damping and external loading is given by:

$$[M][\ddot{u}] + [K][u] = 0$$

The above equation of motion is for un-damped free vibration. This equation after simplifying reduces to:

$$[K]\phi = \omega^2[M]\phi$$

where,
$\phi$ - Mode Shape or Eigenvector
$\omega$ - Circular Natural Frequency
$[K]$ - Stiffness Matrix
$[M]$ - Mass Matrix

### 2.5.2 Response Spectrum Analysis

A linear dynamic analysis where the seismic load is given as a spectrum. It is a very fast method, that takes all the eigen modes into account. As it is a linear analysis there are no failure mechanisms visible.

### 2.5.3 Pushover Analysis

An efficient and reliable method, is a pushover analysis. The lateral forces are distributed over the height of the structure, which is then increased monotonically to push the structure until an ultimate force is reached. The analysis gives key information about the response in terms of story drift, floor displacements, and base shear of the structure. The common outcome of this analysis, is the plotting of a graph between the global base shear and the top displacement $\delta_{top}$ which contains information about storey drift, floor displacements etc.

The load application on the structure can be performed in different ways which defines the type of pushover analysis.

- *Conventional/Monotonic Pushover Analysis*
  An inelastic method, where a constant pattern of monotonically increasing load function is applied throughout the analysis. Generally pushover analysis makes use of small incremental steps which are considered as static and the behaviour in these steps are considered as linear. The load is applied until the target displacement is reached. There are different types of force distribution in the monotonic pushover analysis and this also determines the capacity of the structure.

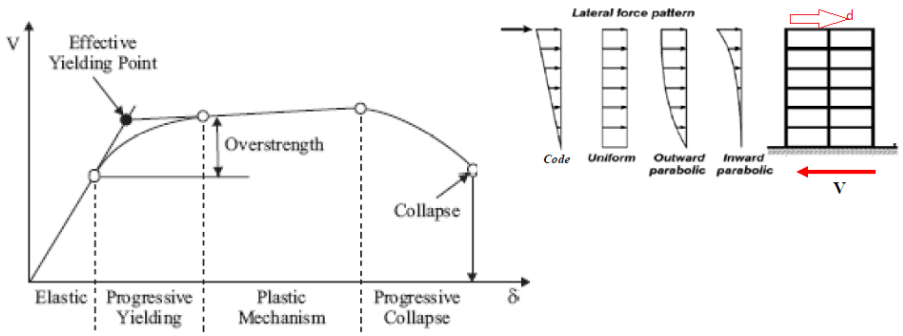


**Fig. 2.10.:** MONOTONIC PUSHOVER ANALYSIS ( UNIVERSITY OF BUFFALO, 2009)

- *Adaptive Pushover Analysis*
  In monotonic pushover, the force pattern is constant throughout the analysis which may not be totally true with the inelastic response of the structure. As a result of which adaptive pushover can be applied where the distribution of inertial forces can be modified. The inertial forces are calculated based on the changing inelastic modal characteristics of the structure. The step sizes are determined by monitoring the total displacement with energy demands (Kalkan and Kunnath, 2007). The final pushover has contribution from each load steps which might have different mode from the initial.

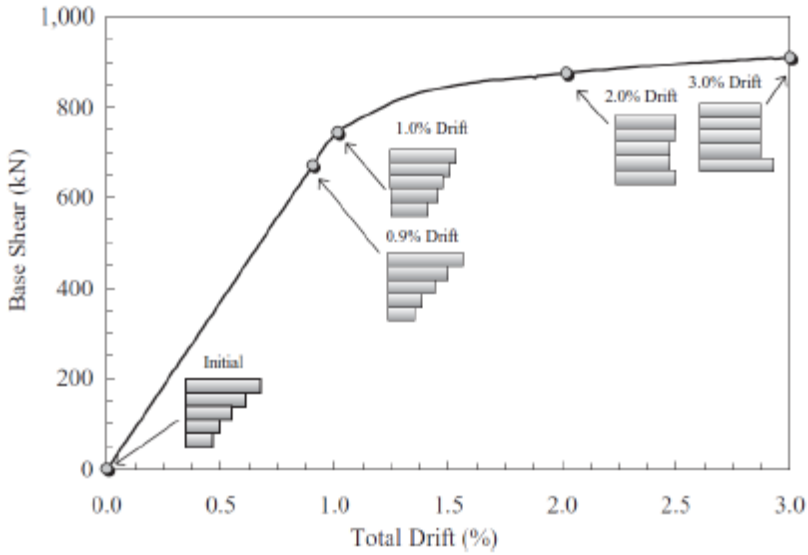


**Fig. 2.11.:** DISTRIBUTION OF INERTIAL FORCES (ADAPTIVE FORCE DISTRIBUTION)( ANTONIOU (2002))

– *Cyclic Pushover Analysis*
The cyclic nature of earthquake loads has a major influence on the structure's behaviour. So the load in positive and negative directions causes the cracks to open, close and re-open. In this analysis each pushover load cases uses the stiffness that is obtained from the end of the previous load step. And with this step it is easy to determine the characteristic hysteric loop as shown in the Figure 2.12. The highlighted area in green, shows the energy dissipated in one cycle.

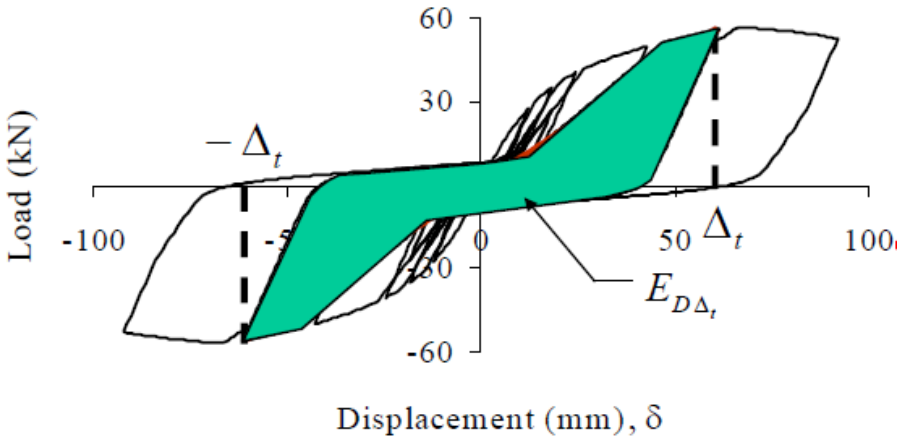


**Fig. 2.12.:** CYCLIC PUSHOVER ANALYSIS ( UNIVERSITY OF BUFFALO, 2009)

According to Eurocode, pushover analysis is a non-linear static analysis performed under constant gravitational loads and monotonically increasing horizontal loads. For masonry structures, capacity is defined in terms of roof displacement. So in this research flexible diaphragms in unreinforced masonry structure are taken in consideration.

### 2.5.4 Non-Linear Time History Analysis

In time history analysis; the seismic action is considered as a time history, a function of acceleration and time applied as a base excitation. The time histories have complete information about the seismic event in a certain location and record three traces. The main advantage with time history analysis is that it takes all modes into account for a single calculation. And possible failure mechanisms are shown for every signal. Even though it is considered as one of the highly sophisticated method, it has its own disadvantages. It is time consuming and the pre-requisite knowledge of signal is required. In this research this analysis procedure is not taken into account.

## 2.6 Assessment of Structures

The key parameters to assess the seismic performance of the structures are ductility factor, force reduction factor, drift limits and target displacement. A small description about drift limits and target displacements will be enumerated.

### 2.6.1 Drift Limits

The maximum inter-story drift, and drift demand are the key factors in performance-based design. The inter-story drifts can give information about distribution of ductility. According to the Eurocode there are specific drift demands for a particular type of limit state which is listed down in the table below:

**Tab. 2.1.:** Drift Limits according to Eurocode, (EN 1998-3, 2005)

| State | Shear(normal force) | Bending(Flexure) |
|---|---|---|
| Limit State of Significant Damage(SD) | $0.004(\frac{H_0}{D})$ | $0.008(\frac{H_0}{D})$ |
| Limit State of Near Collapse(NC) | $0.0053(\frac{H_0}{D})$ | $0.0106(\frac{H_0}{D})$ |

Where:
D - In-plane horizontal dimension of the wall(depth) ;
$H_0$ - Distance between the section where the flexural capacity is attained and the contra flexure point

### 2.6.2 Target Displacement

Pushover curves have become a key tool when it comes to assessment of the seismic performance of buildings. From Performance based Design, for each limit state of interest seismic demand should be estimated. In order to predict the accurate performance, we should take into account the non-linear response of the structure. Based on the above description there are different methods to assess the seismic demand. These methods are given below:

- *Coefficient Method (ASCE-41)*
  In this method, non-linear static procedure is implemented. The target displacement is given by the following equation:

$$\delta_t = C_0.C_1.C_2.S_a.\frac{{T_e}^2}{4\pi^2}.g$$

Where:
$C_0$ – Modification factor that relates to the roof displacement of Multi Degree of Freedom system (MDOF) to an equivalent Single Degree of Freedom System(SDOF);
$C_1$ – Modification factor to relate expected maximum inelastic displacements for linear elastic response;
$C_2$ – Modification factor that takes into account stiffness degradation, pinched hysteric shape, and strength deterioration;
$S_a$ – Response Spectrum Acceleration;
$T_e$ – Effective fundamental period of the structure;
$g$ – Acceleration of gravity.

– *Capacity Spectrum Method (ATC-40)*
In this method a procedure is followed in which a graph is plotted based on expected seismic response of the structure. The demand is expressed by the intersection of the curves i.e. capacity spectrum and response spectrum. The point where it intersects is known as the performance point which indicates strength and displacement of the structure. It consists of four steps to arrive at the performance points : (1) Plotting a pushover curve; (2) Conversion of pushover to capacity spectrum; (3) Conversion of elastic response form standard to A-D format; (4) Displacement Demand. These steps are illustrated in the Figure 2.13.

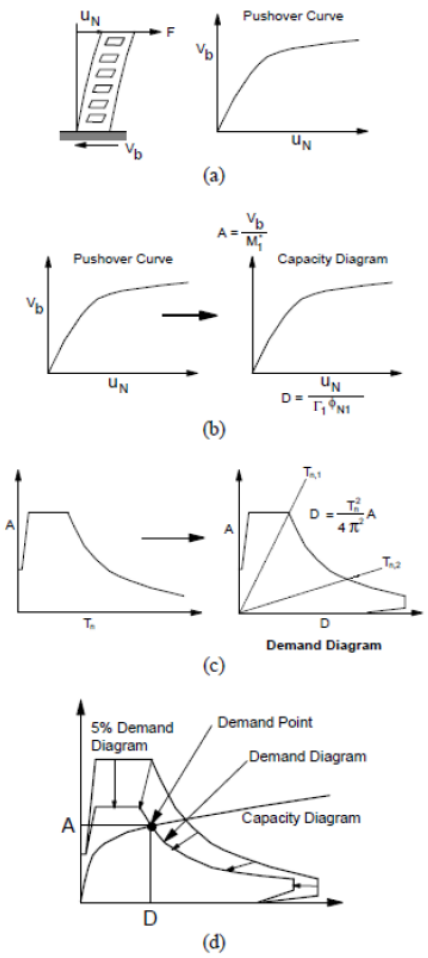


**Fig. 2.13.:** CAPACITY SPECTRUM METHOD ( CHOPRA AND GOEL, 1999)

– *N2 Method (Eurocode-8)*
Another method which is presented in the Eurocode is N2 Method. The capacity curve is based on the bilinear relationship (Allen, Masia, Derakshan, Griffith, Dizhur, and Ingham, 2013) which considers an yield force $H_u = 0.9.H_{max}$ as an approximation to the equal energy method for URM and $H_{cr} = 0.75.H_u$. The approach in the Eurocode 8 is based on actual deformation energy until the plastic mechanism. The method involves

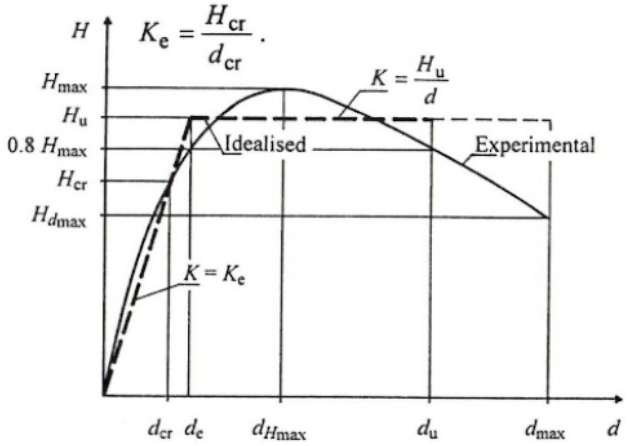


**Fig. 2.14.:** BILINEAR APPROXIMATION OF FORCE DISPLACEMENT CURVE ( ALLEN, MASIA, DERAKSHAN, GRIFFITH, DIZHUR AND INGHAM,2013)

the following steps:

– Step 1: Transformation to equivalent SDOF system;
*Mass of equivalent SDOF*

$$m^* = \sum m_i.\phi_i$$

where:
$m_i$ – Mass in the $i^{th}$ storey;
$\phi_i$ – Normalized displacements.
*Transformation Factor*

$$\Gamma = \frac{m^*}{\sum m_i \phi_i^2}$$

*Force of SDOF System*

$$F^* = \frac{F_b}{\Gamma}$$

where:
$F_b$– Base Shear Force.
*Displacement of SDOF System*

$$d^* = \frac{d_n}{\Gamma}$$

where;
$d_n$– Control node displacement of SDOF.

– Step 2: Determination of idealized elasto-perfectly plastic force-displacement relationship;
– Step 3: Determination of period of the idealized equivalent SDOF system;

$$T^* = 2.\pi.\sqrt{\frac{m^* d_y^*}{F_y^*}}$$

where;
$F_y^*$– Yield Force.
$d_y^*$– Yield Displacement.

– Step 4: Determination of target displacement of equivalent SDOF system;

$$d_{et}^* = S_e(T^*)[\frac{T^*}{2\pi}]^2$$

For $T^* \geq T_c$ (medium and long range);

$$d_t^* = d_{et}^* = S_e(T^*)[\frac{T^*}{2\pi}]^2$$

For $T^* < T_c$ (short range);
if $\frac{F_y^*}{m} \geq S_e(T^*)$,

$$d_t^* = d_{et}^*$$

if $\frac{F_y^*}{m} \leq S_e(T^*)$,

$$d_t^* = \frac{d_{et}^*}{q_u}(1 + (q_u - 1) * (\frac{T_c}{T^*})) \geq d_{et}^*$$

where;
$q_u = \frac{S_e(T^*)m^*}{F_y^*}$
$d_{et}^*$ – Target Displacement of structure with period $T^*$.
$S_e(T^*)$ – Elastic acceleration response spectrum.

– Step 5: Determination of target displacement of equivalent MDOF system;

$$d_t = \Gamma.d_t^*$$

# 3 Modelling Parameters and Assumptions

The development of URM terraced houses in DianaIE involves many user defined parameters. A python script is written based on these user-defined parameters, which can be used to generate automatically a wide variety of terraced houses by defining the parameters. This parametrized script has made the modelling easy during the later stages when geometrical irregularities are taken into account. The basic choices which were adopted in the finite element modelling are presented below:

**Tab. 3.1.:** Model Choices

| Analysis Elements | Choices Adopted |
|---|---|
| Geometry | 2-D Curved Shell Elements |
| Modelling | Macro Modelling |
| Supports | Fixed |

A case study has been taken to implement the parametrised python script. In this model, fixed supports were adopted and foundation and soil-structure interaction is not taken into account to simplify the model. This is adopted as the research mainly focuses on the geometrical variations of the super-structure. A detailed approach would be to include the foundation along with the soil-structure interaction. The choice of opting for a macro model was to make the modelling simplified.
In the following sections, the properties and choices that were made in implementing the python script on the case study are elaborated in detail.

## 3.1 Schematization of the Case Study

The finite element is adopted by just modelling the inner leaf for cavity walls; and the centre of inner leaf is considered here. The outer leaf is modelled as a translational mass element, as it contributes only as an additional mass for the whole structure and not as a structural element by itself. The partition/interior walls are modelled with curved shell elements, that are located in the mid-surface of wall. The floors are modelled by taking the top part of the timber sheets into consideration and the ground floor has been excluded from the model for simplification to reduce the number of elements. And adding to this, the foundation and soil block are not modelled, so the support at bottom is fixed.

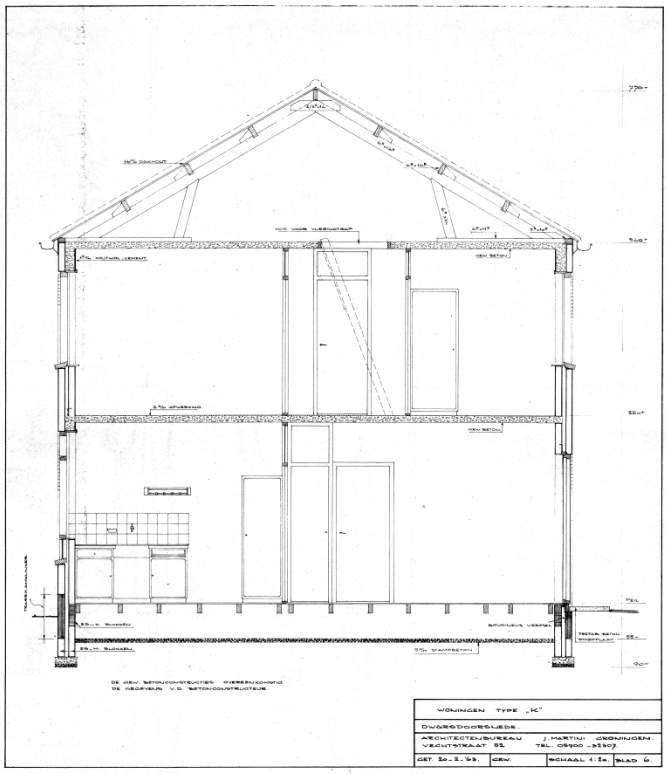

Fig. 3.1.: SECTION VIEW OF CASE STUDY

## 3.2 Finite Element Model

To obtain a realistic crack pattern (related to brick-joints) in the non-linear behaviour of masonry elements, the dimensions of bricks are taken into account. As a result, the size of masonry elements are assigned as 0.2 m. The mesh size for the timber diaphragms, roof and beams is set based on the user defined parameter for beam spacing in the floors. This is done so as to avoid the local modes in an eigenvalue analysis, and also to reduce the total number of elements.

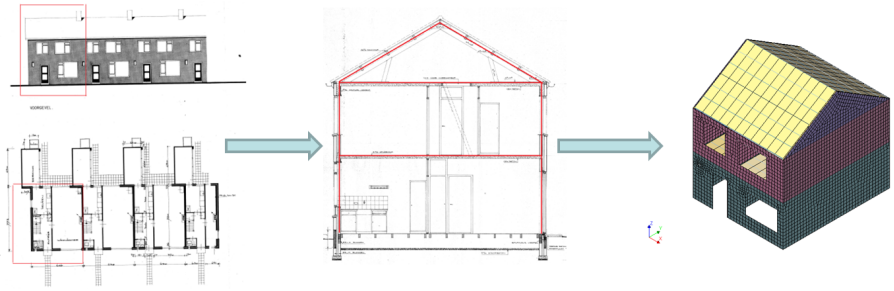

Fig. 3.2.: SCHEMATIZATION OF CASE STUDY

The generated mesh had some irregularities around the openings, and no mesh refinement has been done as parametrizing the mesh refinement for example around the openings is a cumbersome process, and it does not come under the scope of this research. But attention has been given with respect to meshing of the timber floors, so as to avoid eccentricities with the timber beams.

## 3.3 Masonry Walls

Masonry walls that are taken into consideration in the case study are cavity (exterior) walls and solid (interior) walls. The cavity walls consist of two parts: an inner load bearing wall and an outer non bearing wall. They are usually connected together by anchors made of steel ties. The configuration is shown below in the Figure 3.3. In this case study, the inner leaf is modelled as a structural element and the outer leaf is added as translational mass to take into account dynamic effects. The interior walls are solid and of thickness 120mm. The modelling of inner leaf, interior walls, and translational mass are show in the Figure 3.5 and 3.6.

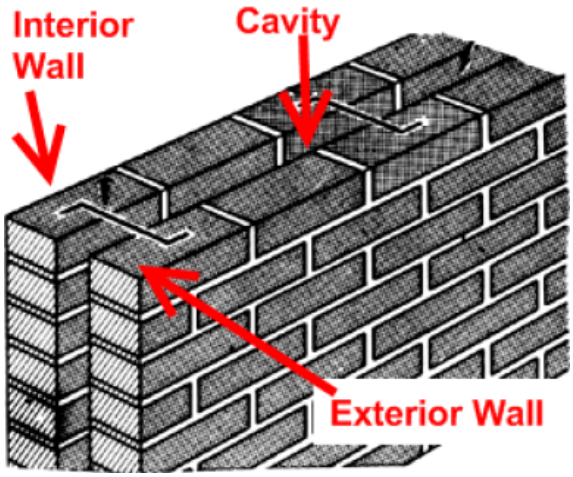


**Fig. 3.3.:** AS BUILT EXTERIOR MASONRY WALLS

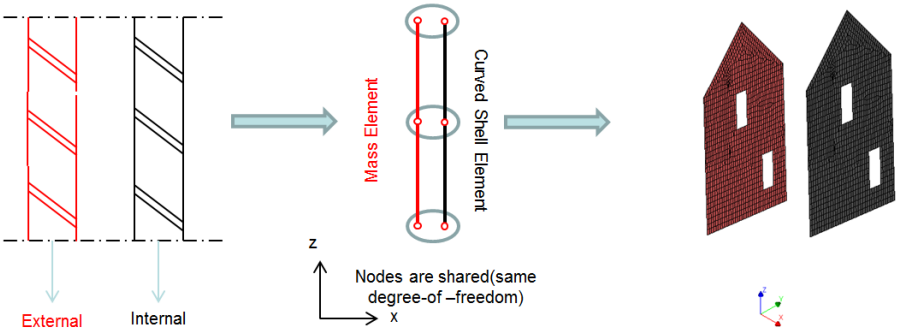


**Fig. 3.4.:** CAVITY WALLS (SCHEMATIZATION)

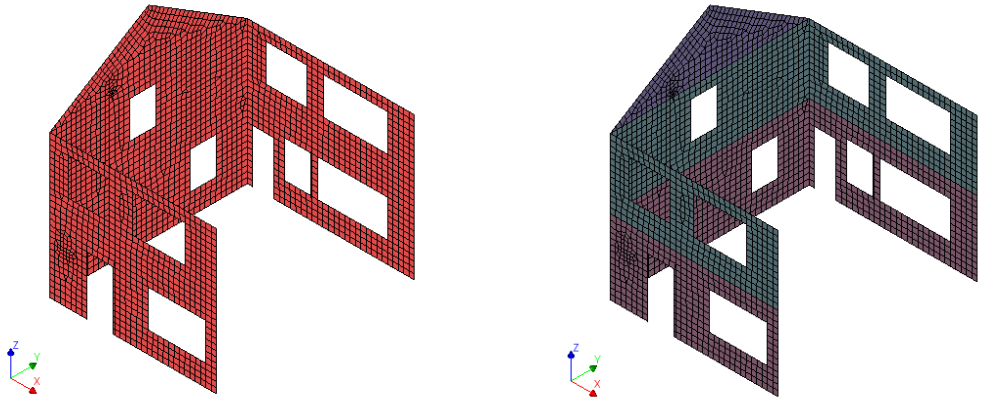

(a) EXTERNAL LEAF (TRANSLATIONAL MASS)
ELE- Q12TM AND T9TM

(b) INTERNAL LEAF (CURVED SHELL)
ELE- Q20SH AND T15SH

**Fig. 3.5.:** MODELLING OF CAVITY WALLS

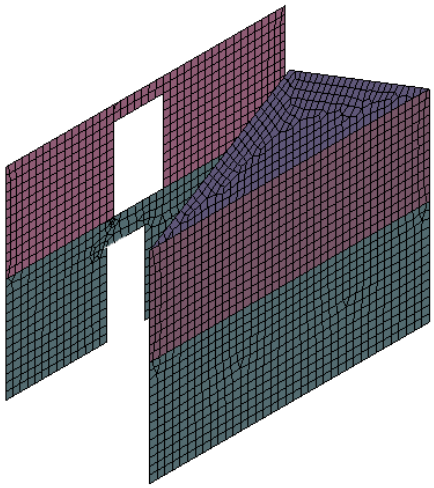

**Fig. 3.6.:** MODELLING OF INTERIOR WALLS

## 3.4 Timber Beams

In the case study, timber beams are connected between the interior and exterior walls. The as built configuration of timber beams are shown in the Figure 3.7. Timber beams are allowed to slide in the horizontal direction, and are restricted in the other two directions; but they are free to rotate in all directions.

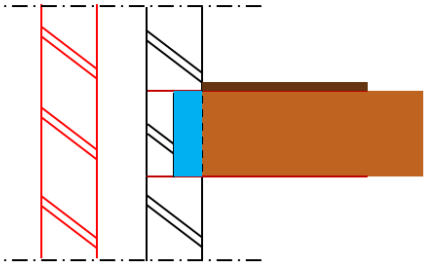

(a) BEAMS TO EXTERIOR WALLS (INNER LEAF)

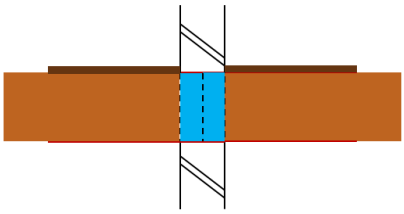

(b) BEAM TO INTERIOR WALL

Fig. 3.7.: CONNECTION OF TIMBER BEAMS TO WALLS

The schematization of the above shown configuration is done by modelling a physical gap between the beams and the walls. And these gaps are then filled by spring elements. The modelling implementation in DianaIE is shown below:

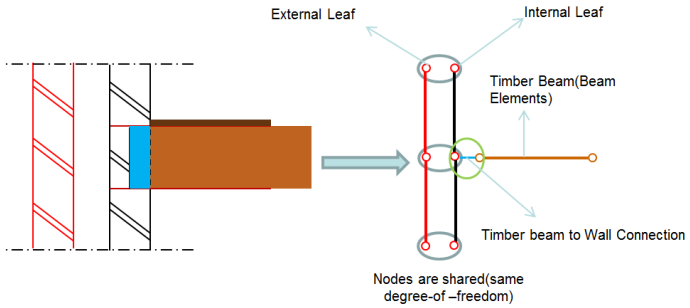


(a) SCHEMATIZATION OF TIMBER BEAM-EXTERIOR WALLS

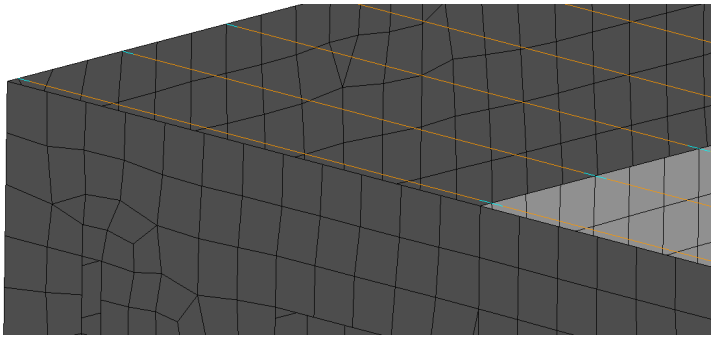

(b) CLOSE-UP VIEW OF BEAM-EXTERIOR WALL CONNECTION(FIRST-FLOOR)

Fig. 3.8.: CONNECTION OF TIMBER BEAMS TO EXTERIOR WALLS

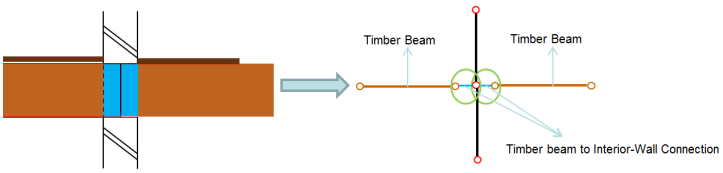


(a) SCHEMATIZATION OF TIMBER BEAM-INTERIOR WALLS

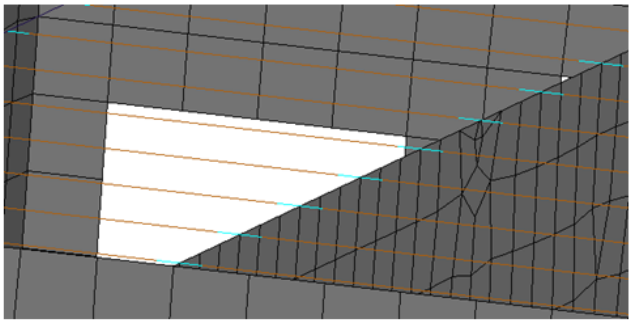

(b) CLOSE-UP VIEW OF BEAM-INTERIOR WALL CONNECTION(FIRST-FLOOR)

**Fig. 3.9.:** CONNECTION OF TIMBER BEAMS TO INTERIOR WALLS

The model which is depicted using springs for connections of the beams to walls, is given an initial stiffness. And the characteristics are based on the linear spring (Diana 10.1 Documentation,2016) which means that the stiffness of the springs remains linear throughout the analysis. A more sophisticated way would be to use the spring based on ultimate forces, as it takes the non-linear behaviour into consideration.
The connection between roof beams are similar to the timber beams. But the dimensions of roof and ridge beams are different and they are taken into account in the modelling. Springs that are used for the roof beams are same as to for ridge beams, with respect to the properties. Further investigation is required in this case, to see if the capacity of floor and roof beams are the same. The investigation can be on the modelling of timber floors and beams by taking into account the effect of friction between them, as in the current model they both share same nodes and degrees of freedom. Another interesting thing to investigate would be the non-linear behaviour of the floors.

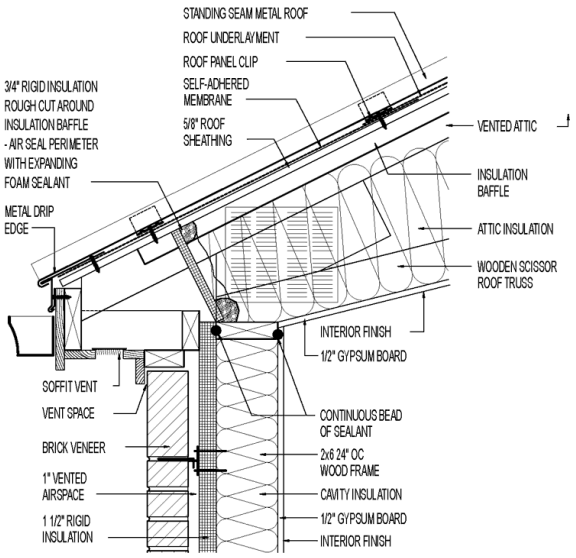


**Fig. 3.10.:** SECTION VIEW OF AS BUILT ROOF

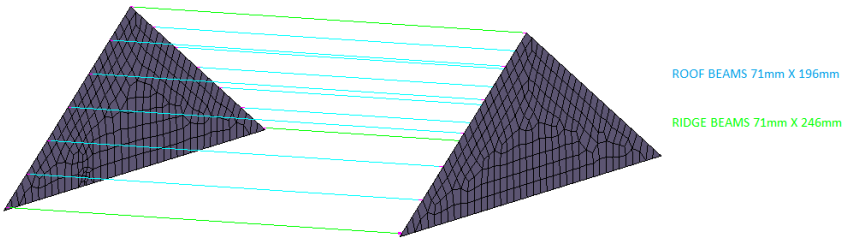


**Fig. 3.11.:** MODELLING OF CONNECTIONS BETWEEN ROOF BEAMS AND MASONRY WALLS

## 3.5 Timber Floors

From the as built configuration shown in timber beams, the floors are just placed on the timber beams (share the same node) and are not connected with the masonry walls. They are connected to the beams by nails, so in reality there will be shear developing between the floor and beam. The floors are schematized by assuming that only the top plank of the floor will play in the structural role (thickness of 22mm), and they are just merged in the finite element model with the timber beams, and the friction effect is not taken into account. The opening of the staircase is taken into account and the openings are covered by stair beams.

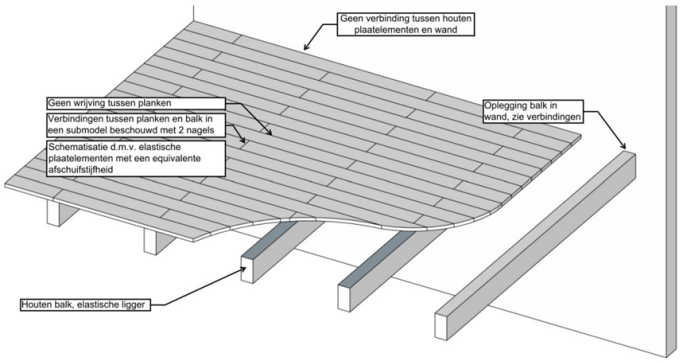


**Fig. 3.12.:** AS BUILT TIMBER FLOORS

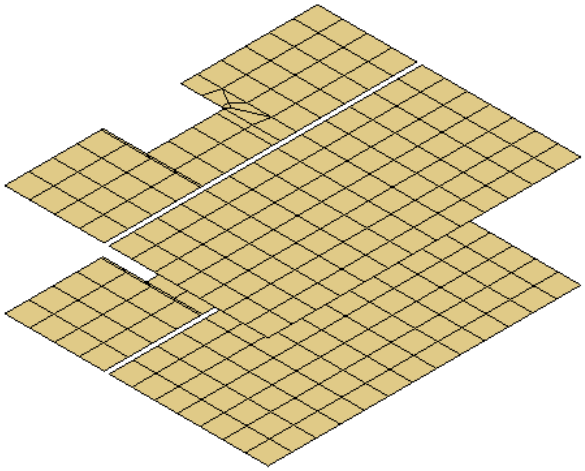

**Fig. 3.13.:** MODELLING OF TIMBER FLOORS

## 3.6 Timber Roofs

In reality, the timber roofs are placed over the ridge beam on the front and back façade, this will result in a development of friction between the roof and wall. It is schematized in such a way that roofs are not connected to the front and back façade. They are just placed over the roof beams.

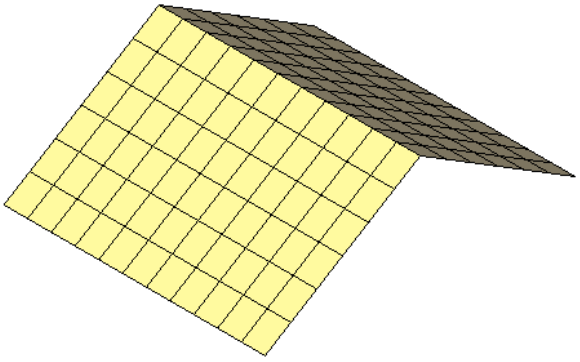

Fig. 3.14.: MODELLING OF TIMBER ROOFS

## 3.7 Lintel Beams

The typical Dutch terraced type houses have lintel beams placed above the openings. But there are different types of design of lintel beams that has been reported. But for the case study, only concrete straight lintel beams are taken into account. The as built configuration is shown below:


Fig. 3.15.: AS BUILT CONFIGURATION OF LINTEL BEAMS

The modelling is done by schematizing the lintel into a beam element, and they share nodes with masonry elements. As they share nodes with the masonry elements, they have a rigid connection and the fact that a slip between the masonry elements and concrete lintel beams is not considered here.

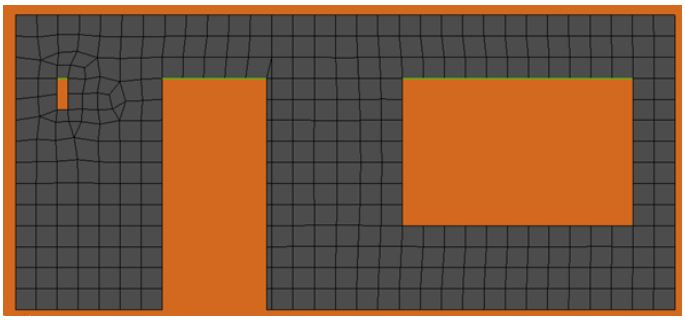

**Fig. 3.16.:** MODELLING OF LINTEL BEAMS

## 3.8 Boundary Conditions

A brief overview is given in this section on choosing certain boundary conditions and the reason behind that assumption.

### 3.8.1 BC at the Base

The ground floor is not included in the model, so as to reduce the number of elements. As the scope of this research is mainly focused on the super-structure, the foundation and soil block are left out of the model. As a result of which, the base is considered as fixed; only one point is given the support condition and rest of the nodes are tied to it. For further investigations and more realistic approach, the foundation and soil-block can be taken into account.

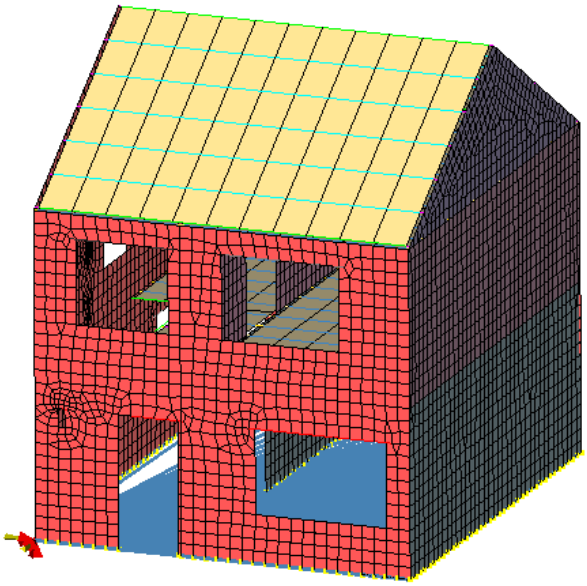

**Fig. 3.17.:** SUPPORT CONDITION AT BASE (TYINGS INCLUDED)

### 3.8.2 Tyings

To mimic the real behaviour, the springs are having a stiffness only in the X-direction, but are tied in the Y and Z-directions. In reality the beams can slide in X-direction and their movement is restricted in the other directions, but are free to rotate in all three directions. The schematization for implementing the above stated conditions is shown below:

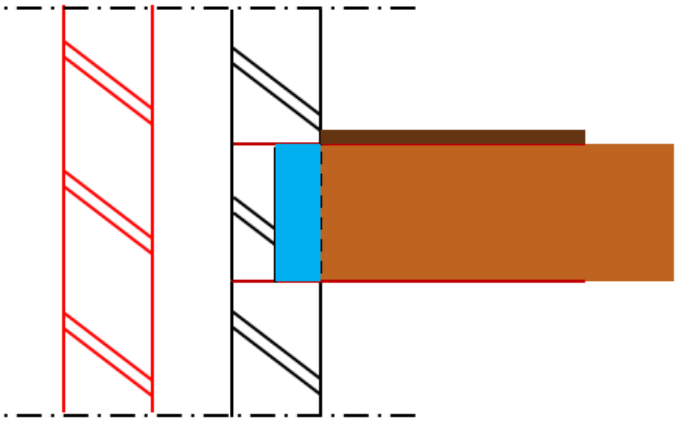

(a) BEAMS TO EXTERIOR WALLS (INNER LEAF)

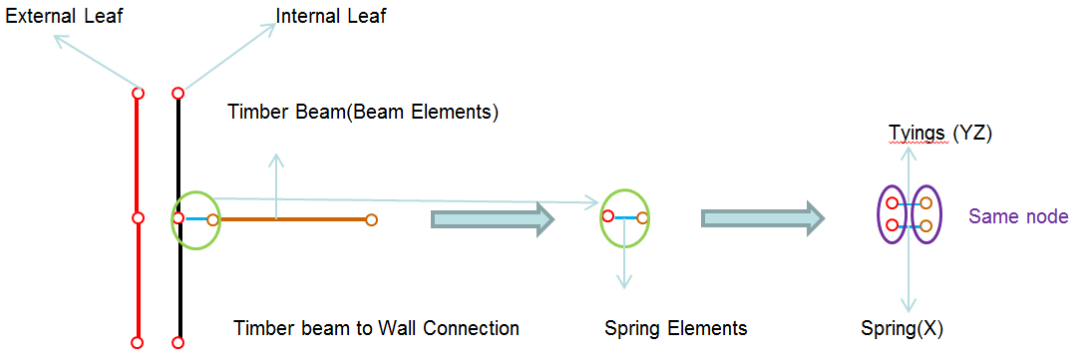


(b) BOUNDARY CONDITIONS-TIMBER BEAMS

**Fig. 3.18.:** MODELLING OF TYINGS

## 3.9 Material Properties

The building consists of different materials. So in this section, material properties of the materials used and the reason behind choosing a certain material model has been explained.

### 3.9.1 Masonry

As suggested before a macro modelling approach is followed and engineering masonry model has been adopted. The main reason behind choosing this model over the existing total strain crack model is because in the later, the model is considered isotropic and no distinguish between shear and tensile cracks (Diana Development Documentation, 2016). For this engineering masonry model was preferred. The material properties that are taken into account are presented in the table.

**Tab. 3.2.:** Masonry Material Properties

| ***Property*** | ***Directions*** | ***Value*** | ***Unit*** |
|---|---|---|---|
| Young's Modulus | $E_x$ | 3600 | $N/mm^2$ |
| | $E_y$ | 5200 | $N/mm^2$ |
| Shear Modulus | $G_{xy}$ | 1500 | $N/mm^2$ |
| Mass Density | $\rho$ | 2000 | $kg/m^3$ |
| Tensile Strength | ele - x direction | 0.21 | $N/mm^2$ |
| | ele - y direction | 0.13 | $N/mm^2$ |
| Fracture Energy(Tension) | $G_{fx}$ | 0.015 | $N/mm$ |
| | $G_{fy}$ | 0.005 | $N/mm$ |
| Compressive Strength | ele - x direction | 7.5 | $N/mm^2$ |
| | ele - y direction | 6 | $N/mm^2$ |
| Fracture Energy(Compression) | $G_{cx}$ | 43.4 | $N/mm$ |
| | $G_{cy}$ | 31.3 | $N/mm$ |
| Factor to Strain (Compressive Strength) | ele - x direction | 4 | |
| | ele - y direction | 4 | |
| Friction Angle | $\phi$ | 23.2678 | degree |
| Cohesion | C | 0.14 | $N/mm^2$ |
| Fracture Energy in Shear | | 0.02 | $N/mm$ |

### 3.9.2 Timber Elements

Timber elements show an orthotropic behaviour which has been taken into account in this case. The timber material properties are applied both for the floors and roofs and are given in the table.

**Tab. 3.3.:** Timber Material Properties (Floors and Roof)

| ***Property*** | ***Directions*** | ***Value*** | ***Unit*** |
|---|---|---|---|
| Young's Modulus | $E_x = E_y = E_z$ | 3600 | $N/mm^2$ |
| Poisson's Ratio | $\nu_{xy} = \nu_{yz} = \nu_{zx}$ | 0.3 | |
| Shear Modulus | $G$ | 4.3 | $N/mm^2$ |
| Mass Density | $\rho$ | 4200 | $kg/m^3$ |

The only modification with properties for timber roofs is the mass density which is given a value of $6000kg/m^3$. The timber beams which are placed below the timber roofs and floors, have been assigned linear properties and are shown in the table.

**Tab. 3.4.:** Timber Material Properties(Beams)

| ***Property*** | ***Directions*** | ***Value*** | ***Unit*** |
|---|---|---|---|
| Young's Modulus | $E$ | 9000 | $N/mm^2$ |
| Poisson's Ratio | $\nu$ | 0.3 | |
| Mass Density | $\rho$ | 600 | $kg/m^3$ |

### 3.9.3 Concrete Elements

The openings are placed with concrete lintel beams in the case study, so we are going to apply linear elastic properties for the concrete as the main interest in this research is about the non-linear behaviour of masonry elements. The properties are given in the table.

**Tab. 3.5.:** Concrete Material Properties (Lintels)

| ***Property*** | ***Directions*** | ***Value*** | ***Unit*** |
|---|---|---|---|
| Young's Modulus | $E$ | 15000 | $N/mm^2$ |
| Poisson's Ratio | $\nu$ | 0.15 | |
| Mass Density | $\rho$ | 2500 | $kg/m^3$ |

# Case Study Interpretation

# 4

The parametrized script can be used to generate different types of buildings. But before varying the geometrical characteristics and performing various types of analysis, a case study from the already constructed terraced house has been taken and analysis are carried out. In this chapter, the results obtained from the analyses are discussed.

## 4.1 Eigenvalue Analysis

An Eigenvalue analysis is always an initial point in the analysis as it helps to understand the characteristics of the modelled structure due to free vibration and not due to any particular loading condition. During an Eigenvalue analysis the mass of the structure is considered as potential energy and the frequency obtained from the response is considered as the natural frequency when maximum energy is absorbed by deformation. In this case study, the first mode shape is related to the sway mode of masonry walls in X-direction. With higher modes we could also see the out-of-plane deformation on the front and back façades. The different mode shapes that are of interest are shown in the Figure 4.1.

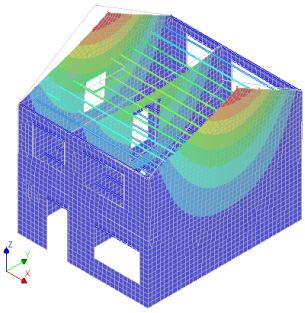

**(a)** Mode 1: $f_1 = 1.8478$

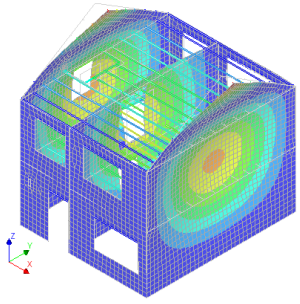

**(b)** Mode 6: $f_6 = 3.7411$

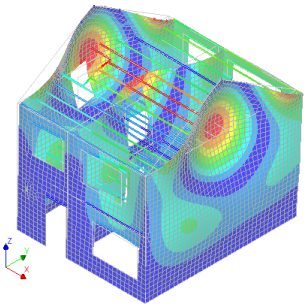

**(c)** Mode 15: $f_{15} = 8.2717$

**Fig. 4.1.:** MODE SHAPES OF THE BUILDING

From the observed mode shapes(1-15) it is found that $60\%$ of cumulative mass participation of the system is achieved. And from the figure presented the highest participating factor was found out to be in X-direction. These eigen modes are used in the Modal Pushover Analysis (MPO) to apply the loads in correspondence to a particular mode shape.

## 4.2 Monotonic Pushover Analysis

The Monotonic Pushover Analysis (MPOA) is a non-linear quasi-static analysis performed to analyse the seismic capacity of a structure. The results of the case study are a starting point for the variation studies, which is elaborated in the forthcoming chapter. Scope here is to assess the overall behaviour of the structure. Henceforth, importance is given to the base shear force that the structure can take and the failure mechanisms associated with it. In this section, a brief description is given about the loads that are applied on the structure, and outcomes are presented.

### 4.2.1 Loading Conditions

The loads that have been applied on the structure includes self-weight; which was done through phased analysis, followed by the application of pushover load in the form of horizontal equivalent acceleration (EQUIAC).

Self-weight was applied by means of phased analysis, so as to make the application of dead load in a more realistic way. Another reason is that, when self-weight is applied as a normal load, there are cracks present in the wall. The phased analysis comprises of three phases:

1 Ground Floor Components.
2 First Floor Components.
3 Roof/Attic Components.

In the first phase, self-weight is added by using start steps. The initial stress was activated by calculating the linear elastic field, as it calculates the stress developed in the active elements by linear elastic analysis. The remove-out-of-balance, was also adopted in the start steps so as to remove the out of balance force in the model. Only in the first phase; an additional load was activated, so as to specify the right-hand side loads (counter balance forces). Adding to this, physical non-linear criteria was added to suppress the displacements due to self-weight, but the elements will still contain the stress, strain and the plastic fields. The most important thing to keep in mind when it comes to phased analysis, the elements that are active in the corresponding phase are the one susceptible to modifications. Application of the above mentioned phased analysis is depicted in the following Figure 4.2.

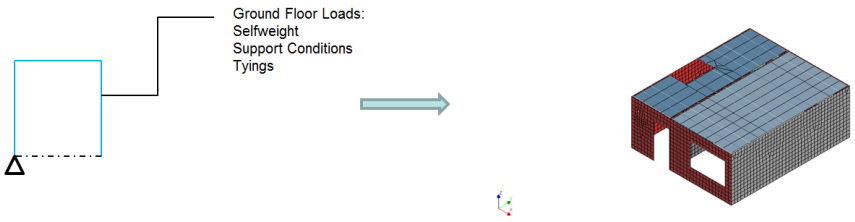


(a) PHASE-I (GROUND FLOOR)

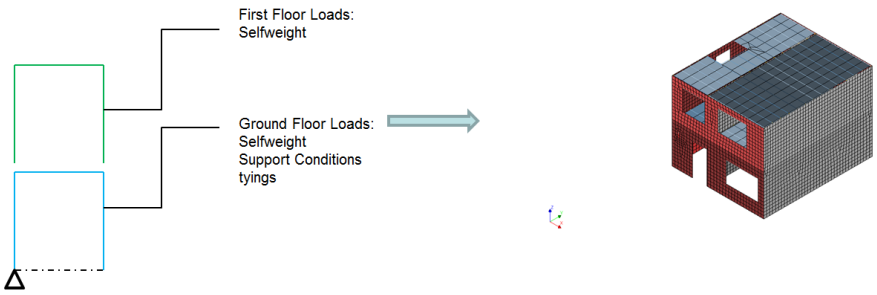


(b) PHASE-II (GROUND, AND FIRST FLOOR)

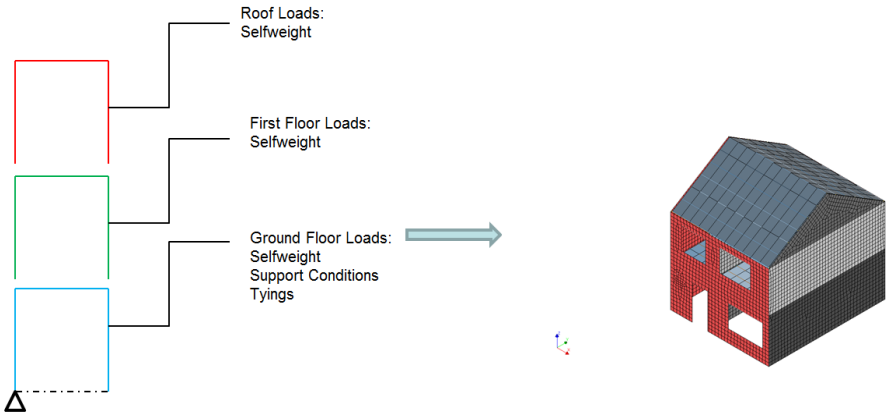


(c) PHASE-III (GROUND, FIRST AND ATTIC FLOOR)

**Fig. 4.2.:** APPLICATION OF SELF-WEIGHT (THROUGH PHASED ANALYSIS)

### 4.2.2 Analysis Results

In this paragraph, the results of pushover analysis performed for the case study are discussed in detail. In-Plane failure of front and back walls are observed. The cracks are concentrated in the back walls as it has more number and wider openings than the front walls. Crack-widths of collapse load are shown in the Figure 4.3 along with failure mechanisms which are highlighted.

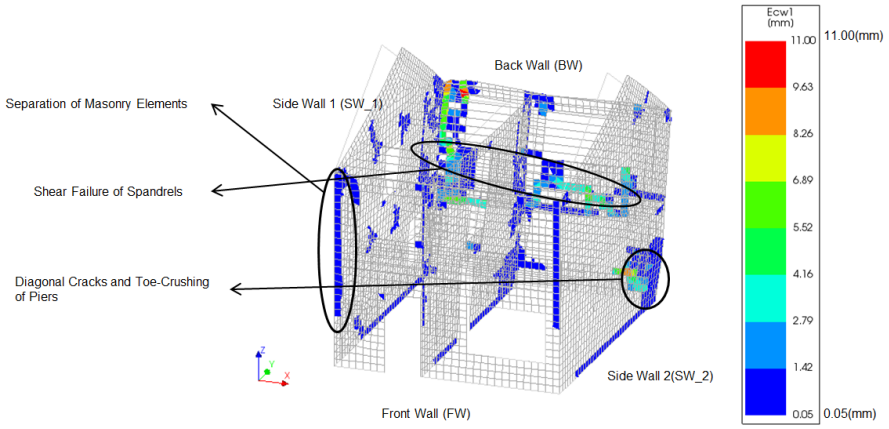


(a) FAILURE MODES

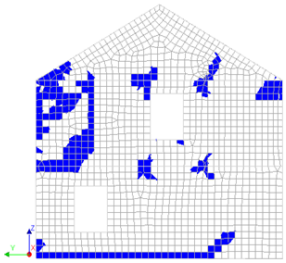

(b) SIDE WALL 1

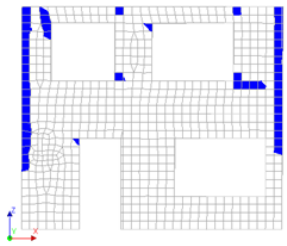

(c) FRONT WALL

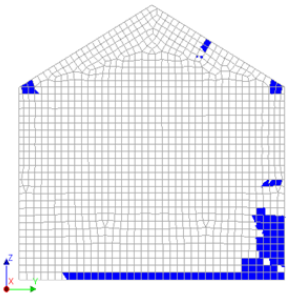

(d) SIDE WALL 2

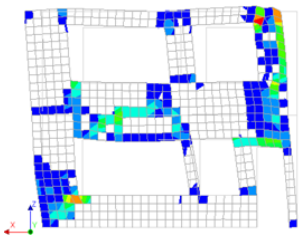

(e) BACK WALL

**Fig. 4.3.:** CRACK WIDTHS AND IDENTIFIED FAILURE MODES

The EQUIAC loads were applied in load steps of 0.002(35)(g) and then modified to smaller load steps 0.001(200)(g). Geometrical non-linearity is activated. Force convergence norm was applied, and the maximum load of the structure was obtained without any divergence. Furthermore, to see the post peak behaviour of the structure arc-length method was adopted in order to deal with local and global softening. The graphs are plotted between the base shear force (at the bottom support) and the top node displacement (located in the roof ( Figure 4.5)). The nodes at the bottom are tied to one point, so that it is easy to obtain the sum of base shear forces at one point (support). The critical parts of the pushover curve are illustrated in the following graph 4.6.

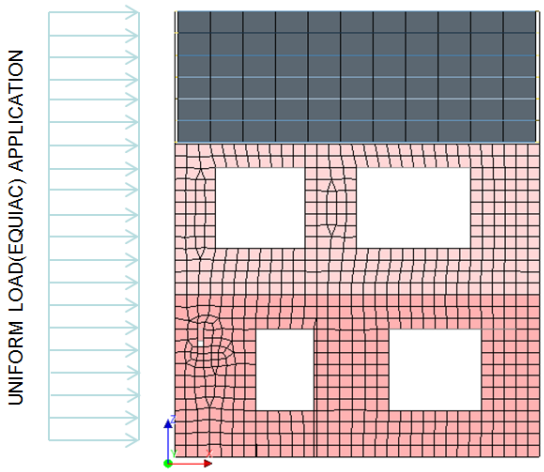


**Fig. 4.4.:** APPLICATION OF LOAD

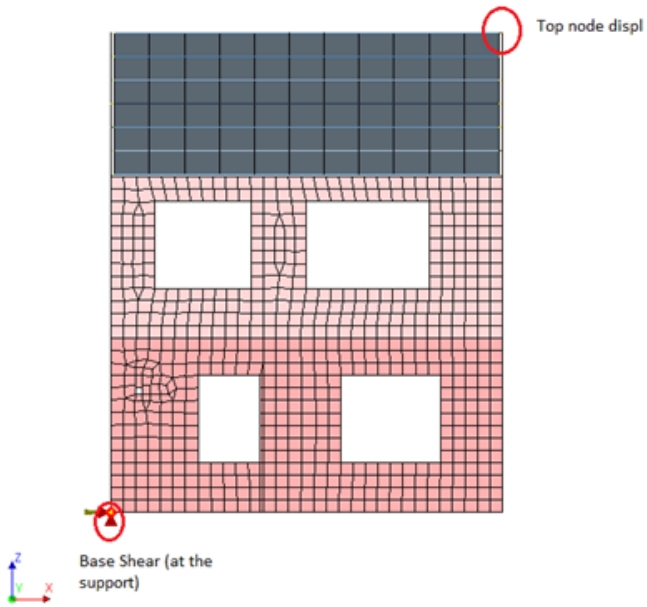


**Fig. 4.5.:** POSITION OF PLOTTED BASE SHEAR AND DISPLACEMENT

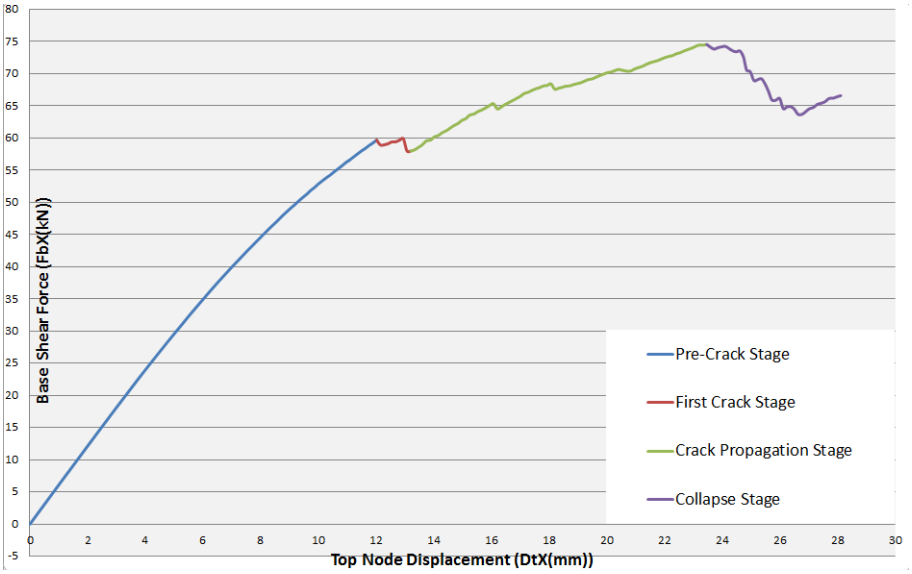


**Fig. 4.6.:** SHEAR-DRIFT CURVES OF THE CASE STUDY

The different stages of the building are depicted in the graph and are disaggregated into:

1. Pre-Crack Stage
2. First Crack Stage
3. Crack Propagation Stage
4. Collapse Stage

The stages are discussed in the order mentioned above in the subsequent sections. The main focus in here is to display the location of the cracks at different stages, and their corresponding widths.

### Pre-Crack Stage

The first step is the application of the gravity loads, which as explained before is done through phased analysis. The first stage is characterized by the shear-drift, which is increasing almost in a linear path. The formation of initial cracks are observed in this stage, which shows that the behaviour is actually non-linear. The cracks are observed between the masonry wall connections and shear cracks appear closer to the openings in the back façade.

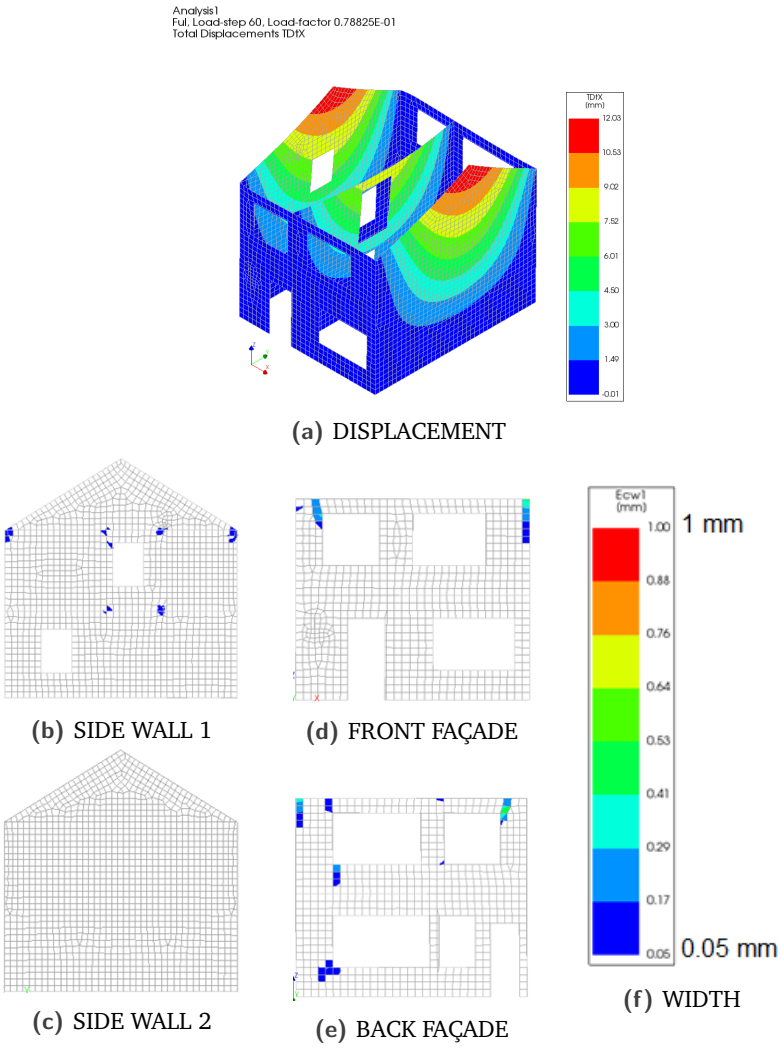


(a) DISPLACEMENT

(b) SIDE WALL 1

(d) FRONT FAÇADE

(c) SIDE WALL 2

(e) BACK FAÇADE

(f) WIDTH

**Fig. 4.7.:** RESULTS AT THE END OF PRE-CRACK STAGE

### First Crack Stage

In this phase some cracks start to localize, having a maximum crack-width of range 1.5-2.5 mm. There are more shear cracks in pier and spandrels. As there are vertical cracks observed between the top and bottom left opening and shear crack over the top right opening of the back façade, this leads to energy release which we can observe in the graph as base shear load decreases during this stage. The shift from a linear curve to a non-linear curves is very much evident from this stage.

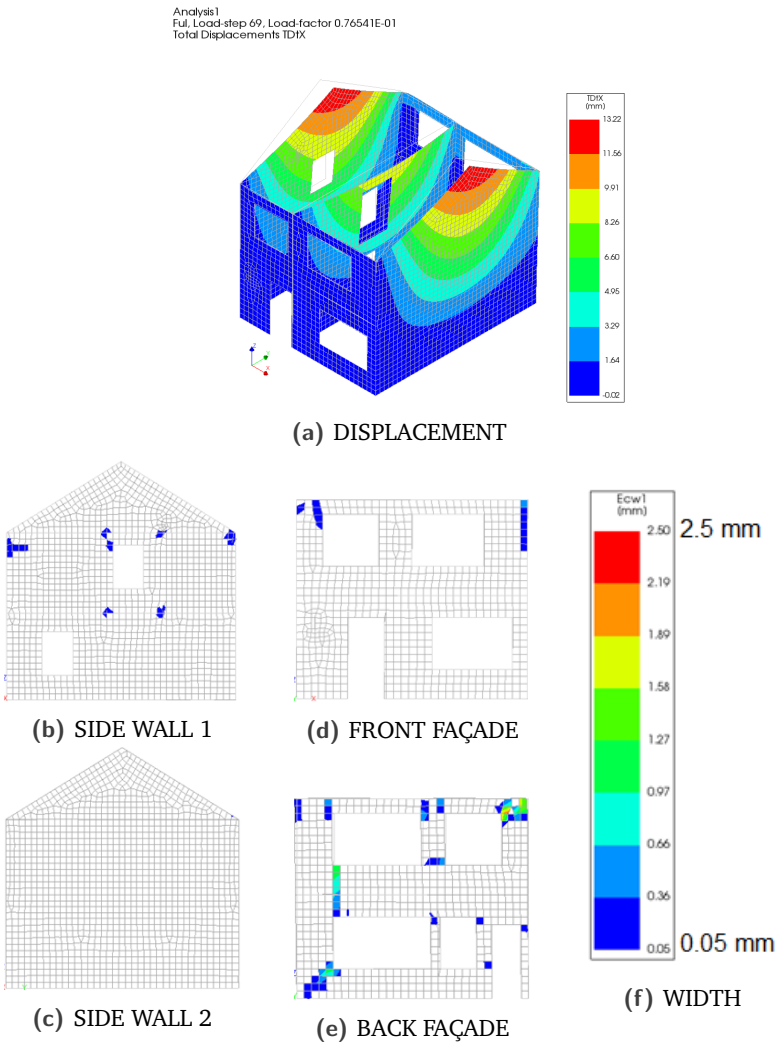


(a) DISPLACEMENT

(b) SIDE WALL 1

(d) FRONT FAÇADE

(c) SIDE WALL 2

(e) BACK FAÇADE

(f) WIDTH

**Fig. 4.8.:** RESULTS AT THE END OF FIRST CRACK STAGE

### Crack Propagation Stage

In this stage, existing cracks open and new cracks are formed. The cracks in the back façade is the governing factor that determines the capacity of the building. It is because, the back façade is having more openings and they are wider; which results in the concentration of cracks in that façade for this particular case. The cracks are observed between the masonry walls, more shear cracks in the back façade, and toe-crushing of piers is also observed in this stage.

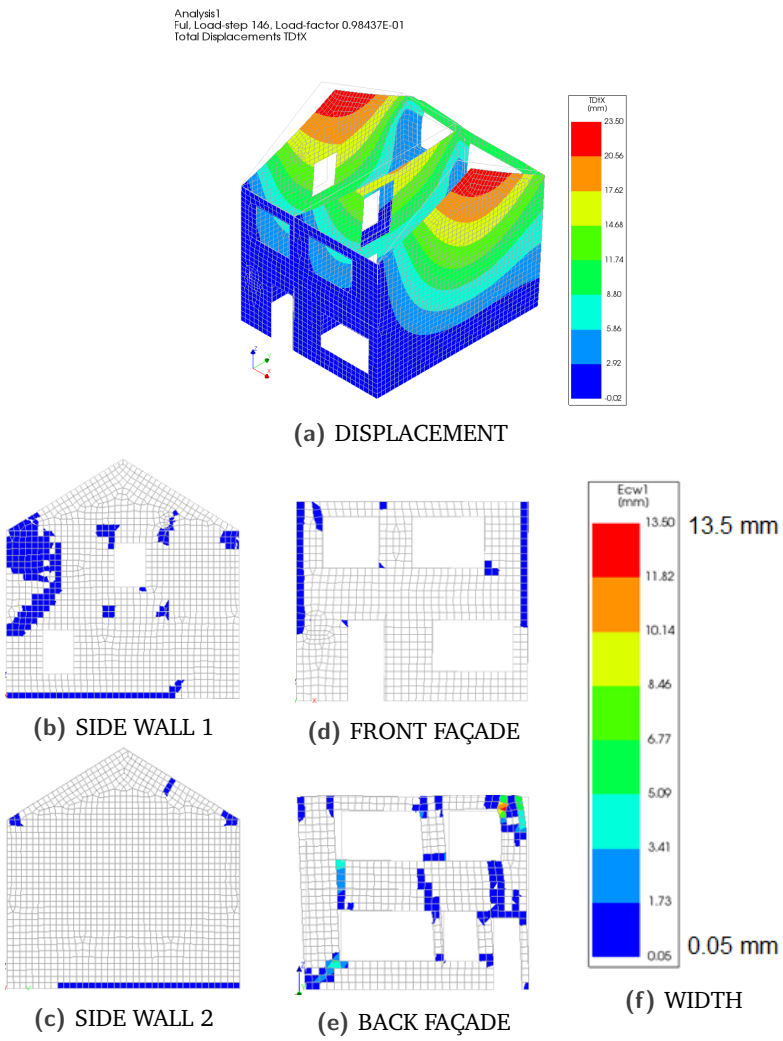


(a) DISPLACEMENT

(b) SIDE WALL 1

(d) FRONT FAÇADE

(f) WIDTH

(c) SIDE WALL 2

(e) BACK FAÇADE

**Fig. 4.9.:** RESULTS AT THE END OF CRACK PROPAGATION STAGE

### Collapse Stage

The last stage is characterized with the arising of more cracks. These cracks are observed in the connection between the masonry walls, toe-crushing of piers, step-wise shear cracks in the back façade. The façade just collapses and the graph after the final step in the collapse stage just drops down drastically.

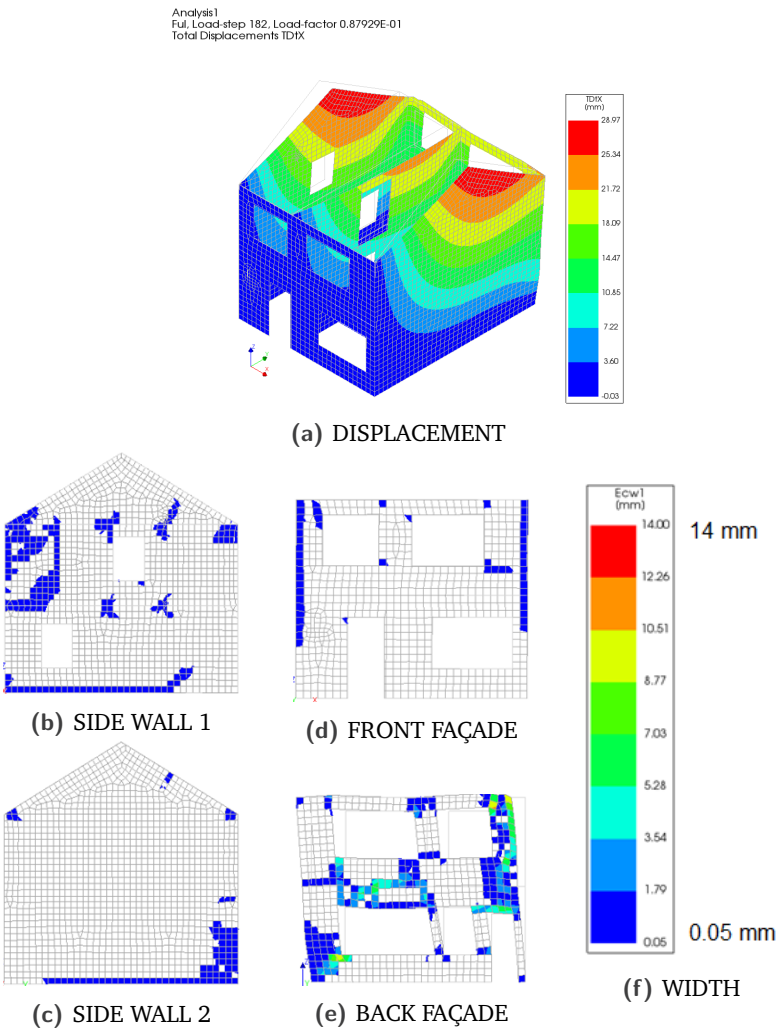


(a) DISPLACEMENT

(b) SIDE WALL 1

(d) FRONT FAÇADE

(f) WIDTH

(c) SIDE WALL 2

(e) BACK FAÇADE

**Fig. 4.10.:** RESULTS AT THE END OF COLLAPSE STAGE

The crack-width results are shown by opting for the maximum value in the 5-layer integration scheme. For more detailed results, the reader is referred to the Appendix where a comparison is given between the normal load control method and arc-length control method. And also crack-widths are displayed for more steps in the analysis.

# 5 Geometrical Variations and Sensitivity Study

The script is parameterized and as a result of which it is easy to change certain parameters to modify the building. The most important aspect of the research is to vary the geometrical characteristics of the building, and by performing monotonic pushover analysis for all the variations, to see the effect on the seismic capacity of the building and comparing them over a sensitivity analysis. The main reason to perform this research is that openings in masonry walls, influences the capacity of the building (also evident from the case study) and also to quantify the effect of the number and size of openings/irregularities on the capacity of the building.
In this chapter, a detailed overview is given on the parameters that are varied and characterization of these parameters by irregularity index. It is then followed by sensitivity analysis done on these variations over a Monotonic Pushover Analysis.

## 5.1 Characterization of Irregularities

To investigate the alteration of seismic capacity by varying the geometrical characteristics, the variations/irregularities are grouped into different classes and they are quantified by indexes. The classification makes it very easy to perform sensitivity analysis.

### 5.1.1 Types of Irregularities

In masonry houses with different openings, the following common irregularities can be identified:

1. **Vertical Irregularity:** The wall has windows(openings) with equal heights at the same story and different lengths.
2. **Horizontal Irregularity:** The wall has openings with different heights at the same story and equal lengths.
3. **Variable Number of Openings:** The wall has variable number of openings per story.

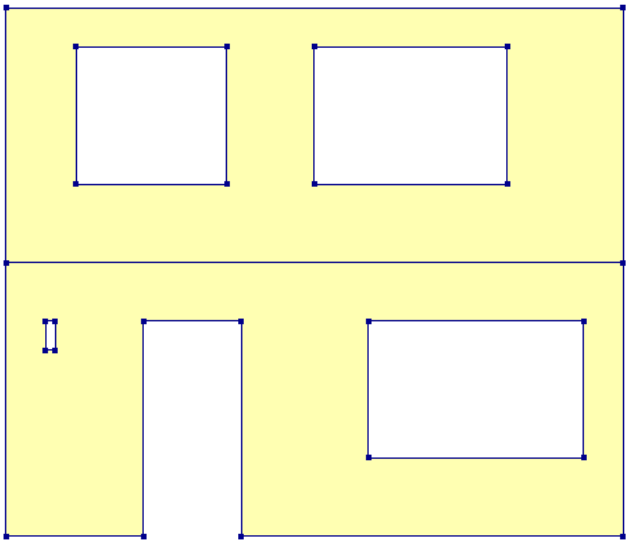

(a) VERTICAL IRREGULARITY

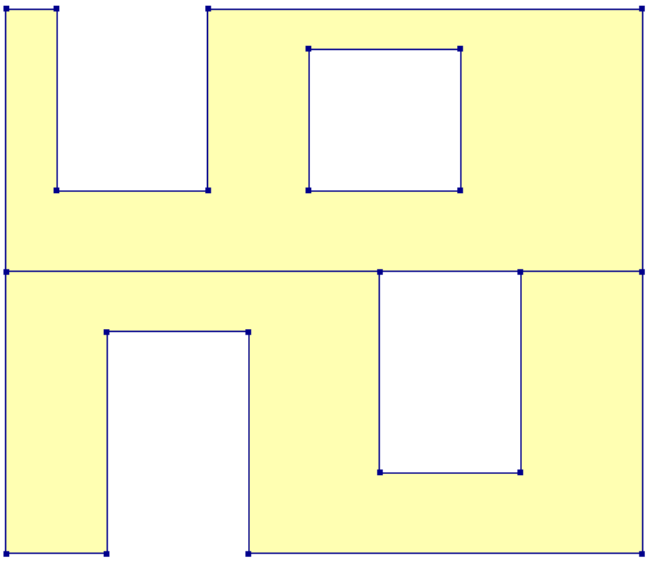

(b) HORIZONTAL IRREGULARITY

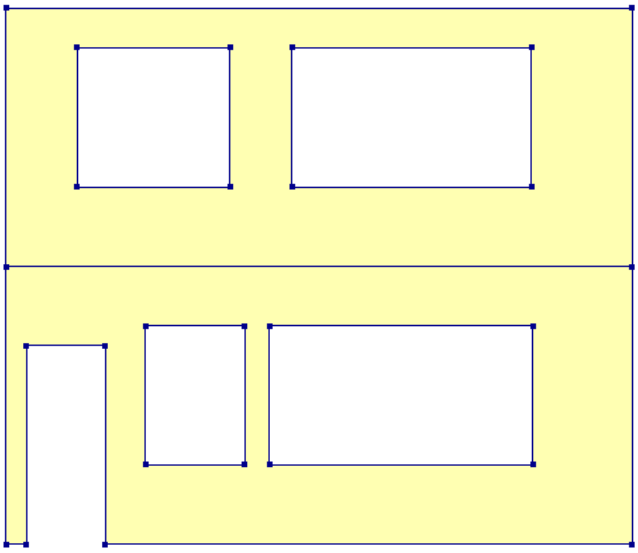

(c) VARIABLE NUMBER OF OPENINGS

**Fig. 5.1.:** TYPES OF IRREGULARITIES

### 5.1.2 Quantification of Irregularities

The main focus of the research is to assess the influence of geometrical variations (irregularities) on non-linear response of masonry houses with openings. To take the variations of irregularities into account, an irregularity index is defined (Parisi, F. and Augenti, N. (2013)). An irregularity index indicates whether a wall in the house is regular(i=0) or not (0<i<1). In this research the irregularity is considered only in the front and back façades, so as to reduce the complexity of the problem.

In case of vertical irregularity, there are two indexes defined; one in the front façade, and one in the back façade. They are given by:

$$I_V^F = \frac{L_{max} - L_{min}}{L_{max} + L_{min}}$$

$$I_V^B = \frac{L_{max} - L_{min}}{L_{max} + L_{min}}$$

where $L_{max}$ and $L_{min}$ are the maximum and minimum opening lengths respectively, $I_V^F$ and $I_V^B$ are the irregularity index for the front and back façade respectively.

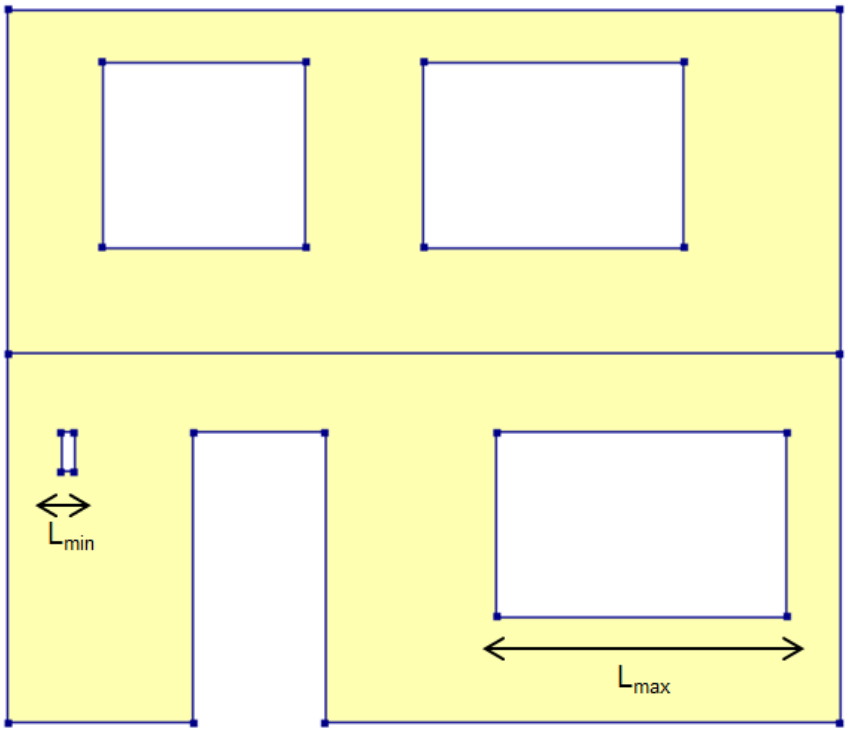


**Fig. 5.2.:** VERTICAL IRREGULARITY REPRESENTATION

The same applies to horizontal irregularity, the indexes are defined for both front and back façade. The indexes are defined by:

$$I_H^F = \frac{H_{max} - H_{min}}{H_{max} + H_{min}}$$

$$I_H^B = \frac{H_{max} - H_{min}}{H_{max} + H_{min}}$$

where $H_{max}$ and $H_{min}$ are the maximum and minimum opening heights respectively, $I_H^F$ and $I_H^B$ are the irregularity index for the front and back façade respectively.

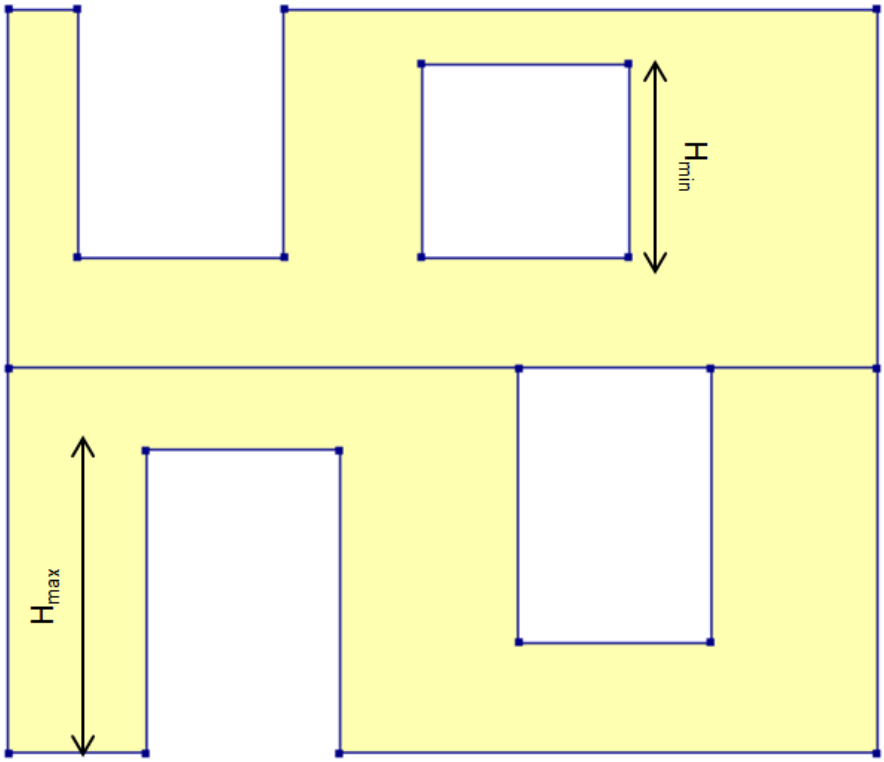


**Fig. 5.3.:** HORIZONTAL IRREGULARITY REPRESENTATION

Finally, the case of variable number of openings. Here the irregularity is defined per story. So the front and back façades each has two irregularities. They are defined by:

$$I_N^{F0} = I_N^{F1} = I_N^{B0} = I_N^{B1} = N$$

where, $N$ is the number of openings per story . $I_N^{F0}$, $I_N^{F1}$, $I_N^{B0}$, and $I_N^{B1}$ are the irregularities of the front and back façades.

## 5.2 Geometrical Variations Excluding the Irregularity

Before any variations are done with respect to the irregularities, initial variations are done by changing certain parameters like increasing the window height (openings) of the masonry houses to first (Z1) and second floor(Z2), inclusion/exclusion of stair case opening (SO, and NSO respectively), and inclusion/exclusion of lintel beams (LB, and NLB respectively).

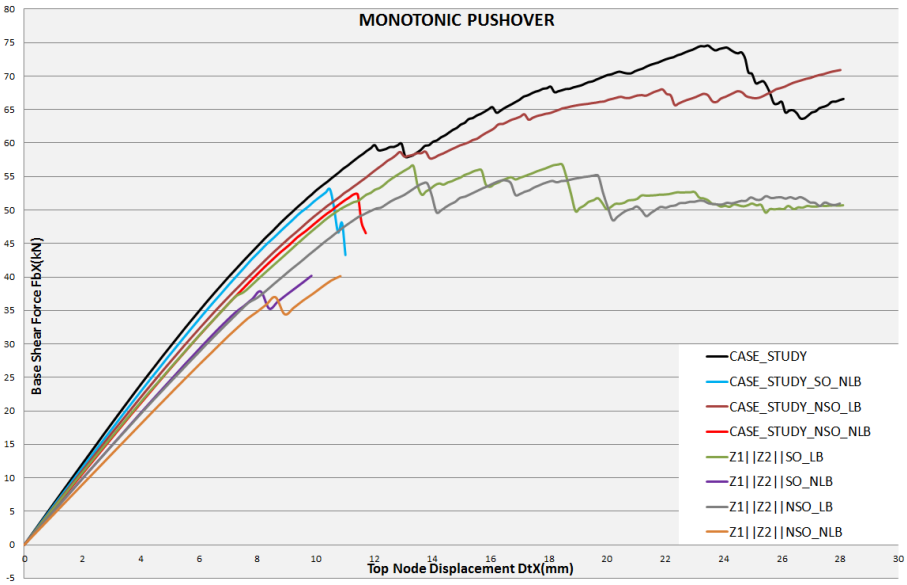


**Fig. 5.4.:** SHEAR-DRIFT CURVES- VARIATIONS BASED ON HEIGHT OF OPENINGS, STAIR-CASE OPENING, AND LINTEL BEAMS

The codes that are stated in the graph are elaborated below. The codes gives the reader an easy way to interpret the results.

- SO – Staircase Opening included;
- NSO – No Staircase Opening;
- LB – Lintel Beams taken into account;
- NLB – Exclusion of Lintel Beams;
- CASE STUDY – Height of Opening (windows) is the same as the height used in the case study;
- Z1||Z2|| – Height of Opening (windows) is increased until the First Floor and Second Floor slabs respectively.

The graph gives us insight about the effect on the seismic capacity of the structure from the afore mentioned parameters that are being varied. The size of the openings affect the seismic capacity of the structure. The capacity of Z1||Z2 with stair case opening(SO) and lintel beams(LB) is 23.8% lower than the case study. The inclusion of staircase opening makes the structure behave a bit more stiffer than when it has been excluded which is evident from the graph. The staircase openings (1.8m) are supported by timber beams, and are directly

connected to the wall which makes the structure stiffer when compared to the exclusion of staircase openings(NSO). Lintel beams have a major influence on the capacity of the structure. The exclusion of the same results in a very poor behaviour of the structure as it leads to extensive cracking over the top of openings in front and back façades. The capacity of the structure where, height of opening is increased to Z1||Z2, no staircase openings (NSO), and no lintel beams (NLB) is reduced by 46.2% and ductility by 61.5% of the case study. To get a better picture of the phenomena observed, the crack-widths are presented for the last step of all variations.

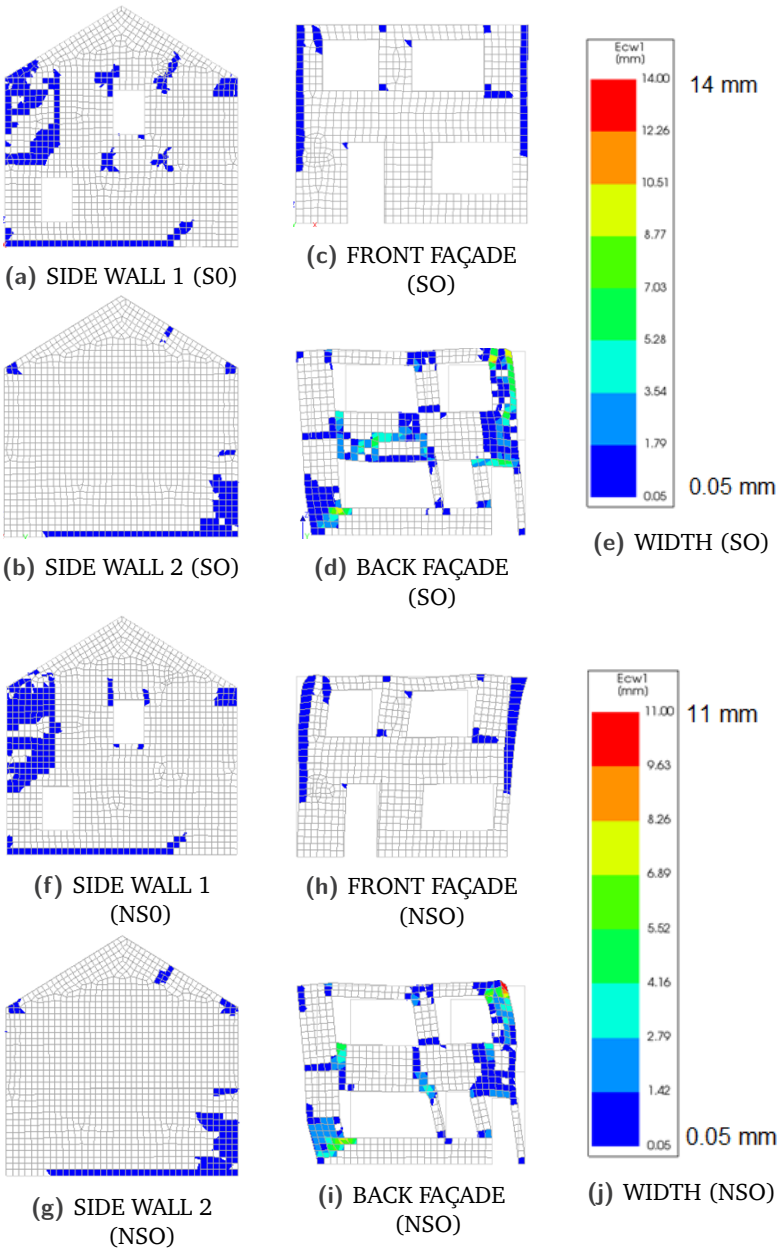


(a) SIDE WALL 1 (S0)

(c) FRONT FAÇADE (SO)

(b) SIDE WALL 2 (SO)

(d) BACK FAÇADE (SO)

(e) WIDTH (SO)

(f) SIDE WALL 1 (NS0)

(h) FRONT FAÇADE (NSO)

(g) SIDE WALL 2 (NSO)

(i) BACK FAÇADE (NSO)

(j) WIDTH (NSO)

Fig. 5.5.: CRACK-WIDTH COMPARISON– CASE STUDY HEIGHT(LB INCLUDED) – INCLUSION(SO) AND EXCLUSION(NSO) OF STAIRCASE OPENINGS

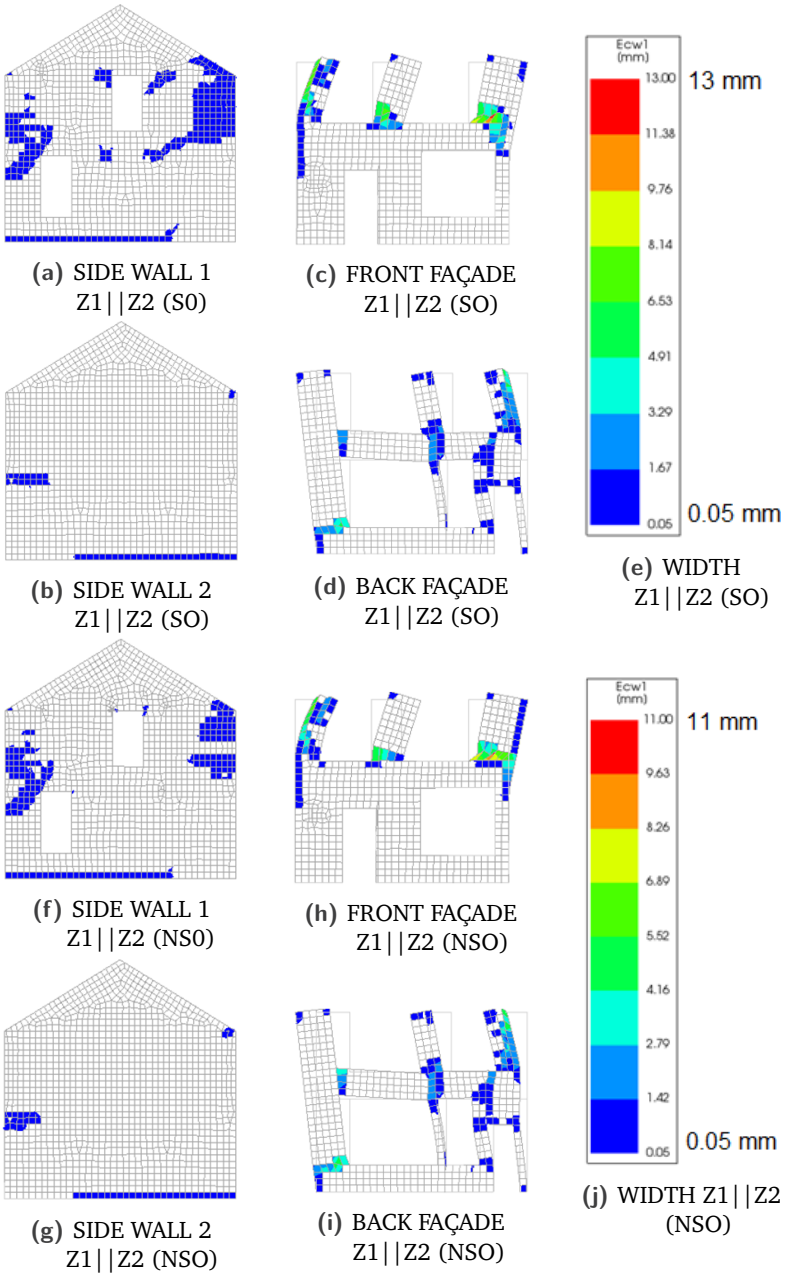


(a) SIDE WALL 1 Z1||Z2 (S0)

(c) FRONT FAÇADE Z1||Z2 (SO)

(e) WIDTH Z1||Z2 (SO)

(b) SIDE WALL 2 Z1||Z2 (SO)

(d) BACK FAÇADE Z1||Z2 (SO)

(f) SIDE WALL 1 Z1||Z2 (NS0)

(h) FRONT FAÇADE Z1||Z2 (NSO)

(j) WIDTH Z1||Z2 (NSO)

(g) SIDE WALL 2 Z1||Z2 (NSO)

(i) BACK FAÇADE Z1||Z2 (NSO)

**Fig. 5.6.:** CRACK-WIDTH COMPARISON– Z1||Z2|| HEIGHT(LB INCLUDED) – INCLUSION(SO) AND EXCLUSION(NSO) OF STAIRCASE OPENINGS

The crack patterns shown in Figure 5.5d and 5.5i are similar, but we see more step cracks (shear failure) with 5.5d. The crack patterns in Figure 5.6d and 5.6i are similar to each other. For more detailed information, please refer to Appendix E

## 5.3 Vertical Irregularity

The variations that are carried out have two main cases:

1 The height of windows(openings) in the front and back façade has been fixed to the adopted height in the case study (1.4 m).
2 The height of windows(openings) in the front and back façade has been fixed to 2m and 1.8m for the ground and first floor respectively.

The variation also included the inclusion/exclusion of stair-case openings in the floor and lintel beams over the openings. The flow chart for the above mentioned variations is represented in the Figure 5.7.

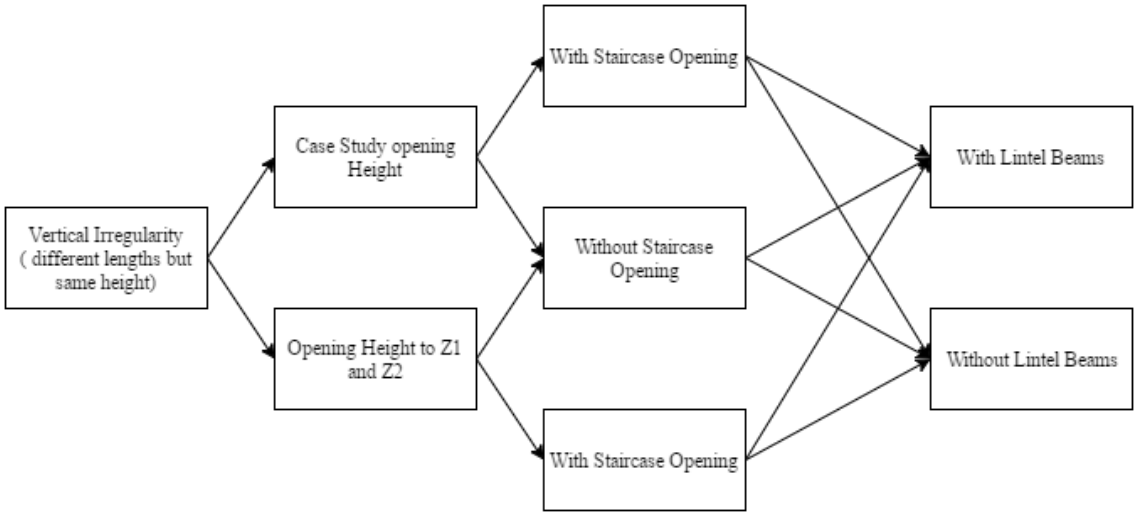


**Fig. 5.7.:** FLOWCHART-VERTICAL IRREGULARITY

Monotonic Pushover analysis was carried out for all the variations stated in the flowchart. A total of 16 variations are analysed under the vertical irregularity. The irregularity index for the front and back façade for the two cases are shown in the Figure 5.8 and 5.9.

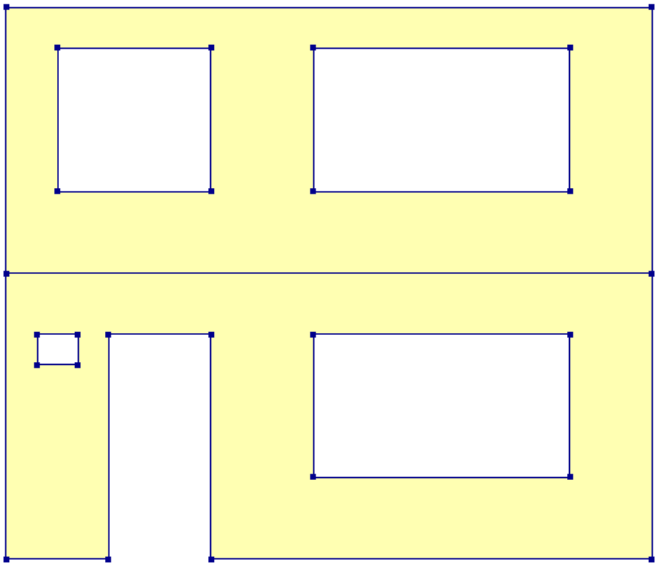

(a) $I_V^F = 0.72$

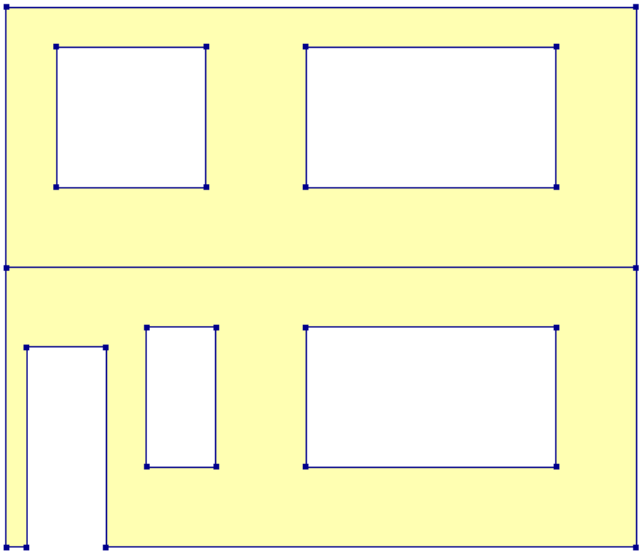

(b) $I_V^B = 0.56$

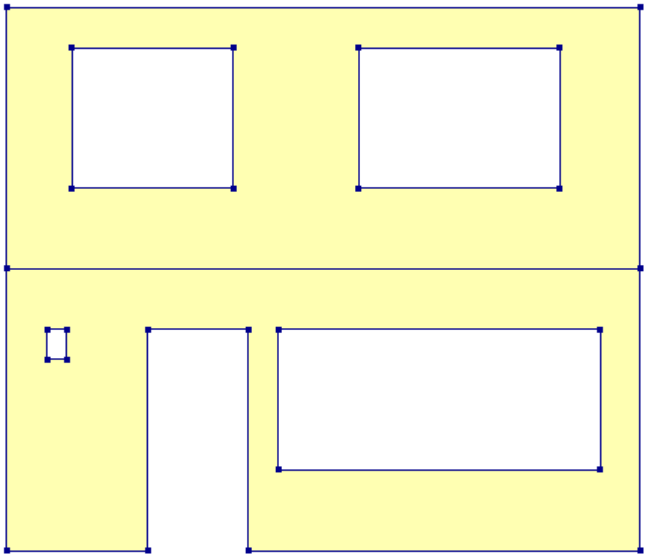

(c) $I_V^F = 0.88$

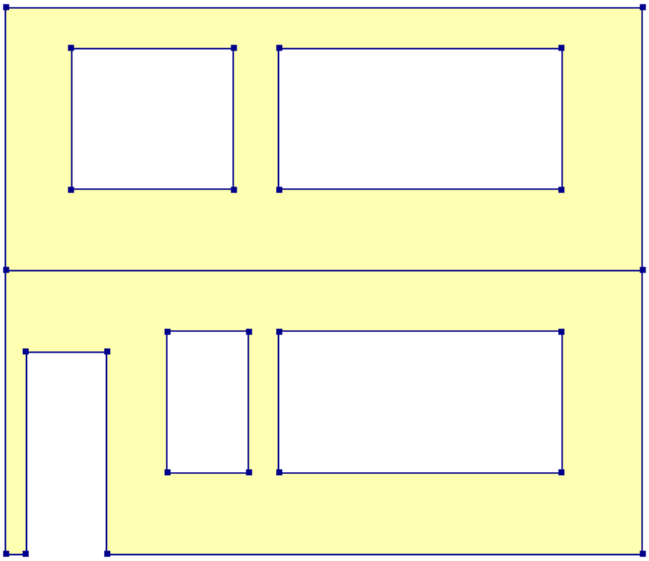

(d) $I_V^B = 0.55$

**Fig. 5.8.:** IRREGULARITY INDEX FOR FRONT AND BACK FAÇADE FOR DIFFERENT VARIATIONS (CASE 1)

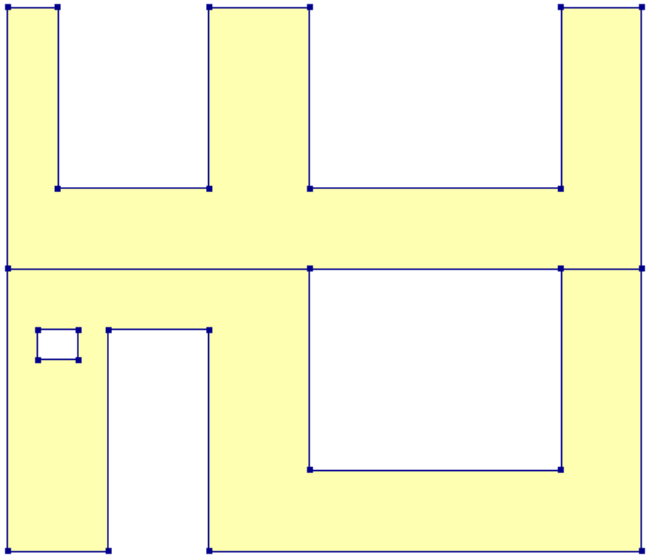

(a) $Z_1||Z_2||I_V^F = 0.72$

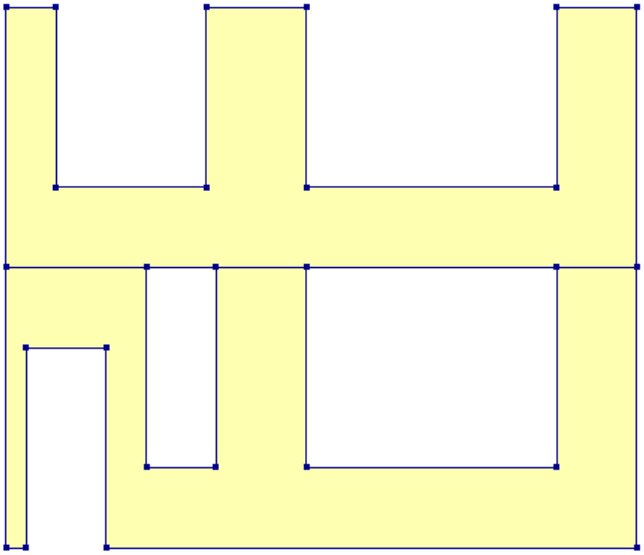

(b) $Z_1||Z_2||I_V^B = 0.56$

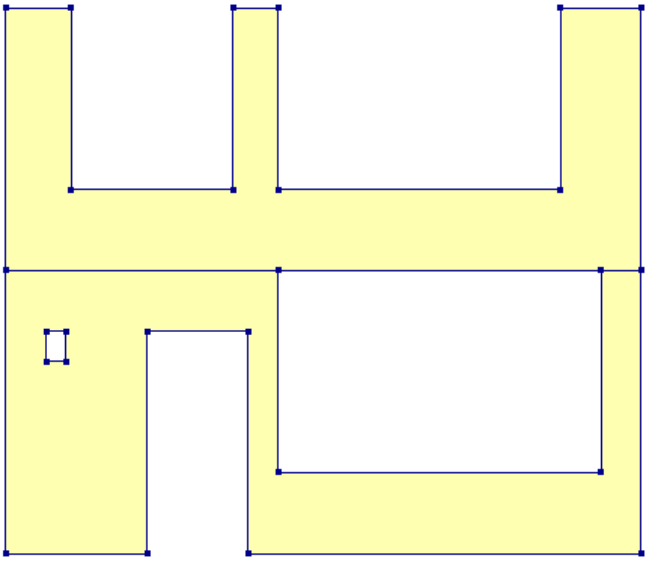

(c) $Z_1||Z_2||I_V^F = 0.88$

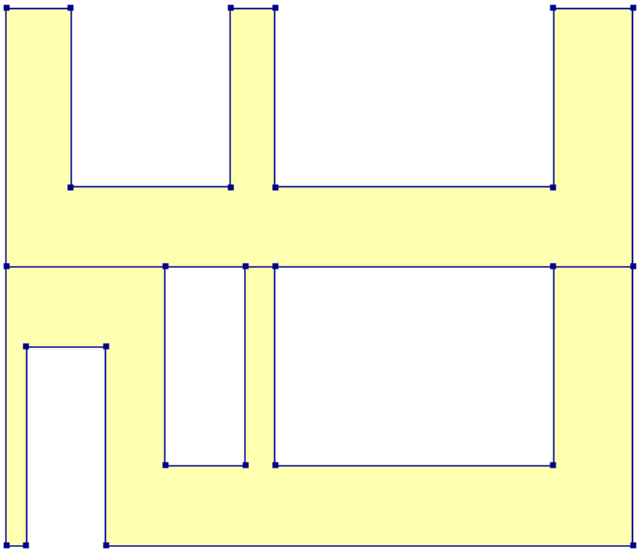

(d) $Z_1||Z_2||I_V^B = 0.55$

**Fig. 5.9.:** IRREGULARITY INDEX FOR FRONT AND BACK FAÇADE FOR DIFFERENT VARIATIONS (CASE 2)

A Graph is plotted between the base shear force and the top node displacement for every case (17 cases). The graph gives us a good picture of the varying seismic capacity with respect to vertical irregularities and other parameters.

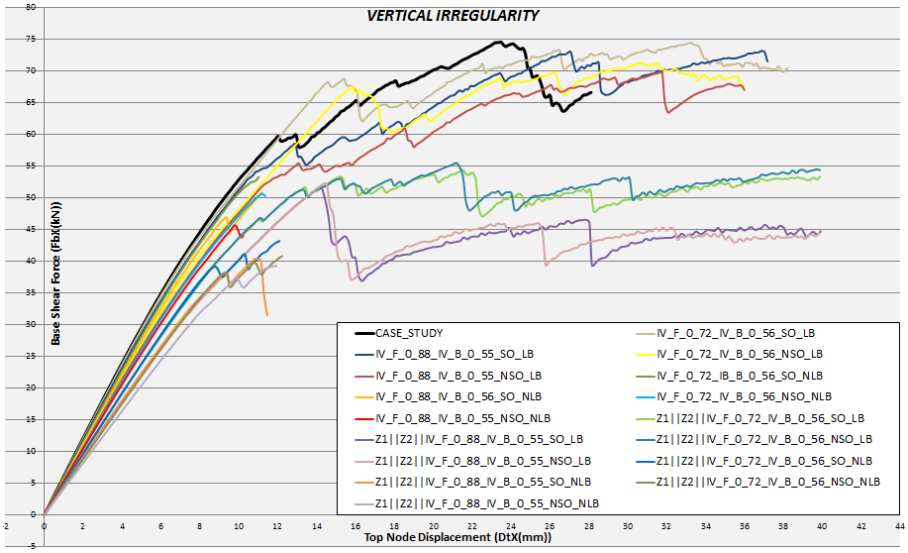


**Fig. 5.10.:** PUSHOVER CURVES - VERTICAL IRREGULARITY

**CASE 1**

In this case, as mentioned earlier the height of windows(openings) is restricted to 1.4 m in both ground and first floor for the front and back façades. A shear-drift curve is plotted for all the variations.

Each of the masonry house is characterized by a set of codes. They start with the type of irregularity, followed by the value of the same for both front and back façades, which is then followed by the inclusion/exclusion of staircase opening (SO/NSO), and finally the inclusion/exclusion of lintel beams in the structure (LB/NLB). With these codes as identification, graphs are plotted for all variations in Case 1.

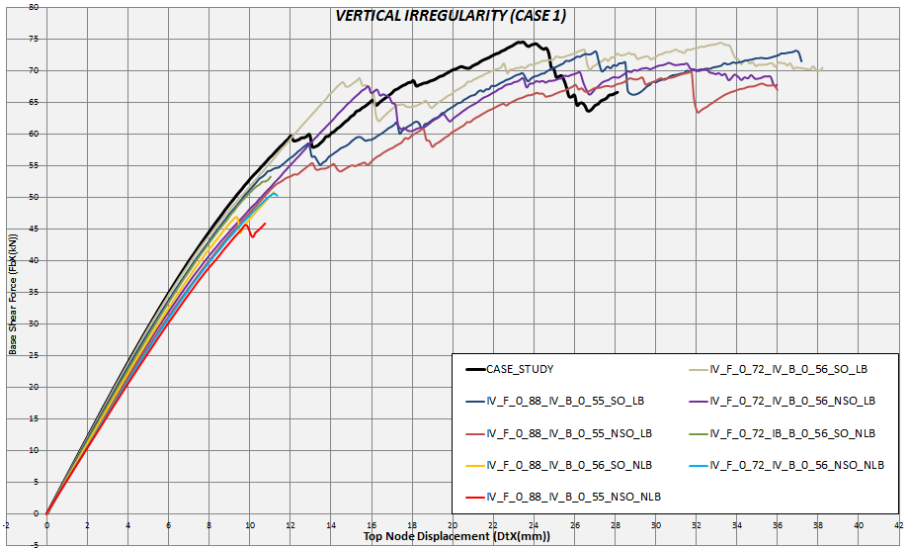


**Fig. 5.11.:** PUSHOVER CURVES - VERTICAL IRREGULARITY (CASE 1)

From the graph it is clear that if we increase the vertical irregularity, it lowers the capacity of the structure, and it becomes less stiff compared to the case study. The inclusion of lintel beams increases the capacity and ductility of the structure.The inclusion of staircase openings (SO), results in a stiffer behaviour of the structure than when it's excluded (NSO). This happens because the staircase opening is supported by timber beams which are rigidly connected to the wall, resulting in a stiffer behaviour. Even though in practice it is not constructed this way, an assumption is made in this study to simplify the modelling aspects. In case of vertical irregularity ($I_V^F = 0.88 \& I_V^B = 0.55$) with inclusion of lintel beams (LB), and no staircase openings (NSO); the capacity of the structure is reduced by 6.5% of the case study. But the exclusion of lintel beams (NLB) from the aforementioned case, has a major influence on the structure; as the capacity is reduced by 38.5% and the ductility by 62%.

**CASE 2**

The height of openings (windows) in the front and back façade has been fixed to 2m and 1.8m for ground and first floor respectively. With similar codes as reference, graphs are plotted for all variations in Case 2.

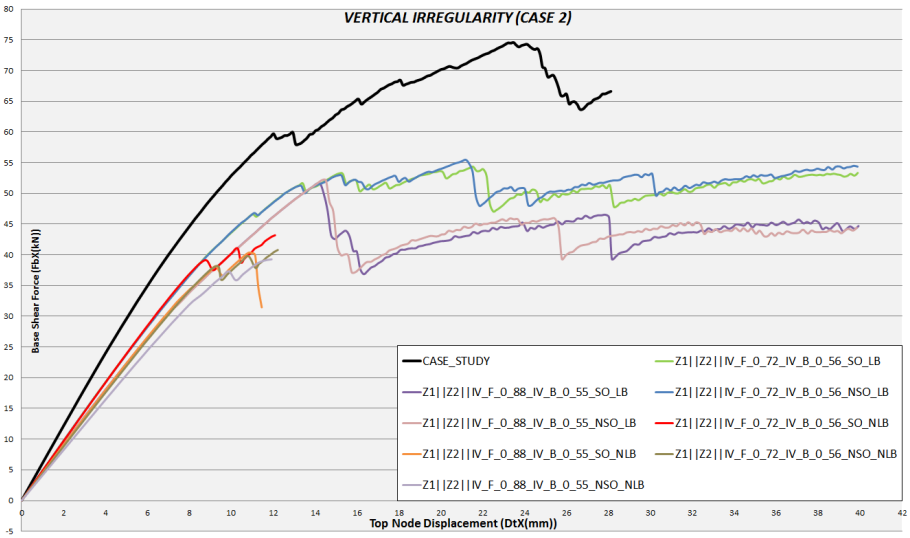


**Fig. 5.12.:** PUSHOVER CURVES - VERTICAL IRREGULARITY (CASE 2)

Increasing the height of openings does have an effect on the capacity. The case where vertical irregularity ($I_V^F = 0.88 \& I_V^B = 0.55$) with inclusion of lintel beams (LB), and no staircase openings (NSO);the capacity of the structure is reduced by 30% of the case study. But with the exclusion of lintel beams (NLB) from the above stated cases, the capacity is reduced by 48% and the ductility by 58% of the case study.
From the above results we can conclude that by increasing the vertical irregularity index the capacity of the structure decreases, and the exclusion of lintel beams has a major influence on the capacity and ductility of the structure. For more detailed information about the crack-widths for all different cases please refer the Appendix F.

## 5.4 Horizontal Irregularity

In horizontal irregularity, two cases were analysed with respect to irregularity index. The variations also include the inclusion/exclusion of stair-case openings in the floor and lintel beams over the openings. The flowchart for above mentioned variations is represented in the Figure 5.13.

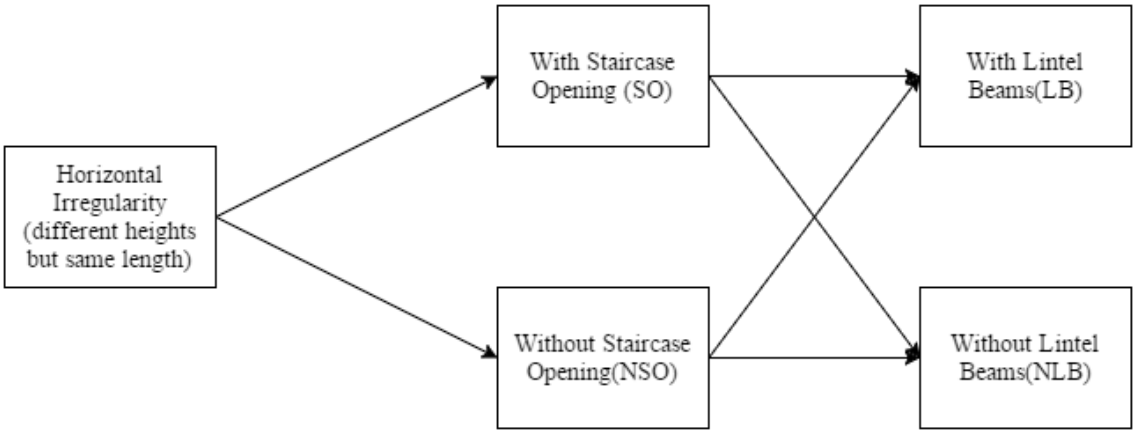


**Fig. 5.13.:** FLOWCHART-HORIZONTAL IRREGULARITY

A total of 8 variations are analysed under the horizontal irregularity. The two cases that were taken into consideration based on the irregularity index for the front and back façade are shown in the Figure 5.14 and 5.15 .

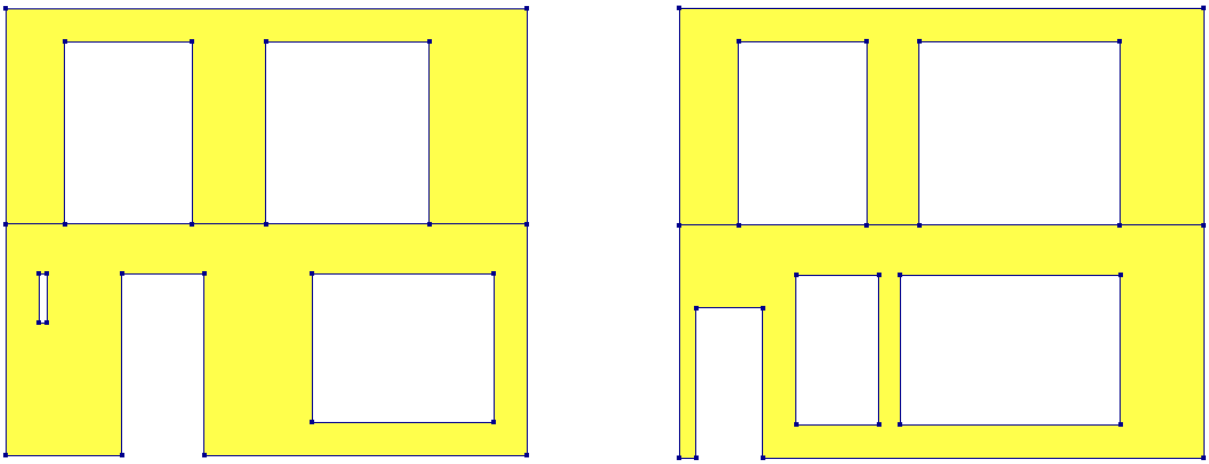

(a) $I_H^F = 0.57$ (b) $I_H^B = 0.1$

**Fig. 5.14.:** CASE 1-IRREGULARITY INDEX FOR FRONT AND BACK FAÇADE

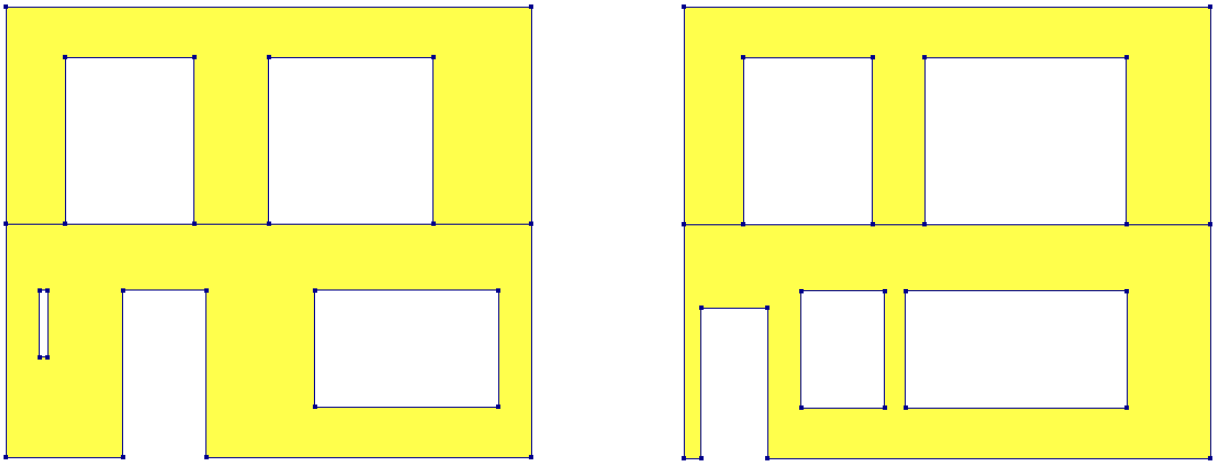

(a) $I_H^F = 0.43$ (b) $I_H^B = 0.18$

**Fig. 5.15.:** CASE 2-IRREGULARITY INDEX FOR FRONT AND BACK FAÇADE

Results were obtained by plotting the graph for Base Shear Force and Top Node Displacement for all the variations including the case study. The graph is representative of horizontal irregularity and is shown in the Figure 5.16. The codes are identified by the following order; irregularity index in front façade, followed by irregularity in back façade, then staircase openings–inclusion (SO)/exclusion (NSO), and finally lintel beams–inclusion (LB)/exclusion (NLB).

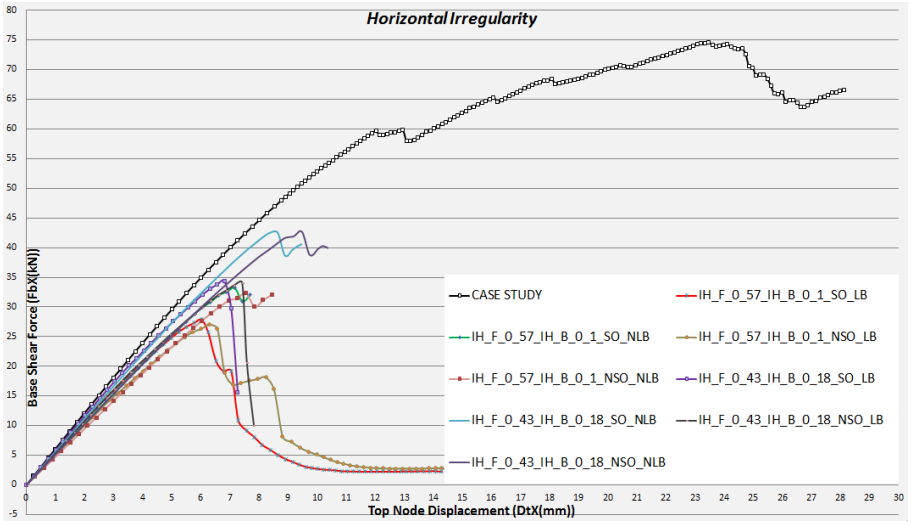


**Fig. 5.16.:** PUSHOVER CURVES - HORIZONTAL IRREGULARITY

**CASE 1** $||I_H^F = 0.57||I_H^B = 0.1||$
The variations were plotted (Figure 5.17).

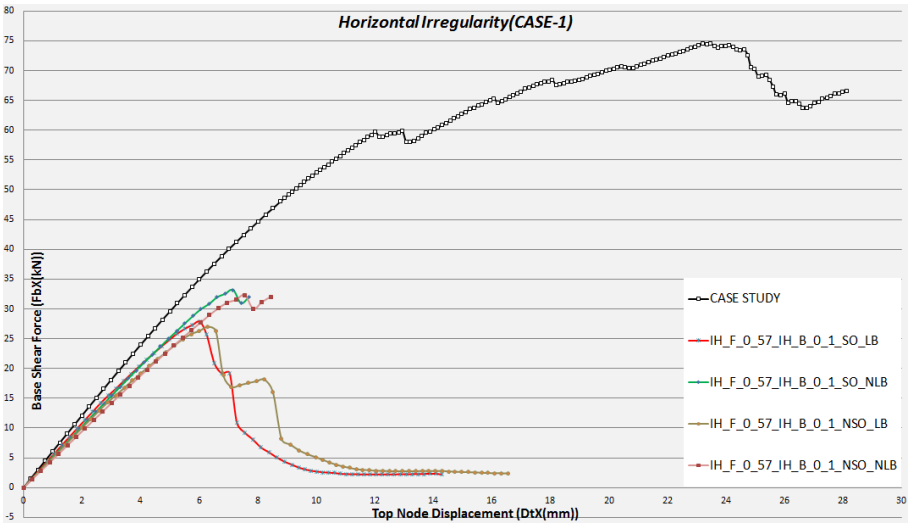


**Fig. 5.17.:** CASE 1- HORIZONTAL IRREGULARITY

The variations have an effect on the capacity of the structure. The inclusion of staircase openings results in a stiffer behaviour of the structure, because the stair beams are directly connected with walls which contributes towards the stiffness. The peculiar behaviour is that, exclusion of lintel beams results in a 4% higher capacity of the structure compared to the inclusion of the same. The absence of lintel beams results in a weaker behaviour of masonry elements above the openings in the front and back façade. This leads to a localised failure in the front and back façade, but a higher global capacity of the structure. However, the inclusion of lintel beams results in a stiffer behaviour of the masonry elements above the openings in the façade. This results in diagonal shear cracks in the back façade near the base, and they are subsequently followed by the base shear failure. Masonry being very weak in tension, results in a lower capacity and brittle behaviour of the structure. The failure mechanisms (crack-widths) for the Case-1 are shown in the Appendix G.1 and G.2.

**CASE 2** $||I_H^F = 0.43||I_H^B = 0.18||$

In this case, the height of the openings are decreased compared to Case 1. The variations of the same are shown in Figure 5.18. Decreasing the height increases the capacity of the structure by 23% with respect to Case 1. But the overall behaviour with respect to the failure mechanisms is similar to Case 1, and it follows the same line of explanation with respect to the inclusion/exclusion of lintel beams.

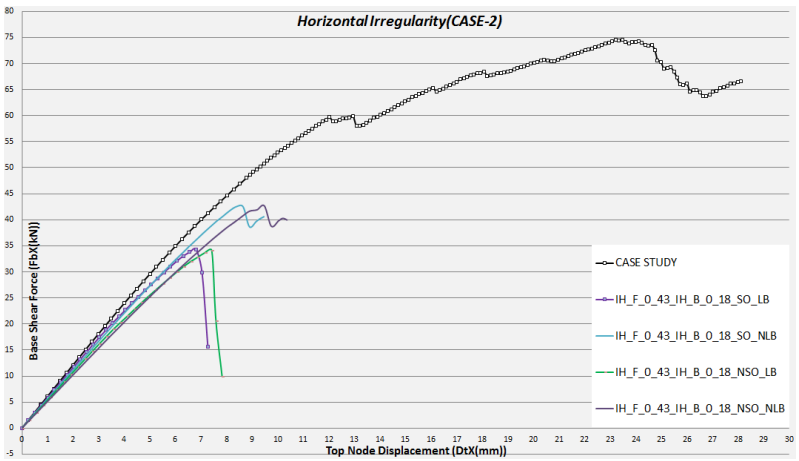


**Fig. 5.18.:** CASE 2- HORIZONTAL IRREGULARITY

The failure mechanisms for Case 2 are shown in Appendix G.3 and G.4.

## 5.5 Number Of Openings

The final variation was with respect to varying the number of openings on every floor in the front and back façades. The variations are done by taking the same number of openings(N) on all floors. This is done to reduce the permutations involved by varying the number N (range of 0–3). The flowchart for the above stated variations are represented in the Figure 5.19.

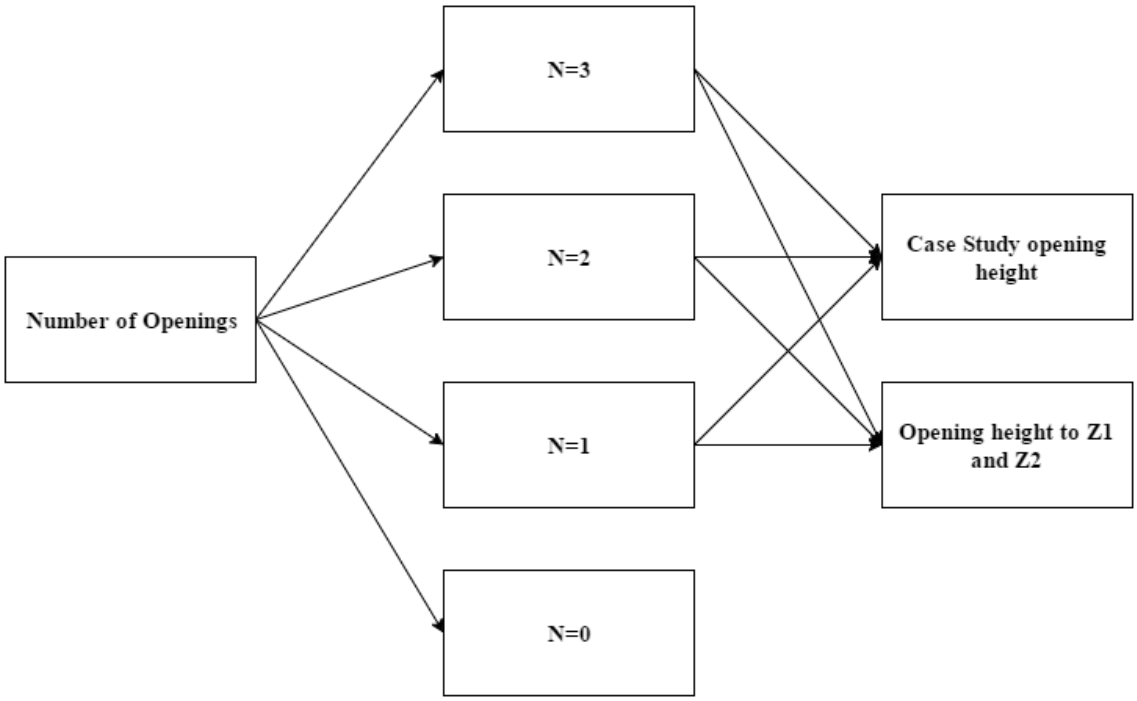


**Fig. 5.19.:** FLOWCHART-NUMBER OF OPENINGS

The variations based on the number of openings are shown in the Figure 5.20,5.21, and 5.22.

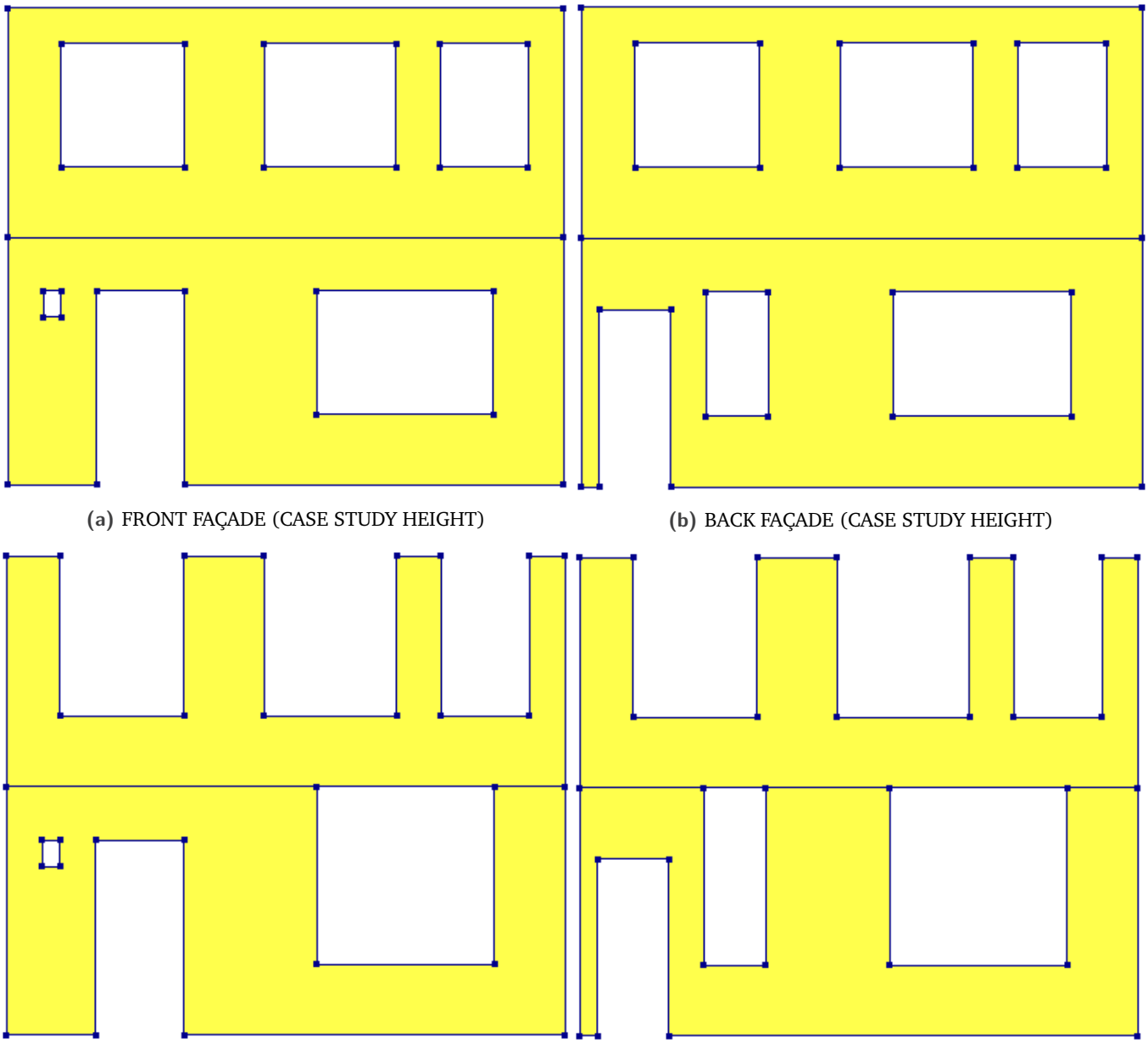

(a) FRONT FAÇADE (CASE STUDY HEIGHT)

(b) BACK FAÇADE (CASE STUDY HEIGHT)

(c) FRONT FAÇADE (Z1||Z2)

(d) BACK FAÇADE (Z1||Z2)

**Fig. 5.20.:** N=3

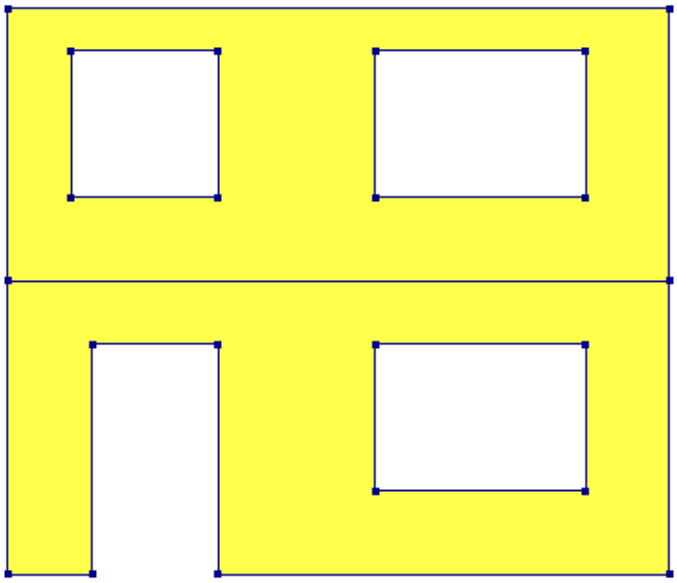

(a) FRONT FAÇADE (CASE STUDY HEIGHT)

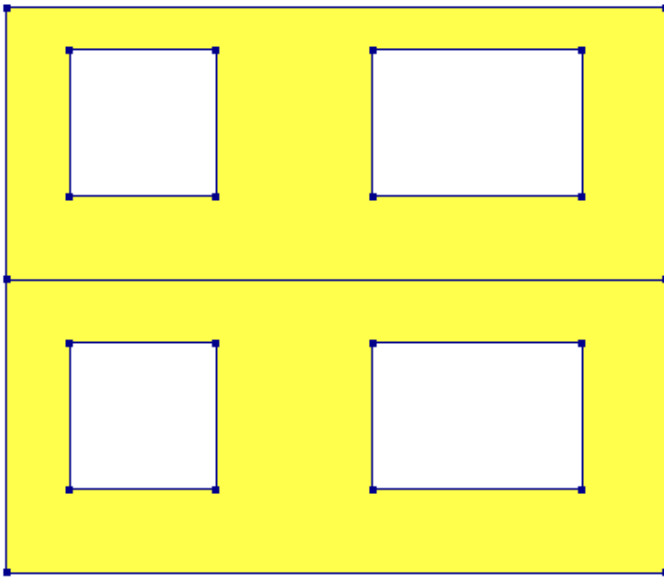

(b) BACK FAÇADE (CASE STUDY HEIGHT)

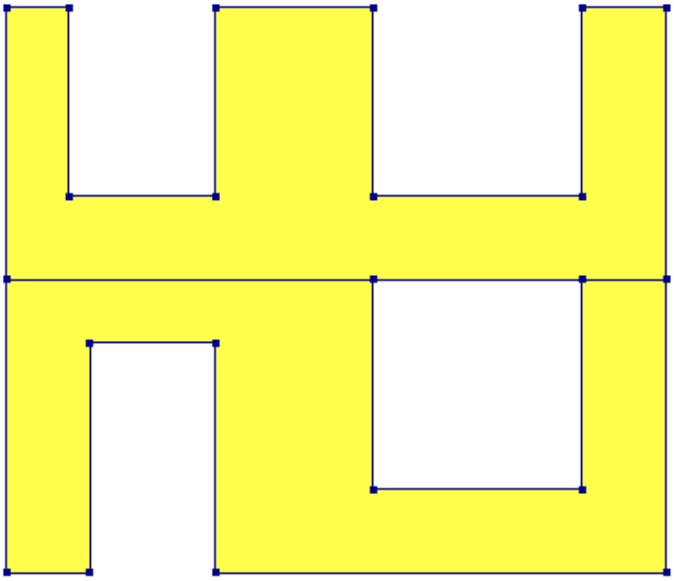

(c) FRONT FAÇADE (Z1||Z2)

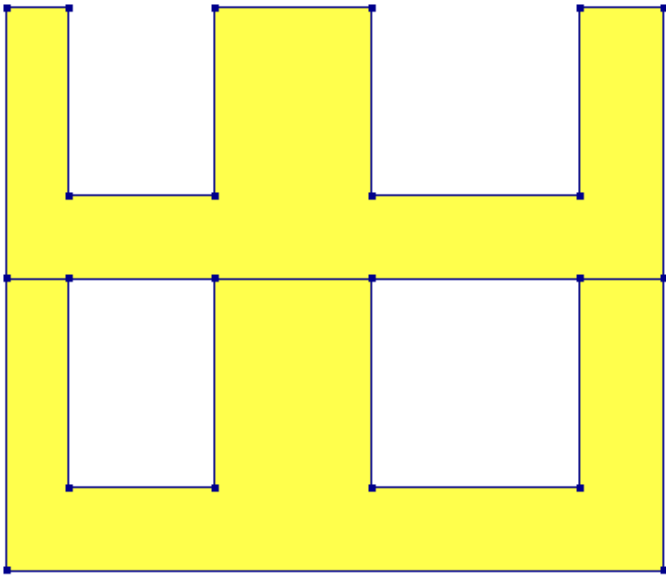

(d) BACK FAÇADE (Z1||Z2)

**Fig. 5.21.:** N=2

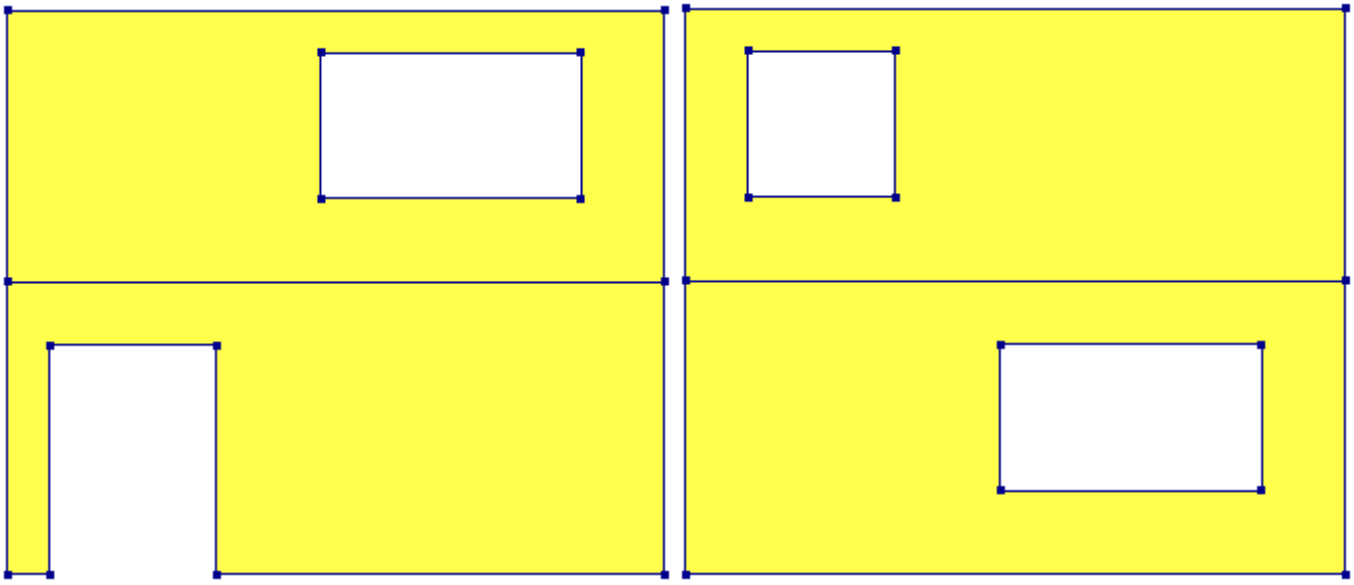

(a) FRONT FAÇADE (CASE STUDY HEIGHT)



(b) BACK FAÇADE (CASE STUDY HEIGHT)

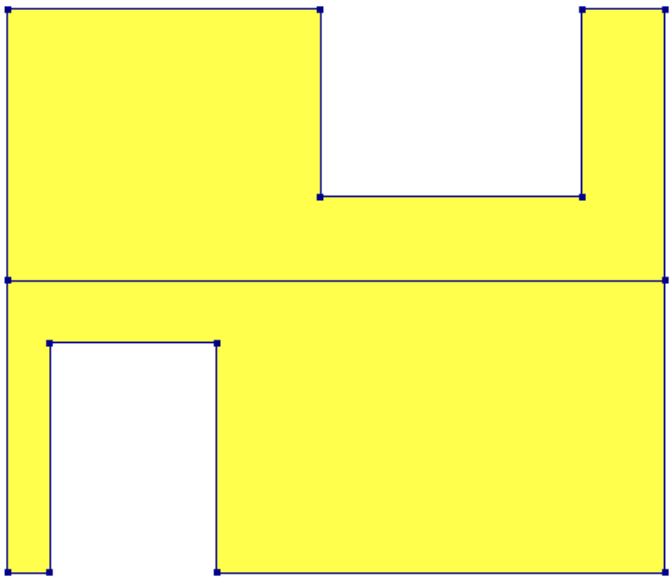

(c) FRONT FAÇADE (Z1||Z2)

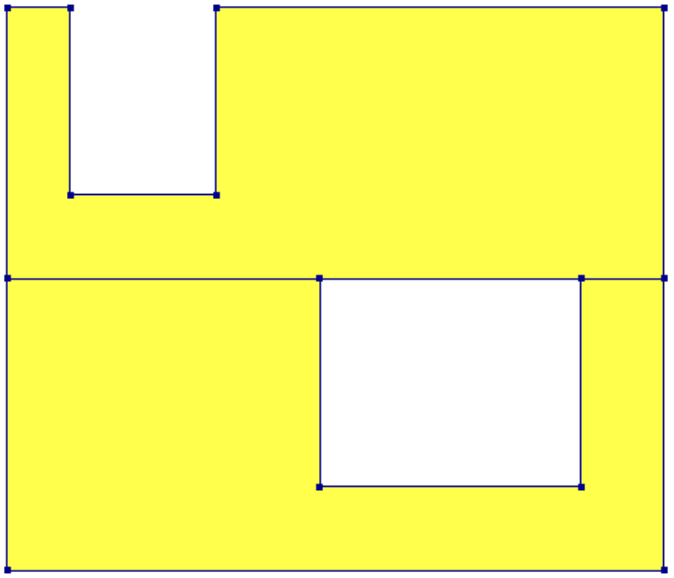

(d) BACK FAÇADE (Z1||Z2)

**Fig. 5.22.:** N=1

For N=0, there are no openings in the front and back façade. As a procedure, pushover analyses are carried out for all the variations. A Graph is then plotted between base shear force and the top node displacement for all the variations. The graph is shown in Figure 5.23.

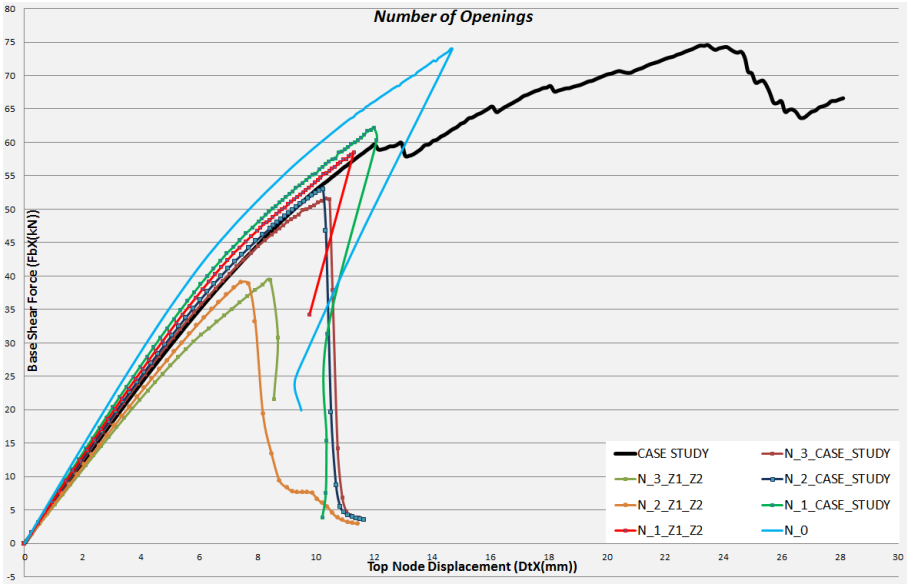


**Fig. 5.23.:** PUSHOVER CURVES - NUMBER OF OPENINGS

For all the variations with number of openings, there are two sub cases; one with the height of openings limited to the height adopted in case study, and the other with height of openings increased to Z1||Z2 (Section 5.2). By considering the variation N=3, the capacity of the building with the height of openings as "case study" is 5% higher than the building with height "Z1||Z2". By decreasing the number of openings, the capacity of the building increases and also the difference between the capacities of the two sub cases is very minimal. In all these variations, after the peak load, the structure experiences base shear failure, as a result of which there is a drastic dissipation of energy leading to the brittle behaviour of the structure. By increasing the angle of friction this can be avoided, but it is not applied here. For more detailed information please refer the Appendix H.

## 5.6 Interpretations on Irregularities

From the above studies, it is evident that varying the irregularity, alters the capacity of the structure. In this section, a comparison between the capacity of the case study, and the altered capacity of the structure caused due to irregularities etc. is done.

### 5.6.1 Effect of Vertical Irregularity Index

A graph is plotted between the irregularity index and the capacity of structure. The graph is only plotted for the front façade and not for the back façade, as the difference in irregularity index is 0.16 and 0.01 respectively.

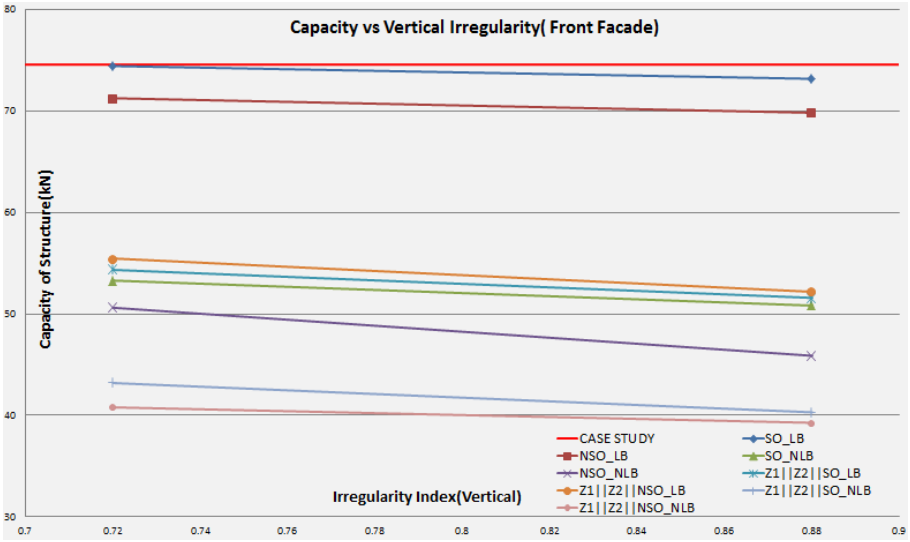


**Fig. 5.24.:** CAPACITY VS VERTICAL IRREGULARITY (FRONT FAÇADE)

Only two cases were performed with respect to the irregularity index, resulting in a linear relation in the graph. By increasing the irregularity index, the capacity of the structure decreases. Increasing the height of the openings results in a lower capacity. Different failure mechanisms were observed in this variation study and a few of them were pointed out in the Figure 5.25.

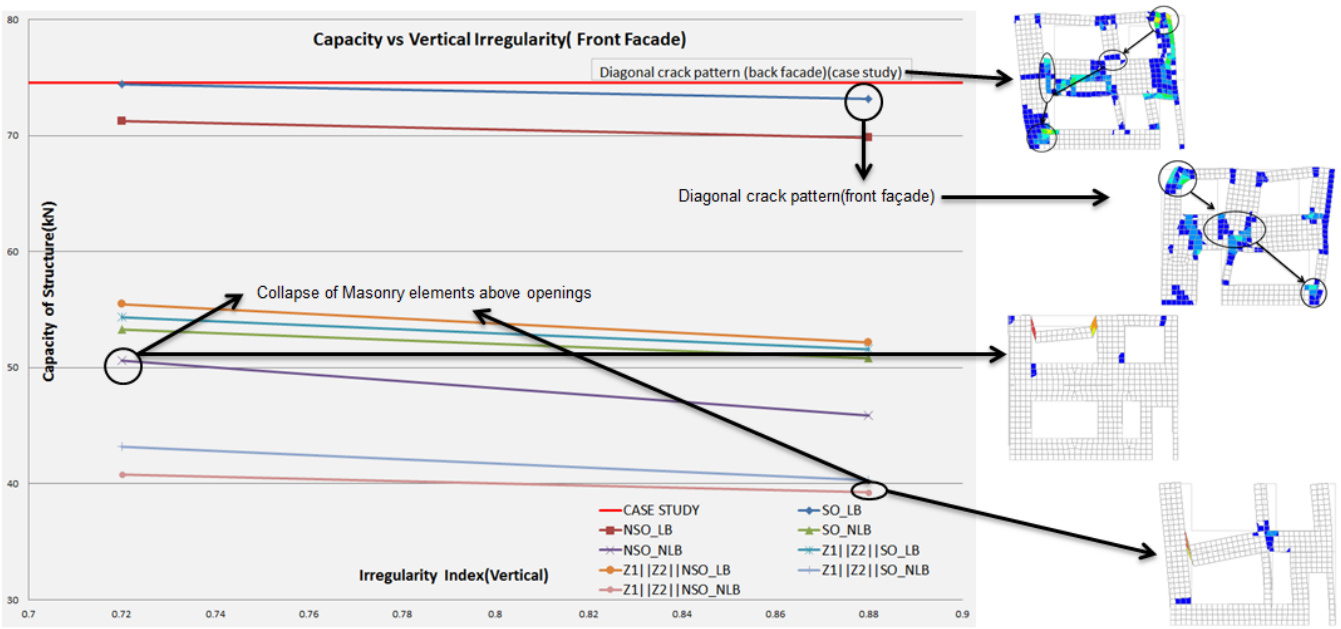


**Fig. 5.25.:** CRACK PATTERNS (VERTICAL IRREGULARITY)

As there are just two variations done with respect to the irregularity index, a linear variation was obtained. By performing additional variation studies ranging from 0-1, a prediction on irregularity index can be obtained with respect to the capacity. By varying the width of the openings, the width of lintel beams are also modified; but there are no modifications done with respect to the properties and the cross section of the lintel. But in practice if the width of the beams are increased, the cross-section of the beams are increased accordingly. As stated before, increasing the vertical irregularity index decreases the capacity of the structure; but by increasing the cross-sectional properties of the lintel beams for higher irregularity index, might results in a stiffer behaviour with a higher capacity of the structure. For more detailed information on crack patterns please refer to Appendix F

### 5.6.2 Effect of Horizontal Irregularity Index

In this variation, height of the openings are varied. A graph is plotted between the irregularity index and the capacity of structure. The graph is only plotted for the front façade and not for the back façade, as the difference in irregularity index is 0.15 and 0.08 respectively.

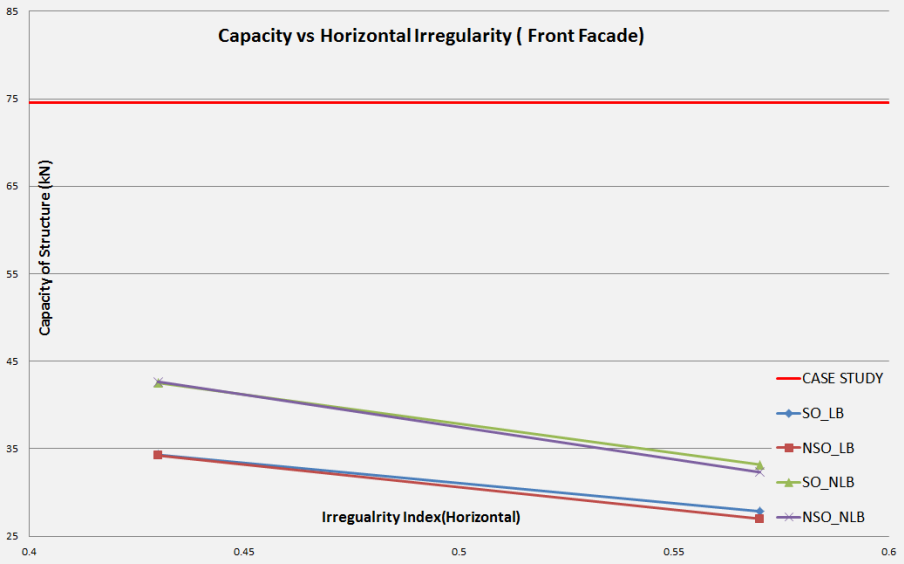


**Fig. 5.26.:** CAPACITY VS HORIZONTAL IRREGULARITY (FRONT FAÇADE)

In this case, with the inclusion of lintel beams (LB) the capacity of the structure is lower than when it is excluded (NLB). The reason behind the lower capacity of the structure with inclusion of lintel beams (LB), is due to the base shear failure of the structure. And this failure occurs in the Side Wall 1, and back façade. But with the exclusion of lintel beams (NLB) the weakest part of the structure was the masonry elements above the openings, as a result it leads to localised failure in the façade. Increasing the irregularity index results in a drop down of capacity of the structure.

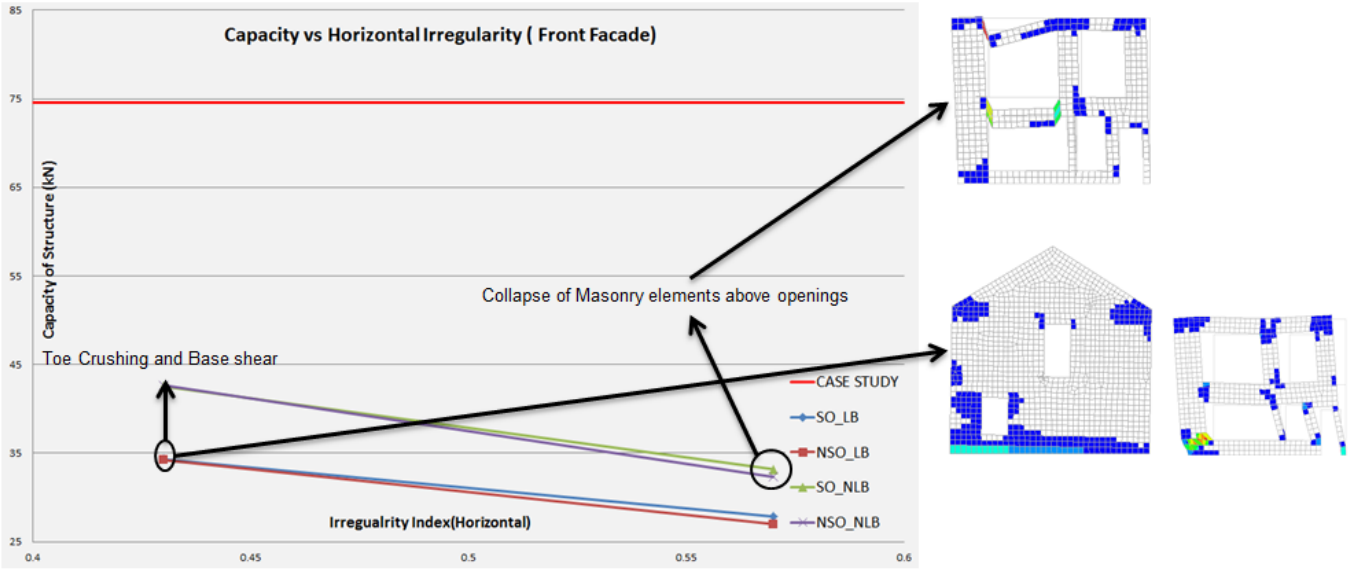


Fig. 5.27.: CRACK PATTERNS(HORIZONTAL IRREGULARITY)

More variations with respect to horizontal irregularity have to be performed to get a better prediction of the influence of the irregularity index with respect to the capacity of the structure.

### 5.6.3 Effect of Number of Openings

The capacity of the structure alters by varying the number of openings. It is represented in the graph as shown in the Figure **??**. The graph is plotted between the capacity of the structure and corresponding number of openings.

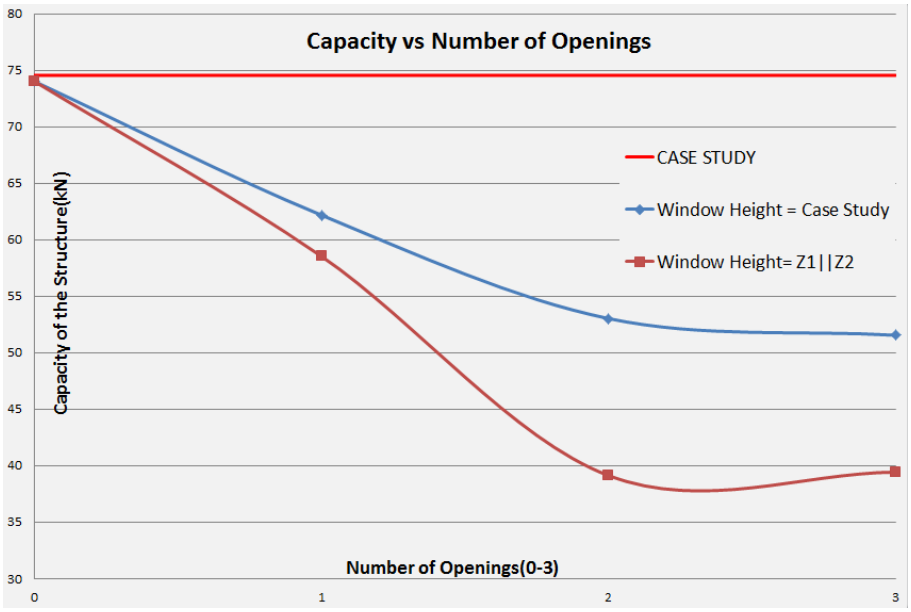


**Fig. 5.28.:** CAPACITY VS NUMBER OF OPENINGS

From the graph, it can be concluded that increasing the number of openings decreases the capacity of the building. And by increasing the height of openings to Z1||Z2 the capacity is furthermore reduced. From the pushover curves (Figure 5.23), for all the variations performed, the structure behaves brittle after reaching the peak load. The main reason behind this mechanism is due to base shear failure of the structure.

# Discussion

# 6

In this report, the research question raised in the introduction, is tried to be answered with a literature study, modelling parameters and assumptions, case study interpretation, and variation studies. In this section, the results obtained are discussed.

The approach that is outlined in this report focussed mainly on assessing the seismic performance of an unreinforced masonry building with timber floors, followed by the variation studies. The results presented in this report are considered to be valid with the assumptions outlined in this report. In the current modelling strategy, the supports are considered to be fixed. But the soil-structure interaction will play an important role in the actual behaviour of the house. The material properties are fixed, and these were adopted from the test results of the newly developed Engineering Masonry Model by DIANA FEA BV. A 2-D element macro modelling was adopted.

The applied earthquake load is hypothetical, a uniform pushover load is adopted. In a real seismic event the loads are cyclic. There are more sophisticated methods to perform these pushover analysis.

The connections were modelled by the use of linear springs. However, the actual behaviour of a terraced house would suggest definition of non-linear properties for the springs, and interfaces between wall-wall connections. The timber beams and planks are considered to be merged in this modelling approach, but a more detailed approach would be to include the shear and flexural deformation of the board, along with friction due to nails slip.

The inclusion of staircase openings (SO) results in a stiffer behaviour of the structure. The reason behind this strange behaviour of the structure is, one: The staircase openings are directly connected to the wall, and second is that they don't have any springs attached to them. So the timber beams transfer all the forces and bending moment to the wall. This results in a conservative approach, as in practice these beams behave in a similar way to that of timber beams supporting the slabs.

The variation studies performed in this report are primitive, as there are only global index defined for the irregularity in front and back façades. A detailed approach is required in classifying these irregularities which includes global and local index, along with percentage of available masonry area. The cross-section of the lintel beams should be taken into account accordingly with respect to the size of the openings. In this study the cross-section is fixed and that results in a lower capacity of the structure.

# Conclusions and Recommendations 7

## 7.1 Conclusions

In this section, an effort is made to answer the research questions raised in the introduction in a systematic way. There are no experimental results available to support the base case study. A sensitivity study was carried out to see the influence on the capacity of structure by varying the geometrical characteristics of the building.

Interpretations were made by taking individual irregularities into consideration and drawing out conclusions, following which a global comparison is done to show the effect of the irregularities.

From the variations studies, it can be concluded that the inclusion of lintel beams does increase the capacity of the structure; as the masonry elements above the openings are resting over the lintel beam. In this research the cross-section and material properties of the lintel beams are fixed; but by varying the size of the openings, according to practice the cross-section and material properties of the lintel beams are modified based on the design estimations. This might result in a higher capacity of the structure than obtained in this research.

The variation of geometrical characteristics is implemented by defining irregularity index. There are four variations done in this study, and conclusions are drawn by taking individual variation into consideration.

**Variations excluding irregularity – Increasing the height of openings, inclusion/exclusion of staircase openings**

- The inclusion of staircase openings results in a stiffer behaviour of the structure. The reason behind this strange behaviour of the structure is, one: The staircase openings are directly connected to the wall, and second is that they don't have any springs attached to them. This implies that the beam shares all degrees of freedom with the masonry wall. This results in a conservative approach, as in practice these beams behave in a similar way to that of timber beams supporting the slabs.
- The exclusion of lintel beams(NLB) results in both loss of capacity (46.2% of case study) and ductility (61.5% of the structure) of the structure.
- Increasing the height of openings to Z1 and Z2 results in a lower capacity of the structure.

**Vertical Irregularity – varying the width of openings**

- In case of vertical irregularity ($I_V^F = 0.88 \& I_V^B = 0.55$) with inclusion of lintel beams (LB), and no staircase openings (NSO); the capacity of the structure is reduced by 6.5% of the case study.
- But the exclusion of lintel beams (NLB) from the aforementioned case, has a major influence on the structure; as the capacity is reduced by 38.5% and the ductility by 62%.
- The case where the height of openings is increased, vertical irregularity ($I_V^F = 0.88 \& I_V^B = 0.55$) with inclusion of lintel beams (LB), and no staircase openings (NSO); the capacity of the structure is reduced by 30% of the case study.

From the above results we can conclude that by increasing the vertical irregularity index the capacity of the structure decreases. The failure mechanisms differ from case to case.

**Horizontal Irregularity – varying the height of openings**

- The absence of lintel beams results in a weaker behaviour of masonry elements above the openings in front and back façade leading to a localised failure.

– However, the inclusion of lintel beams results in a stiffer behaviour of the masonry elements above the openings in the façade, this results in diagonal shear cracks in the back façade near the base, and they are subsequently followed by the base shear failure.

Increasing the horizontal irregularity index results in a reduced capacity of the structure.

**Number of Openings – varying the number of openings per story**

– By considering the variation N=3, the capacity of the building with the height of openings as "case study" is 5% higher than the building with height "Z1||Z2".
– In all these variations, after the peak load, the structure experiences base shear failure, as a result of which there is a drastic dissipation of energy leading to the brittle behaviour of the structure.

By varying the number of openings, it can be concluded that decreasing the number of openings, increases the capacity of the building.

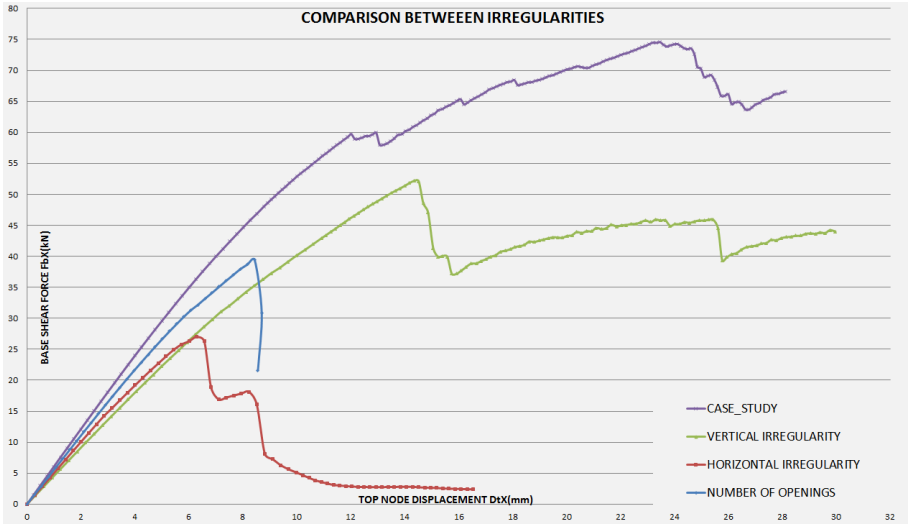


**Fig. 7.1.:** PUSHOVER CURVES - IRREGULARITY COMPARISON

The variations performed in this report gives a clear picture on the influence of the capacity of the structure. Different failure modes were observed in different cases.

From the variation studies shown with the irregularity index, and plotting the graph for the capacity of structure with the corresponding irregularity index; gives the reader a clear picture on predicting the capacity of the structure. The fact that the defined global irregularity index is primitive, this still gives an insight on the capacity of the structure obtained from varying the geometrical parameters. This indeed is the first step to perform sophisticated research on varying the geometrical parameters to develop an empirical model that could predict the capacity of the structure.

## 7.2 Recommendations

This study has shown that irregularities affects the capacity of the structure. However, these are strongly based on the modelling assumptions. The following recommendations are to be taken into account for further research in this field:

- Interfaces can be added to wall-wall connection, to make the model more realistic. Use of non-linear springs instead of linear springs leads to a more sophisticated approach.
- Detailed modelling of cavity walls by taking the external leaf into account as a structural member, and inclusion of anchors between external and internal leaf.
- Detailed research on the behaviour of the timber floor system, as the beams and floors are merged in this research. A more detailed research would involve timber nails and smaller timber sheaths.
- Only linear design of lintel beams are considered in this case, a detailed approach would be to model different types of lintel beams and schematizing it to Finite element programme.
- The base is considered to be fixed throughout this study. Inclusion of soil-structure interaction in the model is considered to be key for further research,
- The irregularity index are defined globally only for the front and back façades in this study. A more detailed approach would be to take into account all the walls, and also defining local index and percentage of area for a better classification, and more sophisticated way of sensitivity study.
- The lintel beams should be altered when it comes to material properties and cross-section, with respect to the size of opening.
- By performing more variations with the irregularity index, a regression analysis can be performed. Regression analysis will describe each capacity parameter under varying irregularity index, which can provide empirical models for the seismic assessment of the structure.

# Bibliography


[1] PAULO B Lourenco. *Computational strategies for masonry structures*. TU Delft, Delft University of Technology, 1996.

[2] K Mosalam, L Glascoe, and J Bernier. „Mechanical properties of unreinforced brick masonry section-1“. In: *Documented to US Department of Energy by Lawrence Livermore National Laboratory* (2009).

[3] M Dhanasekar, AW Page, and PW Kleeman. „The failure of brick masonry under biaxial stresses.“ In: *Proceedings of the Institution of Civil Engineers* 79.2 (1985), pp. 295–313.

[4] Paulo B Lourenço. „Computational strategies for masonry structures: multi-scale modeling, dynamics, engineering applications and other challenges“. In: *Congreso de Métodos Numéricos en Ingeniería*. SEMNI. 2013, pp. 1–17.

[5] L Boussabah and M Bruneau. „Review of the seismic performance of unreinforced masonry walls“. In: *Proc. of the 10th World Conf on Eq. Eng*. 1992, pp. 4537–4540.

[6] Michel Bruneau. „Seismic evaluation of unreinforced masonry buildings-a state-of-the-art report“. In: *Canadian Journal of Civil Engineering* 21.3 (1994), pp. 512–539.

[7] Michel Bruneau. „State-of-the-art report on seismic performance of unreinforced masonry buildings“. In: *Journal of Structural Engineering* 120.1 (1994), pp. 230–251.

[8] Michel Bruneau. „Performance of masonry structures during the 1994 Northridge (Los Angeles) earthquake“. In: *Canadian Journal of Civil Engineering* 22.2 (1995), pp. 378–402.

[9] K Deppe. „The Whittier Narrows, California Earthquake of October 1, 1987-Evaluation of strengthened and unstrengthened unreinforced masonry in Los Angeles city“. In: *Earthquake Spectra* 4.1 (1988), pp. 157–180.

[10] DF Peralta, JM Bracci, and MBD Hueste. „Seismic performance of rehabilitated floor and roof diaphragms“. In: *ST-8 project final report, Mid-America Earthquake Center, National Science Foundation, Texas A&M Univ. Dept. of Civil Eng. College, Texas* (2000).

[11] Miha Tomazevic. *Earthquake-resistant design of masonry buildings*. Vol. 1. World Scientific, 1999.

[12] MA ElGawady, P Lestuzzi, and M Badoux. „Retrofitting of masonry walls using shotcrete“. In: *2006 NZSEE Conference, Paper*. Vol. 45. 2006.

[13] Luis F Restrepo-Velez and Guido Magenes. „Simplified procedure for the seismic risk assessment of unreinforced masonry buildings“. In: *Proceedings of the 13th World Conference on Earthquake Engineering*. 2004.

[14] Fulvio Parisi and Nicola Augenti. „Seismic capacity of irregular unreinforced masonry walls with openings“. In: *Earthquake Engineering & Structural Dynamics* 42.1 (2013), pp. 101–121.

[15] Tianyi Yi, Franklin L Moon, Roberto T Leon, and Lawrence F Kahn. „Lateral load tests on a two-story unreinforced masonry building“. In: *Journal of Structural Engineering* 132.5 (2006), pp. 643–652.

[16] A Brignola, S Podestà, and S Pampanin. „In-plane stiffness of wooden floor“. In: (2008).

[17] Stylianos Antoniou. „Advanced inelastic static analysis for seismic assessment of structures“. PhD thesis. Imperial College London (University of London), 2002.

[18] *University of Buffalo*. `http://civil.eng.buffalo.edu/cie619/3-handouts/cie619-lecture12-nonlinearanalysisstatic.pdf`. [Online; accessed 20-April-2016]. 2009.

[19] Erol Kalkan and Sashi K Kunnath. „Assessment of current nonlinear static procedures for seismic evaluation of buildings“. In: *Engineering Structures* 29.3 (2007), pp. 305–316.

[20] EN 1998-1. „Eurocode 8: Design of structures for earthquake resistance-part 1: general rules, seismic actions and rules for buildings“. In: (2004).

[21] EN 1998-3. „Eurocode 8: Design of structures for earthquake resistance-part 3: Assessment and retrofitting of buildings“. In: (2005).

[22] Anil K Chopra and Rakesh K Goel. „Capacity-demand-diagram methods for estimating seismic deformation of inelastic structures: SDF systems“. In: *Civil and Environmental Engineering* (1999), p. 53.

[23] Clive Allen, MJ Masia, H Derakhshan, et al. „What ductility value should be used when assessing unreinforced masonry buildings?“ In: *NZSEE Conference*. 2013.

[24] C Calderini, S Cattari, S Degli Abbati, et al. „Modelling strategies for seismic global response of building and local mechanisms“. In: *PERPETUATE (EU-FP7 Research Project), Deliverable D* 26 (2012).

[25] ATC ATC. „40, Seismic evaluation and retrofit of concrete buildings“. In: *Applied Technology Council, report ATC-40. Redwood City* (1996).

[26] ARUP. „Implementation Study“. In: (2013).

[27] FEMA356. „Prestandard and Commentary for the Seismic Rehabilitation of Buildings: Rehabilitation Requirement s“. In: American Society of Civil Engineers Washington, DC. 2000.

[28] KNGMG NWO-ALW. „Geo-brief“. In: 2014.

[29] KNMI. „Report on the expected PGV and PGA values for induced earthquakes in the Groningen area“. In: 2013.

[30] Guido Magenes and Andrea Penna. „Existing masonry buildings: general code issues and methods of analysis and assessment“. In: *Workshop: EC*. Vol. 8. 2009.

[31] NAM. „Ontwerpuitgangspunten. Bouwkunding versterken van bestaande gebouwen tegen aardbevingsbelasting in de Groningen regio“. In: 2015.

[32] Jason Ingham and Michael Griffith. „Performance of unreinforced masonry buildings during the 2010 Darfield (Christchurch, NZ) earthquake“. In: *Australian Journal of Structural Engineering* 11.3 (2010), pp. 207–224.

[33] Royal Netherlands Meteorological Institute. „Monitoring induced seismicity in the North of the Netherlands.“ In: 2012.

[34] DIANA FEA BV. „DIANA DEV user's masnual“. In: 2015.

[35] DIANA FEA BV. „DIANA 10.1 user's masnual“. In: 2016.

# List of Figures

# List of Tables

# Appendix

# Target Displacement Calculation

# A

## A.1 Elastic Response Spectrum-NPR

The response spectrum is defined based on the following equations (NPR 9998:2015):

$$T = 0 : S_e(T) = \frac{S_{MS}}{3}$$

$$0 < T \leq T_B : S_e(T) = \frac{S_{MS}}{3} * (1 + \frac{T}{T_B} * [\eta * 3 - 1])$$

$$T_B \leq T \leq T_C : S_e(T) = S_{MS}\eta$$

$$T_C \leq T : S_e(T) = \frac{S_{M1}}{T^2}\eta$$

Where:

- $S_e(T)$ – is the elastic response spectrum, in g;
- $T$ – is the oscillation period of a linear system with one degree of freedom, in s;
- $T_B$ – the lower limit in period of the constant spectral acceleration branch, in s;
- $T_C$ – the upper limit in period of the constant spectral acceleration branch, in s;
- $S_{MS}$ – the spectral acceleration for the short oscillation period, in g;
- $S_{M1}$ – the spectral acceleration for the long-period oscillation, in g;
- $a_g$ – ground acceleration.

The parameters taken into account for the horizontal elastic spectrum are presented in the following table:

**Tab. A.1.:** Horizontal Response Spectrum Parameters

| *S.No* | *Parameter* | *Value* |
|---|---|---|
| 1 | $S_{MS}$ | 0.919(g) |
| 2 | $S_{M1}$ | 0.501(g) |
| 3 | $T_B(s)$ | 0.148 |
| 4 | $T_C(s)$ | 0.738 |
| 5 | $a_g$ | 0.36(g) |

Based on the values from the table and the formulae mentioned, a graph was plotted between elastic spectrum ($S_e(g)$) and time period (T). The graph is shown in Figure A.1.

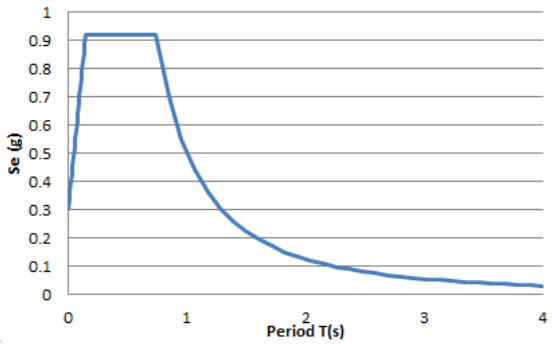


**Fig. A.1.:** HORIZONTAL ELASTIC SPECTRUM

## A.2 Conversion of Elastic Spectrum to A-D Format

For the transformation, the following formula is considered:

$$S_d = S_a . \frac{T^2}{4\pi^2}$$

| T | $S_e(T)$ (0 m | Sa (m/s2 | Sd(m) |
|---|---|---|---|
| (s) | (g) | | |
| 0.000 | 0.306 | 3.0051 | 0 |
| 0.007 | 0.337 | 3.3056 | 4.5605E-06 |
| 0.015 | 0.368 | 3.6062 | 1.99E-05 |
| 0.022 | 0.398 | 3.9067 | 4.8507E-05 |
| 0.030 | 0.429 | 4.2072 | 9.2868E-05 |
| 0.037 | 0.460 | 4.5077 | 0.00015547 |
| 0.044 | 0.490 | 4.8082 | 0.0002388 |
| 0.052 | 0.521 | 5.1087 | 0.00034535 |
| 0.059 | 0.552 | 5.4092 | 0.00047761 |
| 0.066 | 0.582 | 5.7097 | 0.00063805 |
| 0.074 | 0.613 | 6.0103 | 0.00082918 |
| 0.081 | 0.644 | 6.3108 | 0.00105347 |
| 0.089 | 0.674 | 6.6113 | 0.00131342 |
| 0.096 | 0.705 | 6.9118 | 0.00161151 |
| 0.103 | 0.735 | 7.2123 | 0.00195023 |
| 0.111 | 0.766 | 7.5128 | 0.00233206 |
| 0.118 | 0.797 | 7.8133 | 0.0027595 |
| 0.125 | 0.827 | 8.1138 | 0.00323504 |
| 0.133 | 0.858 | 8.4144 | 0.00376115 |
| 0.140 | 0.889 | 8.7149 | 0.00434033 |
| 0.148 | 0.919 | 9.0154 | 0.00497507 |
| 0.738 | 0.919 | 9.0154 | 0.12437671 |
| 0.847 | 0.698 | 6.8486 | 0.12437671 |
| 0.955 | 0.548 | 5.3786 | 0.12437671 |
| 1.064 | 0.442 | 4.3356 | 0.12437671 |
| 1.173 | 0.364 | 3.569 | 0.12437671 |
| 1.282 | 0.305 | 2.9891 | 0.12437671 |
| 1.390 | 0.259 | 2.5399 | 0.12437671 |
| 1.499 | 0.223 | 2.1848 | 0.12437671 |
| 1.608 | 0.194 | 1.8993 | 0.12437671 |
| 1.717 | 0.170 | 1.6663 | 0.12437671 |
| 1.825 | 0.150 | 1.4737 | 0.12437671 |
| 1.934 | 0.134 | 1.3127 | 0.12437671 |
| 2.043 | 0.120 | 1.1766 | 0.12437671 |
| 2.152 | 0.108 | 1.0607 | 0.12437671 |
| 2.260 | 0.098 | 0.9611 | 0.12437671 |
| 2.369 | 0.089 | 0.8749 | 0.12437671 |
| 2.478 | 0.082 | 0.7998 | 0.12437671 |
| 2.586 | 0.075 | 0.734 | 0.12437671 |
| 2.695 | 0.069 | 0.676 | 0.12437671 |
| 2.804 | 0.064 | 0.6245 | 0.12437671 |
| 2.913 | 0.059 | 0.5788 | 0.12437671 |
| 3.021 | 0.055 | 0.5379 | 0.12437671 |
| 3.130 | 0.051 | 0.5012 | 0.12437671 |
| 3.239 | 0.048 | 0.4681 | 0.12437671 |
| 3.348 | 0.045 | 0.4382 | 0.12437671 |
| 3.456 | 0.042 | 0.411 | 0.12437671 |
| 3.565 | 0.039 | 0.3863 | 0.12437671 |
| 3.674 | 0.037 | 0.3638 | 0.12437671 |
| 3.783 | 0.035 | 0.3432 | 0.12437671 |
| 3.891 | 0.033 | 0.3243 | 0.12437671 |
| 4.000 | 0.031 | 0.3069 | 0.12437671 |

**Fig. A.2.:** CONVERSION TO AD FORMAT

## A.3 Conversion of MDOF to SDOF system

$$m^* = \Sigma m_i.\phi_i = \frac{60.317}{2}(1 + 0.5) = 45.2377$$

$$\Gamma = \frac{m^*}{\Sigma m_i \phi^2} = 1.2$$

Bi-Linear approximation:

**Tab. A.2.:** Idealized Curve

| $F^*(kN)$ | $d^*(m)$ | $\frac{F^*}{m^*} ms^{-2}$ |
|---|---|---|
| 0 | 0 | 0 |
| 32.6798 | 0.008 | 0.72 |
| 54.4664 | 0.01399 | 1.2 |
| 54.4664 | 0.025 | 1.2 |

Capacity curves and bilinear approximation are shown in Figure A.3.

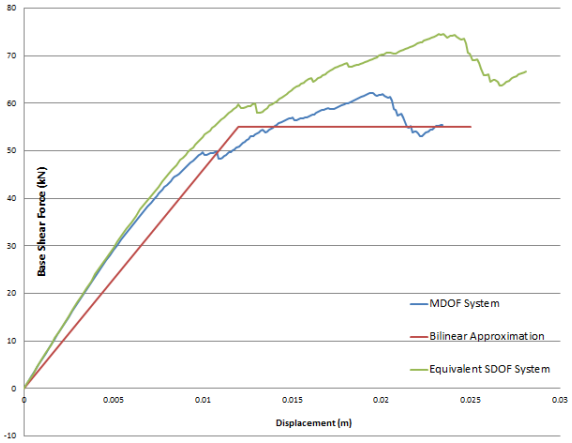


**Fig. A.3.:** CAPACITY CURVES

## A.4 Period and Target Displacement of SDOF System

Period:

$$T^* = 2\pi\sqrt{\frac{m^* d_y^*}{F_y^*}} = 0.6s$$

Target Displacement:

$$d_{et}^* = S_e(T^*)[\frac{T^*}{2\pi}]^2 = 0.035m$$

As $T^* < T_C$ and $\frac{F_y^*}{m^*} \leq S_e(T^*)$ :

$$d_t^* = d_{et}^* = 0.035m$$

## A.5 MDOF Target Displacement

$$d_t = \Gamma.d_t^* = 0.042m$$

# Case Study

# B

## B.1 Drawings

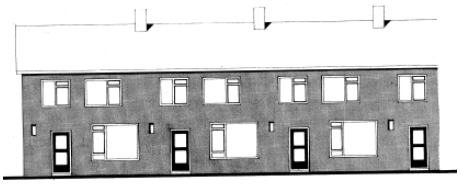

(a) FRONT VIEW

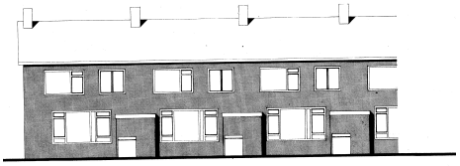

(b) BACK VIEW

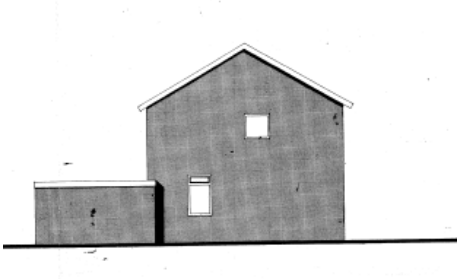

(c) SIDE VIEW (LEFT END)

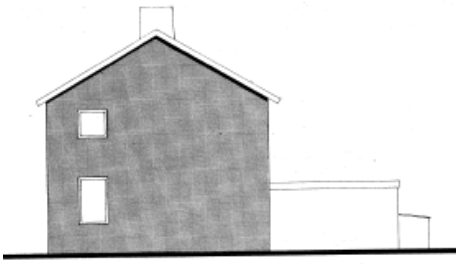

(d) SIDE VIEW (RIGHT END)

**Fig. B.1.:** ROW OF TERRACED HOUSES

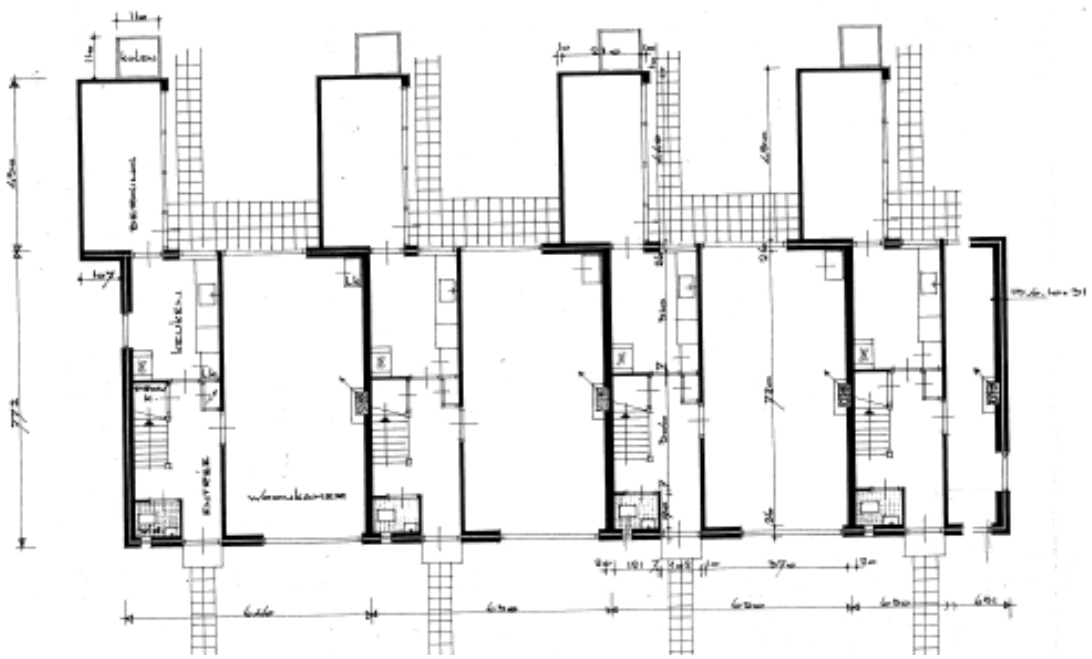

(a) GROUND FLOOR

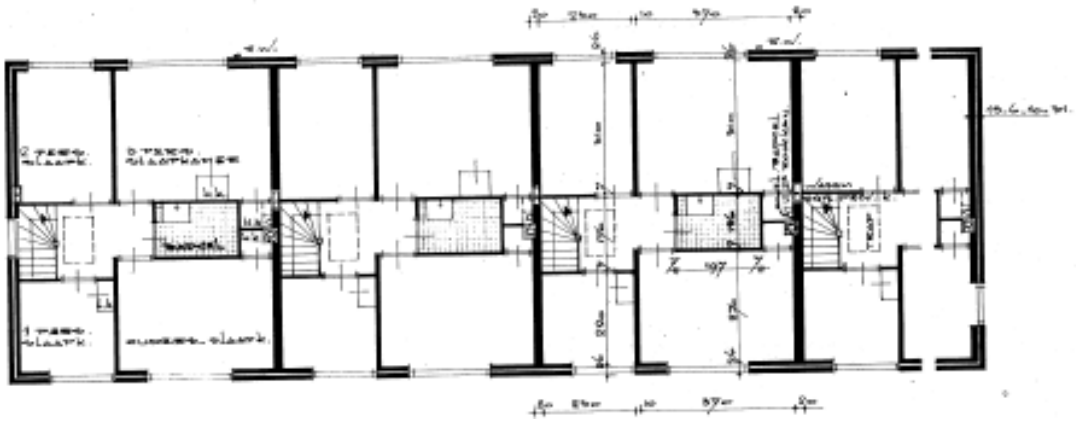

(b) FIRST FLOOR

Fig. B.2.: PLAN VIEW- ROW OF TERRACED HOUSES

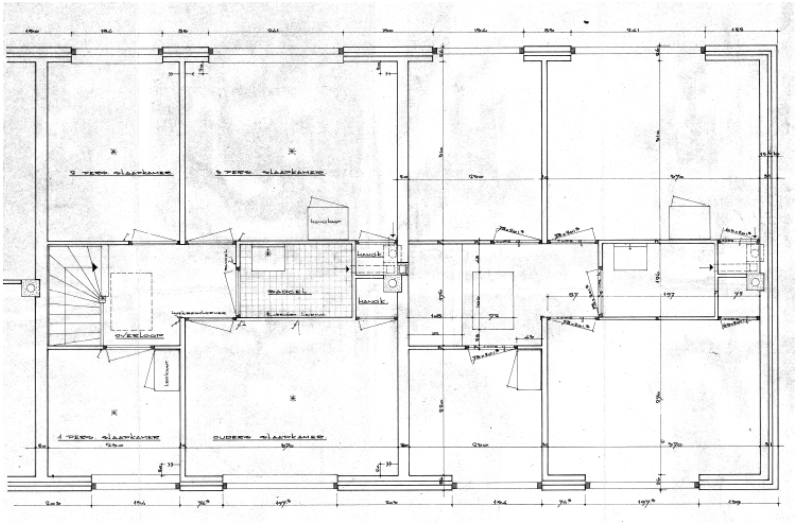

Fig. B.3.: FIRST FLOOR PLAN - SINGLE TERRACED HOUSE

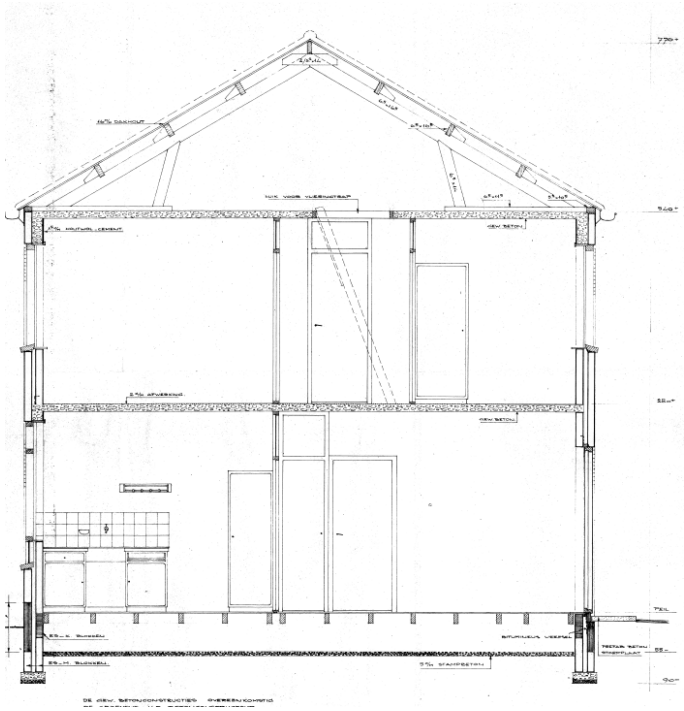

Fig. B.4.: SECTION - SINGLE TERRACED HOUSE

## B.2 Solving Procedures Comparison

The pushover analysis is performed under a force convergence norm, but due to the lack of poor convergence after the peak load; arc-length method is activated. The arc-length is controlled by certain set of node sets. These nodes are located where displacements for the pushover curves are obtained. And they are controlled in X-direction. A snippet of the command file is shown in Figure B.5.

```
BEGIN EXECUT
  BEGIN LOAD
    LOADNR 2
    BEGIN STEPS
      BEGIN EXPLIC
        SIZES 0.00200000(35) 0.00100000(500)
        ARCLEN REGULA SET NODES 4175 4180 4184 4199-4206 4236 4250 \
                                4339-4345(2) 4350 4352 4354 4407 4409 4411 \
                                4416 4436 /
      END EXPLIC
    END STEPS
  END LOAD
  BEGIN ITERAT
    MAXITE 100
    METHOD NEWTON
    BEGIN CONVER
      BEGIN FORCE
        TOLCON 0.001
```

Control Sets for arc-length

**Fig. B.5.:** CONTROL SETS - ARC LENGTH (COMMAND FILE)

The comparison between the stated methods are shown in Figure B.6.

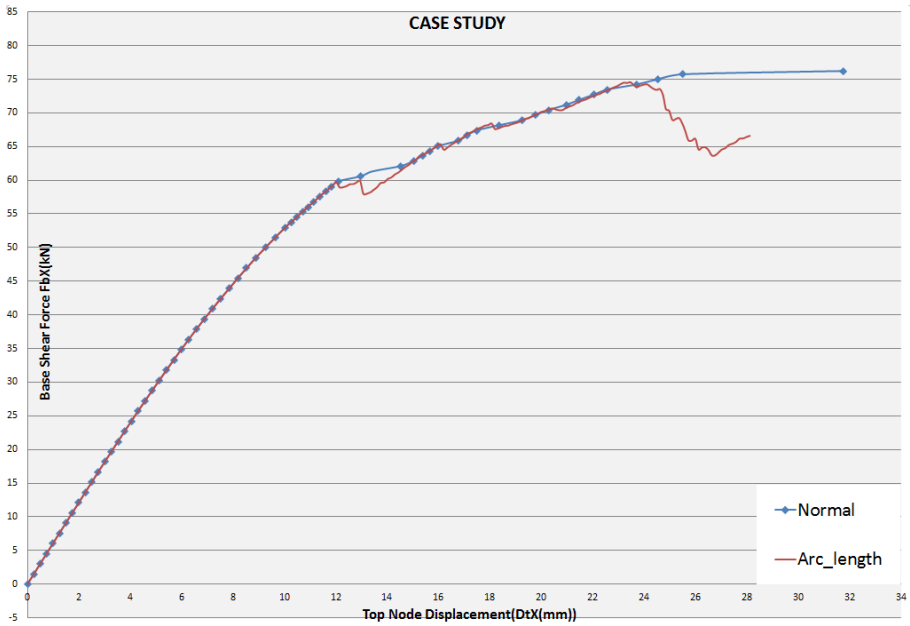


**Fig. B.6.:** PUSHOVER CURVES COMPARISON

## B.3 Inter-Story Drift and Displacements

In this section, graphs are plotted between the base shear force at the bottom of the building and the corresponding displacements at the mid-point of floors, including the top node(roof) and are shown in Figure B.7. The drift is defined as follows:

$$u_i = \frac{d_i}{H_i}$$

where:
$u_i$ – Drift at $i^{th}$ floor;
$d_i$ – Displacement at $i^{th}$ floor;
$H_i$ – Height of $i^{th}$ floor.
The graphs for the same are shown in Figure B.8.

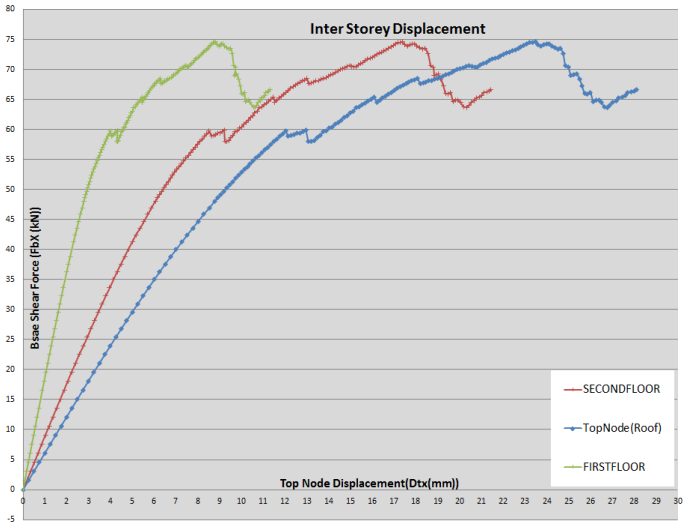


**Fig. B.7.:** INTER-STORY DISPLACEMENT

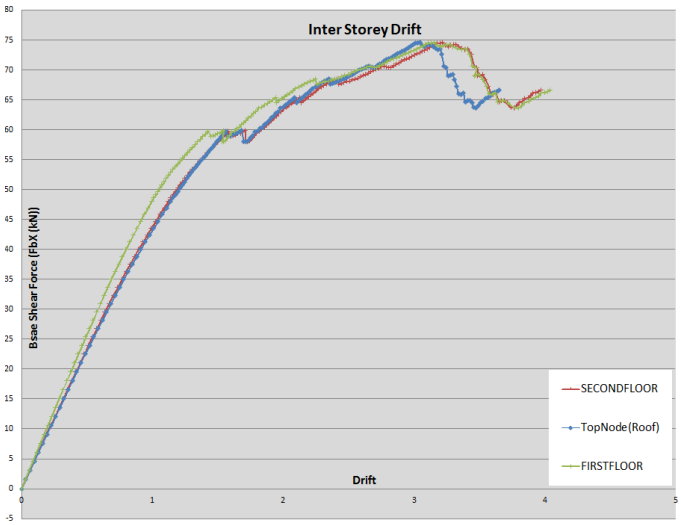


**Fig. B.8.:** INTER-STORY DRIFT

## B.4 Crack-Widths

The crack-widths of selected steps are represented in the graph (Figure B.9).

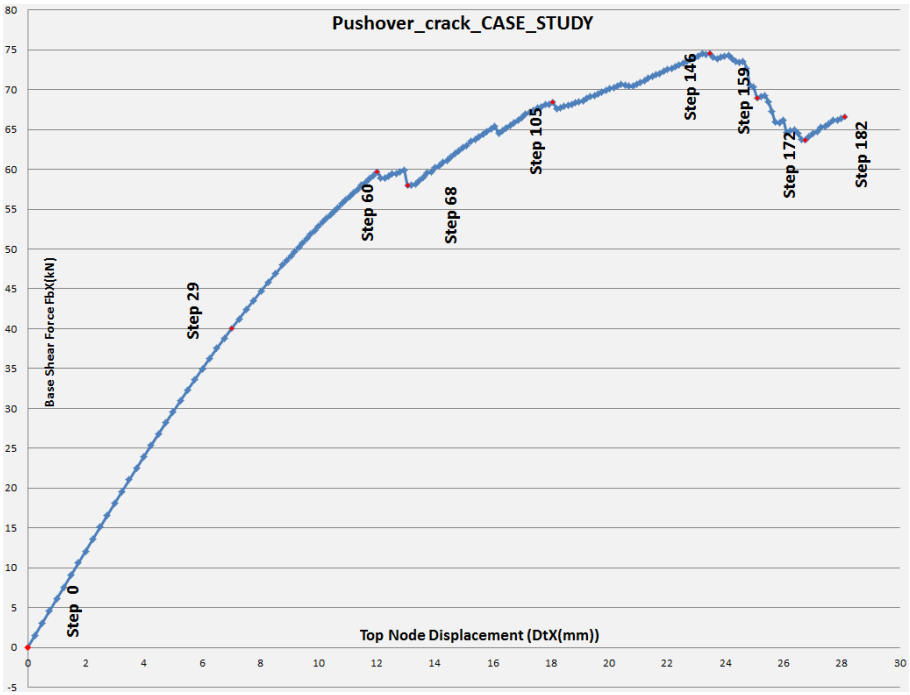


**Fig. B.9.:** PUSHOVER CURVE (STEPS- CRACK-WIDTH)

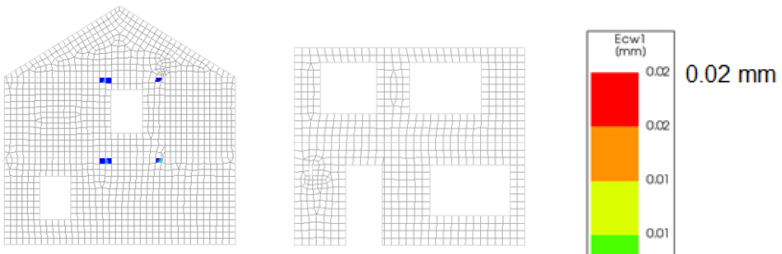


(a) SIDE WALL 1 (c) FRONT FAÇADE (e) WIDTH

(b) SIDE WALL 2 (d) BACK FAÇADE

Fig. B.10.: CRACK-WIDTH STEP 0

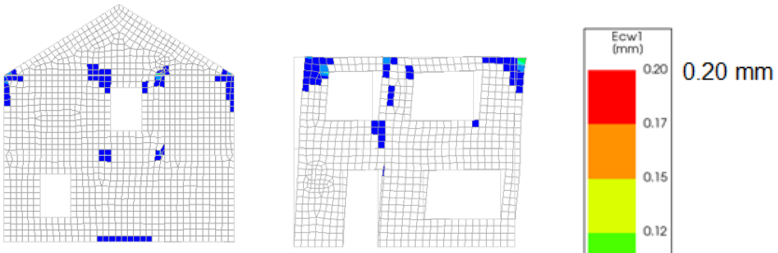


(a) SIDE WALL 1 (c) FRONT FAÇADE (e) WIDTH

(b) SIDE WALL 2 (d) BACK FAÇADE

Fig. B.11.: CRACK-WIDTH STEP 29

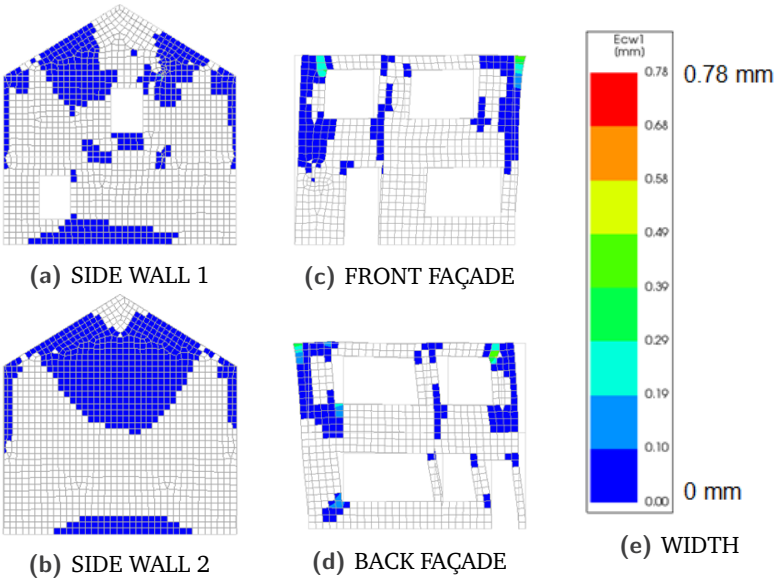


(a) SIDE WALL 1 (c) FRONT FAÇADE

(b) SIDE WALL 2 (d) BACK FAÇADE (e) WIDTH

**Fig. B.12.:** CRACK-WIDTH STEP 60

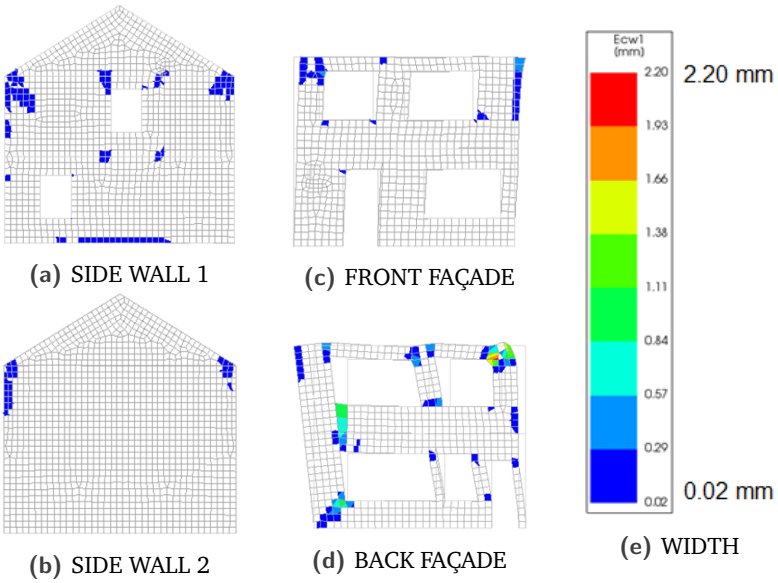


(a) SIDE WALL 1 (c) FRONT FAÇADE

(b) SIDE WALL 2 (d) BACK FAÇADE (e) WIDTH

**Fig. B.13.:** CRACK-WIDTH STEP 68

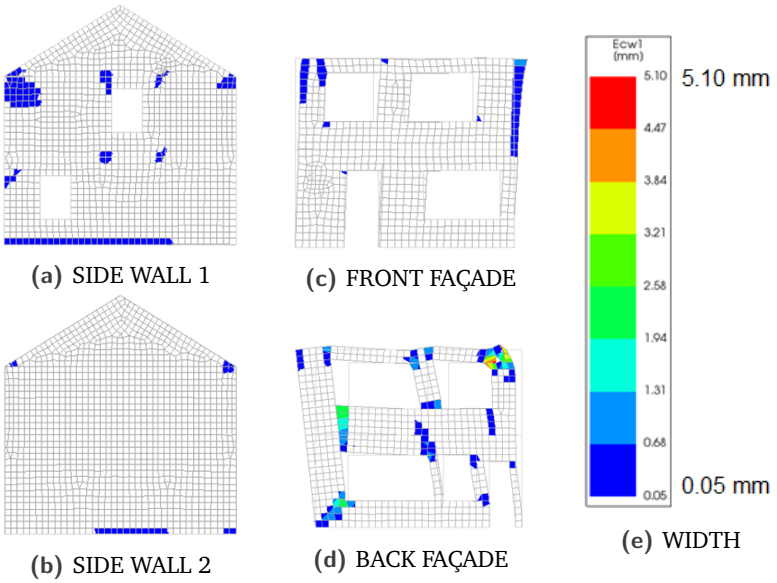


(a) SIDE WALL 1 (c) FRONT FAÇADE

(b) SIDE WALL 2 (d) BACK FAÇADE

(e) WIDTH

Fig. B.14.: CRACK-WIDTH STEP 105

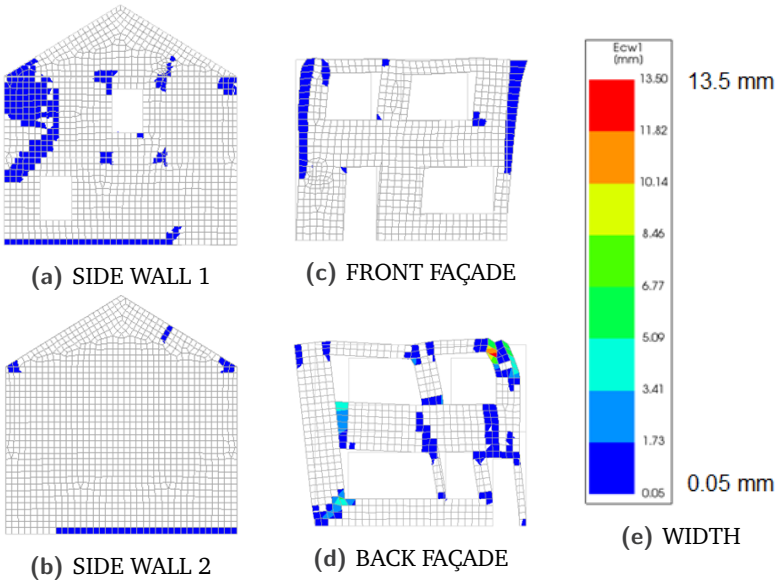


(a) SIDE WALL 1 (c) FRONT FAÇADE

(b) SIDE WALL 2 (d) BACK FAÇADE

(e) WIDTH

Fig. B.15.: CRACK-WIDTH STEP 146

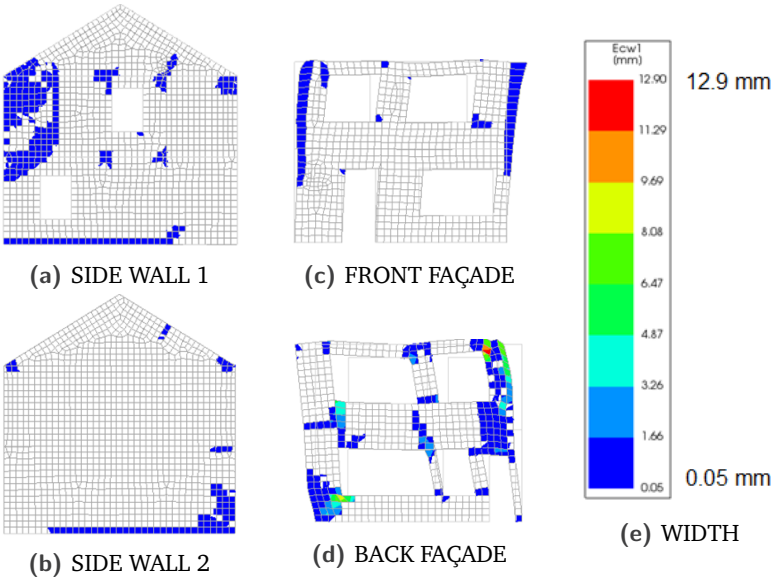


(a) SIDE WALL 1 (c) FRONT FAÇADE

(b) SIDE WALL 2 (d) BACK FAÇADE

(e) WIDTH

Fig. B.16.: CRACK-WIDTH STEP 159

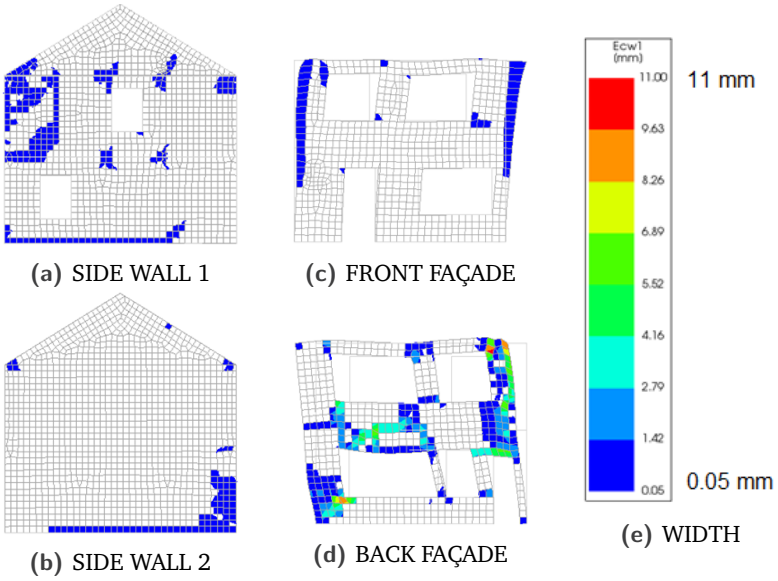


(a) SIDE WALL 1 (c) FRONT FAÇADE

(b) SIDE WALL 2 (d) BACK FAÇADE

(e) WIDTH

Fig. B.17.: CRACK-WIDTH STEP 172

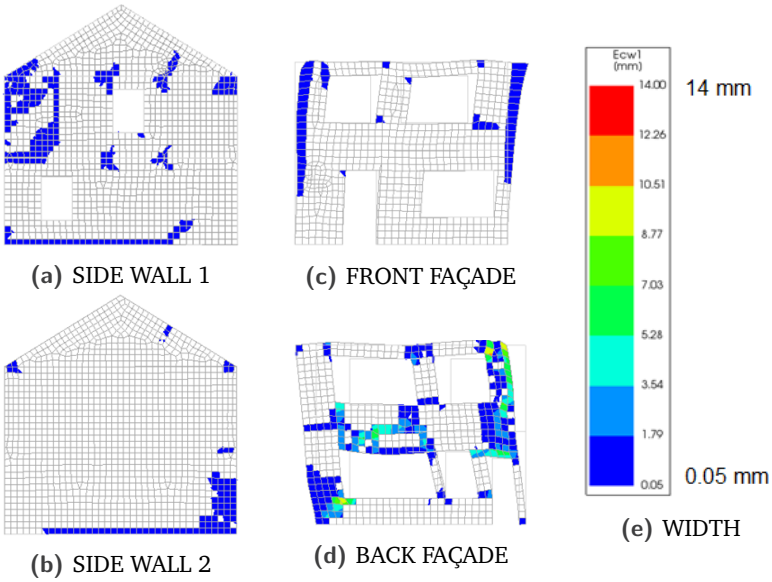


(a) SIDE WALL 1 (c) FRONT FAÇADE (e) WIDTH

(b) SIDE WALL 2 (d) BACK FAÇADE

**Fig. B.18.:** CRACK-WIDTH STEP 182

# Python Script

C

## C.1 User-Defined Parameters

```
#Terraced_Houses

#### PARAMETER STARTS
#First a list is made for all parameters,that  the user has freedom to enter
newProject( "parametrised_house", 100 )

#
#1. Length,breadth and Height of House
#everything in meters
#Length=6.3              Breadth=7.46     Height= 7.7
x_min=0
y_min=0
z_min=0
x_max=6.3
y_max=7.46
z_max=7.7


#2. Number of Floors( including GF)=3
#height of floors ( 0, 2.8, 5.4 )
Z_0=z_min
Z_1=z_max/(7.7/2.8)
Z_2=z_max/(7.7/5.4)

#Floor_1 and 2 co-ord
x_F_1_S= x_max/(6.3/0.06)
x_F_1_E= x_max/(6.3/1.31)
y_F_1_E= y_max/(7.46/2.365)
y_F_1_S= y_max/(7.46/0.06)
#1 co-ord [ x_F_1_S, y_F_1_S, Z_1(Z_2) ], [ x_F_1_E, y_F_1_E, Z_1(Z_2) ]
x_F_2_S= x_max/(6.3/1.38)
x_F_2_E= x_max/(6.3/2.39)
y_F_2_S= y_max/(7.46/0.06)
y_F_2_E= y_max/(7.46/1.1)
#2 co-ord [ x_F_2_S, y_F_2_S, Z_1 ], [ x_F_2_E, y_F_2_E, Z_1 ]
x_F_3_S= x_max/(6.3/0.06)
x_F_3_E= x_max/(6.3/2.39)
y_F_3_S= y_max/(7.46/1.1)
y_F_3_E= y_max/(7.46/2.33)
#3 co-ord [ x_F_3_S, y_F_3_S, Z_1 ], [ x_F_3_E, y_F_3_E, Z_1 ]
x_F_4_S= x_max/(6.3/1.08)
x_F_4_E= x_max/(6.3/2.39)
y_F_4_S= y_max/(7.46/2.365)
y_F_4_E= y_max/(7.46/4.195)
#4 co-ord [ x_F_4_S, y_F_4_S, Z_1(Z_2) ], [ x_F_4_E, y_F_4_E, Z_1(Z_2) ]
x_F_5_S= x_max/(6.3/0.06)
x_F_5_E= x_max/(6.3/2.39)
y_F_5_S= y_max/(7.46/4.195)
y_F_5_E= y_max/(7.46/7.40)
#5 co-ord [ x_F_5_S, y_F_5_S, Z_1(Z_2) ], [ x_F_5_E, y_F_5_E, Z_1(Z_2) ]
x_F_6_S= x_max/(6.3/2.51)
x_F_6_E= x_max/(6.3/6.24)
y_F_6_S= y_max/(7.46/0.06)
y_F_6_E= y_max/(7.46/2.83)
#6 co-ord [ x_F_6_S, y_F_6_S, Z_1(Z_2) ], [ x_F_6_E, y_F_6_E, Z_1(Z_2) ]
y_F_7_S= y_max/(7.46/2.9)
y_F_7_E= y_max/(7.46/4.16)
#7 co-ord [ x_F_6_S, y_F_7_S, Z_1(Z_2) ], [ x_F_6_E, y_F_7_E, Z_1(Z_2) ]
y_F_8_S= y_max/(7.46/4.23)
y_F_8_E= y_max/(7.46/7.40)
#8 co-ord [ x_F_6_S, y_F_8_S, Z_1(Z_2) ], [ x_F_6_E, y_F_8_E, Z_1(Z_2) ]

#Foundation

#3. Roof_walls
#there can be two different types of orientation
#for the moment just one orientation is considered
#RoofWalls
Roof_Wall=[ x_min, x_max ]

#4. Roof Slabs
#here there can be two options either include the slab, just as a self weight or include it as a material
#for now only as a geometry it is going to be taken

#5.Interior_walls dialog box will appear for 0_1_Level
#For the walls we get the input from user,
#start and the end location of walls are given
#Walls co-ord [ x1, y1, z1 ], [ x2, y2, z2 ]
#After which the sheets for the walls will be created
#first in Xdirection and then in Y direction
#and the user can enter the start and  end co-ordinates of individual Walls
#Walls in X Direction
y_IW_1= y_max/(7.46/1.065)
x_IW_1= x_max/(6.3/1.345)
```

```
#IW_1 co-ord [ 0, y_IW_1, Z_0], [ x_IW_1, y_IW_1, Z_1 ]
#
y_IW_2= y_max/(7.46/4.195)
x_IW_2= x_max/(6.3/2.45)
#IW_2 co-ord [  0, y_IW_2, Z_0], [ x_IW_2, y_IW_2, Z_1 ]
#
#Walls in Y Direction
x_IW_3= x_max/(6.3/1.345)
y_IW_3= y_IW_1
#IW_3 co-ord [ x_IW_3, y_min, Z_0 ], [ x_IW_3, y_IW_3, Z_1 ]
#
x_IW_4= x_IW_2
#IW_4 co-ord [ x_IW_4, y_min, Z_0 ], [ x_IW_4, y_max, Z_1 ]


#6. After The interior wall are conMasonry_Walltructed the user is asked for openings in the walls in the particular levels
#The idea is to ask for opening if yes then make a list of the walls in the walls in the floor
#and allow the user to select the walls that has openings
#once selection has been made , system selects every wall and asks for location of opening
#and also add opening dialgoue box should be placed for more openings in the same walls
#
#Openings
#maximum height of openings
z_0_H_1= z_max/(7.7/2.2)
#Wall_F_0
x_O_1_S= x_max/(6.3/0.4)
x_O_1_E= x_max/(6.3/0.5)
z_O_1_S= z_max/(7.7/1.9)
#O_1 co-ord [ x_O_1_S, y_min, z_O_1_S ], [ x_O_1_E, y_min, z_0_H_1 ]
x_D_1_S= x_max/(6.3/1.4)
x_D_1_E= x_max/(6.3/2.4)
#D_1 co-ord [ x_D_1_S, y_min, Z_0 ], [ x_D_1_E, y_min, z_0_H_1 ]
x_W_1_S= x_max/(6.3/3.7)
x_W_1_E= x_max/(6.3/5.9)
z_W_1_S= z_max/(7.7/0.8)
#W_1 co-ord [ x_W_1_S, y_min, z_W_1_S ], [ x_W_1_E, y_min, z_0_H_1 ]

#Wall_B_0
x_D_2_S= x_max/(6.3/0.2)
x_D_2_E= x_max/(6.3/1)
z_D_2_E= z_max/(7.7/2)
#D_2 co-ord [ x_D_2_S, y_max, Z_0 ], [ x_D_2_E, y_max, z_D_2_E ]
x_W_2_S= x_max/(6.3/1.4)
x_W_2_E= x_max/(6.3/2.4)
z_W_2_S= z_W_1_S
#W_2 co-ord [ x_W_2_S, y_max, z_W_2_S ], [ x_W_2_E, y_max, z_0_H_1 ]
x_W_3_S= x_max/(6.3/2.65)
x_W_3_E= x_max/(6.3/5.3)
z_W_3_S= z_W_1_S
#W_3 co-ord [ x_W_3_S, y_max, z_W_3_S ], [x_W_3_E, y_max, z_0_H_1 ]

#Wall_S1_0
y_W_4_S= y_max/(7.46/5.3)
y_W_4_E= y_max/(7.46/6.3)
z_W_4_S= z_W_1_S
#W_4 co-ord [ x_min, y_W_4_S, z_W_4_S ], [ x_min, y_W_4_E, z_0_H_1 ]

#Wall_S2_0
#y_W_5_S= y_max/(7.46/1.5)
#y_W_5_E= y_max/(7.46/2.5)
#z_W_5_S= z_W_1_S
#W_5 co-ord [ x_max, y_W_5_S, z_W_5_S ], [ x_max, y_W_5_E, z_0_H_1 ]

#IW_1
y_D_3= y_max/(7.46/1.065)
x_D_3_S= x_max/(6.3/0.3)
x_D_3_E= x_max/(6.3/1.3)
#D_3 co-ord [ x_D_3_S, y_D_3, Z_0 ], [ x_D_3_E, y_D_3, z_0_H_1 ]

#IW_2
y_D_4= y_max/(7.46/4.195)
x_D_4_S= x_max/(6.3/1)
x_D_4_E= x_max/(6.3/2)
#D_4 co-ord [ x_D_4_S, y_D_4, Z_0 ], [ x_D_4_E, y_D_4, z_0_H_1 ]

#IW_4
x_D_5= x_IW_2
y_D_5_S= y_max/(7.46/2.7)
y_D_5_E= y_max/(7.46/3.7)
#D_5 co-ord [ x_D_5, y_D_5_S, Z_0 ], [ x_D_5, y_D_5_E, z_0_H_1 ]
#


#7. After all the openings are created the next is to enter the Interior walls between floor 1 and 2
#following the same procedure
#Interior_walls ( betweeen Z_1 and Z_2)
#Walls in X Direction
y_IW_5= y_max/(7.46/2.365)
x_IW_5_E= x_max/(6.3/2.45)
#IW_5 co-ord [ x_min, y_IW_5, Z_1 ], [ x_IW_5_E, y_IW_5, Z_2 ]
#
y_IW_6= y_max/(7.46/2.865)
x_IW_6_S= x_max/(6.3/2.45)
#IW_6 co-ord [ x_IW_6_S, y_IW_6, Z_1 ], [ x_max, y_IW_6, Z_2 ]
#
y_IW_7= y_max/(7.46/3.53)
x_IW_7_S= x_max/(6.3/5.445)
#IW_7 co-ord [ x_IW_7_S, y_IW_7, Z_1 ], [ x_max, y_IW_7, Z_2 ]
```

```
#
y_IW_8= y_max/(7.46/4.195)
#IW_8 co—ord [ x_min, y_IW_8, Z_1 ], [ x_max, y_IW_8, Z_2 ]
#Walls in Y Direction
x_IW_9= x_max/(6.3/2.45)
y_IW_9_E= y_max/(7.46/2.865)
#IW_9 co—ord [ x_IW_9, y_min, Z_1 ], [ x_IW_9, y_IW_9_E, Z_2 ]
#
x_IW_10= x_IW_9
y_IW_10_S= y_IW_6
y_IW_10_E= y_IW_8
z_IW_10_S= z_max/(7.7/5)
#IW_10 co—ord [ x_IW_10, y_IW_10_S, z_IW_10_S ], [ x_IW_10, y_IW_10_E, Z_2 ]
#
x_IW_11= x_IW_9
y_IW_11_S= y_max/(7.46/4.195)
#IW_11 co—ord [ x_IW_11, y_IW_11_S, Z_1 ], [ x_IW_9, y_max, Z_2 ]
#
x_IW_12= x_max/(6.3/3.405)
y_IW_12_S= y_max/(7.46/2.865)
y_IW_12_E= y_max/(7.46/4.195)
#IW_12 co—ord [ x_IW_12, y_IW_12_S, Z_1 ], [ x_IW_12, y_IW_12_E, Z_2 ]
#
x_IW_13= x_max/(6.3/5.445)
y_IW_13_S= y_max/(7.46/2.865)
y_IW_13_E= y_max/(7.46/4.195)
#IW_13 co—ord [ x_IW_13, y_IW_13_S, Z_1 ], [ x_IW_11, y_IW_13_E, Z_2 ]


#8. Openings in the Walls between floor 1 and 2
#maximum height of Openings
z_1_H_2= z_max/(7.7/5)
z_W_S= z_max/(7.7/3.6)
#
x_W_6_S= x_max/(6.3/0.71)
x_W_6_E= x_max/(6.3/2.25)
x_W_7_S= x_max/(6.3/3.145)
x_W_7_E= x_max/(6.3/5.12)
#W_6 co—ord [ x_W_6_S, y_min, z_W_S ], [ x_W_6_E, y_min, z_1_H_2 ]
#W_7 co—ord [ x_W_7_S, y_min, z_W_S ], [ x_W_7_E, y_min, z_1_H_2 ]
#
x_W_8_S= x_max/(6.3/0.71)
x_W_8_E= x_max/(6.3/2.25)
x_W_9_S= x_max/(6.3/2.88)
x_W_9_E= x_max/(6.3/5.29)
#W_8 co—ord [ x_W_8_S, y_max z_W_S ], [ x_W_8_E, y_max, z_1_H_2 ]
#W_9 co—ord [ x_W_9_S, y_max z_W_S ], [ x_W_9_E, y_max, z_1_H_2 ]
#
y_W_10_S= y_max/(7.46/3)
y_W_10_E= y_max/(7.46/4)
#W_10 co—ord [ x_min, y_W_10_S, z_W_S ], [ x_min, y_W_10_E, z_1_H_2 ]
#
x_D_6_S= x_max/(6.3/1.27)
x_D_6_E= x_max/(6.3/2.02)
y_D_6= y_IW_5
#D_6 co—ord [ x_D_6_S, y_D_6, Z_1 ], [ x_D_6_E, y_D_6, z_1_H_2 ]
#
x_D_7_S= x_max/(6.3/2.55)
x_D_7_E= x_max/(6.3/3.3)
x_D_8_S= x_max/(6.3/5.5575)
x_D_8_E= x_max/(6.3/6.1875)
#D_7 co—ord [ x_D_7_S, y_IW_6, Z_1 ], [ x_D_7_E, y_IW_6, z_1_H_2 ]
#D_8 co—ord [ x_D_8_S, y_IW_6, Z_1 ], [ x_D_8_E, y_IW_6, z_1_H_2 ]
#
x_D_9_S= x_max/( 6.3/1.5)
x_D_9_E= x_max/(6.3/2.25)
x_D_10_S= x_max/(6.3/2.55)
x_D_10_E= x_max/(6.3/3.3)
x_D_11_S= x_max/(6.3/5.5575)
x_D_11_E= x_max/(6.3/6.1875)
#D_9 co—ord [ x_D_9_S, y_IW_8, Z_1 ], [ x_D_9_E, y_IW_8, z_1_H_2]
#D_10 co—ord [ x_D_10_S, y_IW_8, Z_1 ], [ x_D_10_E, y_IW_8, z_1_H_2 ]
#D_11 co—ord [ x_D_11_S, y_IW_8, Z_1 ], [ x_D_11_E, y_IW_8, z_1_H_2 ]
#
y_D_12_S= y_max/(7.46/3.065)
y_D_12_E= y_max/(7.46/3.815)
x_D_12= x_IW_11
#D_12 co—ord [ x_D_12, y_D_12_S, Z_1 ], [ x_D_12, y_D_12_E, z_1_H_2 ]
#


#9. If the staircase opening have to be included A dialog should be added,
# which will ask for the start and end location in every floor
#
#Stairs_opening
x_ST_E= x_max/(6.3/1.02)
y_ST_S= y_max/(7.46/2.365)
y_ST_E= y_max/(7.46/4.195)
#1_ST_2 co—ord [ x_min, y_ST_S, Z_1 ], [ x_ST_E, y_ST_E, Z_1 ]
#ATTIC STAIRS AT_ST co—ord [ x_min, y_ST_S, Z_2 ], [ x_ST_E, y_ST_E, Z_2 ]
#
#StairCase_Beams
#Level_1
#beam_1 co—ord [ x_min, y_ST_S, Z_1 ], [ x_ST_E, y_ST_S, Z_1 ]
#beam_2 co—ord [ x_ST_E, y_ST_S, Z_1 ], [ x_ST_E, y_ST_E, Z_1 ]
#beam_3 co—ord [ x_min, y_ST_E, Z_1 ], [ x_ST_E, y_ST_E, Z_1 ]
#Level_2
#beam_1 co—ord [ x_min, y_ST_S, Z_2 ], [ x_ST_E, y_ST_S, Z_2 ]
```

```
#beam_2 co-ord [ x_ST_E, y_ST_S, Z_2 ], [ x_ST_E, y_ST_E, Z_2 ]
#beam_3 co-ord [ x_min, y_ST_E, Z_2 ], [ x_ST_E, y_ST_E, Z_2 ]

#10. In the Roof slabs a dialogue box will appear
#here we create one beam after which spacing between the beams will be asked and also the number of beams


#11. Floor Beams
#here the user will have the freedom to choose the how many beams he wants to have in every floor and also give the spacing between them.
#All Floor Beams
#Number of beams and The spacings between the beam can be specified by the user
#the beams are modelled betweeen the ouer ND interior walls
#And  the are connected to the walls by springs as in practice the beams can move horizontally
#number of beams = 12
FF_spacing= (y_F_8_E-y_F_1_S)/13
#FirstFloor Beam locations( only start and end of x-cord)
#beam_first_ 0.06-2.39 beam_second_ 2.51-6.24
#beam_first_ 1.08-2.39 beam_second_ 2.51-6.24
beam_first_a_S= x_max/(6.3/0.06)
beam_first_a_E= x_max/(6.3/2.39)
beam_second_S= x_max/(6.3/2.51)
beam_second_E= x_max/(6.3/6.24)
beam_first_b_S= x_max/(6.3/1.08)
beam_first_b_E= x_max/(6.3/2.39)
#SecondFloor_beam location (only start and end of x-cord)
#beam_first_ 0.06-2.39 beam_second_ 2.51-6.24
#beam_first_ 1.08-2.39 beam_second_ 2.51-6.24
#beam_first_ 0.06-3.345 beam_second_ 3.465-6.24
#beam_first_c_S= x_max/(6.3/1.08)
#beam_first_c_E= x_max/(6.3/3.345)
#beam_second_c_S= x_max/(6.3/3.465)
#beam_second_c_E= x_max/(6.3/6.24)




#12.Lintel Beams
#Lintel Beams
#After the opening are made , the next dialogue box
#will be for Lintel Beams on the openings#if yes then the start and end location of beams,
#only beam elements are used as curvedshell wouldn't behave very well in the out of plane direction

#in every floor the linel beam co-ordinates are asked and a loop is made that generates the beams
#the list and also makes an imprint on the surface

#Lintel beams between 0 and 1
z_0_LB_1= z_max/(7.7/2.2)
#
#Wall_F_0
x_LB_1_S= x_O_1_S#LB co-ord
x_LB_1_E= x_O_1_E#LB co-ord
#O_1 co-ord [ [ x_LB_1_S, y_min, z_0_LB_1 ], [ x_LB_1_E, y_min, z_0_LB_1 ] ]
x_LB_2_S= x_D_1_S
x_LB_2_E= x_D_1_E
#D_1 co-ord [ [ x_LB_2_S, y_min, z_0_LB_1 ], [ x_LB_2_E, y_min, z_0_LB_1 ] ]
x_LB_3_S= x_W_1_S
x_LB_3_E= x_W_1_E
#D_1 co-ord [ [ x_LB_3_S, y_min, z_0_LB_1 ], [ x_LB_3_E, y_min, z_0_LB_1 ] ]
#Wall_B_0
x_LB_4_S= x_D_2_S
x_LB_4_E= x_D_2_E
#D_2 co-ord [ [ x_LB_4_S, y_max, z_D_2_E ], [ x_LB_4_E, y_max, z_D_2_E ] ]
x_LB_5_S= x_W_2_S
x_LB_5_E= x_W_2_E
x_LB_8_S= x_W_3_S
x_LB_8_E= x_W_3_E
#W_2 & W_3 co-ord [ [ x_LB_5_S, y_max, z_0_LB_1 ], [ x_LB_5_E, y_max, z_0_LB_1 ], [ x_LB_8_S, y_max, z_0_LB_1 ], [ x_LB_8_E, y_max, z_0_LB_1 ] ]
#Wall_S1_0
y_LB_6_S= y_W_4_S
y_LB_6_E= y_W_4_E
#W_4 co-ord [ [ x_min, y_LB_6_S, z_0_LB_1 ], [ x_min, y_LB_6_E, z_0_LB_1 ] ]
#Wall_S2_0
#y_LB_7_S= y_max/(7.46/1.4)
#y_LB_7_E= y_max/(7.46/2.6)
#W_5 co-ord [ [ x_max, y_LB_7_S, z_0_LB_1 ], [ x_max, y_LB_7_E, z_0_LB_1 ] ]
#IW_4
y_LB_10_S= y_D_5_S
y_LB_10_E= y_D_5_E
#D_5 co-ord [ [ x_D_5, y_LB_10_S, z_0_LB_1 ], [ x_D_5, y_LB_10_E, z_0_LB_1 ] ]

#Lintel Beams between 1 and 2
z_1_LB_2= z_max/(7.7/5)
#Wall_F_1
x_LB_11_S= x_W_6_S
x_LB_11_E= x_W_6_E
#W_6 co-ord [ [ x_LB_11_S, y_min, z_1_LB_2 ], [ x_LB_11_E, y_min, z_1_LB_2 ] ]
x_LB_12_S= x_W_7_S
x_LB_12_E= x_W_7_E
#W_7 co-ord [ [ x_LB_12_S, y_min, z_1_LB_2 ], [ x_LB_12_E, y_min, z_1_LB_2 ] ]
#Wall_B_1
x_LB_13_S= x_W_8_S
x_LB_13_E= x_W_8_E
#W_8 co-ord [ [ x_LB_13_S, y_max, z_1_LB_2 ], [ x_LB_13_E, y_max, z_1_LB_2 ] ]
x_LB_14_S= x_W_9_S
x_LB_14_E= x_W_9_E
```

```
#W_9 co-ord [ [ x_LB_14_S, y_max, z_1_LB_2 ], [ x_LB_14_E, y_max, z_1_LB_2 ] ]
#Wall_S1_1
y_LB_15_S= y_W_10_S
y_LB_15_E= y_W_10_E
#W_10 co-ord [ [ x_min, y_LB_15_S, z_1_LB_2 ], [ x_min, y_LB_15_E, z_1_LB_2 ] ]
#IW_5
x_LB_16_S= x_max/(6.3/1.17)
x_LB_16_E= x_max/(6.3/2.12)
#D_6 co-ord [ [ x_LB_16_S, y_D_6, z_1_LB_2 ], [ x_LB_16_E, y_D_6, z_1_LB_2 ] ]
#IW_6
x_LB_17_S= x_max/(6.3/2.45)
x_LB_17_E= x_max/(6.3/3.4)
#D_7 co-ord [ [ x_LB_17_S, y_IW_6, z_1_LB_2 ], [ x_LB_17_E, y_IW_6, z_1_LB_2 ] ]
x_LB_18_S= x_max/(6.3/5.4575)
x_LB_18_E= x_max/(6.3/6.3)
#D_8 co-ord [ [ x_LB_18_S, y_IW_6, z_1_LB_2 ], [ x_LB_18_E, y_IW_6, z_1_LB_2 ] ]
#IW_8
x_LB_19_S= x_max/(6.3/1.4)
x_LB_19_E= x_max/(6.3/2.35)
#D_9 co-ord [ [ x_LB_19_S, y_IW_8, z_1_LB_2 ], [ x_LB_19_E, y_IW_8, z_1_LB_2 ] ]
x_LB_20_S= x_max/(6.3/2.45)
x_LB_20_E= x_max/(6.3/3.4)
#D_10 co-ord [ [ x_LB_20_S, y_IW_8, z_1_LB_2 ], [ x_LB_20_E, y_IW_8, z_1_LB_2 ] ]
x_LB_21_S= x_max/(6.3/5.4575)
x_LB_21_E= x_max/(6.3/6.3)
#D_11 co-ord [ [ x_LB_21_S, y_IW_8, z_1_LB_2 ], [ x_LB_18_E, y_IW_8, z_1_LB_2 ] ]
#IW_11
y_LB_22_S= y_max/(7.46/2.965)
y_LB_22_E= y_max/(7.46/3.915)
#D_12 co-ord [ [ x_D_12, y_LB_22_S, z_1_LB_2 ], [ x_D_12, y_LB_22_E, z_1_LB_2 ] ]

#13. Boundary Conditions
#supports are going to be assumed as fixed
```

## C.2 Script Commands

```
#SCRIPTING STARTS
Levels=[ Z_0, Z_1, Z_2 ]
Floor=[]
GroundFloor=[]
Side_Walls=[]
Facade=[]
Roof_Slab=[]

# FLOOR

for i in range( 0, len(Levels) ):
        if i==0:
                createSheet( "Floor_"+str(i), [ [ x_min, y_min, Levels[i] ], [ x_max, y_min, Levels[i] ], [ x_max, y_max, Levels[i] ], [ x_min, y_max, Levels[i] ] ] )
        elif i ==1:
                createSheet( "Floor_"+str(i)+str(i+1), [ [ x_F_1_S, y_F_1_S, Levels[i] ], [ x_F_2_E, y_F_1_S, Levels[i] ], [ x_F_2_E, y_F_1_E, Levels[i] ], [ x_F_1_S, y_F_1_E, Levels[i] ] ] )
                createSheet( "Floor_"+str(i)+str(i+4), [ [ x_F_4_S, y_F_4_S, Levels[i] ], [ x_F_4_E, y_F_4_S, Levels[i] ], [ x_F_4_E, y_F_4_E, Levels[i] ], [ x_F_4_S, y_F_4_E, Levels[i] ] ] )
                createSheet( "Floor_"+str(i)+str(i+5), [ [ x_F_5_S, y_F_5_S, Levels[i] ], [ x_F_5_E, y_F_5_S, Levels[i] ], [ x_F_5_E, y_F_5_E, Levels[i] ], [ x_F_5_S, y_F_5_E, Levels[i] ] ] )
                createSheet( "Floor_"+str(i)+str(i+6), [ [ x_F_6_S, y_F_6_S, Levels[i] ], [ x_F_6_E, y_F_6_S, Levels[i] ], [ x_F_6_E, y_F_8_E, Levels[i] ], [ x_F_6_S, y_F_8_E, Levels[i] ] ] )

        else:
                createSheet( "Floor_"+str(i)+str(i+1), [ [ x_F_1_S, y_F_1_S, Levels[i] ], [ x_F_2_E, y_F_1_S, Levels[i] ], [ x_F_2_E, y_F_1_E, Levels[i] ], [ x_F_1_S, y_F_1_E, Levels[i] ] ] )
                createSheet( "Floor_"+str(i)+str(i+4), [ [ x_F_4_S, y_F_4_S, Levels[i] ], [ x_F_4_E, y_F_4_S, Levels[i] ], [ x_F_4_E, y_F_4_E, Levels[i] ], [ x_F_4_S, y_F_4_E, Levels[i] ] ] )
                createSheet( "Floor_"+str(i)+str(i+5), [ [ x_F_5_S, y_F_5_S, Levels[i] ], [ x_F_5_E, y_F_5_S, Levels[i] ], [ x_F_5_E, y_F_5_E, Levels[i] ], [ x_F_5_S, y_F_5_E, Levels[i] ] ] )
                createSheet( "Floor_"+str(i)+str(i+6), [ [ x_F_6_S, y_F_6_S, Levels[i] ], [ x_F_6_E, y_F_6_S, Levels[i] ], [ x_F_6_E, y_F_8_E, Levels[i] ], [ x_F_6_S, y_F_8_E, Levels[i] ] ] )

sew( [ "Floor_12", "Floor_15", "Floor_16" ], 1e-05 )
sew( [ "Floor_23", "Floor_26", "Floor_27" ], 1e-05 )
Floor= [ "Floor_12", "Floor_17", "Floor_23", "Floor_28" ]

removeShape("Floor_0")

## WALLS ##

for i in range( 0, 2 ):
        createSheet( "Wall_F_"+str(i), [ [ x_min, y_min, Levels[i] ], [ x_max, y_min, Levels[i] ], [ x_max, y_min, Levels[i+1] ], [ x_min, y_min, Levels[i+1] ] ] )
        createSheet( "Wall_B_"+str(i), [ [ x_min, y_max, Levels[i] ], [ x_max, y_max, Levels[i] ], [ x_max, y_max, Levels[i+1] ], [ x_min, y_max, Levels[i+1] ] ] )
        createSheet( "Wall_S1_"+str(i), [ [ x_min, y_min, Levels[i] ], [ x_min, y_min, Levels[i+1] ], [ x_min, y_max, Levels[i+1] ], [ x_min, y_max, Levels[i] ] ] )
        createSheet( "Wall_S2_"+str(i), [ [ x_max, y_min, Levels[i] ], [ x_max, y_min, Levels[i+1] ], [ x_max, y_max, Levels[i+1] ], [ x_max, y_max, Levels[i] ] ] )
        Facade.append( "Wall_F_"+str(i) )
        Facade.append( "Wall_B_"+str(i) )
        Side_Walls.append( "Wall_S1_"+str(i) )
        Side_Walls.append( "Wall_S2_"+str(i) )
```

```
45
for i in range( 0,2 ):
47          createSheet( "Roof_Wall_"+str(i+1), [ [ Roof_Wall[i], y_min, Z_2 ], [ Roof_Wall[i], y_max/2, z_max ], [ Roof_Wall[i], y_max,
        Z_2 ] ] )
            Side_Walls.append( "Roof_Wall_"+str(i+1) )
49
# StairCase_Beams
51
Stair_beams_X=[]
53 Stair_beams_Y=[]
stairs_level= [ Z_1, Z_2 ]
55 for i in range( 0, len(stairs_level) ):
            createLine( "stair_beams_"+str(i+1)+str(i), [ x_min, y_ST_S, stairs_level[i] ], [ x_ST_E, y_ST_S, stairs_level[i] ] )
57          createLine( "stair_beams_"+str(i+1)+str(i+1), [ x_ST_E, y_ST_S, stairs_level[i] ], [ x_ST_E, y_ST_E, stairs_level[i] ] )
            createLine( "stair_beams_"+str(i+1)+str(i+2), [ x_min, y_ST_E, stairs_level[i] ], [ x_ST_E, y_ST_E, stairs_level[i] ] )
59          Stair_beams_X.append( "stair_beams_"+str(i+1)+str(i) )
            Stair_beams_Y.append( "stair_beams_"+str(i+1)+str(i+1) )
61          Stair_beams_X.append( "stair_beams_"+str(i+1)+str(i+2) )


63
# Roof_beams
65
createLine( "Roof_beam_1", [ x_max/(6.3/0.06), y_max/(7.46/0.06), Z_R ],[ x_max/(6.3/6.24), y_max/(7.46/0.06), Z_R ] )
67 arrayCopy( [ "Roof_beam_1" ], [ x_min, ((y_max/2)-(y_max/(7.46/0.06)))/6 , ( ( z_max-Z_R )/6 ) ], [ 0, 0, 0 ], [ 0, 0, 0 ], 6 )
arrayCopy( [ "Roof_beam_7" ], [ x_min, ((y_max/2)-(y_max/(7.46/0.06)))/6, -( ( z_max-Z_R )/6 ) ], [ 0, 0, 0 ], [ 0, 0, 0 ], 6 )
69
# Springs on Attic Floor
71
createLine( "spring_S1", [ x_min, y_max/(7.46/0.06), Z_R ], [ x_max/(6.3/0.06), y_max/(7.46/0.06), Z_R ] )
73 createLine( "spring_E1", [ x_max/(6.3/6.24), y_max/(7.46/0.06), Z_R ], [ x_max, y_max/(7.46/0.06), Z_R ] )
arrayCopy( [ "spring_S1" ], [ x_min, ((y_max/2)-(y_max/(7.46/0.06)))/6, ( ( z_max-Z_R )/6 ) ], [ 0, 0, 0 ], [ 0, 0, 0 ], 6 )
75 arrayCopy( [ "spring_E1" ], [ x_min, ((y_max/2)-(y_max/(7.46/0.06)))/6, ( ( z_max-Z_R )/6 ) ], [ 0, 0, 0 ], [ 0, 0, 0 ], 6 )
arrayCopy( [ "spring_S7" ], [ x_min, ((y_max/2)-(y_max/(7.46/0.06)))/6, -( ( z_max-Z_R )/6 ) ], [ 0, 0, 0 ], [ 0, 0, 0 ], 6 )
77 arrayCopy( [ "spring_E7" ], [ x_min, ((y_max/2)-(y_max/(7.46/0.06)))/6, -( ( z_max-Z_R )/6 ) ], [ 0, 0, 0 ], [ 0, 0, 0 ], 6 )

79 Roof_springs_S=[ "spring_S1", "spring_S2", "spring_S3", "spring_S4", "spring_S5", "spring_S6", "spring_S7", "spring_S8", "spring_S9",
        "spring_S10", "spring_S11", "spring_S12", "spring_S13" ]
Roof_springs_E=[ "spring_E1", "spring_E2", "spring_E3", "spring_E4", "spring_E5", "spring_E6", "spring_E7", "spring_E8", "spring_E9",
        "spring_E10", "spring_E11", "spring_E12", "spring_E13" ]
81
# All Floor Beams
83 # Number of beams and The spacings between the beam can be specified by the user
Ground_beams=[]
85 FirstFloor_beams=[]
SecondFloor_beams=[]
87 Ground_Storage_Beams=[]
Elevation_Storage_Beams=[]
89 Roof_beams=[ "Roof_beam_2", "Roof_beam_3", "Roof_beam_4", "Roof_beam_5", "Roof_beam_6", "Roof_beam_8", "Roof_beam_9", "Roof_beam_10",
        "Roof_beam_11", "Roof_beam_12" ]
Ridge_beams= [ "Roof_beam_1", "Roof_beam_7", "Roof_beam_13" ]
91
Beam_Ls=[]
93 for i in range(0, len (Levels)):
            if i==0 or i==1:
95                  for j in range(0,14):
                            if i==0:
97                                  createLine( "beam_"+str(i)+str(j+1), [ x_min, FF_spacing* (j+1), Levels[i] ],[ x_max, FF_spacing* (j
        +1), Levels[i] ] )
                                    if i==0:
99                                          removeShape( "beam_"+str(i)+str(j+1) )
                            elif i==1 and ( (FF_spacing* (j)<=y_ST_S or (FF_spacing* (j)>=y_ST_E ):
101                                 createLine( "beam_first_"+str(i)+str(j),  [ beam_first_a_S, y_F_1_S + FF_spacing* (j), Levels[i] ],[
        beam_first_a_E, y_F_1_S + FF_spacing* (j), Levels[i] ] )
                                    createLine( "beam_second_"+str(i)+str(j), [ beam_second_S, y_F_1_S + FF_spacing* (j), Levels[i] ], [
        beam_second_E, y_F_1_S + FF_spacing* (j), Levels[i] ] )
103                         else:
                                    createLine( "beam_first_"+str(i)+str(j), [ beam_first_b_S, y_F_1_S + FF_spacing* (j), Levels[i] ],[
        beam_first_b_E, y_F_1_S + FF_spacing* (j), Levels[i] ] )
105                                 createLine( "beam_second_"+str(i)+str(j), [ beam_second_S, y_F_1_S + FF_spacing* (j), Levels[i] ],[
        beam_second_E, y_F_1_S + FF_spacing* (j), Levels[i] ] )
                            if Levels[i]==0:
107                                 Ground_beams.append( "beam_"+str(i)+str(j+1) )
                            else:
109                                 FirstFloor_beams.append( "beam_first_"+str(i)+str(j) )
                                    FirstFloor_beams.append( "beam_second_"+str(i)+str(j) )
111         else:
                    for j in range(0,14):
113                         if FF_spacing* (j)<=y_ST_S or FF_spacing* (j)>=y_ST_E:
                                    createLine( "beam_first_"+str(i)+str(j),  [ beam_first_a_S, y_F_1_S + FF_spacing* (j), Levels[i] ],[
        beam_first_a_E, y_F_1_S + FF_spacing* (j), Levels[i] ] )
115                                 createLine( "beam_second_"+str(i)+str(j), [ beam_second_S, y_F_1_S + FF_spacing* (j), Levels[i] ], [
        beam_second_E, y_F_1_S + FF_spacing* (j), Levels[i] ] )
                            else:
117                                 createLine( "beam_first_"+str(i)+str(j), [ beam_first_b_S, y_F_1_S + FF_spacing* (j), Levels[i] ],[
        beam_first_b_E, y_F_1_S + FF_spacing* (j), Levels[i] ] )
                                    createLine( "beam_second_"+str(i)+str(j), [ beam_second_S, y_F_1_S + FF_spacing* (j), Levels[i] ],[
        beam_second_E, y_F_1_S + FF_spacing* (j), Levels[i] ] )
119                         SecondFloor_beams.append( "beam_first_"+str(i)+str(j) )
                            SecondFloor_beams.append( "beam_second_"+str(i)+str(j) )
121


123
# Springs on the floor
125 Springs_FF=[]
Springs_SF=[]
127 timber_floor= [ Z_1, Z_2 ]

129 for i in range( 0, len(timber_floor ) ):
```

```
        if i==0:
131             for j in range(0, 14 ):
                    if (FF_spacing* (j))<=y_ST_S or (FF_spacing* (j))>=y_ST_E:
133                         createLine( "spring_first_S_"+str(i+1)+str(j), [ x_min, y_F_1_S + FF_spacing* (j), timber_floor[i] ],
      [ beam_first_a_S, y_F_1_S + FF_spacing* (j), timber_floor[i] ] )
                            createLine( "spring_first_E_"+str(i+1)+str(j), [ beam_first_a_E, y_F_1_S + FF_spacing* (j),
      timber_floor[i] ], [ x_max/(6.3/2.45), y_F_1_S + FF_spacing* (j), timber_floor[i] ] )
135                         createLine( "spring_second_S_"+str(i+1)+str(j), [ x_max/(6.3/2.45), y_F_1_S + FF_spacing* (j),
      timber_floor[i] ], [ beam_second_S, y_F_1_S + FF_spacing* (j), timber_floor[i] ] )
                            createLine( "spring_second_E_"+str(i+1)+str(j), [ beam_second_E, y_F_1_S + FF_spacing* (j),
      timber_floor[i] ], [ x_max, y_F_1_S + FF_spacing* (j), timber_floor[i] ] )
137                     else:
                            createLine( "spring_first_S_"+str(i+1)+str(j), [ x_ST_E, y_F_1_S + FF_spacing* (j), timber_floor[i]
      ], [ beam_first_b_S, y_F_1_S + FF_spacing* (j), timber_floor[i] ] )
139                         createLine( "spring_first_E_"+str(i+1)+str(j), [ beam_first_b_E, y_F_1_S + FF_spacing* (j),
      timber_floor[i] ], [ x_max/(6.3/2.45), y_F_1_S + FF_spacing* (j), timber_floor[i] ] )
                            createLine( "spring_second_S_"+str(i+1)+str(j), [ x_max/(6.3/2.45), y_F_1_S + FF_spacing* (j),
      timber_floor[i] ], [ beam_second_S, y_F_1_S + FF_spacing* (j), timber_floor[i] ] )
141                         createLine( "spring_second_E_"+str(i+1)+str(j), [ beam_second_E, y_F_1_S + FF_spacing* (j),
      timber_floor[i] ], [ x_max, y_F_1_S + FF_spacing* (j), timber_floor[i] ] )
                        Springs_FF.append( "spring_first_S_"+str(i+1)+str(j) )
143                     Springs_FF.append( "spring_first_E_"+str(i+1)+str(j) )
                        Springs_FF.append( "spring_second_S_"+str(i+1)+str(j) )
145                     Springs_FF.append( "spring_second_E_"+str(i+1)+str(j) )
        else:
147             for j in range(0, 14 ):
                    if FF_spacing* (j)<y_ST_S or FF_spacing* (j)>y_ST_E:
149                         createLine( "spring_first_S_"+str(i+1)+str(j), [ x_min, y_F_1_S + FF_spacing* (j), timber_floor[i] ],
      [ beam_first_a_S, y_F_1_S + FF_spacing* (j), timber_floor[i] ] )
                            createLine( "spring_first_E_"+str(i+1)+str(j), [ beam_first_a_E, y_F_1_S + FF_spacing* (j),
      timber_floor[i] ], [ x_max/(6.3/2.45), y_F_1_S + FF_spacing* (j), timber_floor[i] ] )
151                         createLine( "spring_second_S_"+str(i+1)+str(j), [ x_max/(6.3/2.45), y_F_1_S + FF_spacing* (j),
      timber_floor[i] ], [ beam_second_S, y_F_1_S + FF_spacing* (j), timber_floor[i] ] )
                            createLine( "spring_second_E_"+str(i+1)+str(j), [ beam_second_E, y_F_1_S + FF_spacing* (j),
      timber_floor[i] ], [ x_max, y_F_1_S + FF_spacing* (j), timber_floor[i] ] )
153                     else:
                            createLine( "spring_first_S_"+str(i+1)+str(j), [ x_ST_E, y_F_1_S + FF_spacing* (j), timber_floor[i]
      ], [ beam_first_b_S, y_F_1_S + FF_spacing* (j), timber_floor[i] ] )
155                         createLine( "spring_first_E_"+str(i+1)+str(j), [ beam_first_b_E, y_F_1_S + FF_spacing* (j),
      timber_floor[i] ], [ x_max/(6.3/2.45), y_F_1_S + FF_spacing* (j), timber_floor[i] ] )
                            createLine( "spring_second_S_"+str(i+1)+str(j), [ x_max/(6.3/2.45), y_F_1_S + FF_spacing* (j),
      timber_floor[i] ], [ beam_second_S, y_F_1_S + FF_spacing* (j), timber_floor[i] ] )
157                         createLine( "spring_second_E_"+str(i+1)+str(j), [ beam_second_E, y_F_1_S + FF_spacing* (j),
      timber_floor[i] ], [ x_max, y_F_1_S + FF_spacing* (j), timber_floor[i] ] )
                        Springs_SF.append( "spring_first_S_"+str(i+1)+str(j) )
159                     Springs_SF.append( "spring_first_E_"+str(i+1)+str(j) )
                        Springs_SF.append( "spring_second_S_"+str(i+1)+str(j) )
161                     Springs_SF.append( "spring_second_E_"+str(i+1)+str(j) )

163 # LB co-ord 0 and 1 LINTEL BEAMS

165 LB_0_1_X= []
    LB_0_1_Y= []
167 LB_1_2_X= []
    LB_1_2_Y= []
169 LintelBeam_Coord_0_1= [ [ [ x_LB_1_S, y_min, z_0_LB_1 ], [ x_LB_1_E, y_min, z_0_LB_1 ] ], [ [ x_LB_2_S, y_min, z_0_LB_1 ], [ x_LB_2_E
      , y_min, z_0_LB_1 ] ], [ [ x_LB_3_S, y_min, z_0_LB_1 ], [ x_LB_3_E, y_min, z_0_LB_1 ] ], [ [ x_LB_4_S, y_max, z_D_2_E ], [
      x_LB_4_E, y_max, z_D_2_E ] ], [ [ x_LB_5_S, y_max, z_0_LB_1 ], [ x_LB_5_E, y_max, z_0_LB_1 ] ], [ [ x_LB_8_S, y_max, z_0_LB_1
      ], [ x_LB_8_E, y_max, z_0_LB_1 ] ],[ [ x_min, y_LB_6_S, z_0_LB_1 ], [ x_min, y_LB_6_E, z_0_LB_1 ] ], [ [ x_D_5, y_LB_10_S,
      z_0_LB_1 ], [ x_D_5, y_LB_10_E, z_0_LB_1 ] ] ]
    for i in range( 0, len (LintelBeam_Coord_0_1)):
171     createLine( "Lintbeam_"+str(i+1), LintelBeam_Coord_0_1[i][0], LintelBeam_Coord_0_1[i][1] )
        if LintelBeam_Coord_0_1[i][0][1]==LintelBeam_Coord_0_1[i][1][1]:
173             LB_0_1_X.append( "Lintbeam_"+str(i+1))
        else:
175             LB_0_1_Y.append( "Lintbeam_"+str(i+1))


177


179 # LB co-ord 1 and 2

181 LintelBeam_Coord_1_2= [ [ [ x_LB_11_S, y_min, z_1_LB_2 ], [ x_LB_11_E, y_min, z_1_LB_2 ] ], [ [ x_LB_12_S, y_min, z_1_LB_2 ], [
      x_LB_12_E, y_min, z_1_LB_2 ] ], [ [ x_LB_13_S, y_max, z_1_LB_2 ], [ x_LB_13_E, y_max, z_1_LB_2 ] ], [ [ x_LB_14_S, y_max,
      z_1_LB_2 ], [ x_LB_14_E, y_max, z_1_LB_2 ] ], [ [ x_min, y_LB_15_S, z_1_LB_2 ], [ x_min, y_LB_15_E, z_1_LB_2 ] ] ]
    for i in range( 0, len(LintelBeam_Coord_1_2)):
183     createLine( "Lintbeam_"+str(i+11), LintelBeam_Coord_1_2[i][0], LintelBeam_Coord_1_2[i][1] )
        if LintelBeam_Coord_1_2[i][0][1]==LintelBeam_Coord_1_2[i][1][1]:
185             LB_1_2_X.append( "Lintbeam_"+str(i+11))
        else:
187             LB_1_2_Y.append( "Lintbeam_"+str(i+11))


189
    LB_120 = [ "Lintbeam_1", "Lintbeam_2", "Lintbeam_3", "Lintbeam_4", "Lintbeam_5", "Lintbeam_6","Lintbeam_7", "Lintbeam_11", "
      Lintbeam_12", "Lintbeam_13", "Lintbeam_14", "Lintbeam_15" ]
191 LB_70 = [ "Lintbeam_8"]

193 # Tyings

195 spring_first_S_1=[]
    spring_first_E_1=[]
197 spring_first_S_2=[]
    spring_first_E_2=[]
199 spring_second_S_1=[]
    spring_second_E_1=[]
201 spring_second_S_2=[]
    spring_second_E_2=[]
203 for i in range(0,2):
        for j in range (0,14):
```

```
                if i==0:
                        spring_first_S_1.append( "spring_first_S_"+str(i+1)+str(j) )
                        spring_first_E_1.append( "spring_first_E_"+str(i+1)+str(j) )
                        spring_second_S_1.append( "spring_second_S_"+str(i+1)+str(j) )
                        spring_second_E_1.append( "spring_second_E_"+str(i+1)+str(j) )
                elif i==1:
                        spring_first_S_2.append( "spring_first_S_"+str(i+1)+str(j) )
                        spring_first_E_2.append( "spring_first_E_"+str(i+1)+str(j) )
                        spring_second_S_2.append( "spring_second_S_"+str(i+1)+str(j) )
                        spring_second_E_2.append( "spring_second_E_"+str(i+1)+str(j) )

tying_first_S_1=[]
tying_first_C_1=[]
tying_first_S_2=[]
tying_first_C_2=[]
#tying_second_S_1=[]
tying_second_E_1=[]
#tying_second_S_2=[]
tying_second_E_2=[]
for i in range(0,2):
        for j in range (0,14):
                if i==0:
                        tying_first_S_1.append( "tying_first_S_"+str(i+1)+str(j) )
                        tying_first_C_1.append( "tying_first_C_"+str(i+1)+str(j) )
                        tying_second_E_1.append( "tying_second_E_"+str(i+1)+str(j) )
                elif i==1:
                        tying_first_S_2.append( "tying_first_S_"+str(i+1)+str(j) )
                        tying_first_C_2.append( "tying_first_C_"+str(i+1)+str(j) )
                        tying_second_E_2.append( "tying_second_E_"+str(i+1)+str(j) )

tying_springs_S=[]
tying_springs_E=[]
for i in range(0,14):
        tying_springs_S.append("spring_S"+str(i) )
        tying_springs_E.append("spring_E"+str(i) )

# Floor_1

for i in range( 0, len(tying_first_S_1) ):
        if (FF_spacing*(i))<y_ST_S or (FF_spacing*(i))>y_ST_E:
                a= 0
                c= 0.06
        else:
                c= beam_first_b_S
                a= x_max/(6.3/1.02)
        createPointTying( tying_first_S_1[i], "TY_FLOOR_1" )
        setParameter( GEOMETRYTYING, tying_first_S_1[i], "TRANSL", [ 0, 1, 1 ] )
        attachTo( GEOMETRYTYING, tying_first_S_1[i], "SLAVE", spring_first_S_1[i], [ [ a, y_F_1_S + FF_spacing*(i), Z_1 ] ] )
        attachTo( GEOMETRYTYING, tying_first_S_1[i], "MASTER", spring_first_S_1[i], [ [ c, y_F_1_S + FF_spacing*(i), Z_1 ] ] )

for i in range( 0, len(tying_first_C_1) ):
        a= beam_first_a_E
        b= y_F_1_S + FF_spacing*(i)
        c= x_max/(6.3/2.45)
        d= beam_second_S
        createPointTying( tying_first_C_1[i], "TY_FLOOR_1" )
        setParameter( GEOMETRYTYING, tying_first_C_1[i], "TRANSL", [ 0, 1, 1 ] )
        attachTo( GEOMETRYTYING, tying_first_C_1[i], "SLAVE", spring_first_E_1[i], [ [ a, b, Z_1 ] ] )
        attachTo( GEOMETRYTYING, tying_first_C_1[i], "SLAVE", spring_second_S_1[i], [ [ d, b, Z_1 ] ] )
        attachTo( GEOMETRYTYING, tying_first_C_1[i], "MASTER", spring_first_E_1[i], [ [ c, b, Z_1 ] ] )

for i in range( 0, len(tying_second_E_1) ):
        a= beam_second_E
        b= y_F_1_S + FF_spacing*(i)
        c= x_max
        createPointTying( tying_second_E_1[i], "TY_FLOOR_1" )
        setParameter( GEOMETRYTYING, tying_second_E_1[i], "TRANSL", [ 0, 1, 1 ] )
        attachTo( GEOMETRYTYING, tying_second_E_1[i], "SLAVE", spring_second_E_1[i], [ [ c, b, Z_1 ] ] )
        attachTo( GEOMETRYTYING, tying_second_E_1[i], "MASTER", spring_second_E_1[i], [ [ a, b, Z_1 ] ] )




# Floor_2

for i in range( 0, len(tying_first_S_2) ):
        if FF_spacing*(i)<y_ST_S or FF_spacing*(i)>y_ST_E:
                a= x_min
                c= x_max/(6.3/0.06)
        else:
                c= beam_first_b_S
                a= x_max/(6.3/1.02)
        createPointTying( tying_first_S_2[i], "TY_FLOOR_2" )
        setParameter( GEOMETRYTYING, tying_first_S_2[i], "TRANSL", [ 0, 1, 1 ] )
        attachTo( GEOMETRYTYING, tying_first_S_2[i], "SLAVE", spring_first_S_2[i], [ [ a, y_F_1_S + FF_spacing*(i), Z_2 ] ] )
        attachTo( GEOMETRYTYING, tying_first_S_2[i], "MASTER", spring_first_S_2[i], [ [ c, y_F_1_S + FF_spacing*(i), Z_2 ] ] )

for i in range( 0, len(tying_first_C_2) ):
        a= beam_first_a_E
        b= y_F_1_S + FF_spacing*(i)
        c= x_max/(6.3/2.45)
        d= beam_second_S
        createPointTying( tying_first_C_2[i], "TY_FLOOR_2" )
        setParameter( GEOMETRYTYING, tying_first_C_2[i], "TRANSL", [ 0, 1, 1 ] )
        attachTo( GEOMETRYTYING, tying_first_C_2[i], "SLAVE", spring_first_E_2[i], [ [ a, b, Z_2 ] ] )
        attachTo( GEOMETRYTYING, tying_first_C_2[i], "SLAVE", spring_second_S_2[i], [ [ d, b, Z_2 ] ] )
        attachTo( GEOMETRYTYING, tying_first_C_2[i], "MASTER", spring_first_E_2[i], [ [ c, b, Z_2 ] ] )
```

```
303
for i in range( 0, len(tying_second_E_2) ):
305         a= beam_second_E
            b= y_F_1_S + FF_spacing*(i)
307         c= x_max
            createPointTying( tying_second_E_2[i], "TY_FLOOR_2" )
309         setParameter( GEOMETRYTYING, tying_second_E_2[i], "TRANSL", [ 0, 1, 1 ] )
            attachTo( GEOMETRYTYING, tying_second_E_2[i], "SLAVE", spring_second_E_2[i], [ [ c, b, Z_2 ] ] )
311         attachTo( GEOMETRYTYING, tying_second_E_2[i], "MASTER", spring_second_E_2[i], [ [ a, b, Z_2 ] ] )


313

315 for i in range ( 0, len(Roof_springs_S) ):
            if i<=6:
317                 a= (((y_max/2)-(y_max/(7.46/0.06)))/6)*(i+1)
                    b= ( ( z_max-Z_R )/6 )*(i+1)
319         else:
                    a= (((y_max/2)-(y_max/(7.46/0.06)))/6)*(i+1)
321                 b= -( ( z_max-Z_R )/6 )*(i+1)
            createPointTying( tying_springs_S[i], "TY_ROOF" )
323         setParameter( GEOMETRYTYING, tying_springs_S[i], "TRANSL", [ 0, 1, 1 ] )
            attachTo( GEOMETRYTYING, tying_springs_S[i], "SLAVE", Roof_springs_S[i], [ [ x_min, a, b ] ] )
325         attachTo( GEOMETRYTYING, tying_springs_S[i], "MASTER", Roof_springs_S[i], [ [ x_max/(6.3/0.06), a, b ] ] )

327 for i in range ( 0, len(Roof_springs_E) ):
            if i<=6:
329                 a= (((y_max/2)-(y_max/(7.46/0.06)))/6)*(i+1)
                    b= ( ( z_max-Z_R )/6 )*(i+1)
331         else:
                    a= (((y_max/2)-(y_max/(7.46/0.06)))/6)*(i+1)
333                 b= -( ( z_max-Z_R )/6 )*(i+1)
            createPointTying( tying_springs_E[i], "TY_ROOF" )
335         setParameter( GEOMETRYTYING, tying_springs_E[i], "TRANSL", [ 0, 1, 1 ] )
            attachTo( GEOMETRYTYING, tying_springs_E[i], "SLAVE", Roof_springs_E[i], [ [ x_max, a, b ] ] )
337         attachTo( GEOMETRYTYING, tying_springs_E[i], "MASTER", Roof_springs_E[i], [ [ x_max/(6.3/6.24), a, b ] ] )

339 # Mesh

341 all = [ l for l in shapes() ]
    setElementSize( all , 0.20 )
343 timber=[]
    timber=  Floor + Stair_beams_X + Stair_beams_Y + FirstFloor_beams + SecondFloor_beams + Roof_beams + Ridge_beams + Roof_Slab
345 setElementSize( timber, FF_spacing )
    generateMesh( [] )
347 #
    hideView( "GEOM" )
```

# DIANA Input Files

D

## D.1 DAT File

```
: Diana Datafile written by Diana Dev (Latest update: 2016-09-01)
'UNITS'
LENGTH M
MASS KG
'DIRECTIONS'
   1   1.00000E+00   0.00000E+00   0.00000E+00
   2   0.00000E+00   1.00000E+00   0.00000E+00
   3   0.00000E+00   0.00000E+00   1.00000E+00
'MODEL'
GRAVDI 3
GRAVAC  -9.81000E+00
'COORDINATES'
   1   2.45000E+00   0.00000E+00   2.80000E+00
   2   2.45000E+00   0.00000E+00   0.00000E+00
   3   1.40000E+00   0.00000E+00   2.20000E+00
   4   2.40000E+00   0.00000E+00   2.20000E+00
   5   3.70000E+00   0.00000E+00   8.00000E-01
   6   5.90000E+00   0.00000E+00   8.00000E-01
   7   3.70000E+00   0.00000E+00   2.20000E+00
   8   5.90000E+00   0.00000E+00   2.20000E+00
   9   2.40000E+00   0.00000E+00   0.00000E+00
  10   1.40000E+00   0.00000E+00   0.00000E+00
...
5579   1.02000E+00   2.88308E+00   2.80000E+00
5580   1.02000E+00   4.01231E+00   5.40000E+00
5581   1.02000E+00   3.44769E+00   5.40000E+00
5582   1.02000E+00   2.88308E+00   5.40000E+00
'MATERI'
   1 NAME   "Concrete_Linear"
     MCNAME CONCR
     MATMDL LEI
     YOUNG    1.50000E+10
     POISON   1.50000E-01
     DENSIT   2.50000E+03
     ASPECT RAYDAM
     RAYLEI   5.20000E-01   2.70000E-03
   2 NAME   "Floor_orthotropic"
     MCNAME CONCR
     MATMDL LEO
     YOUNG    3.00000E+10   5.00000E+09   1.50000E+10
     POISON   1.50000E-01   1.50000E-01   1.50000E-01
     SHRMOD   1.00000E+08   6.52000E+09   6.52000E+09
```

```
  DENSIT   1.00000E+00
  ASPECT RAYDAM
  RAYLEI   5.20000E-01   2.70000E-03
3 NAME   "Masonry_Wall"
  MCNAME CONCR
  MATMDL MASONR
  DENSIT   2.00000E+03
  ENGMAS
  YOUNG    3.60000E+09   5.20000E+09
  SHRMOD   1.50000E+09
  TENSTR   2.10000E+05   1.30000E+05
  GF1      1.50000E+01   5.00000E+00
  UNLFAC   1.00000E+00
  COMSTR   7.50000E+06   6.00000E+06
  GC       4.34000E+04   3.13000E+04
  EPSCFA   4.00000E+00   4.00000E+00
  PHI      4.06100E-01
  COHESI   1.40000E+05
  CRKCOH
  GFS      2.00000E+01
  CBSPEC GOVIND
  ASPECT RAYDAM
  RAYLEI   5.20000E-01   2.70000E-03
4 NAME   "Timber_Beams"
  MCNAME MCSTEL
  MATMDL ISOTRO
  YOUNG    9.00000E+09
  POISON   3.00000E-01
  DENSIT   6.00000E+02
  ASPECT RAYDAM
  RAYLEI   5.20000E-01   2.70000E-03
5 NAME   "Timber_Floors"
  MCNAME MCSTEL
  MATMDL ORTHOT
  YOUNG    9.00000E+09   9.00000E+09   9.00000E+09
  POISON   3.00000E-01   3.00000E-01   3.00000E-01
  SHRMOD   4.30000E+06   3.40000E+09   3.40000E+09
  DENSIT   4.20000E+03
  ASPECT RAYDAM
  RAYLEI   5.20000E-01   2.70000E-03
6 NAME   "Timber_Roof"
  MCNAME MCSTEL
  MATMDL ORTHOT
  YOUNG    9.00000E+09   9.00000E+09   9.00000E+09
  POISON   3.00000E-01   3.00000E-01   3.00000E-01
  SHRMOD   4.30000E+06   3.40000E+09   3.40000E+09
  DENSIT   6.00000E+03
  ASPECT RAYDAM
  RAYLEI   5.20000E-01   2.70000E-03
```

```
   7 NAME   "spring_flr"
     MCNAME SPRING
     MATMDL LINETR
     SPRING   1.00000E+07
   8 NAME   "springs"
     MCNAME SPRING
     MATMDL LINETR
     SPRING   5.00000E+06
   9 NAME   "tr_mass_1"
     MCNAME MASSEL
     MATMDL SURFMA
     MASSSU   1.85000E+02   1.85000E+02   1.85000E+02
     ASPECT
'GEOMET'
   1 NAME   "concrete_floor_thk"
     GCNAME SHEET
     GEOMDL CURSHL
     XAXIS    1.00000E+00   0.00000E+00   0.00000E+00
     THICK    2.50000E-01
   2 NAME   "wall_thk_x"
     GCNAME SHEET
     GEOMDL CURSHL
     XAXIS    1.00000E+00   0.00000E+00   0.00000E+00
     EPFLAT   1.00000E-03
     THICK    1.20000E-01
   3 NAME   "wall_thk_y"
     GCNAME SHEET
     GEOMDL CURSHL
     XAXIS    0.00000E+00   1.00000E+00   0.00000E+00
     EPFLAT   1.00000E-03
     THICK    1.20000E-01
   4 NAME   "IW_thk_1"
     GCNAME SHEET
     GEOMDL CURSHL
     XAXIS    0.00000E+00   0.00000E+00   1.00000E+00
     EPFLAT   1.00000E-03
     THICK    7.00000E-02
   5 NAME   "IW_thk_2"
     GCNAME SHEET
     GEOMDL CURSHL
     XAXIS    0.00000E+00   0.00000E+00   1.00000E+00
     EPFLAT   1.00000E-03
     THICK    7.00000E-02
   6 NAME   "floor_thk"
     GCNAME SHEET
     GEOMDL CURSHL
     EPFLAT   1.00000E-03
     THICK    2.20000E-02
   7 NAME   "Lintel_section_1"
```

```
      GCNAME LINE
      GEOMDL CLS2B3
      RECTAN   2.00000E-01   1.20000E-01
    8 NAME   "Lintel_section_2"
      GCNAME LINE
      GEOMDL CLS2B3
      RECTAN   1.50000E-01   7.00000E-02
    9 NAME   "timber_beam"
      GCNAME LINE
      GEOMDL CLS2B3
      RECTAN   1.96000E-01   7.10000E-02
      ZAXIS    0.00000E+00   1.00000E+00   0.00000E+00
   10 NAME   "stair_beam_x"
      GCNAME LINE
      GEOMDL CLS2B3
      RECTAN   2.50000E-01   1.00000E-01
      ZAXIS    0.00000E+00   1.00000E+00   0.00000E+00
   11 NAME   "stair_beam_y"
      GCNAME LINE
      GEOMDL CLS2B3
      RECTAN   2.50000E-01   1.00000E-01
      ZAXIS    1.00000E+00   0.00000E+00   0.00000E+00
   12 NAME   "ridge_beam"
      GCNAME LINE
      GEOMDL CLS2B3
      RECTAN   2.46000E-01   7.10000E-02
      ZAXIS    0.00000E+00   1.00000E+00   0.00000E+00
   13 NAME   "timber_flr_thk"
      GCNAME SHEET
      GEOMDL CURSHL
      EPFLAT   1.00000E-03
      THICK    2.20000E-02
   14 NAME   "int_wall_thk"
      GCNAME SHEET
      GEOMDL CURSHL
      XAXIS    0.00000E+00   1.00000E+00   0.00000E+00
      EPFLAT   1.00000E-03
      THICK    1.20000E-01
'DATA'
    1 NAME   "Wall_Data"
      THINTE 5
    2 NAME   "floor_data"
'ELEMENTS'
SET  "Wall_F_0"
CONNECT
    1 Q20SH  197 193 191 196
    2 Q20SH  146 183 185 145
    3 Q20SH  296 119 120 298
    4 Q20SH  251 252 210 212
```

```
   5 Q20SH  122 301 300 121
....
 336 T15SH  364 370 363
 337 T15SH  373 386 374
 338 T15SH  4 21 20
 339 T15SH  389 385 388
MATERIAL 3
GEOMETRY 2
DATA 1
SET  "Wall_F_3"
CONNECT
.....
SET  "spring_second_E_213"
CONNECT
8280 SP2TR  3006 3653
MATERIAL 7
'LOADS'
CASE 1
NAME SW
WEIGHT
CASE 2
NAME "Pushover"
EQUIAC
   1   9.80600E+00
CASE 3
NAME "ele_PO"
ELEMEN
/ "Wall_F_3" /
     EQUIAC   9.80600E+00
     DIRECT 1
/ "Wall_B_3" /
     EQUIAC   9.80600E+00
     DIRECT 1
/ "Wall_S1_3" /
     EQUIAC   9.80600E+00
     DIRECT 1
/ "Wall_F_2" /
     EQUIAC   9.80600E+00
     DIRECT 1
/ "Wall_B_2" /
     EQUIAC   9.80600E+00
     DIRECT 1
/ "Wall_S1_2" /
     EQUIAC   9.80600E+00
     DIRECT 1
/ "Roof_Wall_3" /
     EQUIAC   9.80600E+00
     DIRECT 1
COMBIN
```

```
   1 1   1.00000E+00
   2 2   1.00000E+00 3   1.00000E+00
'SUPPOR'
NAME "Base"
17   TR 1
17   TR 2
17   TR 3
17   RO 1
17   RO 2
'TYINGS'
NAME TY_FLOOR_1
EQUAL TR 2 TR 3
5577 2738
....
EQUAL TR 2 TR 3
4179 4531
NAME TY_SUPPORT
EQUAL TR 1 TR 2 TR 3 RO 1 RO 2
/ 2 9 10 16 103-126 415 426 427 429 430 535-558 789 828-862 3108-3143 4611 4612
4637-4667 / 17
'END'
```

## D.2 DCF File

```
NUMTHR 4
*FILOS
INITIA
*INPUT
*PHASE LABEL=GF_FF
  BEGIN ACTIVE
    ELEMEN "Wall_F_0" "Wall_F_3" "Wall_B_0" "Wall_B_3" "Wall_S1_0" \
           "Wall_S1_3" "Floor_12" "beam_first_111" "beam_first_19" \
           "beam_first_17" "beam_first_15" "beam_first_13" "beam_first_11" \
....
           "spring_first_E_113" "spring_second_S_113" "spring_second_E_113" /
    SUPPOR "Base"
    TYINGS TY_FLOOR_1 TY_SUPPORT
  END ACTIVE
*NONLIN LABEL="Structural nonlinear"
  TYPE GEOMET
  BEGIN EXECUT
    TEXT "new execute block 2"
    BEGIN START
      BEGIN LOAD
        PREVIO OFF
        ADD LOADNR 1
      END LOAD
      INITIA STRESS CALCUL LOAD 1
      STEPS EXPLIC
    END START
```

```
    BEGIN PHYSIC
      SUPPRE
      LIQUEF OFF
    END PHYSIC
    BEGIN ITERAT
      MAXITE 100
      METHOD NEWTON
      CONVER DISPLA OFF
    END ITERAT
  END EXECUT
  SOLVE PARDIS
....
  BEGIN EXECUT
    BEGIN LOAD
      LOADNR 2
      BEGIN STEPS
        BEGIN EXPLIC
          SIZES 0.00200000(35) 0.00100000(500)
          ARCLEN REGULA SET NODES 4175 4180 4184 4199-4206 4236 4250 \
                                  4339-4345(2) 4350 4352 4354 4407 4409 4411 \
                                  4416 4436 /
        END EXPLIC
      END STEPS
    END LOAD
    BEGIN ITERAT
      MAXITE 100
      METHOD NEWTON
      BEGIN CONVER
        BEGIN FORCE
          TOLCON 0.001
          CONTIN
        END FORCE
        DISPLA OFF
      END CONVER
    END ITERAT
  END EXECUT
  SOLVE PARDIS
  BEGIN OUTPUT
    TEXT "Output"
    BINARY
    SELECT STEPS ALL /
    DISPLA TOTAL TRANSL GLOBAL X Y Z
    STRAIN CRACK GREEN
    BEGIN STRAIN
      BEGIN CRKWDT
        BEGIN GREEN
          BEGIN PRINCI
            "1" "2" "3"
            INTPNT
```

```
        END PRINCI
      END GREEN
    END CRKWDT
  END STRAIN
  STRAIN TOTAL FORCE LOCAL X Y Z
  BEGIN STRESS
    BEGIN TOTAL
      BEGIN CAUCHY
        BEGIN GLOBAL
          XX YY ZZ XY
          INTPNT
        END GLOBAL
      END CAUCHY
    END TOTAL
  END STRESS
  STRESS CRACK CAUCHY LOCAL
  STRESS TOTAL FORCE LOCAL X Y Z
  FORCE REACTI TRANSL GLOBAL X Y Z
END OUTPUT
*END
```

# Variations Excluding Irregularity

E

In this chapter graphs for individual cases are shown, and the crack-widths for maximum base shear force is displayed; but in case of no lintel beams(NLB) crack-widths for maximum base shear force and the collapse of façade is shown.

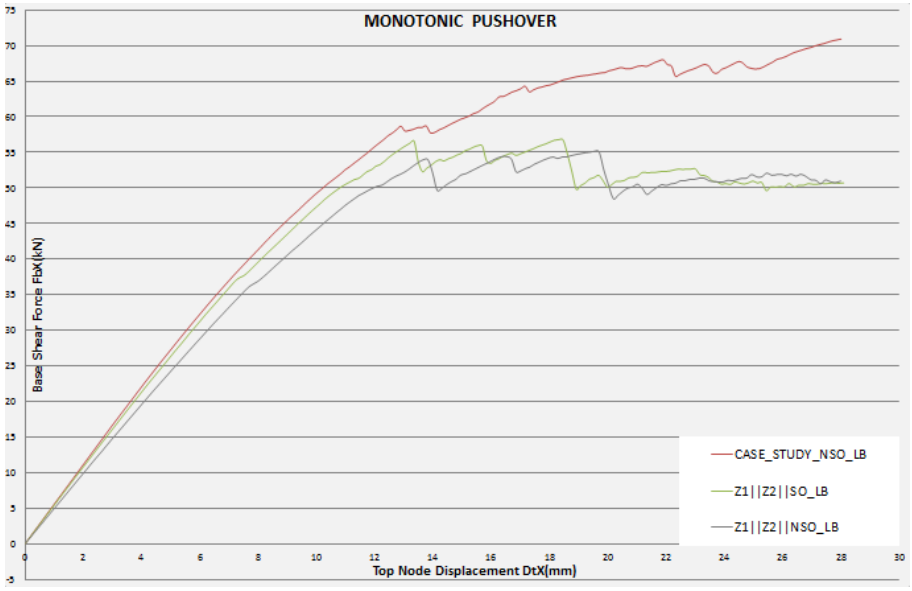


**Fig. E.1.:** PUSHOVER CURVE–EXCLUDING IRREGULARITIES (INCLUSION OF LINTEL BEAMS)

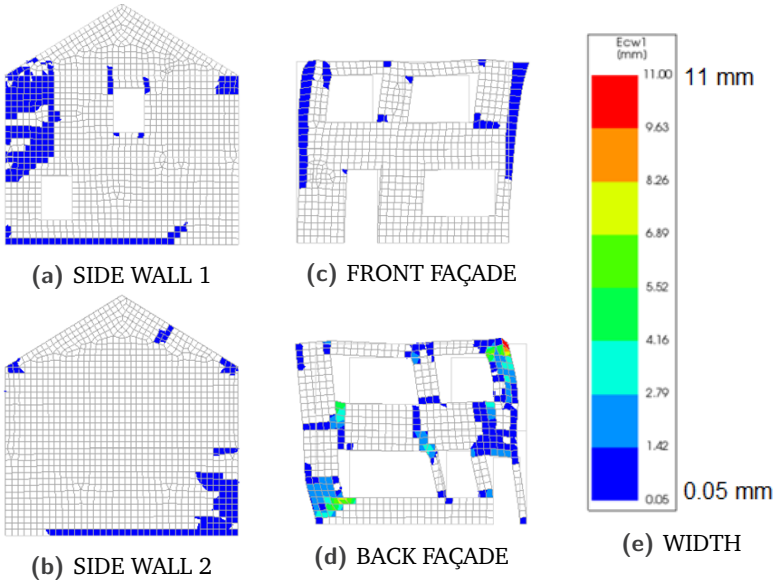


(a) SIDE WALL 1 (c) FRONT FAÇADE (e) WIDTH

(b) SIDE WALL 2 (d) BACK FAÇADE

**Fig. E.2.:** CRACK-WIDTH–CASE STUDY–NSO–LB

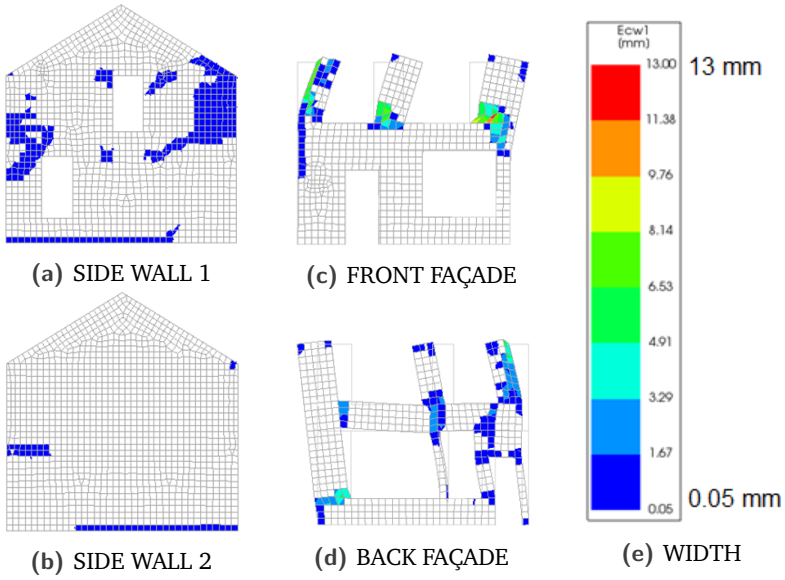


(a) SIDE WALL 1 (c) FRONT FAÇADE (e) WIDTH

(b) SIDE WALL 2 (d) BACK FAÇADE

**Fig. E.3.:** CRACK-WIDTH–Z1||Z2–SO–LB

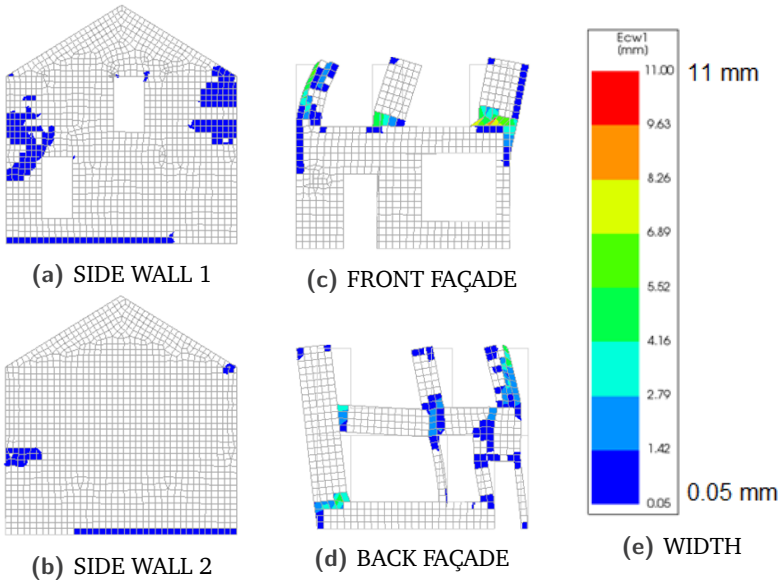


(a) SIDE WALL 1 (c) FRONT FAÇADE (e) WIDTH

(b) SIDE WALL 2 (d) BACK FAÇADE

**Fig. E.4.:** CRACK-WIDTH–Z1||Z2–NSO–LB

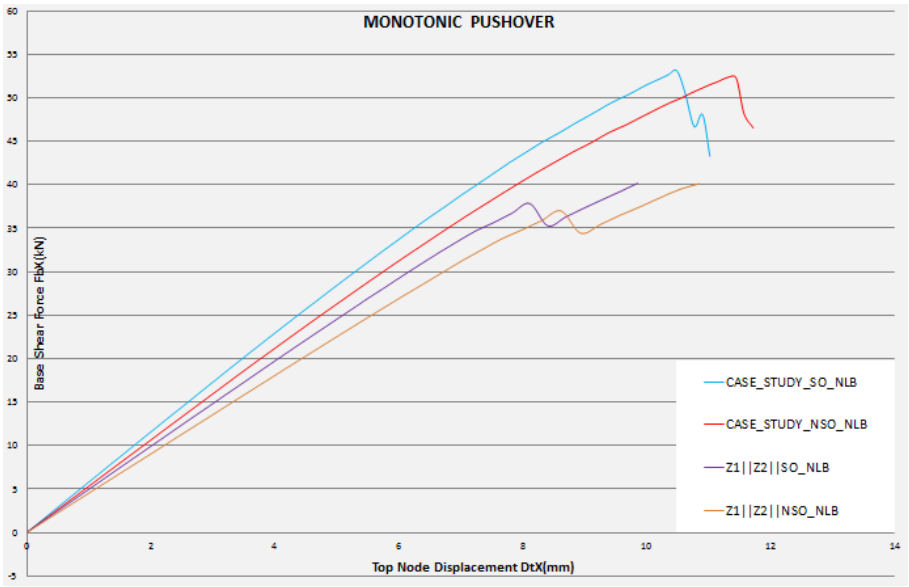


**Fig. E.5.:** PUSHOVER CURVE–EXCLUDING IRREGULARITIES (EXCLUSION OF LINTEL BEAMS)

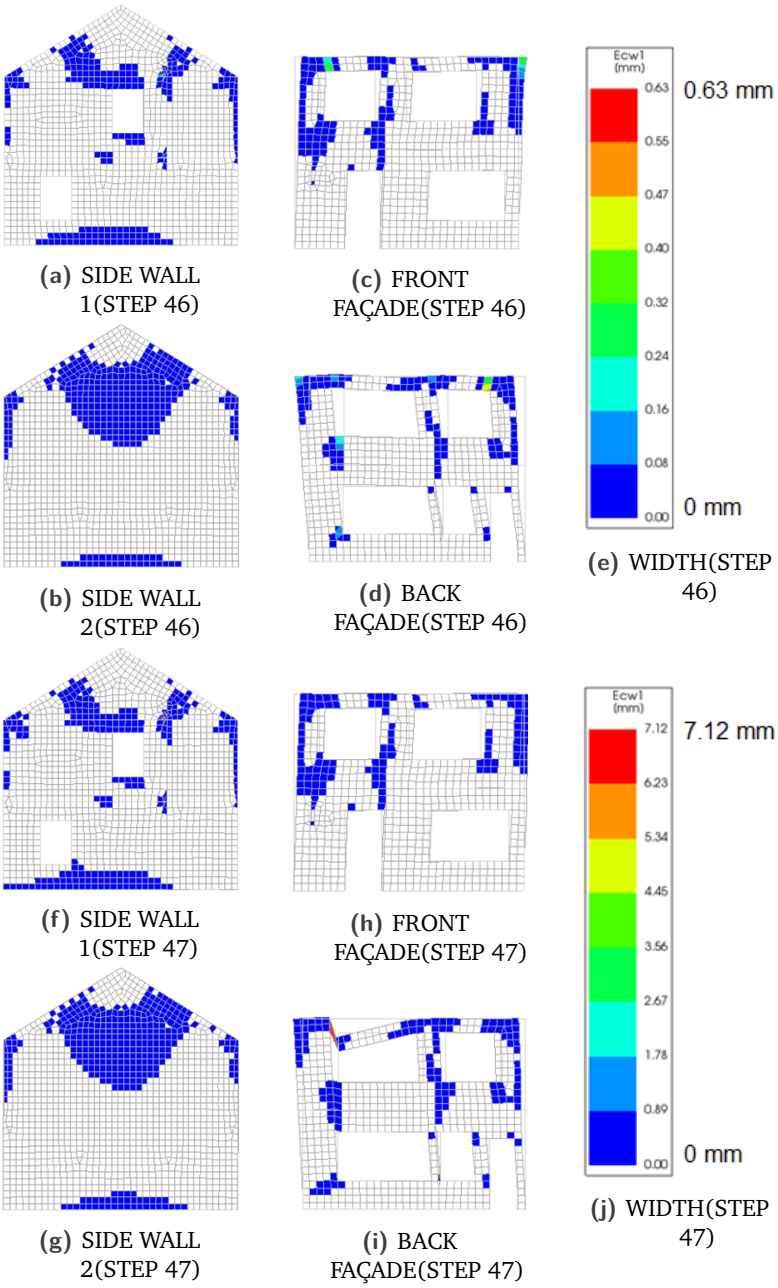


(a) SIDE WALL 1(STEP 46)

(c) FRONT FAÇADE(STEP 46)

(e) WIDTH(STEP 46)

(b) SIDE WALL 2(STEP 46)

(d) BACK FAÇADE(STEP 46)

(f) SIDE WALL 1(STEP 47)

(h) FRONT FAÇADE(STEP 47)

(j) WIDTH(STEP 47)

(g) SIDE WALL 2(STEP 47)

(i) BACK FAÇADE(STEP 47)

**Fig. E.6.:** CRACK-WIDTH–CASE STUDY–SO–NLB

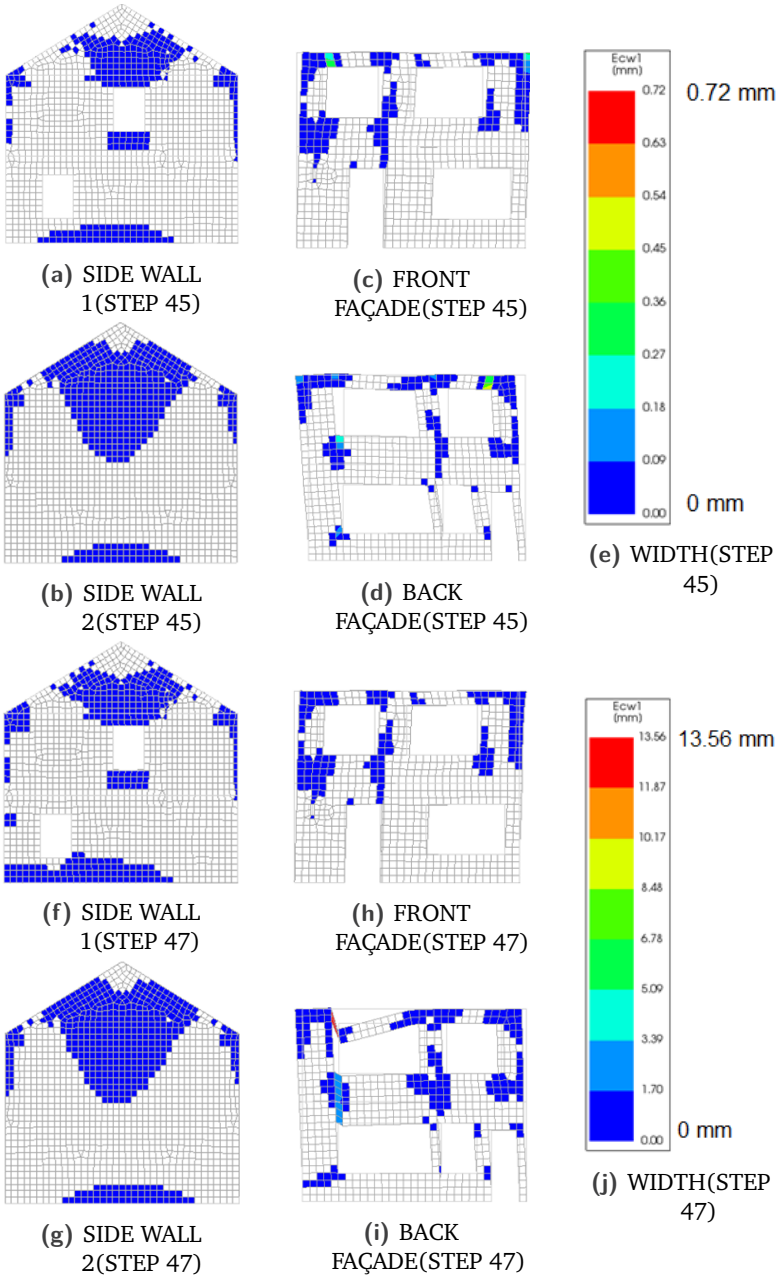


(a) SIDE WALL 1(STEP 45)

(b) SIDE WALL 2(STEP 45)

(c) FRONT FAÇADE(STEP 45)

(d) BACK FAÇADE(STEP 45)

(e) WIDTH(STEP 45)

(f) SIDE WALL 1(STEP 47)

(g) SIDE WALL 2(STEP 47)

(h) FRONT FAÇADE(STEP 47)

(i) BACK FAÇADE(STEP 47)

(j) WIDTH(STEP 47)

**Fig. E.7.:** CRACK-WIDTH–CASE STUDY–NSO–NLB

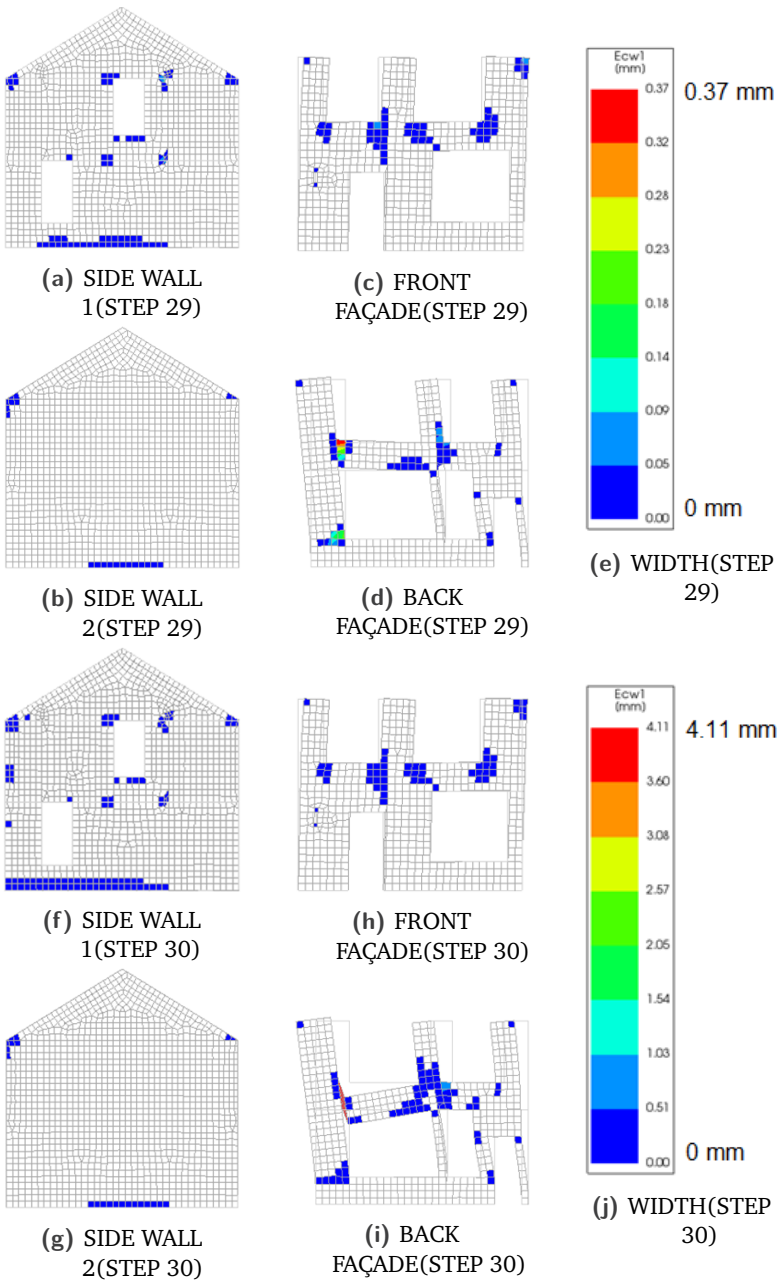


(a) SIDE WALL 1(STEP 29)

(c) FRONT FAÇADE(STEP 29)

(e) WIDTH(STEP 29)

(b) SIDE WALL 2(STEP 29)

(d) BACK FAÇADE(STEP 29)

(f) SIDE WALL 1(STEP 30)

(h) FRONT FAÇADE(STEP 30)

(j) WIDTH(STEP 30)

(g) SIDE WALL 2(STEP 30)

(i) BACK FAÇADE(STEP 30)

**Fig. E.8.:** CRACK-WIDTH–Z1||Z2–SO–NLB

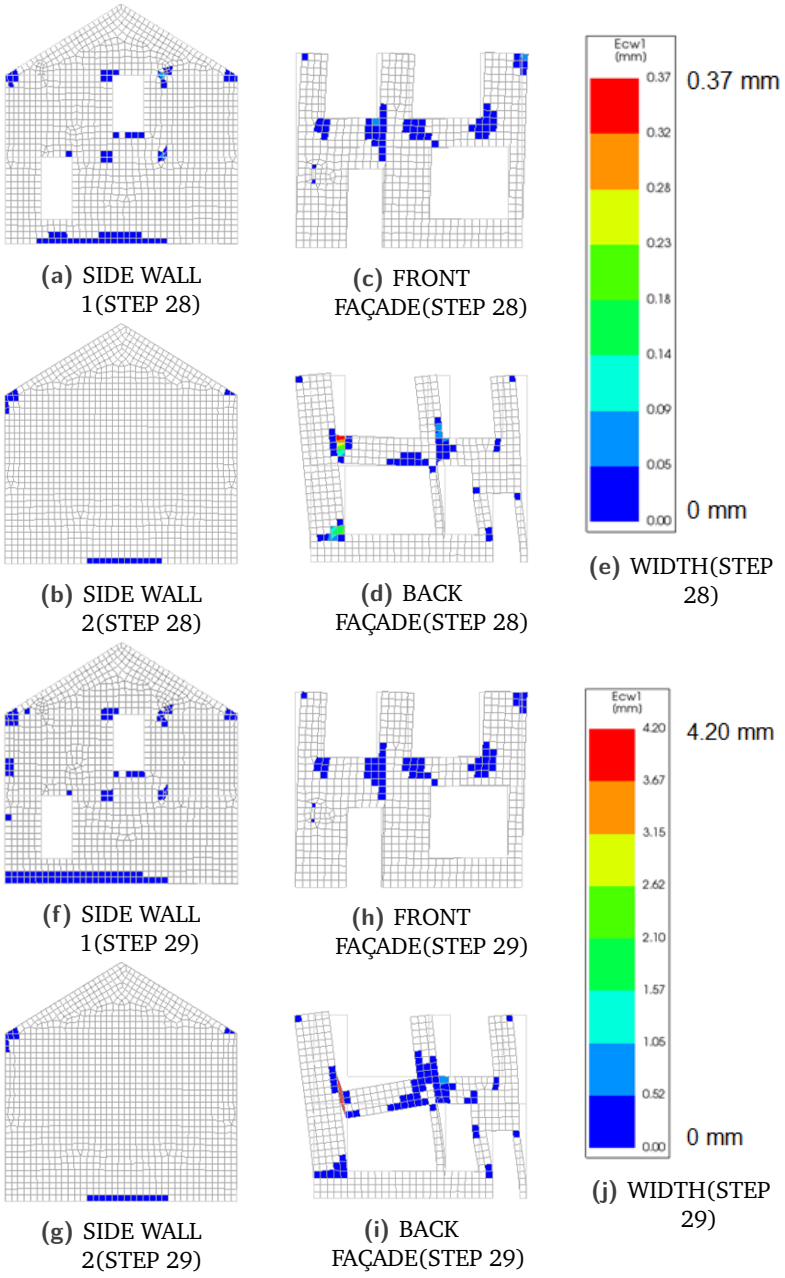


(a) SIDE WALL 1(STEP 28)

(c) FRONT FAÇADE(STEP 28)

(e) WIDTH(STEP 28)

(b) SIDE WALL 2(STEP 28)

(d) BACK FAÇADE(STEP 28)

(f) SIDE WALL 1(STEP 29)

(h) FRONT FAÇADE(STEP 29)

(j) WIDTH(STEP 29)

(g) SIDE WALL 2(STEP 29)

(i) BACK FAÇADE(STEP 29)

**Fig. E.9.:** CRACK-WIDTH–Z1||Z2–NSO–NLB

# Vertical Irregularity

F

In this section, crack-widths for different variations are presented. They go by the following order:

1. Case 1 with lintel beams(LB)
2. Case 1 without lintel beams(NLB)
3. Case 2 with lintel beams(LB)
4. Case 2 without lintel beams(NLB)

## F.1 Case 1–SO/NSO and LB

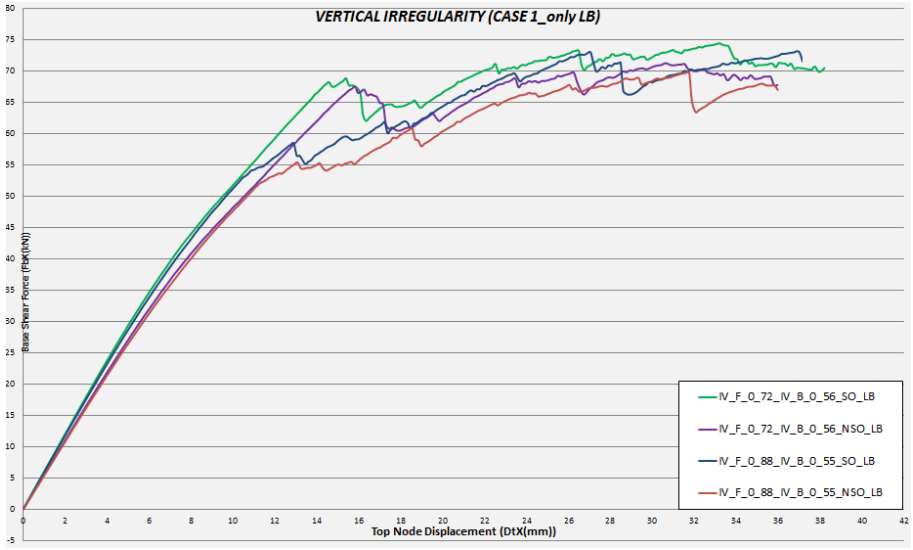


**Fig. F.1.:** PUSHOVER CURVE–VERTICAL IRREGULARITY CASE 1(SO/NSO AND INCLUSION OF LINTEL BEAMS)

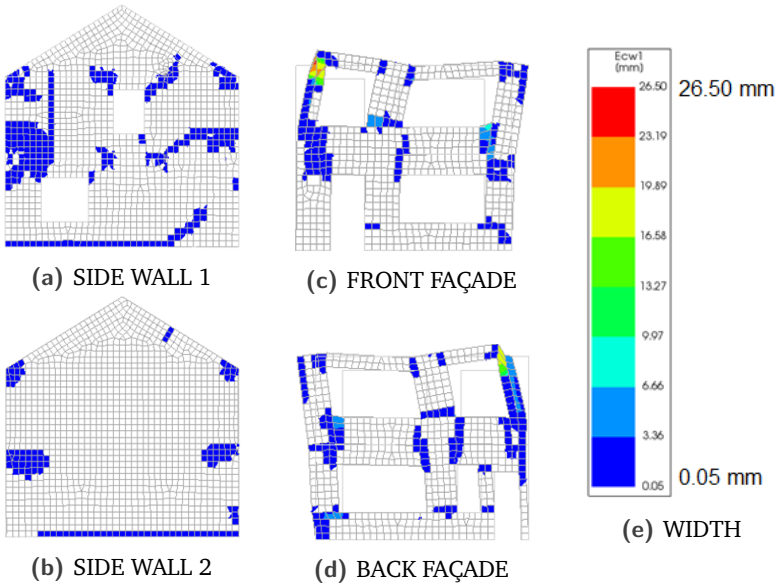


(a) SIDE WALL 1 (c) FRONT FAÇADE (e) WIDTH

(b) SIDE WALL 2 (d) BACK FAÇADE

**Fig. F.2.:** CRACK-WIDTH–$I_V^F = 0.72 I_V^B = 0.56$–SO–LB

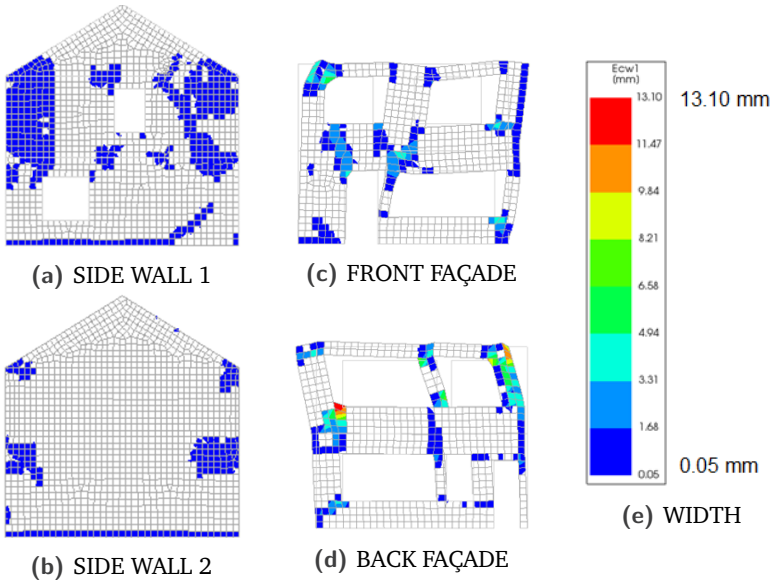


(a) SIDE WALL 1 (c) FRONT FAÇADE (e) WIDTH

(b) SIDE WALL 2 (d) BACK FAÇADE

**Fig. F.3.:** CRACK-WIDTH–$I_V^F = 0.88 I_V^B = 0.55$–SO–LB

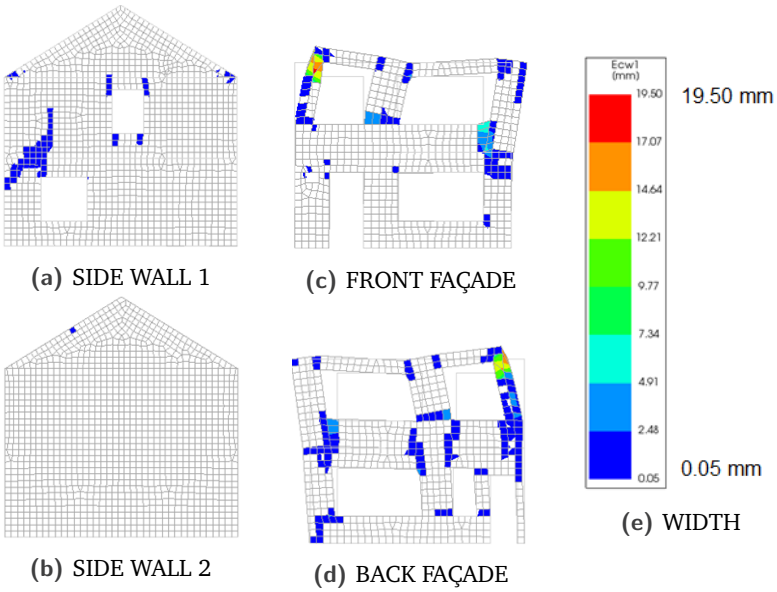


(a) SIDE WALL 1 (c) FRONT FAÇADE

(e) WIDTH

(b) SIDE WALL 2 (d) BACK FAÇADE

**Fig. F.4.:** CRACK-WIDTH–$I_V^F = 0.72 I_V^B = 0.56$–NSO–LB

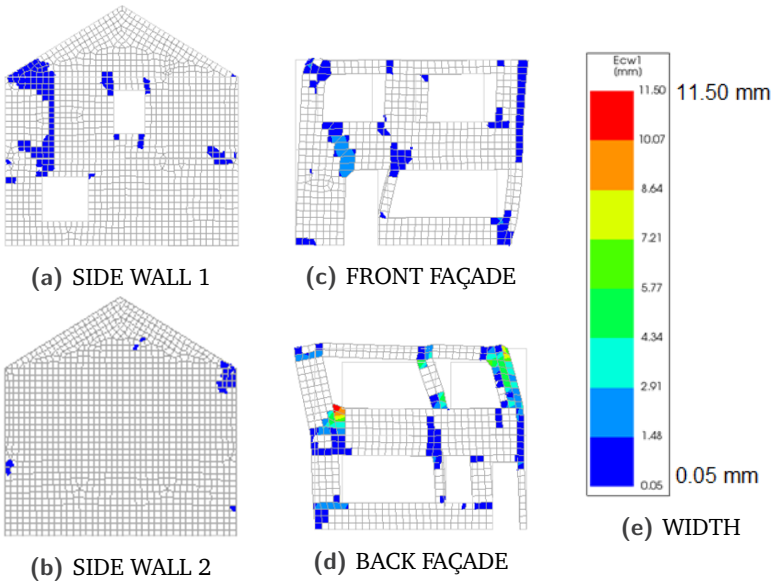


(a) SIDE WALL 1 (c) FRONT FAÇADE

(e) WIDTH

(b) SIDE WALL 2 (d) BACK FAÇADE

**Fig. F.5.:** CRACK-WIDTH–$I_V^F = 0.88 I_V^B = 0.55$–NSO–LB

## F.2 Case 1–SO/NSO and NLB

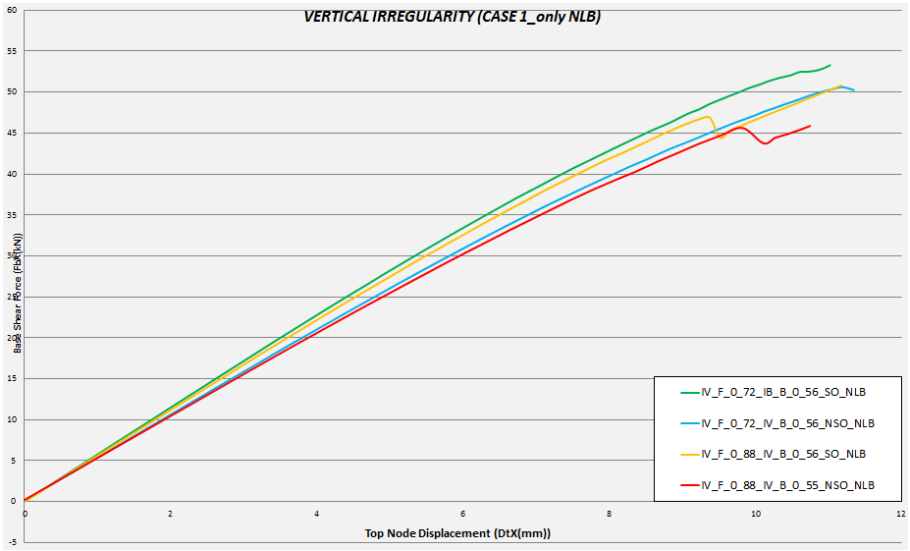


**Fig. F.6.:** PUSHOVER CURVE–VERTICAL IRREGULARITY CASE 1(SO/NSO AND EXCLUSION OF LINTEL BEAMS)

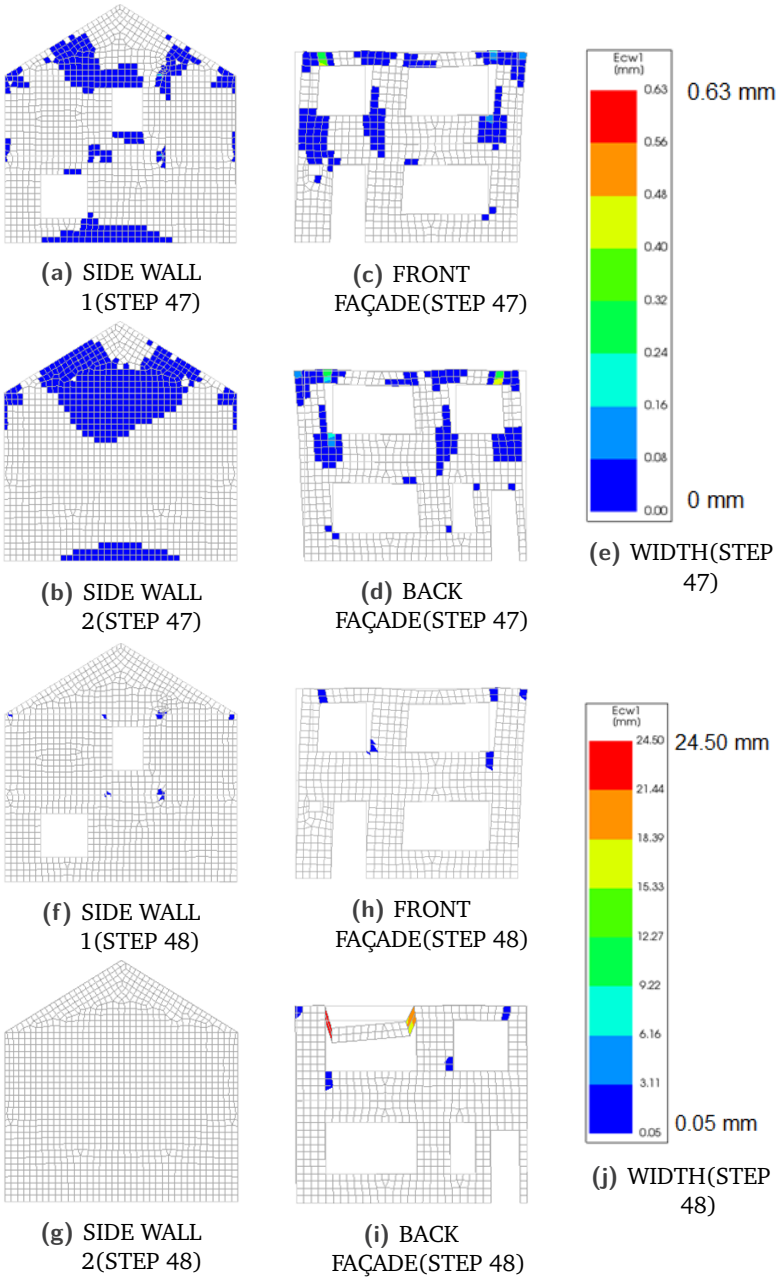


(a) SIDE WALL 1(STEP 47)

(c) FRONT FAÇADE(STEP 47)

(e) WIDTH(STEP 47)

(b) SIDE WALL 2(STEP 47)

(d) BACK FAÇADE(STEP 47)

(f) SIDE WALL 1(STEP 48)

(h) FRONT FAÇADE(STEP 48)

(j) WIDTH(STEP 48)

(g) SIDE WALL 2(STEP 48)

(i) BACK FAÇADE(STEP 48)

**Fig. F.7.:** CRACK-WIDTH–$I_V^F = 0.72 I_V^B = 0.56$–SO–NLB

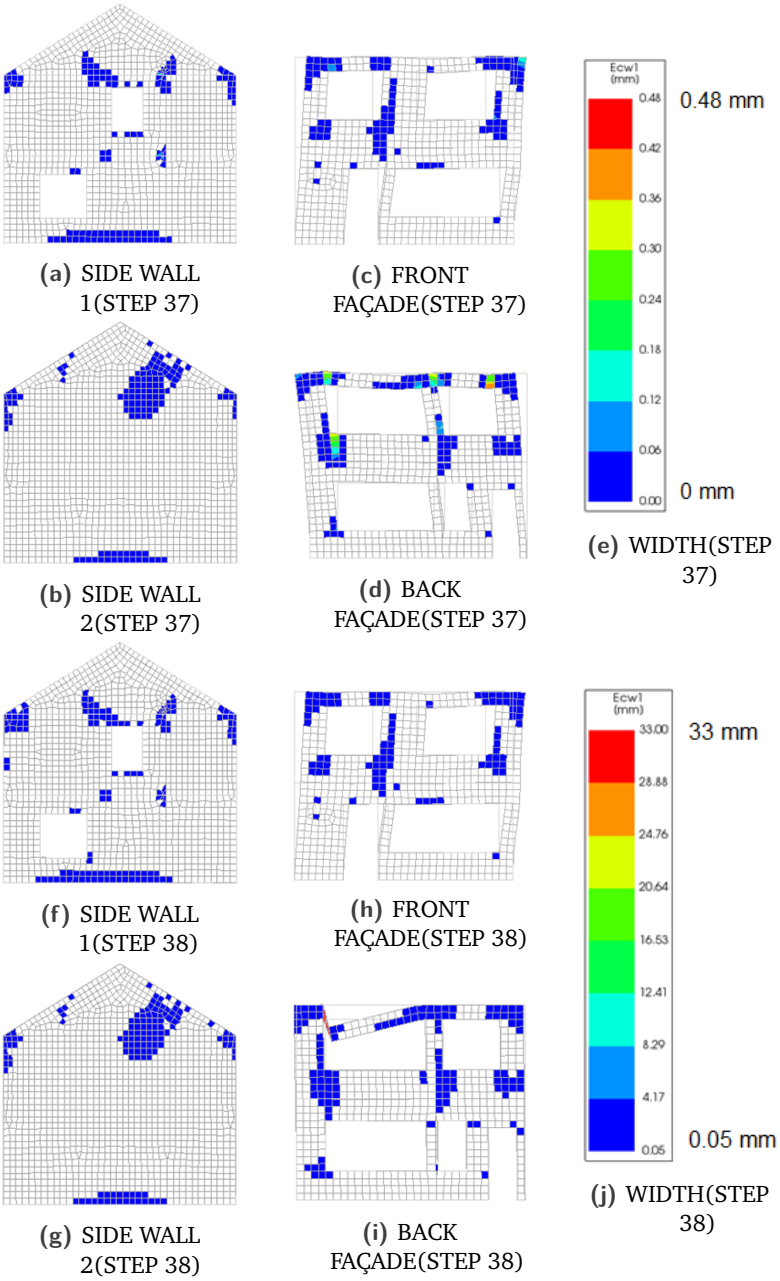


(a) SIDE WALL 1(STEP 37)

(b) SIDE WALL 2(STEP 37)

(c) FRONT FAÇADE(STEP 37)

(d) BACK FAÇADE(STEP 37)

(e) WIDTH(STEP 37)

(f) SIDE WALL 1(STEP 38)

(g) SIDE WALL 2(STEP 38)

(h) FRONT FAÇADE(STEP 38)

(i) BACK FAÇADE(STEP 38)

(j) WIDTH(STEP 38)

**Fig. F.8.:** CRACK-WIDTH–$I_V^F = 0.88 I_V^B = 0.55$–SO–NLB

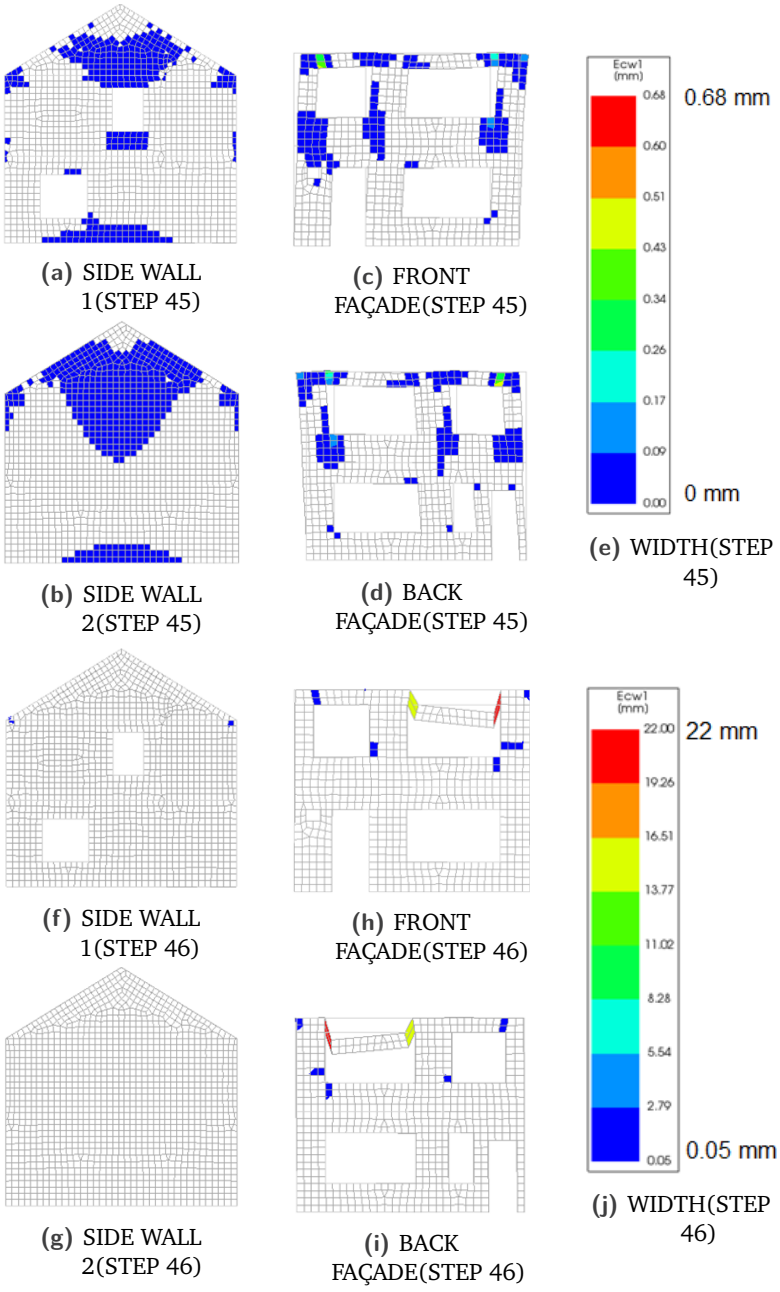


(a) SIDE WALL 1(STEP 45)

(c) FRONT FAÇADE(STEP 45)

(e) WIDTH(STEP 45)

(b) SIDE WALL 2(STEP 45)

(d) BACK FAÇADE(STEP 45)

(f) SIDE WALL 1(STEP 46)

(h) FRONT FAÇADE(STEP 46)

(j) WIDTH(STEP 46)

(g) SIDE WALL 2(STEP 46)

(i) BACK FAÇADE(STEP 46)

**Fig. F.9.:** CRACK-WIDTH–$I_V^F = 0.72 I_V^B = 0.56$–NSO–NLB

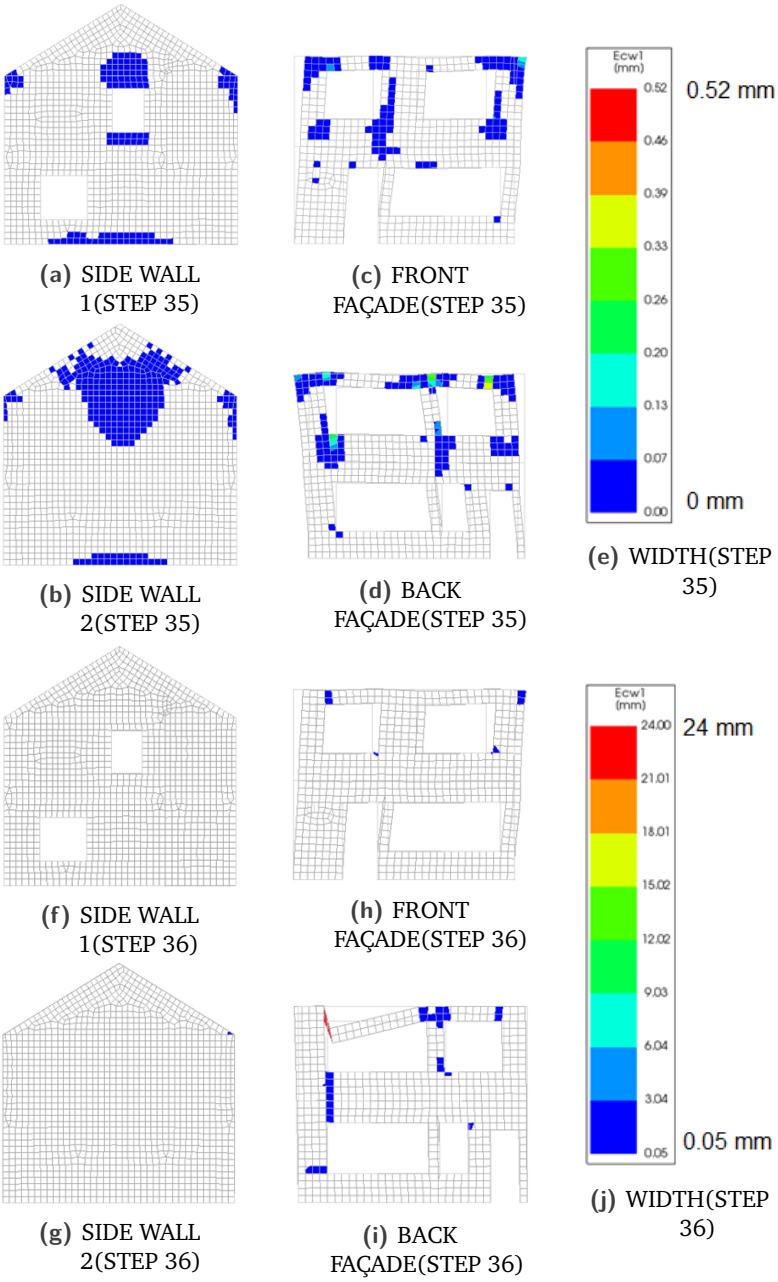


(a) SIDE WALL 1(STEP 35)

(c) FRONT FAÇADE(STEP 35)

(e) WIDTH(STEP 35)

(b) SIDE WALL 2(STEP 35)

(d) BACK FAÇADE(STEP 35)

(f) SIDE WALL 1(STEP 36)

(h) FRONT FAÇADE(STEP 36)

(j) WIDTH(STEP 36)

(g) SIDE WALL 2(STEP 36)

(i) BACK FAÇADE(STEP 36)

**Fig. F.10.:** CRACK-WIDTH–$I_V^F = 0.88 I_V^B = 0.55$–NSO–NLB

## F.3 Case 2–SO/NSO and LB

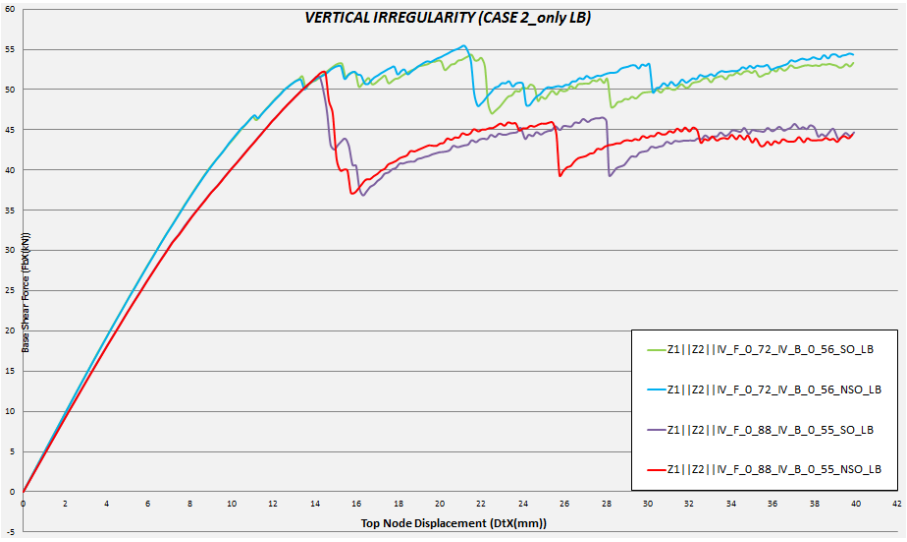


**Fig. F.11.:** PUSHOVER CURVE–VERTICAL IRREGULARITY CASE 2(SO/NSO AND INCLUSION OF LINTEL BEAMS)

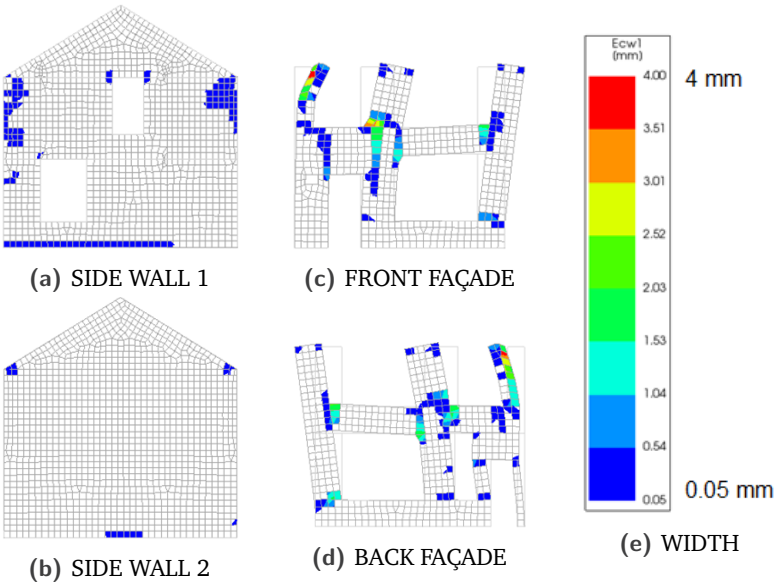


(a) SIDE WALL 1 (c) FRONT FAÇADE

(b) SIDE WALL 2 (d) BACK FAÇADE (e) WIDTH

**Fig. F.12.:** CRACK-WIDTH–$Z1||Z2||I_V^F = 0.72 I_V^B = 0.56$–SO–LB

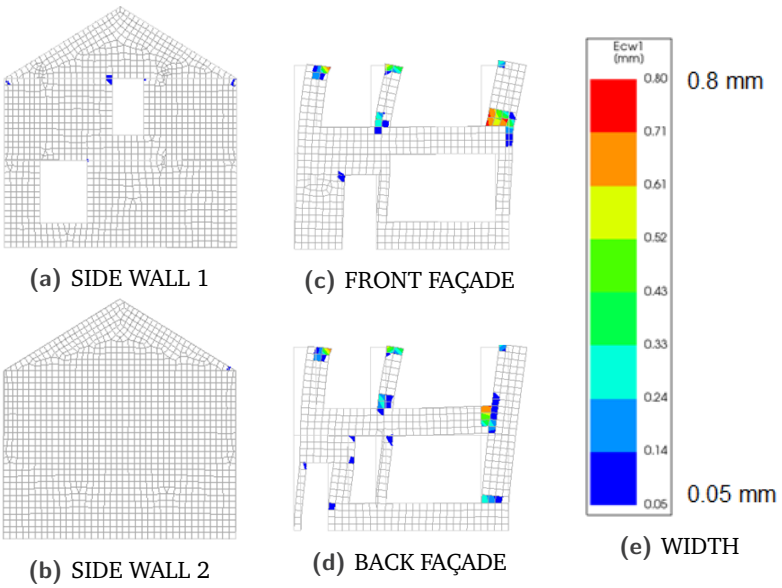


(a) SIDE WALL 1 (c) FRONT FAÇADE

(b) SIDE WALL 2 (d) BACK FAÇADE (e) WIDTH

**Fig. F.13.:** CRACK-WIDTH–$Z1||Z2||I_V^F = 0.88 I_V^B = 0.55$–SO–LB

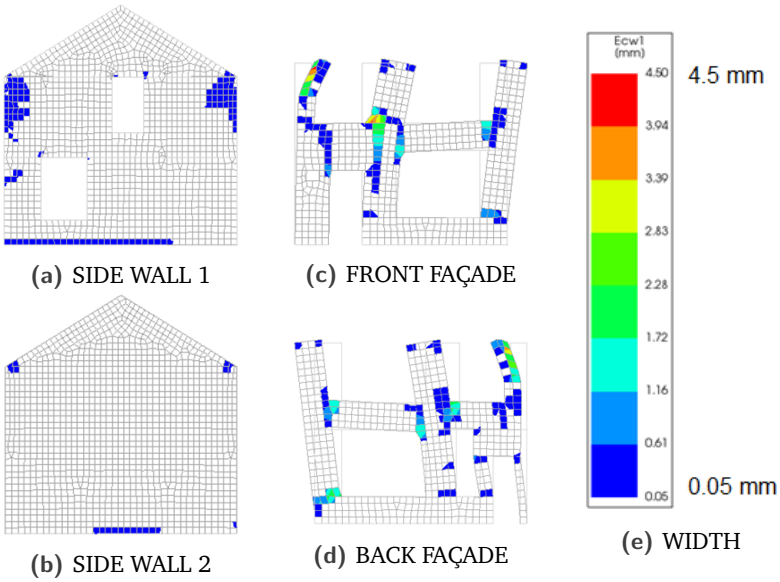


(a) SIDE WALL 1 (c) FRONT FAÇADE

(b) SIDE WALL 2 (d) BACK FAÇADE (e) WIDTH

**Fig. F.14.:** CRACK-WIDTH–$Z1||Z2||I_V^F = 0.72 I_V^B = 0.56$–NSO–LB

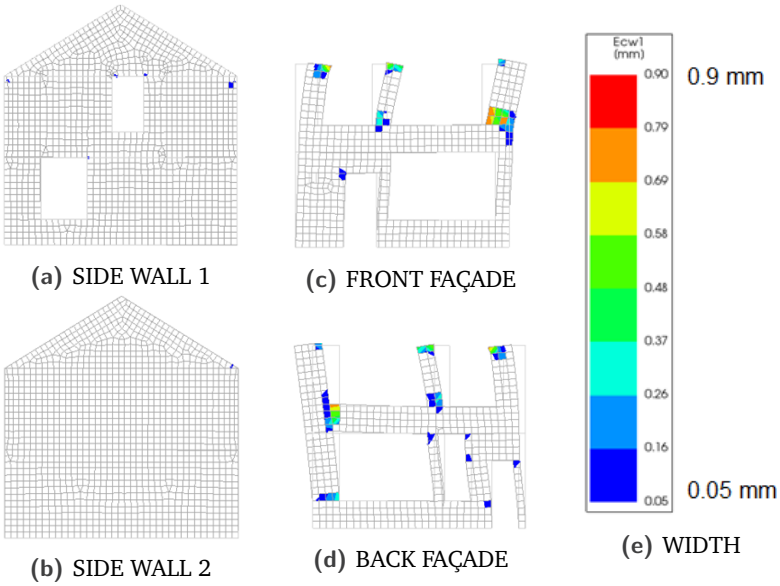


(a) SIDE WALL 1 (c) FRONT FAÇADE

(b) SIDE WALL 2 (d) BACK FAÇADE (e) WIDTH

**Fig. F.15.:** CRACK-WIDTH–$Z1||Z2||I_V^F = 0.88 I_V^B = 0.55$–NSO–LB

## F.4 Case 2–SO/NSO and NLB

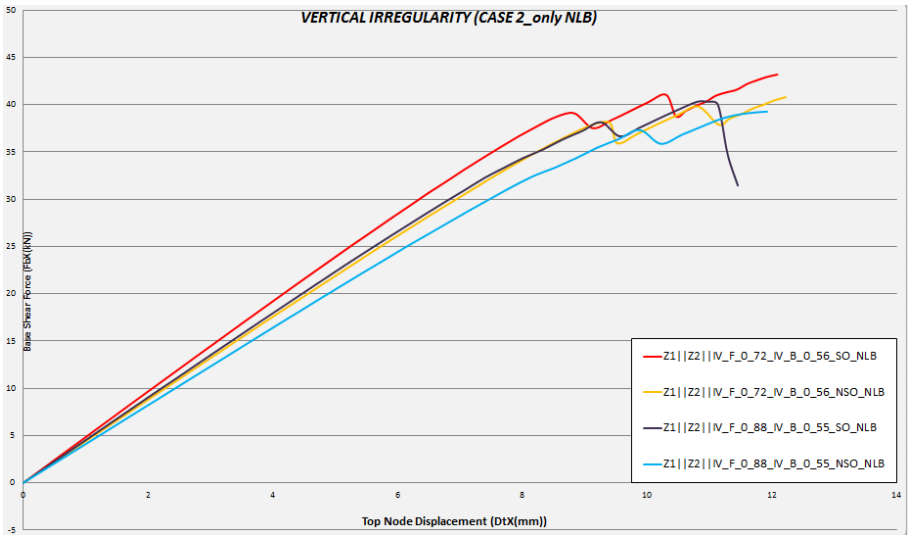


**Fig. F.16.:** PUSHOVER CURVE–VERTICAL IRREGULARITY CASE 2(SO/NSO AND EXCLUSION OF LINTEL BEAMS)

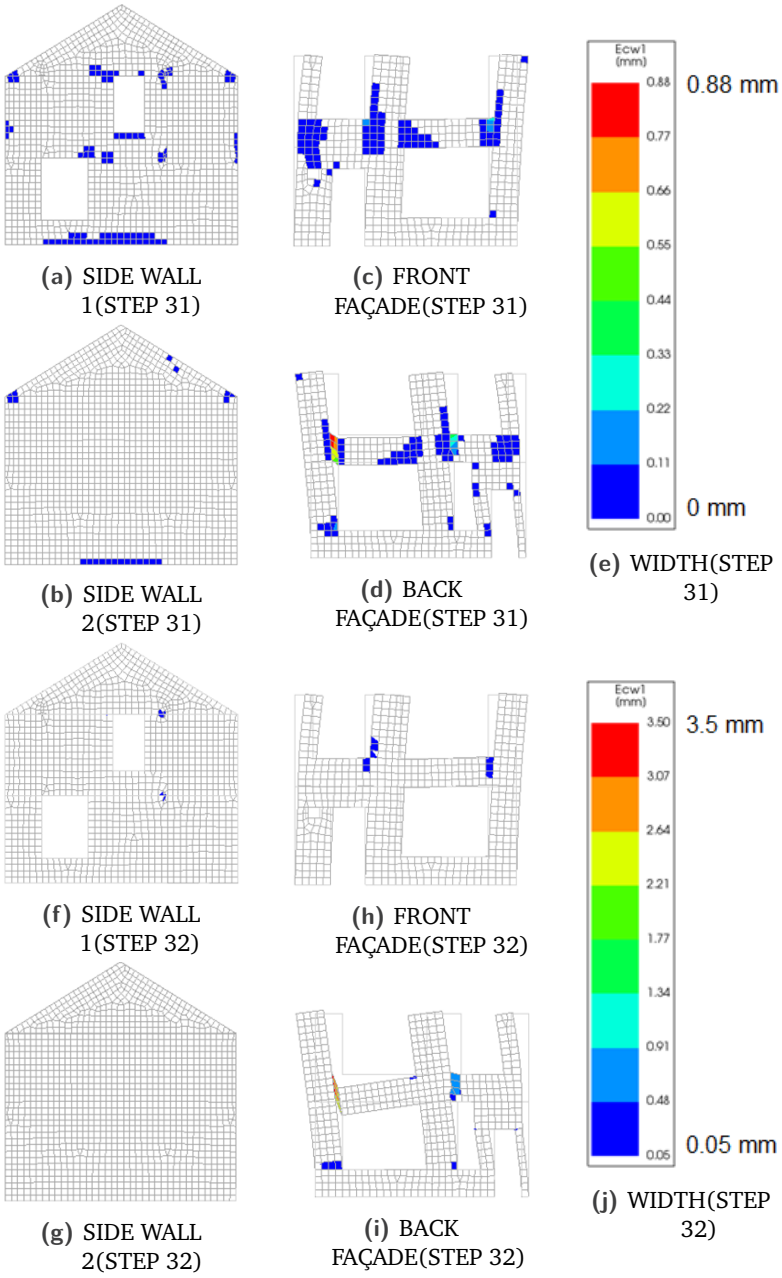


(a) SIDE WALL 1(STEP 31)

(c) FRONT FAÇADE(STEP 31)

(e) WIDTH(STEP 31)

(b) SIDE WALL 2(STEP 31)

(d) BACK FAÇADE(STEP 31)

(f) SIDE WALL 1(STEP 32)

(h) FRONT FAÇADE(STEP 32)

(j) WIDTH(STEP 32)

(g) SIDE WALL 2(STEP 32)

(i) BACK FAÇADE(STEP 32)

**Fig. F.17.:** CRACK-WIDTH–$Z1||Z2||I_V^F = 0.72 I_V^B = 0.56$–SO–NLB

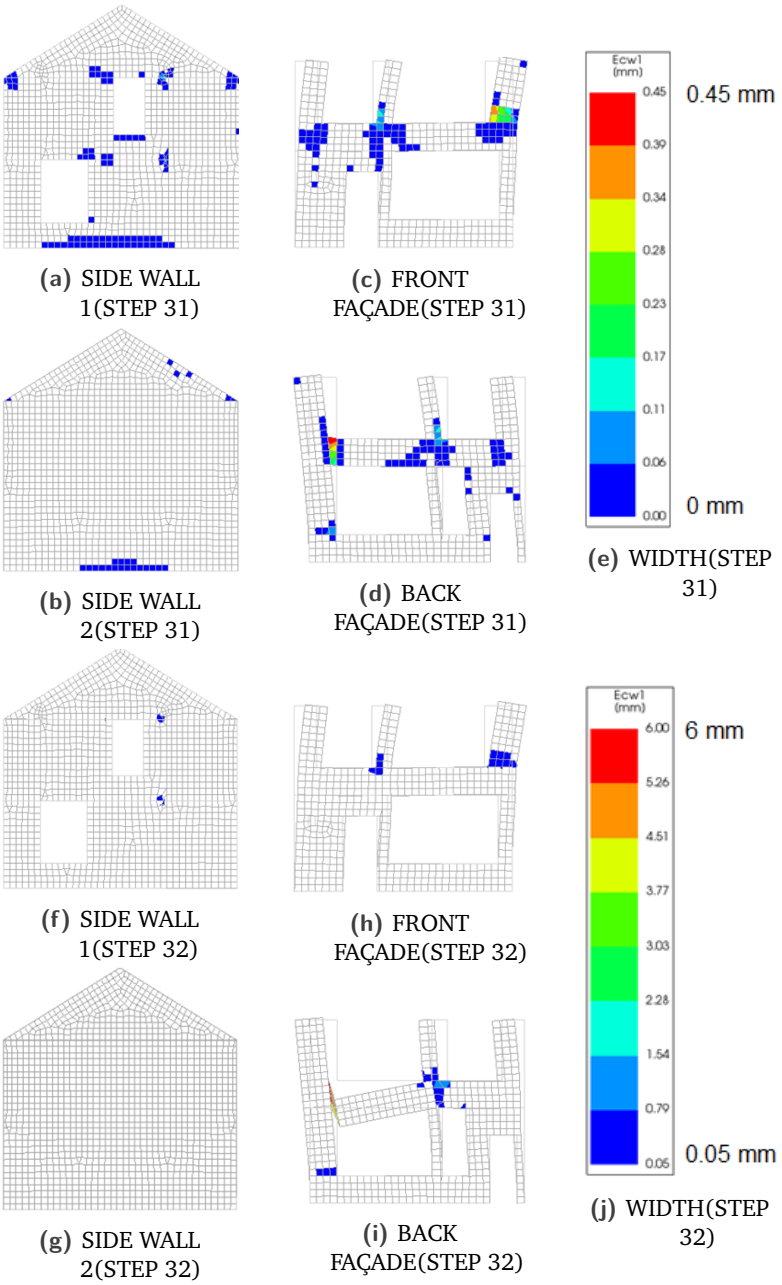


(a) SIDE WALL 1(STEP 31)

(c) FRONT FAÇADE(STEP 31)

(e) WIDTH(STEP 31)

(b) SIDE WALL 2(STEP 31)

(d) BACK FAÇADE(STEP 31)

(f) SIDE WALL 1(STEP 32)

(h) FRONT FAÇADE(STEP 32)

(j) WIDTH(STEP 32)

(g) SIDE WALL 2(STEP 32)

(i) BACK FAÇADE(STEP 32)

**Fig. F.18.:** CRACK-WIDTH–$Z1||Z2||I_V^F = 0.88 I_V^B = 0.55$–SO–NLB

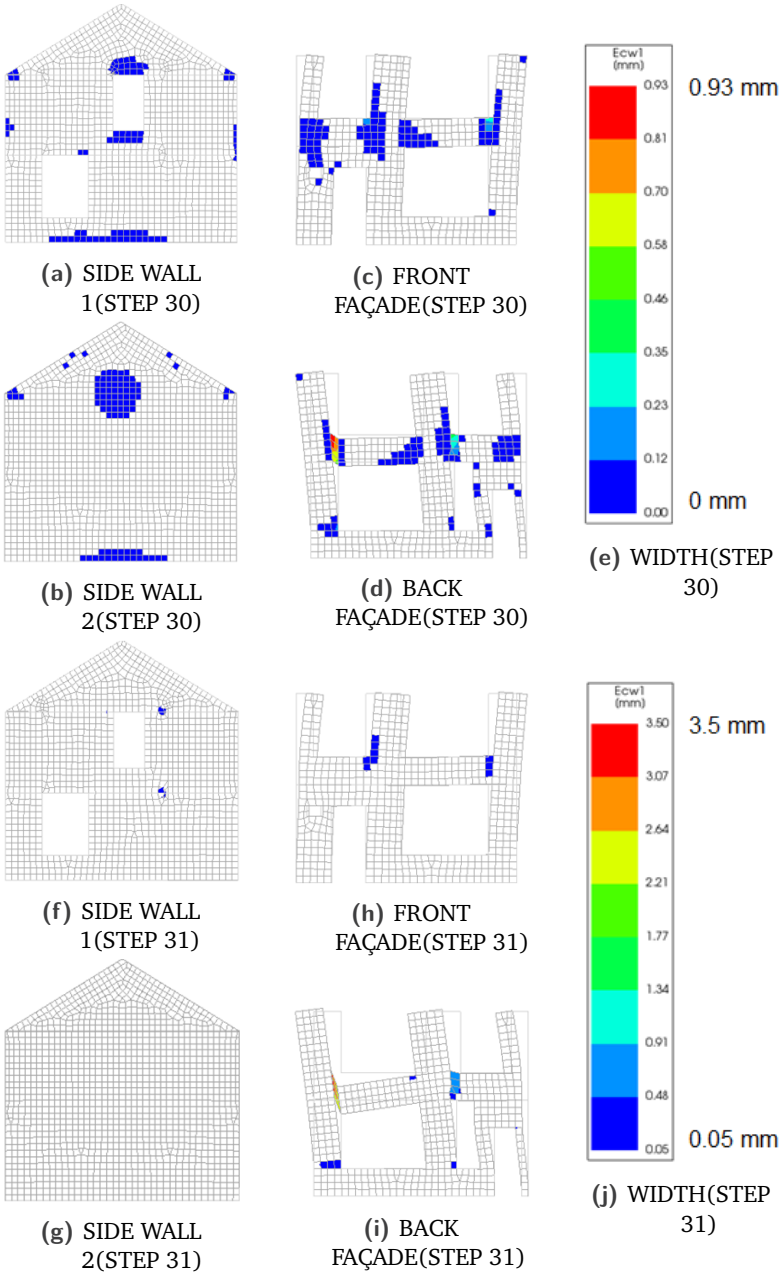


(a) SIDE WALL 1(STEP 30)

(b) SIDE WALL 2(STEP 30)

(c) FRONT FAÇADE(STEP 30)

(d) BACK FAÇADE(STEP 30)

(e) WIDTH(STEP 30)

(f) SIDE WALL 1(STEP 31)

(g) SIDE WALL 2(STEP 31)

(h) FRONT FAÇADE(STEP 31)

(i) BACK FAÇADE(STEP 31)

(j) WIDTH(STEP 31)

**Fig. F.19.:** CRACK-WIDTH–$Z1||Z2||I_V^F = 0.72 I_V^B = 0.56$–NSO–NLB

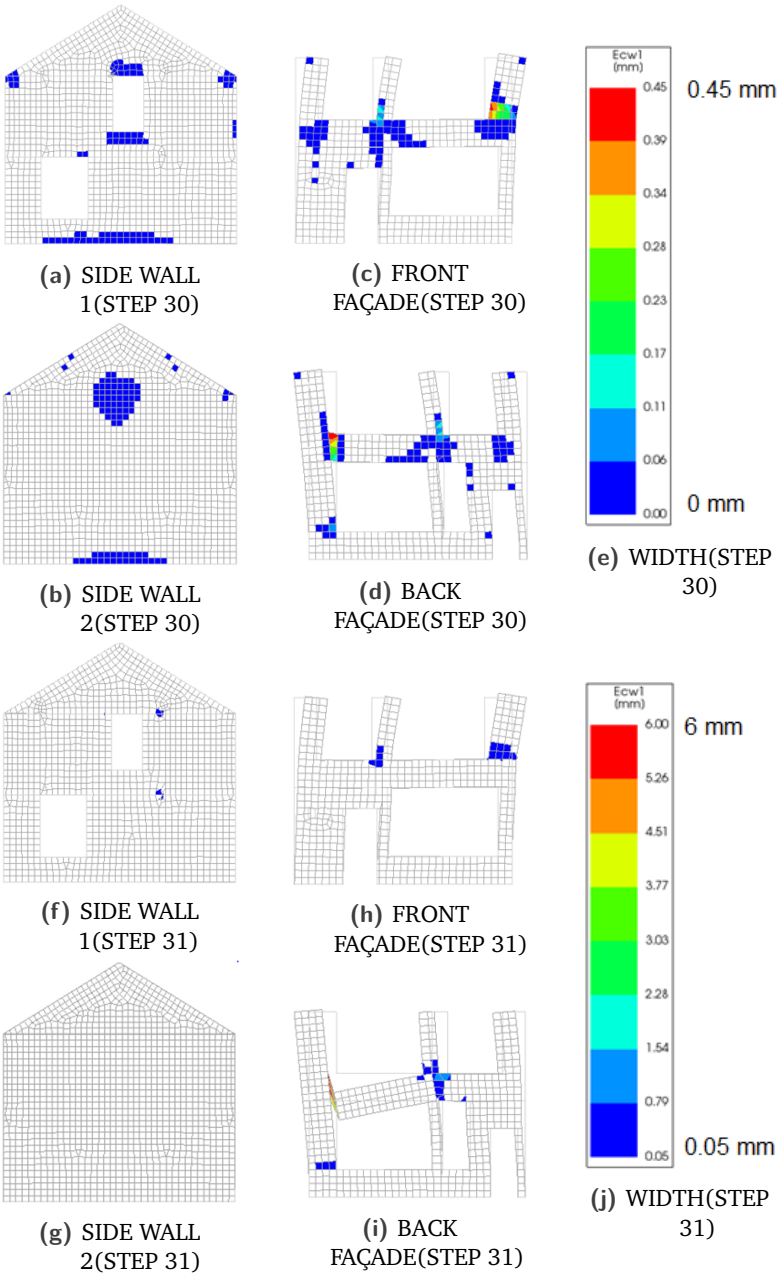


(a) SIDE WALL 1(STEP 30)

(c) FRONT FAÇADE(STEP 30)

(e) WIDTH(STEP 30)

(b) SIDE WALL 2(STEP 30)

(d) BACK FAÇADE(STEP 30)

(f) SIDE WALL 1(STEP 31)

(h) FRONT FAÇADE(STEP 31)

(j) WIDTH(STEP 31)

(g) SIDE WALL 2(STEP 31)

(i) BACK FAÇADE(STEP 31)

**Fig. F.20.:** CRACK-WIDTH–$Z1||Z2||I_V^F = 0.88 I_V^B = 0.55$–NSO–NLB

# Horizontal Irregularity

G

## G.1 Case 1–SO/NSO and LB

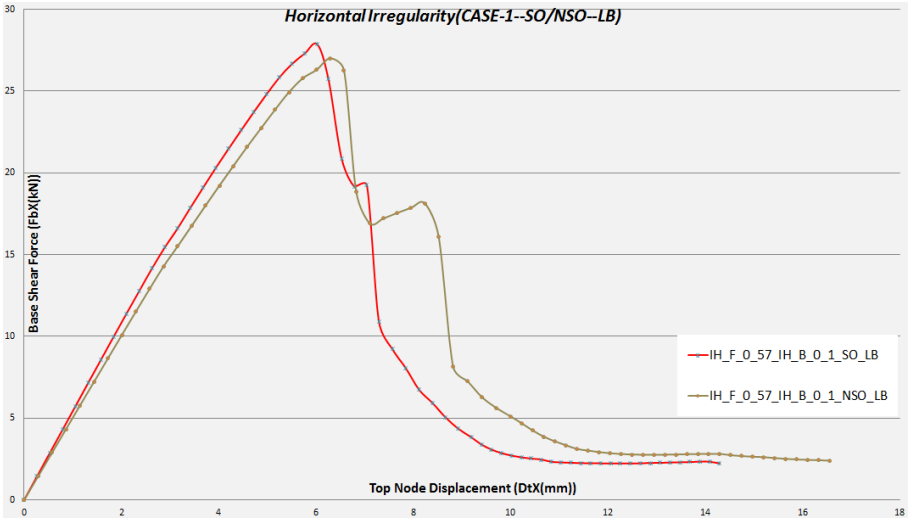


Fig. G.1.: PUSHOVER CURVE–HORIZONTAL IRREGULARITY CASE 1$[I_H^F = 0.57||I_H^B = 0.1]$ (SO/NSO AND INCLUSION OF LINTEL BEAMS)

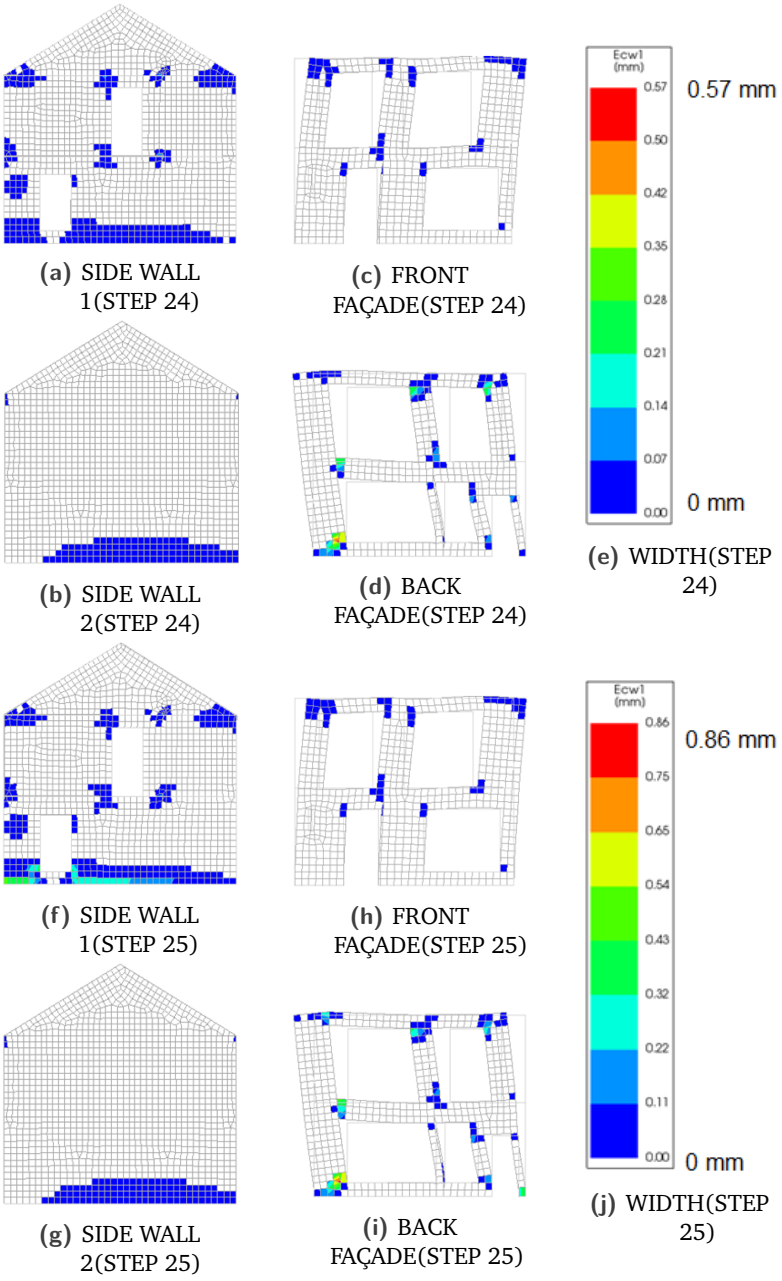


(a) SIDE WALL 1(STEP 24)

(b) SIDE WALL 2(STEP 24)

(c) FRONT FAÇADE(STEP 24)

(d) BACK FAÇADE(STEP 24)

(e) WIDTH(STEP 24)

(f) SIDE WALL 1(STEP 25)

(g) SIDE WALL 2(STEP 25)

(h) FRONT FAÇADE(STEP 25)

(i) BACK FAÇADE(STEP 25)

(j) WIDTH(STEP 25)

**Fig. G.2.:** CRACK-WIDTH–$I_H^F = 0.57 I_H^B = 0.1$–SO–LB

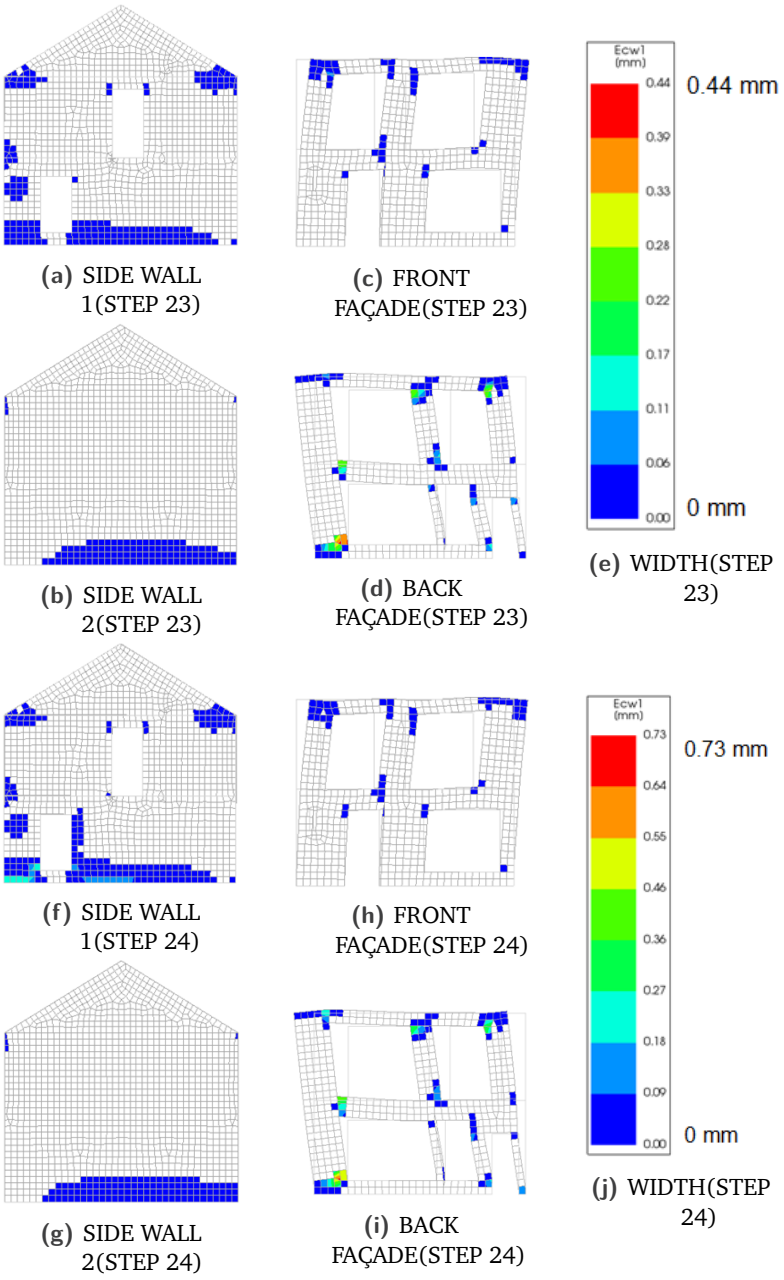


(a) SIDE WALL 1(STEP 23)

(b) SIDE WALL 2(STEP 23)

(c) FRONT FAÇADE(STEP 23)

(d) BACK FAÇADE(STEP 23)

(e) WIDTH(STEP 23)

(f) SIDE WALL 1(STEP 24)

(g) SIDE WALL 2(STEP 24)

(h) FRONT FAÇADE(STEP 24)

(i) BACK FAÇADE(STEP 24)

(j) WIDTH(STEP 24)

**Fig. G.3.:** CRACK-WIDTH–$I_H^F = 0.57 I_H^B = 0.1$–NSO–LB

## G.2 Case 1–SO/NSO and NLB

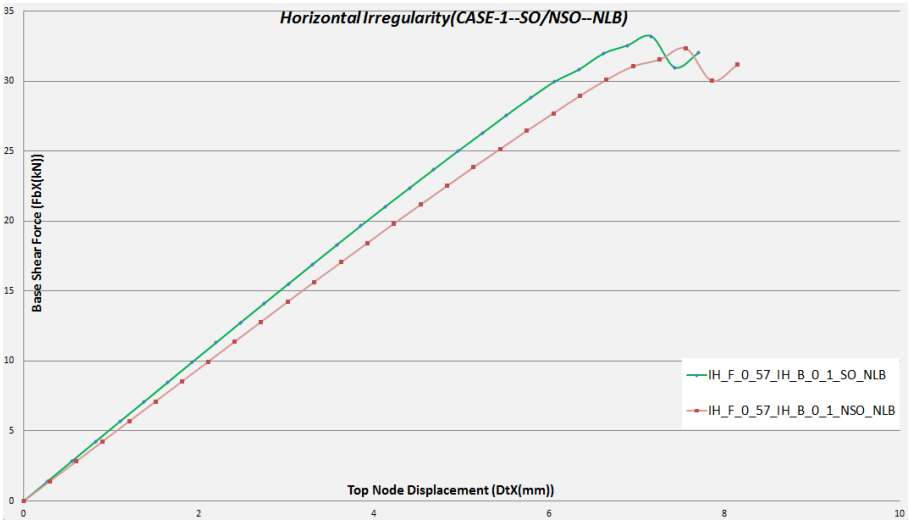


**Fig. G.4.:** PUSHOVER CURVE–HORIZONTAL IRREGULARITY CASE 1$[I_H^F = 0.57||I_H^B = 0.1]$ (SO/NSO AND EXCLUSION OF LINTEL BEAMS)

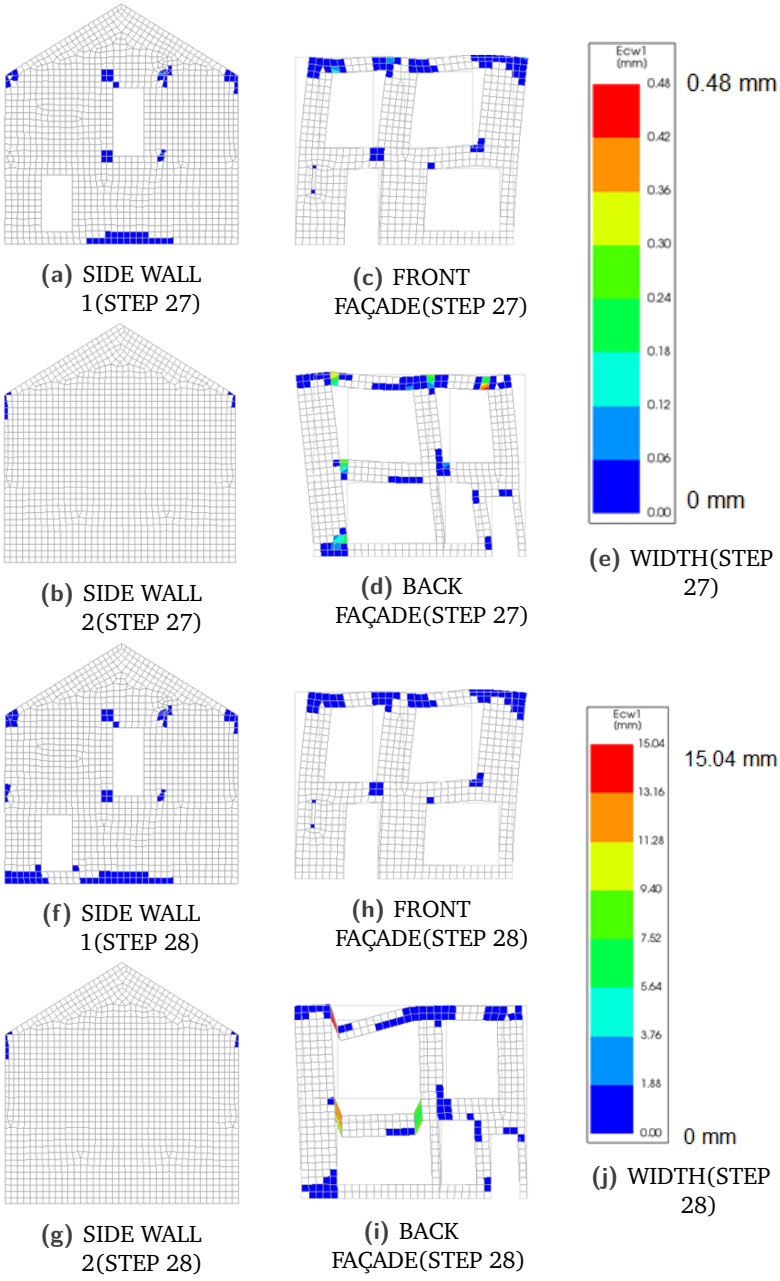


(a) SIDE WALL 1(STEP 27)

(b) SIDE WALL 2(STEP 27)

(c) FRONT FAÇADE(STEP 27)

(d) BACK FAÇADE(STEP 27)

(e) WIDTH(STEP 27)

(f) SIDE WALL 1(STEP 28)

(g) SIDE WALL 2(STEP 28)

(h) FRONT FAÇADE(STEP 28)

(i) BACK FAÇADE(STEP 28)

(j) WIDTH(STEP 28)

**Fig. G.5.:** CRACK-WIDTH–$I_H^F = 0.57 I_H^B = 0.1$–SO–NLB

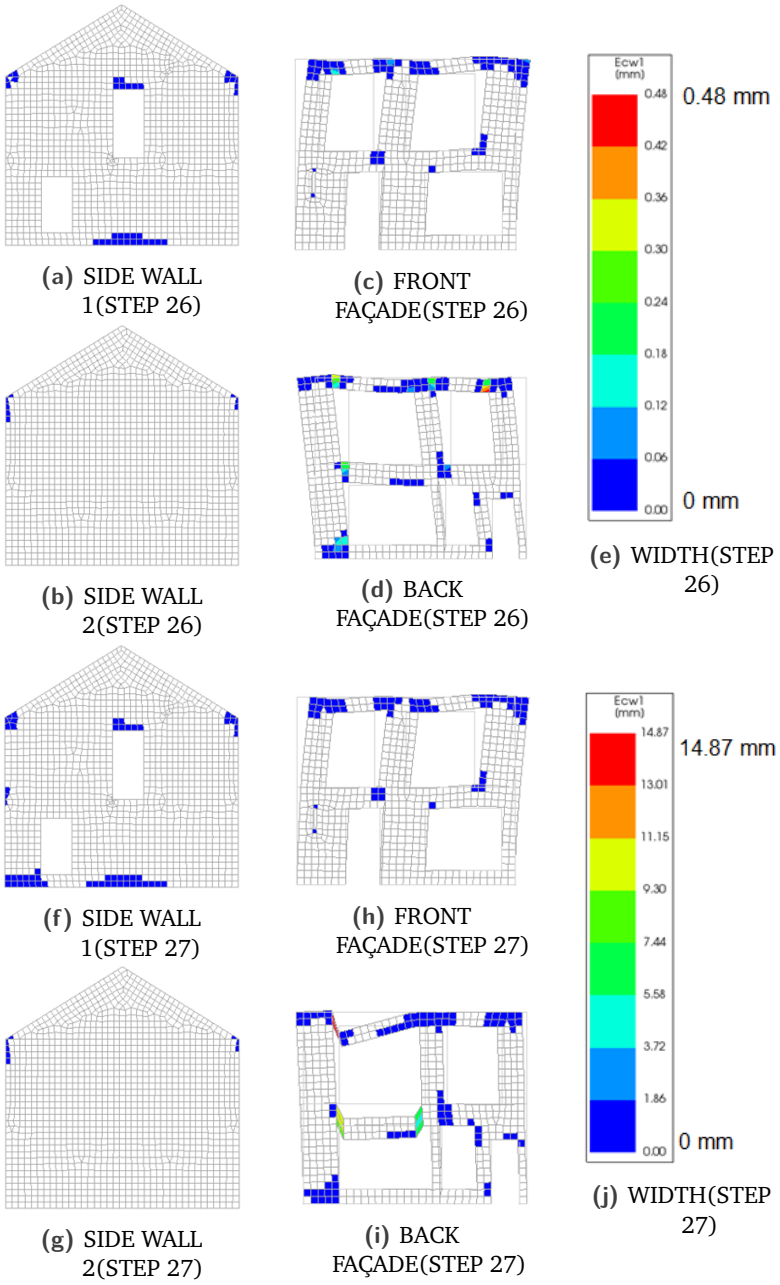


(a) SIDE WALL 1(STEP 26)

(b) SIDE WALL 2(STEP 26)

(c) FRONT FAÇADE(STEP 26)

(d) BACK FAÇADE(STEP 26)

(e) WIDTH(STEP 26)

(f) SIDE WALL 1(STEP 27)

(g) SIDE WALL 2(STEP 27)

(h) FRONT FAÇADE(STEP 27)

(i) BACK FAÇADE(STEP 27)

(j) WIDTH(STEP 27)

**Fig. G.6.:** CRACK-WIDTH–$I_H^F = 0.57 I_H^B = 0.1$–NSO–NLB

## G.3 Case 2–SO/NSO and LB

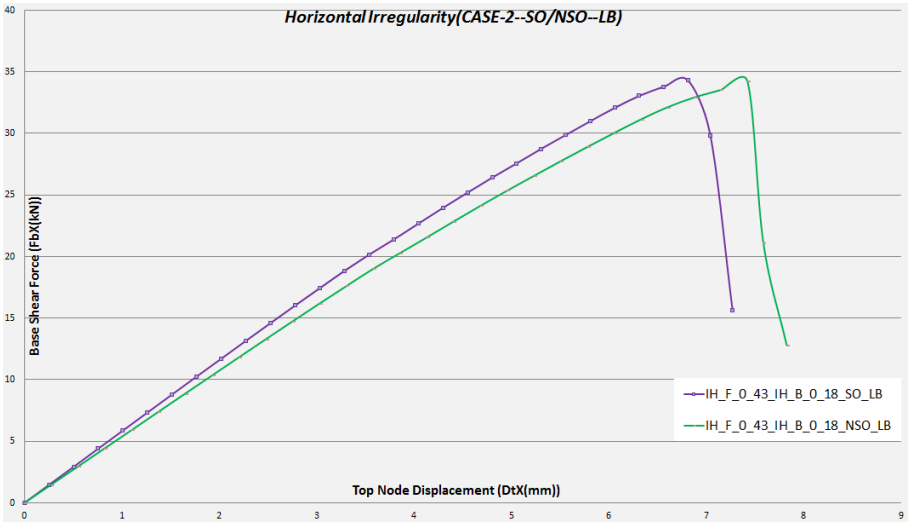


**Fig. G.7.:** PUSHOVER CURVE–HORIZONTAL IRREGULARITY CASE $1[I_H^F = 0.43||I_H^B = 0.18]$ (SO/NSO AND INCLUSION OF LINTEL BEAMS)

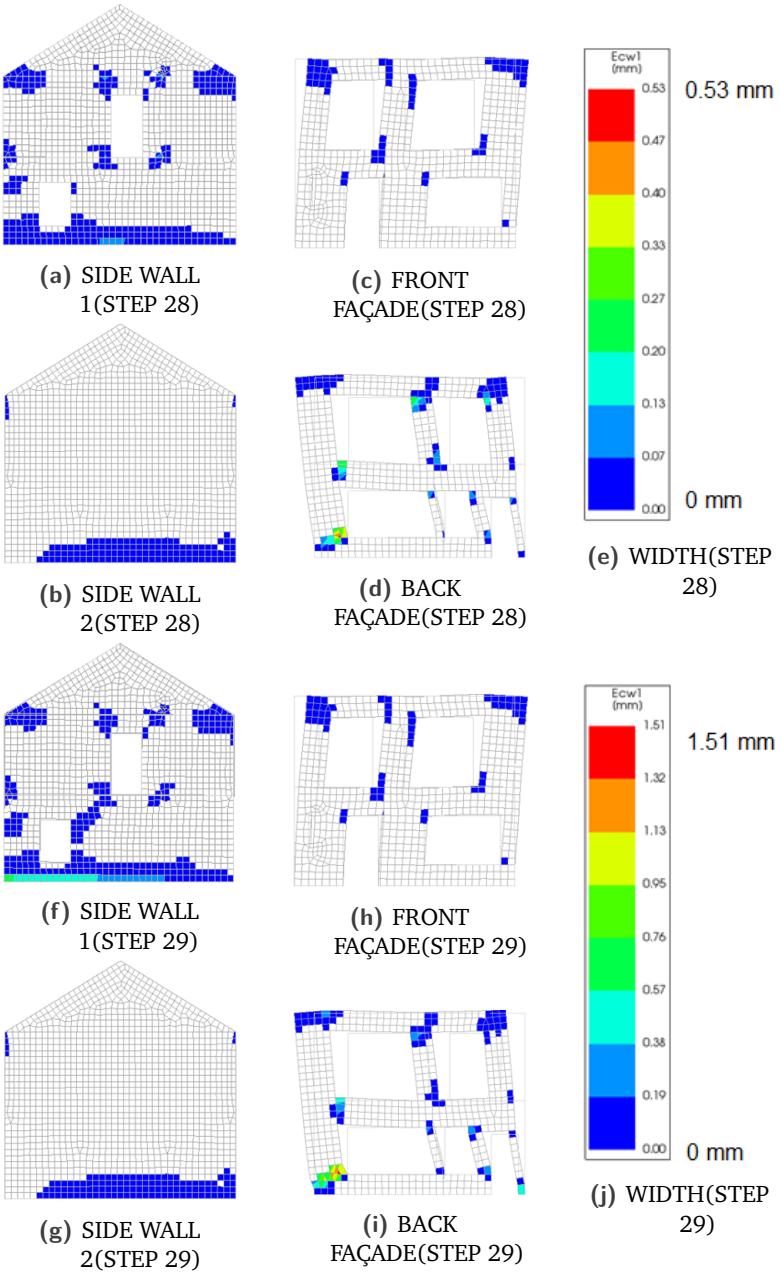


(a) SIDE WALL 1(STEP 28)

(b) SIDE WALL 2(STEP 28)

(c) FRONT FAÇADE(STEP 28)

(d) BACK FAÇADE(STEP 28)

(e) WIDTH(STEP 28)

(f) SIDE WALL 1(STEP 29)

(g) SIDE WALL 2(STEP 29)

(h) FRONT FAÇADE(STEP 29)

(i) BACK FAÇADE(STEP 29)

(j) WIDTH(STEP 29)

**Fig. G.8.:** CRACK-WIDTH–$I_H^F = 0.43 I_H^B = 0.18$–SO–LB

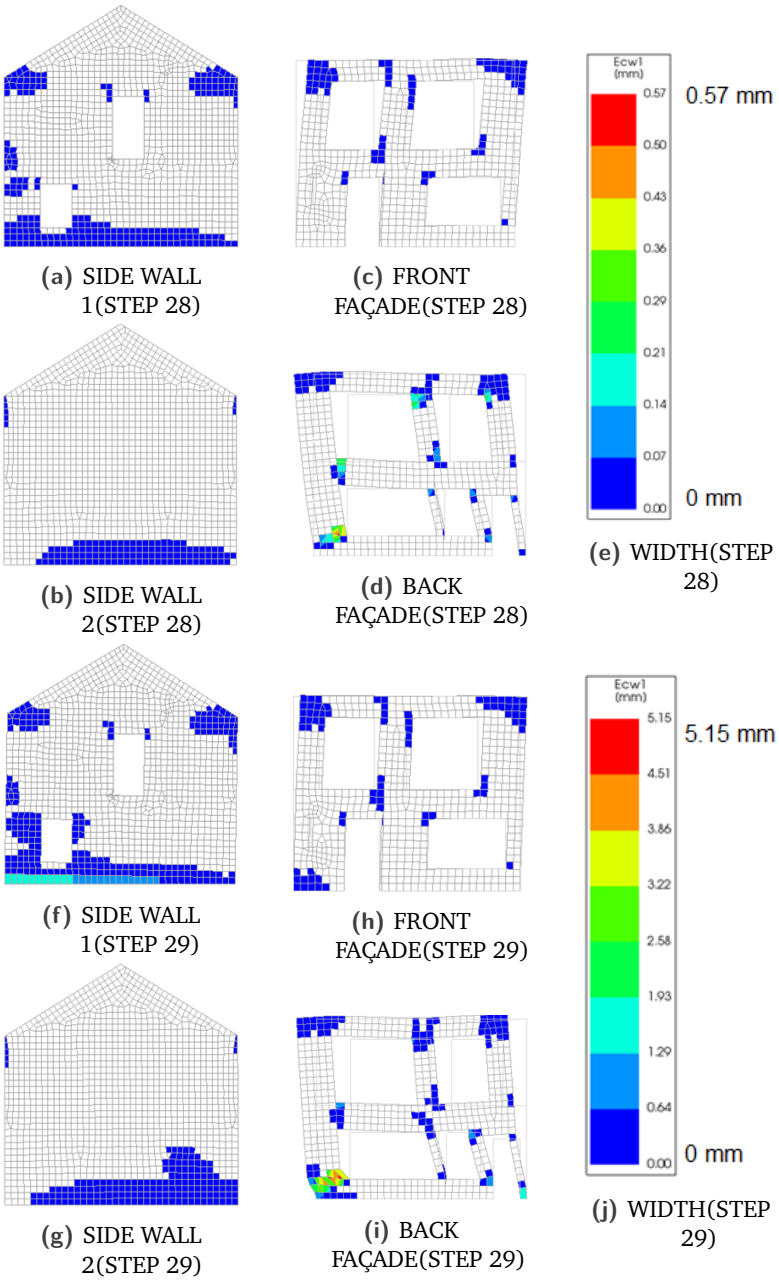


(a) SIDE WALL 1(STEP 28)

(c) FRONT FAÇADE(STEP 28)

(e) WIDTH(STEP 28)

(b) SIDE WALL 2(STEP 28)

(d) BACK FAÇADE(STEP 28)

(f) SIDE WALL 1(STEP 29)

(h) FRONT FAÇADE(STEP 29)

(j) WIDTH(STEP 29)

(g) SIDE WALL 2(STEP 29)

(i) BACK FAÇADE(STEP 29)

**Fig. G.9.:** CRACK-WIDTH–$I_H^F = 0.43 I_H^B = 0.18$–NSO–LB

## G.4 Case 2–SO/NSO and NLB

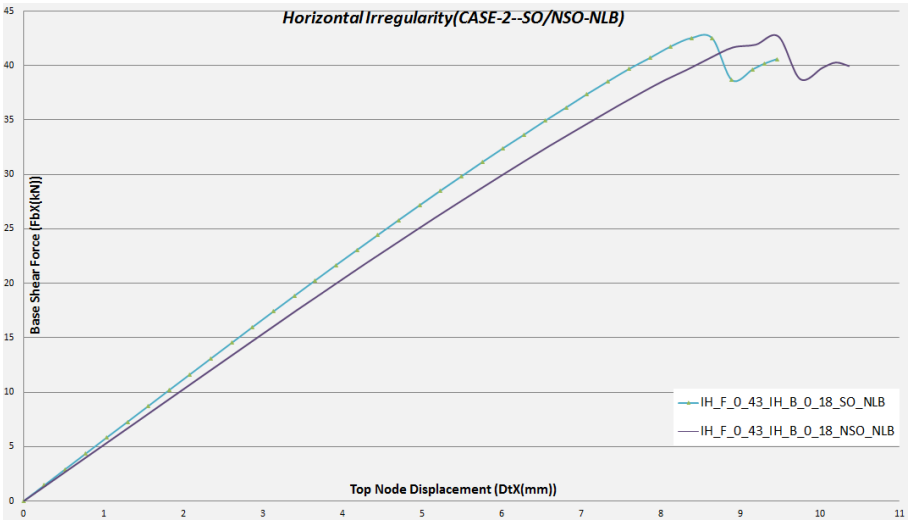


**Fig. G.10.:** PUSHOVER CURVE–HORIZONTAL IRREGULARITY CASE $1[I_H^F = 0.43||I_H^B = 0.18]$ (SO/NSO AND EXCLUSION OF LINTEL BEAMS)

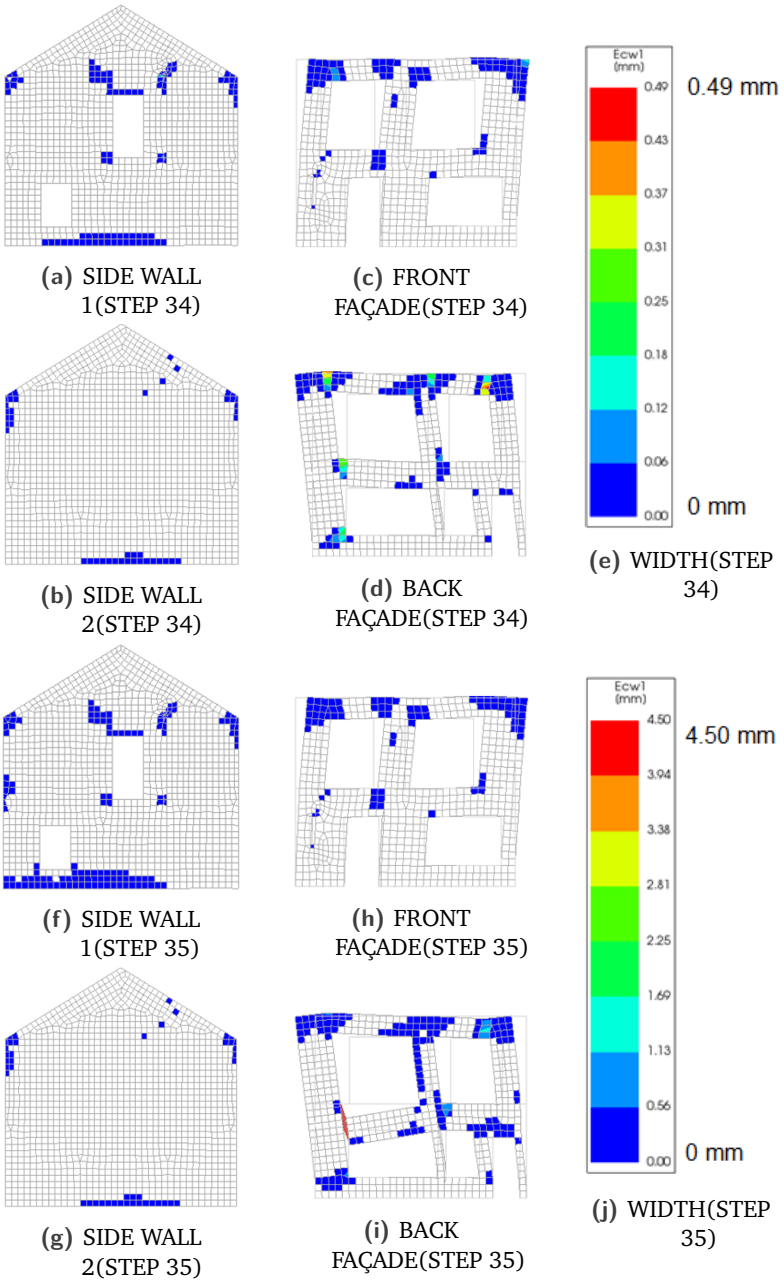


(a) SIDE WALL 1(STEP 34)

(c) FRONT FAÇADE(STEP 34)

(e) WIDTH(STEP 34)

(b) SIDE WALL 2(STEP 34)

(d) BACK FAÇADE(STEP 34)

(f) SIDE WALL 1(STEP 35)

(h) FRONT FAÇADE(STEP 35)

(j) WIDTH(STEP 35)

(g) SIDE WALL 2(STEP 35)

(i) BACK FAÇADE(STEP 35)

**Fig. G.11.:** CRACK-WIDTH–$I_H^F = 0.43 I_H^B = 0.18$–SO–NLB

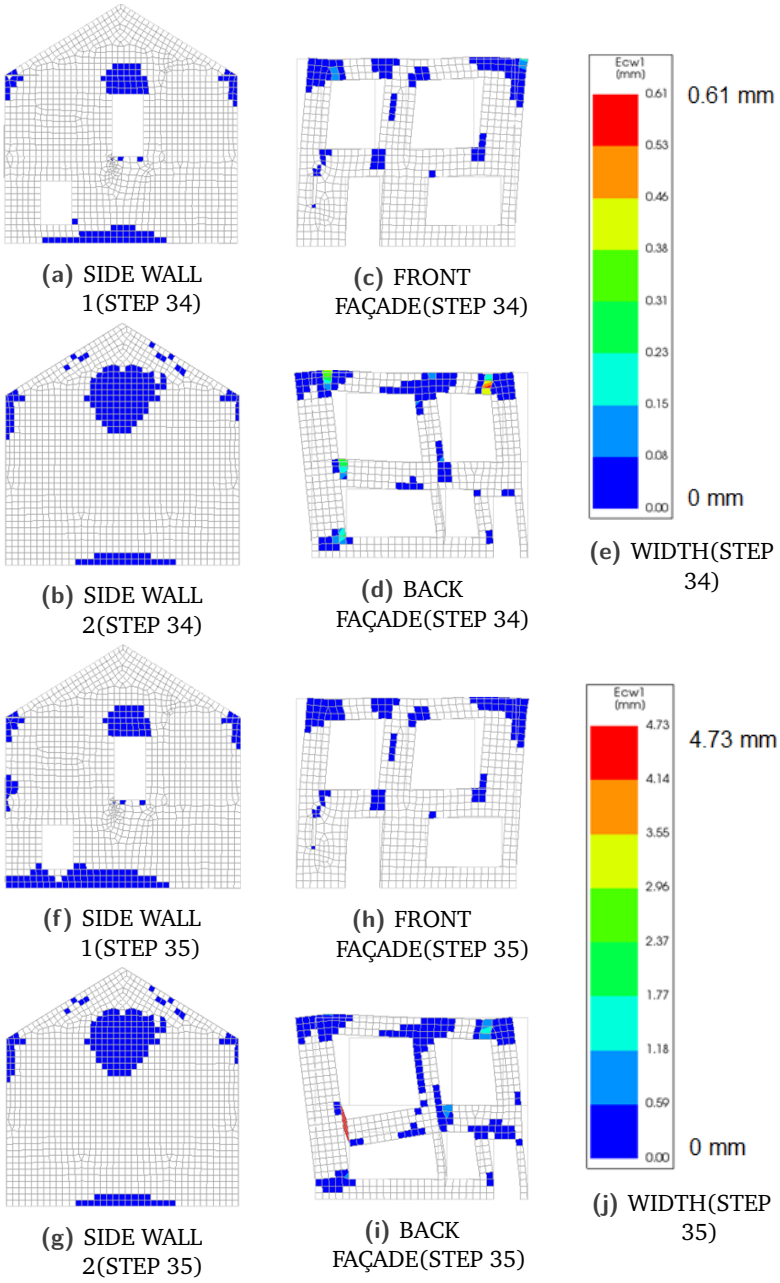


(a) SIDE WALL 1(STEP 34)

(b) SIDE WALL 2(STEP 34)

(c) FRONT FAÇADE(STEP 34)

(d) BACK FAÇADE(STEP 34)

(e) WIDTH(STEP 34)

(f) SIDE WALL 1(STEP 35)

(g) SIDE WALL 2(STEP 35)

(h) FRONT FAÇADE(STEP 35)

(i) BACK FAÇADE(STEP 35)

(j) WIDTH(STEP 35)

**Fig. G.12.:** CRACK-WIDTH–$I_H^F = 0.43 I_H^B = 0.18$–NSO–NLB

# Number of Openings

H

## H.1 Case 1–Case Study Height

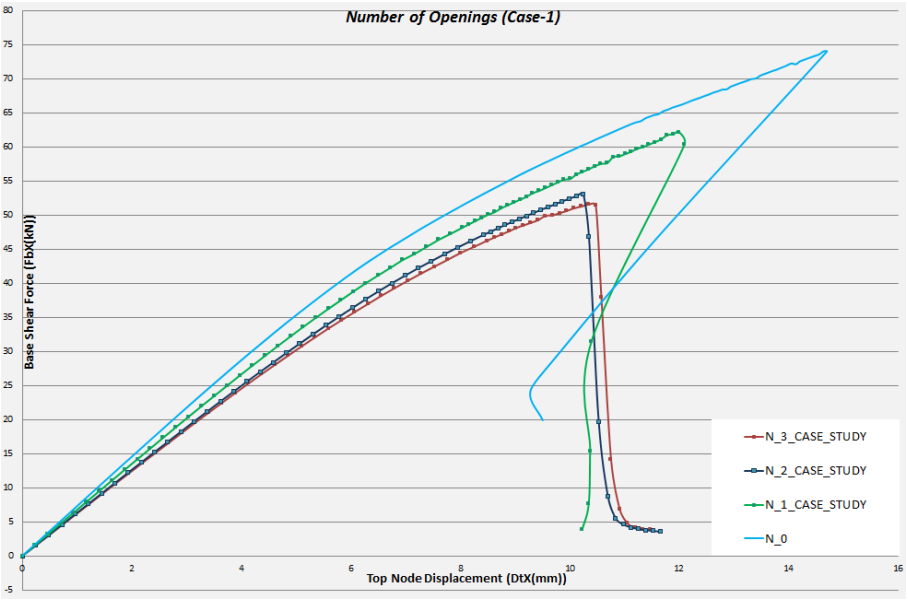


**Fig. H.1.:** PUSHOVER CURVE–NUMBER OF OPENINGS CASE 1[CASE STUDY HEIGHT]

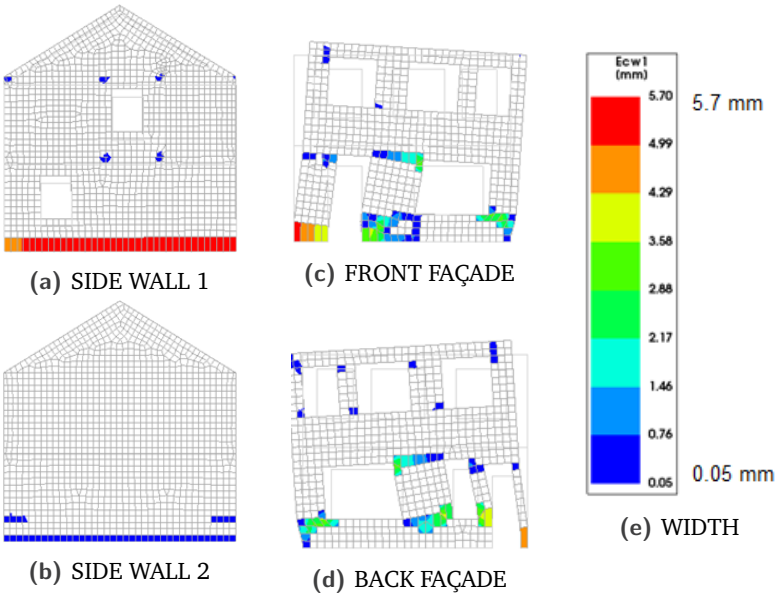


(a) SIDE WALL 1 (c) FRONT FAÇADE (e) WIDTH

(b) SIDE WALL 2 (d) BACK FAÇADE

**Fig. H.2.:** CRACK-WIDTH($N = 3$)

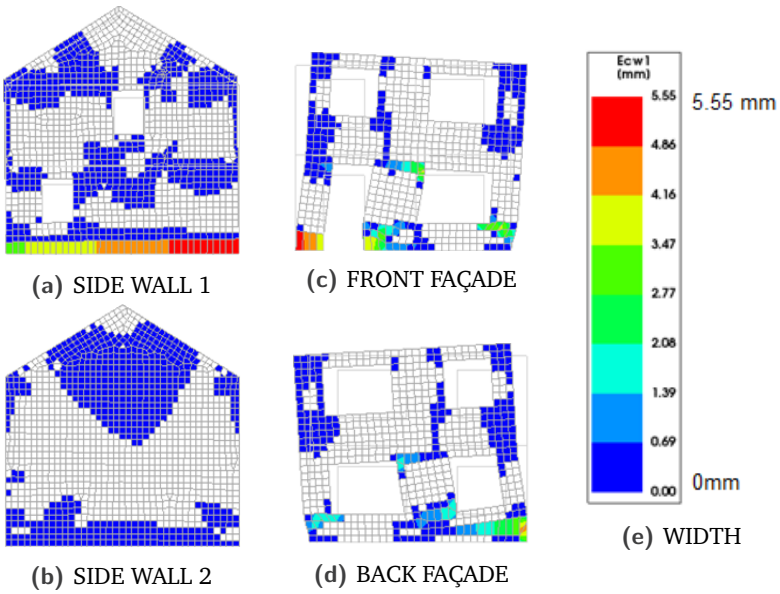


(a) SIDE WALL 1 (c) FRONT FAÇADE (e) WIDTH

(b) SIDE WALL 2 (d) BACK FAÇADE

**Fig. H.3.:** CRACK-WIDTH($N = 2$)

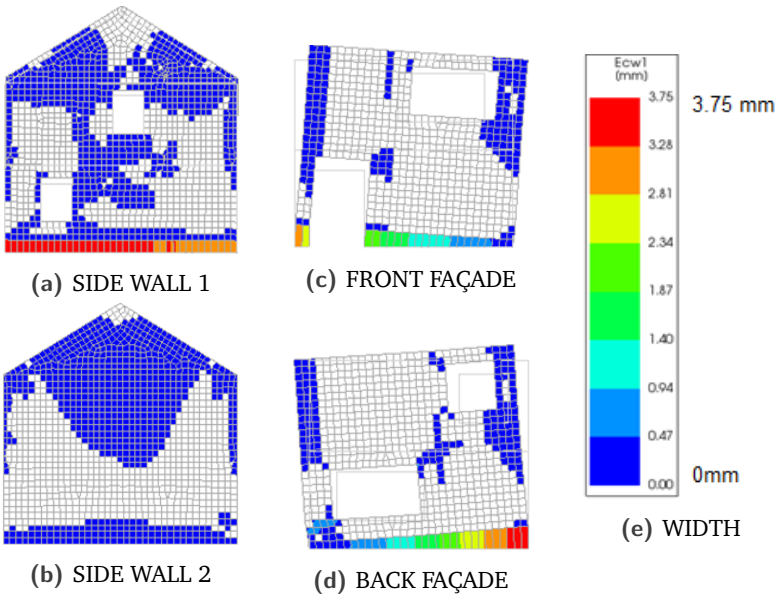


(a) SIDE WALL 1 (c) FRONT FAÇADE (e) WIDTH

(b) SIDE WALL 2 (d) BACK FAÇADE

**Fig. H.4.:** CRACK-WIDTH($N = 1$)

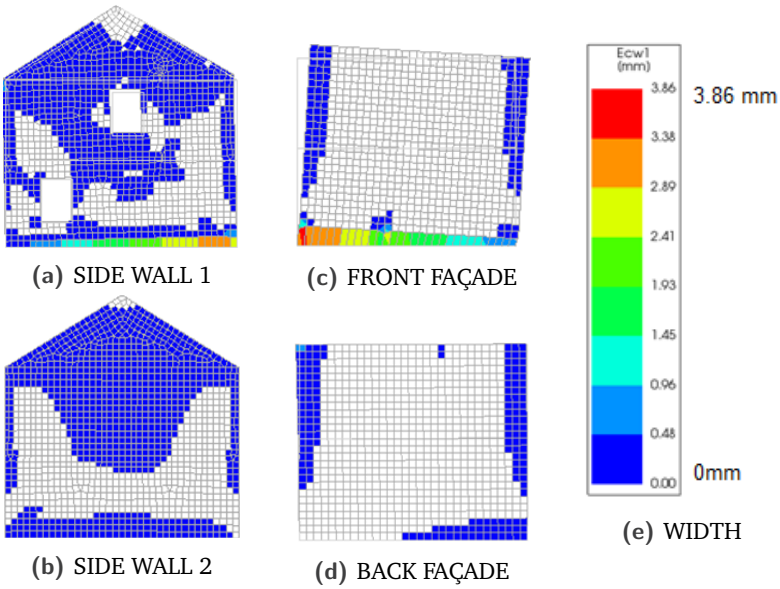


(a) SIDE WALL 1 (c) FRONT FAÇADE (e) WIDTH

(b) SIDE WALL 2 (d) BACK FAÇADE

**Fig. H.5.:** CRACK-WIDTH($N = 0$)

## H.2 Case 2–Height of Openings(Z1||Z2)

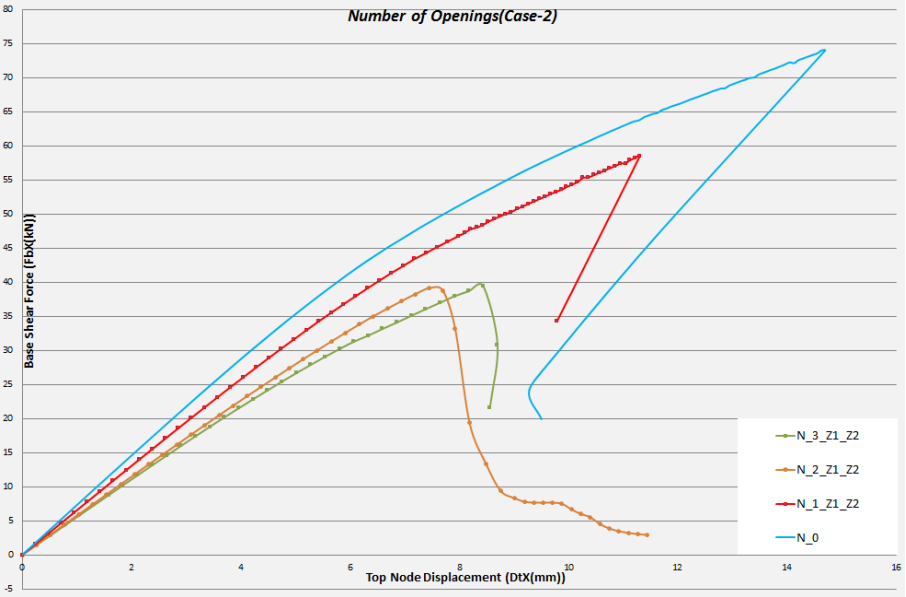


**Fig. H.6.:** PUSHOVER CURVE–NUMBER OF OPENINGS CASE 2[Z1||Z2 HEIGHT]

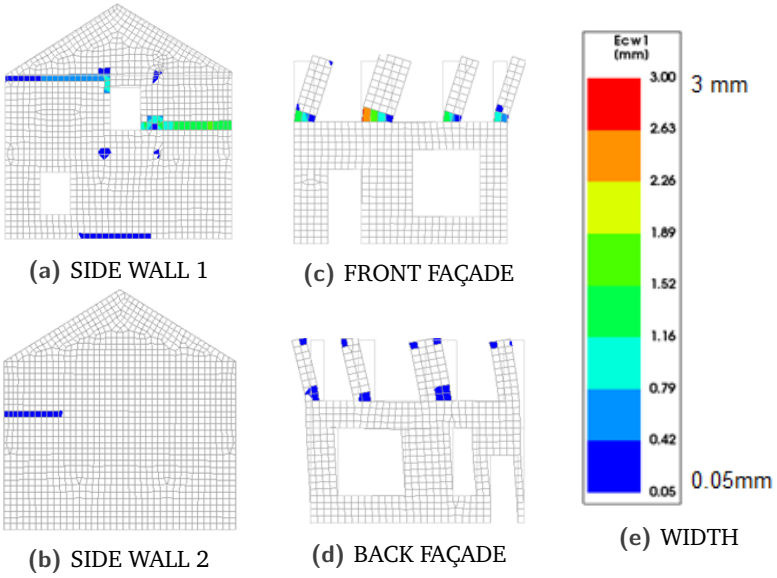


(a) SIDE WALL 1 (c) FRONT FAÇADE (e) WIDTH

(b) SIDE WALL 2 (d) BACK FAÇADE

**Fig. H.7.:** CRACK-WIDTH($N = 3||Z1||Z2||$)

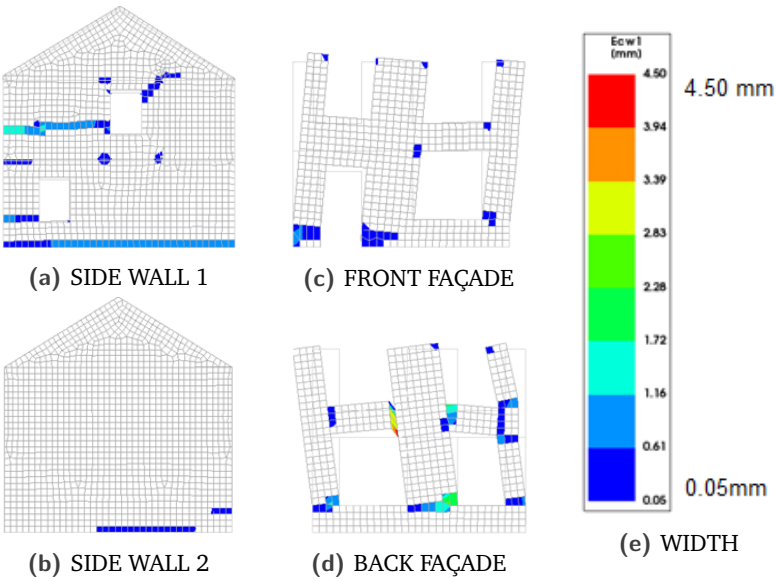


(a) SIDE WALL 1 (c) FRONT FAÇADE (e) WIDTH

(b) SIDE WALL 2 (d) BACK FAÇADE

**Fig. H.8.:** CRACK-WIDTH($N = 2||Z1||Z2||$)

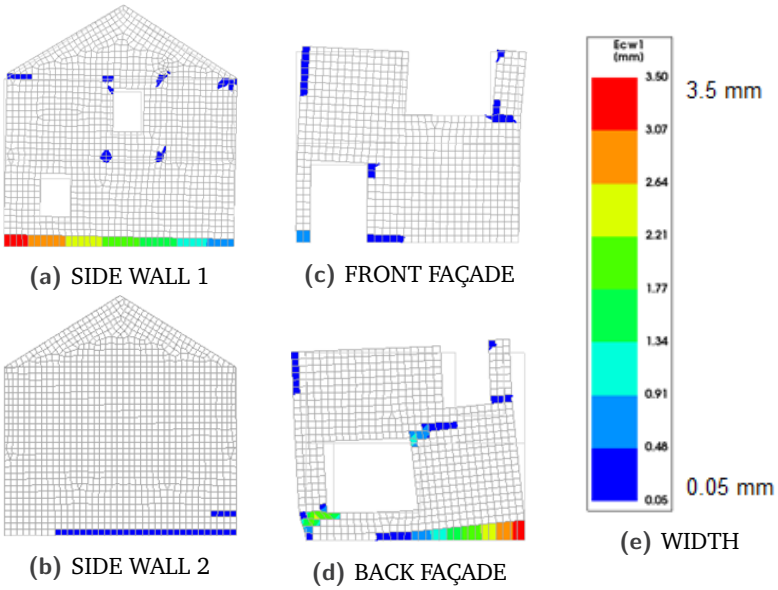


(a) SIDE WALL 1 (c) FRONT FAÇADE (e) WIDTH

(b) SIDE WALL 2 (d) BACK FAÇADE

**Fig. H.9.:** CRACK-WIDTH($N = 1||Z1||Z2||$)